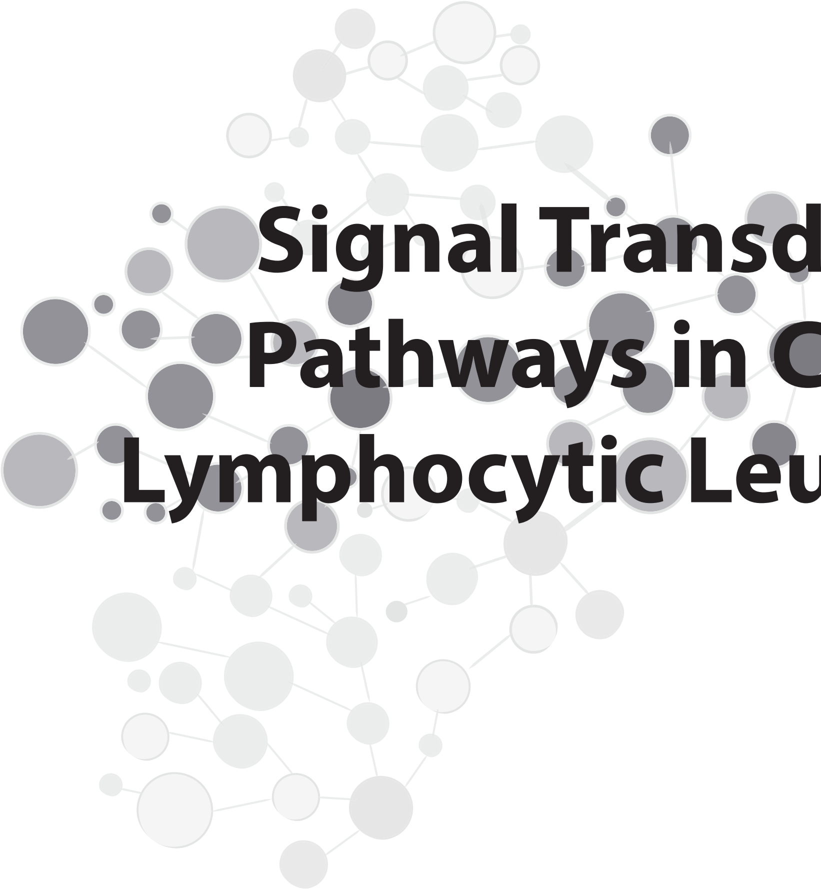

Signal Transduction Pathways in Chronic Lymphocytic Leukemia

Simar Pal Singh

Molecular Medicine
Postgraduate School

No parts of this thesis may be reproduced or transmitted in any form by any means, electronic or mechanical, including photocopying, recording or any information storage and retrieval system, without permission in writing from the author.

The research for this thesis was performed within the framework of the Erasmus MC Postgraduate School Molecular Medicine.

The studies described in this thesis were performed at the Department of Pulmonary Medicine and Laboratory for Medical Immunology, Department of Immunology, Erasmus MC, Rotterdam, the Netherlands.

The studies were financially supported by the Post graduate school Molecular Medicine, the Dutch Cancer Society and the Departments of Pulmonary Medicine and Immunology, Erasmus MC Rotterdam.

The research and printing of this thesis was supported by Post graduate school Molecular Medicine, Department of Pulmonary Medicine, Erasmus MC and Erasmus University Rotterdam.

ISBN: 978-94-91811-22-7

Cover design: Simar Pal Singh
Lay-out: Daniëlle Korpershoek & Bibi van Bodegom
Printing: Ridderprint BV, Alblasserdam

Copyright © 2019 by Simar Pal Singh. All rights reserved.

Signal Transduction Pathways in Chronic Lymphocytic Leukemia

Signaaltransductie Routes in Chronische Lymfatische Leukemie

Thesis

to obtain the degree of Doctor from the
Erasmus University Rotterdam
by command of the
rector magnificus

Prof.dr. R.C.M.E. Engels

and in accordance with the decision of the Doctoral Board
The Public defense will be held on

Tuesday 29 October 2019 at 11:30 hours

by

Simar Pal Singh

born in Delhi, India

Erasmus University Rotterdam

DOCTORAL COMMITEE

Promotor
Prof.dr. R.W. Hendriks

Other Members
Prof.dr. A.P. Kater
Prof.dr. H.R. Delwel
Dr. J.E.J. Guikema

Copromotor
Dr. A.W. Langerak

CONTENTS

CHAPTER 1 9
General introduction

CHAPTER 2 23
Role of Bruton's tyrosine kinase in B cells and malignancies.
Molecular Cancer 2018; 17(1):57

CHAPTER 3 71
Transcriptome analysis links BCR, BTK and anti-CD40 signaling to CLL pathogenesis.
In preparation

CHAPTER 4 95
Cell lines generated from a chronic lymphocytic leukemia mouse model exhibit constitutive Btk and Akt signaling.
Oncotarget 2017; 8(42)

CHAPTER 5 129
Overexpression of SH2-containing inositol phosphatase contributes to chronic lymphocytic leukemia survival.
Under revision

CHAPTER 6 165
Identification of distinct unmutated chronic lymphocytic leukemia subsets in mice based on their T cell dependency.
Frontiers in Immunology 2018; 9(1996)

CHAPTER 7 193
Differential roles of BTK and ERK activity in the integration of B cell receptor and CD40 signaling in chronic lymphocytic leukemia.
Submitted

CHAPTER 8 209
General discussion

ADDENDUM 233
Abbreviations 235
Summary 239
Samenvatting 243
Acknowledgements 247
About the author 253
PhD Portfolio 255
Publications 257

Chapter 1

General Introduction

Part of this chapter was published in Muggen A.F. et al.,
Targeting Signaling Pathways in Chronic Lymphocytic Leukemia
Current Cancer Drug Targets, 2016, 16, 669-688

GENERAL INTRODUCTION

Chronic lymphocytic leukemia (CLL) is the most frequently occurring type of leukemia in adults in the Western world. CLL is characterized by the accumulation of a monoclonal population of small B cells with a typical immunophenotype (CD19$^+$, CD20^{dim}, CD5$^+$, CD23$^+$, CD27$^+$, CD43$^+$, surface Ig^{dim}) in blood. Over 95% of cases are diagnosed above 50 years of age. To date, the overall 5-year relative survival for CLL patients is 79.2%[1]. Nevertheless, there is a large difference in survival between individual CLL patients, varying from several months to a normal life expectancy[1]. This heterogeneity in survival reflects the known biological heterogeneity in CLL, which is considered a multifactorial disease.

Clinical features of CLL

Many people with CLL have no clinical symptoms at first, and the disease may only be discovered during a routine blood test or a blood test for another medical condition. The diagnosis of CLL requires the presence of $\geq 5 \times 10^9$/L B lymphocytes in the peripheral blood, sustained for at least 3 months[2]. The leukemic cells found in the blood smear are characteristically small, mature lymphocytes with a narrow border of cytoplasm and a dense nucleus lacking discernable nucleoli and partially aggregated chromatin. To stratify patients according to disease risk, several prognostic factors are included in daily clinical practice. These include clinical staging, molecular genetics and B-cell receptor (BCR) characteristics.

Clinical staging. Clinical staging of CLL is performed by one of the two widely accepted staging systems used in both patient care and clinical trials: Rai and Binet. Both of these rely solely on a physical examination and standard laboratory tests, as described in **Table 1**.

Molecular Genetics. In CLL several genetic aberrations are found that have prognostic value. For instance, there are multiple chromosomal aberrations that together occur in approximately 80% of CLL cases. These mainly concern deletions of chromosomal regions 17p, 11q, or 13q, and trisomy of chromosome 12. These chromosomal deletions are associated with the loss of the *TP53* and *ATM* genes, and the *miR15a* and *miR16-1* microRNA genes, respectively; so far, the relevant gene(s) involved in trisomy 12 is unknown. Deletion of 17p and deletion of 11q are associated with a poor disease outcome, while deletion of 13q as a single event is associated with a milder form of disease (reviewed in[3]). Over the last few years several novel mutations with prognostic value have been identified by next generation sequencing approaches. Mutations found in the *NOTCH1*[4] and *SF3B1* genes[5] are associated with progressive disease, while mutations in *MYD88*[4] are rare and appear to be associated with an indolent form of disease. Although some of the identified mutations appear to act as early driver mutations playing a role in disease onset, mutations are never

Table 1: Clinical Staging for CLL

RAI and BINET clinical staging for CLL	
RAI SYSTEM	
Rai Stage	Clinical Characteristics
O	Lymphocytosis with leukemia cells in the blood and/or marrow
I	Lymphocytosis and enlarged lymph nodes
II	Lymphocytosis and enlarged spleen and/or liver
III	Lymphocytosis and anemia (hemoglobin,[Hb] < 1 g/dL)
IV	Lymphocytosis and thrombocytopenia (platelet <100 X 10^9/L)
Modified Rai classification defines CLL into three main categories • Low-risk disease (include Rai stage 0) • Intermediate-risk disease (include Rai stage I or II) • High-risk disease: (include Rai stage III or IV)	
BINET SYSTEM	
Binet Stage	Clinical Characteristics
A	Hb ≥10 g/dL and platelets ≥100 X 10^9/L and ≤ 2 lymph node areas involved
B	Hb ≥10 g/dL and platelets ≥100 X 10^9/L and ≥ 3 lymph node areas involved
C	Hb <10 g/dL and/or a platelet count <100 X 10^9/L.
Lymph node areas • Head and neck, including the Waldeyer ring (this counts as 1 area, even if ≥1 group of nodes is enlarged). • Axillae (involvement of both axillae counts as just 1 area). • Groins, including superficial femorals (involvement of both groins counts as just 1 area). • Palpable spleen. Palpable liver (clinically enlarged).	

present in 100% of the clones[6]. Other mutations may act later during evolution of the CLL clone and seem to be more important for disease progression. From all genetic studies it is however clear that neither the B cell receptor (BCR) itself, nor its signaling pathway is directly targeted by mutations.

BCR characteristics. On the basis of somatic hypermutation (SHM) status of the immunoglobulin heavy chain variable (IGHV) genes of the BCR, it is clear that CLL cells can derive from pre- or post-GC B cells. CLL patients can thus be grouped into unmutated CLL (U-CLL) and mutated CLL (M-CLL). This division is also clinically relevant, because U-CLL tend to have an unfavorable prognosis with a more aggressive course of the disease and shorter time to first treatment, while M-CLL is associated with a more indolent disease form with a relatively favorable prognosis[7, 8].

Approximately one-third of all CLL cases can be further grouped on the basis of their restricted IGHV, IGHD, and IGHJ gene usage, and similarities in length and amino acid sequence of the complementarity determining region 3 (CDR3)[9]. These so-called stereotypic BCRs are found in multiple CLL patients and the analyses of large cohorts of CLL patients enabled their clustering into at least 19 major subsets which contain ~12% of all CLL cases; another 18% of CLL cases belong to minor stereotypic subsets, as was found in a study which included 7424 CLL patients[9]. The finding of BCR stereotypy is indicative of a contribution of similar antigens, thus implicating antigenic stimulation and thereby BCR specificity in CLL pathogenesis[9]. It has been shown that BCR stereotypy in CLL not only has biological impact, but also bears clinical significance. Distinct BCR stereotypic subsets appeared to associate with differences in time to first treatment, thus showing added prognostic value over U-CLL / M-CLL status per se and cytogenetic aberrations[10,11]. The role of BCR characteristics and downstream signaling pathway is further introduced in **Chapter 2** of this thesis.

CLL mouse models

Mouse models of human cancers provide a useful tool to elucidate the mechanisms that account for the natural history and pathogenesis of the disease and to evaluate the effect of different therapeutic approaches prior to human clinical trials. To date, various CLL-like mouse models have been generated using transgenesis and gene targeting approaches (see Simonetti *et al.* for an excellent review[12]). Of these various CLL mouse models only the *Eμ-TCL1* and *IgH.TEμ* models showed complete disease penetrance (100%), with no obvious monoclonal B-cell lymphocytosis stage preceding CLL development. Here we will introduce the characteristics and usefulness of these two CLL models for the study of human disease.

The *Eμ-TCL1* mouse model was generated based on overexpression of TCL1 under the control of a IGHV promoter and the IGH intronic enhancer (Eμ) in the B-cell lineage[13]. The immunophenotypic profiling of *Eμ-TCL1* mice revealed that these animals spontaneously develop hyperplasia of $CD5^+IgM^+$ B-cells, initially in the peritoneal cavity and then in lymph nodes, spleen, bone marrow and peripheral blood. Sequence analysis of BCR rearrangements from *Eμ-TCL1* mice demonstrated a skewed murine IGHV repertoire with particular involvement of IGHV11, IGHV12 and IGHV4 gene families. Furthermore, analysis of IGHV gene SHM status demonstrated that TCL1-derived leukemias are identical and minimally divergent from germ-line sequences, similar to human U-CLL. The HCDR3s in *Eμ-TCL1* mice are often long and contain multiple neutral tyrosine and serine residues. They also contain many (~55%) positively and negatively charged residues at or adjacent to the IGHV-IGHD and IGHD-IGHJ junctions, deriving from simple and complex rearrangement events including insertion of non-templated nucleotides[14].

Since the *Eμ-TCL1* mouse model very much resembles human CLL in terms of leukemia phenotype, antigen-receptor and disease course, it has been extensively used to study pathogenic mechanisms leading to CLL[12]. Recently, it has also been applied as a pre-clinical tool to investigate the efficacy and potential side effects of novel therapeutic agents. The *Eμ-TCL1* leukemias have been tested for the effects of the BTK inhibitor, ibrutinib, or the SYK inhibitor, fostamatinib, (described below), following adoptive transfer in immunodeficient severe combined immunodeficiency or syngeneic mice respectively[15,16]. Both inhibitors delayed CLL disease progression in these adoptive transfer *Eμ-TCL1* leukemia mouse models. Mimicking clinical observations in patients[17,18], treatment of mice transplanted with *Eμ-TCL1*-derived leukemias with the small molecule kinase inhibitors ibrutinib or fostamatinib resulted in a transient increase in CLL numbers in the peripheral blood concurrently with a decreased tumor load in the spleen[15,16].

A second model, the *IgH.TEμ* CLL mouse model, was generated based on sporadic expression of the SV40 T oncogene in mature B-cells[19]. SV40 T is a potent oncogene able to transform many cell types and has been implicated in the etiology of various cancers, including B-cell malignancies[20]. Sporadic expression was achieved by insertion of a SV40 T antigen gene in opposite transcriptional orientation in the IGH locus between the IGHD and IGHJ regions, in the presence (*IgH.TEμ*) or absence (*IgH.T*) of an extra copy of the Eμ enhancer[19]. Leukemic cells present in these mice displayed many characteristics that are also found in human CLL, in particular in U-CLL patients. At 6-9 months of age, most *IgH.TEμ* mice showed accumulation of a monoclonal $CD5^+IgM^+$ IgD^{low} B-cell population. IGHV sequence analysis revealed preferential usage of unmutated VH11.2 and non-stochastic usage of D and J genes, strikingly similar to those observed in *Eμ-TCL1* mice. Interestingly, unlike *Eμ-TCL1* mice, two $VHJ558^+$ leukemias from *IgH.TEμ* CLL mice manifested extensive SHM, thereby providing an animal model for both U-CLL and M-CLL and demonstrating that pathways activated by the SV40 T antigen play important roles in CLL pathogenesis. The HCDR3s of *IgH.TEμ* mice were enriched for serine/tyrosine residues and contained multiple charged amino acids that might confer CDR3 flexibility and favor poly-reactivity.

Furthermore, the *IgH.TEμ* CLL mouse model came up as the first mouse model to demonstrate the importance of the BCR downstream signaling molecule Bruton's tyrosine kinase (BTK) in CLL development. CLL formation was absent in BTK-deficient *IgH.TEμ* mice[21]. Conversely, transgenic overexpression of human BTK specifically in B cells under the control of the CD19 promoter (CD19-hBTK transgene) accelerated and increased CLL formation in *IgH.TEμ* mice. Increased CLL susceptibility of BTK-overexpressing B cells in *IgH.TEμ*. CD19-hBTK tumors was associated with frequent occurrence of CLL clones that expressed non-stereotypical BCRs. These BCR characteristics comprise of increased Igλ usage and the presence of long HCDR3 regions, frequently containing tyrosine stretches, thereby further substantiating the contribution of BTK-mediated BCR signaling to CLL development[21].

In conclusion, due to complete disease penetrance and phenotypic relatedness to CLL disease in humans, both *Eμ-TCL1* mice and *IgH.TEμ* mice provide useful pre-clinical models for understanding the pathogenesis of CLL. In this regard, the *Eμ-TCL1* mouse model has been extensively used in elucidating the functional role of specific molecules in the onset and progression of CLL *in vivo* in crosses of *Eμ-TCL1* mice with several transgenic and knockout mouse models[12].

AIM OF THIS THESIS

Several lines of evidence, as described above, indicate that important prognostic information for CLL resides in the BCR that is expressed. Moreover, the high response rates of small molecule inhibitors such as the BTK inhibitor ibrutinib, and the phosphatidyl-inositol-3-kinase δ-isoform (PI3Kδ) inhibitor idelalisib, in patients with CLL underline the importance of BCR signaling in the CLL pathogenesis. However, recent clinical studies have provided evidence that the therapeutic effect of various kinase inhibitors of the BCR signaling pathway, is also dependent on the role of these kinases in micro-environmental signaling. In this regard, T cell-mediated signals such as CD40L may be particularly important, because they were shown to promote proliferation of CLL cells in vitro[22]. In addition, CD40 stimulation in leukemic cells has the capacity to enhance their anti-apoptotic profile by upregulating anti-apoptotic proteins including Mcl-1, Bfl-1, and Bcl-XL and downregulating the pro-apoptotic protein Noxa[23-25]. These findings support the notion that CD40 signaling tips the balance between anti-apoptotic and pro-apoptotic proteins, which was shown to result in increased drug resistance[26,27]. In this thesis we describe studies that aim to unravel the role of B-cell intrinsic factors (such as BCR signaling) and extrinsic factors (such as signaling induced by CD40L, which is expressed on activated T cells) in the pathogenesis of the CLL.

In the current chapter (**Chapter 1**) we have introduced CLL diagnosis and prognosis, as well as two mouse models relevant for understanding CLL development and pathogenesis *in vivo*. In **Chapter 2**, we discuss the role of BTK in B-cell differentiation and B-cell malignancies and highlight the importance of BTK inhibition in cancer therapy. Additionally, we describe BTK functions in several myeloid cell populations that represent important components of the tumor microenvironment.

IGHV sequence analysis revealed preferential usage of stereotypical unmutated VH11.2 in approximately 35% CLL from *IgH.TEμ* mice. This suggests a role for antigenic stimulation in CLL development. Furthermore, Btk expression levels are critical for CLL development in *IgH.TEμ* mice. As described above, Btk-deficiency completely abrogated CLL development in *IgH.ET*μ mice[21]. Conversely, B cell-specific overexpression of Btk (CD19-hBTK) accelerated CLL and increased overall CLL incidence, thereby substantiating contribution of BTK-mediated BCR signaling in *IgH.TEμ* mice. In **Chapter 3**, we aimed to identify genomic pathways downstream of the BCR and/or Btk that play a role in early CLL incidence in *IgH.ETμ* mice. To this end we compared genome-wide RNA expression profiles of *IgH.ETμ* CLL cells with naïve wild-type splenic B cells or CD19-hBTK B cells, either unstimulated or following *in vitro* BCR stimulation by α-IgM antibodies. In addition, we also aimed to investigate the role of antigenic stimulation via T cell help (α-CD40/IL-4) in CLL development in *IgH.ETμ* mice. To this end, we compared our *IgH.ETμ* CLL cells with previously reported genome-wide expression data from unstimulated and α-CD40/IL4-stimulated follicular B-cells[28].

Mouse models, as described above, have provided important insights into the pathogenesis of several diseases including CLL. However, despite their proven usefulness as pre-clinical tools, transgenic mouse models take substantial time (>6 months) to develop CLL and are not suitable for large-scale screens of novel compounds or combination therapies. Therefore, in **Chapter 4** we aimed to obtain stable CLL cell lines from *IgH.TEμ* mice splenocytes (hereafter named EMC cells) by exploiting their constitutive active kinase signaling phenotype. In addition, we tested the potential of these EMC cell lines to serve as a platform for the investigation of CLL signal transduction as well as the *in vitro* and *in vivo* efficacy of small molecule inhibitors in CLL.

In addition to kinases, optimal activity of phosphatases downstream of the BCR is essential for B cell function and selection at various cellular differentiation checkpoints. Although the role of aberrant kinase activation for survival of CLL cells is well established[29], it is currently unclear how the activity of phosphatases is dysregulated in CLL. In **Chapter 5** we explored the expression of phosphatases in CLL and investigated the role of phosphatase signaling in the pathogenesis of CLL. In particular, we aimed to identify the involvement of the SH2-containing inositol phosphatases SHIP1 and SHIP2 in CLL pathogenesis. Also, we explored the therapeutic potential of small molecule inhibitors of the SHIP phosphatases in CLL.

In addition to B cell-intrinsic signaling pathways, CLL cells have been shown to exhibit a variable dependence on various components of tumor micro-environment including macrophages, T cells and stromal cells. Differences regarding antigenic reactivity have fueled several theories concerning the cellular origins of M-CLL and U-CLL. Marginal zone B-cells[30], post-germinal center (GC) memory B-cells[31], $CD5^+$ B-cells[32,33], and IL-10 expressing regulatory B-cells[34] have all been mentioned as the normal B cell counterpart from which CLL cells would derive. SHM status and genome-wide transcription profiling indicated that U-CLL and M-CLL are derived from $CD5^+CD27^-$ pre- and $CD5^+CD27^+$ post-germinal center (GC) B-cells, respectively[35,32]. However, direct *in vivo* evidence for such origin of CLL subgroups is not established. In **Chapter 6** we addressed the impact of antigenic pressure on BCR selection in CLL. To this end we analyzed the effects of defective T cell help and GC formation, as well as robust antigenic stimulation on the development and BCR repertoire of U-CLL in *IgH.TEμ* mice.

In addition to direct effects on CLL survival, the tumor microenvironment also affects the expression and reactivity of the BCR on CLL cells. This is evident from the characteristics of CLL cells derived from lymph nodes, including low surface IgM (sIgM) expression, elevated basal calcium (Ca^{2+}) signaling and unresponsiveness to BCR stimulation[36-38]. In these aspects, CLL cells resemble anergic B-cells. Such phenotype is reported for both U-CLL and M-CLL. However, to which extent U-CLL and M-CLL vary in their dependence on BCR and micro-environmental stimuli such as CD40L (via T helper cells or through stromal cells)[22] has not been fully elucidated. Furthermore, it remains unclear if the anergic phenotype of CLL cells, as characterized by reduced BCR responsiveness[39], also involves reduced responses to CD40 triggering. In **Chapter 7,** we used phospho-specific flow cytometry to study signaling properties of CLL cells, both in the BCR and the CD40 pathway.

Finally, in **Chapter 8** we summarize the various findings of our studies and discuss future research directions as well as clinical implications of our study results.

REFERENCES

1. DeSantis CE, Lin CC, Mariotto AB, Siegel RL, Stein KD, Kramer JL, *et al.* Cancer treatment and survivorship statistics, 2014. *CA Cancer J Clin* 2014 Jun 1.
2. Hallek M, Cheson BD, Catovsky D, Caligaris-Cappio F, Dighiero G, Dohner H, *et al.* iwCLL guidelines for diagnosis, indications for treatment, response assessment, and supportive management of CLL. *Blood* 2018 Jun 21; **131**(25)**:** 2745-2760.
3. Zenz T, Mertens D, Kuppers R, Dohner H, Stilgenbauer S. From pathogenesis to treatment of chronic lymphocytic leukaemia. *Nat Rev Cancer* 2010 Jan; **10**(1)**:** 37-50.
4. Puente XS, Pinyol M, Quesada V, Conde L, Ordonez GR, Villamor N, *et al.* Whole-genome sequencing identifies recurrent mutations in chronic lymphocytic leukaemia. *Nature* 2011 Jul 7; **475**(7354)**:** 101-105.
5. Quesada V, Conde L, Villamor N, Ordonez GR, Jares P, Bassaganyas L, *et al.* Exome sequencing identifies recurrent mutations of the splicing factor SF3B1 gene in chronic lymphocytic leukemia. *Nat Genet* 2012 Jan; **44**(1)**:** 47-52.
6. Landau DA, Carter SL, Stojanov P, McKenna A, Stevenson K, Lawrence MS, *et al.* Evolution and impact of subclonal mutations in chronic lymphocytic leukemia. *Cell* 2013 Feb 14; **152**(4)**:** 714-726.
7. Damle RN, Wasil T, Fais F, Ghiotto F, Valetto A, Allen SL, *et al.* Ig V gene mutation status and CD38 expression as novel prognostic indicators in chronic lymphocytic leukemia. *Blood* 1999 Sep 15; **94**(6)**:** 1840-1847.
8. Hamblin TJ, Davis Z, Gardiner A, Oscier DG, Stevenson FK. Unmutated Ig V(H) genes are associated with a more aggressive form of chronic lymphocytic leukemia. *Blood* 1999 Sep 15; **94**(6)**:** 1848-1854.
9. Agathangelidis A, Darzentas N, Hadzidimitriou A, Brochet X, Murray F, Yan XJ, *et al.* Stereotyped B-cell receptors in one-third of chronic lymphocytic leukemia: a molecular classification with implications for targeted therapies. *Blood* 2012 May 10; **119**(19)**:** 4467-4475.
10. Baliakas P, Agathangelidis A, Hadzidimitriou A, Sutton LA, Minga E, Tsanousa A, *et al.* Not all IGHV3-21 chronic lymphocytic leukemias are equal: prognostic considerations. *Blood* 2015 Jan 29; **125**(5)**:** 856-859.

11. Baliakas P, Hadzidimitriou A, Sutton LA, Minga E, Agathangelidis A, Nichelatti M*, et al.* Clinical effect of stereotyped B-cell receptor immunoglobulins in chronic lymphocytic leukaemia: a retrospective multi-centre study. *Lancet Haematol* 2014 Nov; **1**(2)**:** e74-84.
12. Simonetti G, Bertilaccio MT, Ghia P, Klein U. Mouse models in the study of chronic lymphocytic leukemia pathogenesis and therapy. *Blood* 2014 Aug 14; **124**(7)**:** 1010-1019.
13. Bichi R, Shinton SA, Martin ES, Koval A, Calin GA, Cesari R*, et al.* Human chronic lymphocytic leukemia modeled in mouse by targeted TCL1 expression. *Proc Natl Acad Sci U S A* 2002 May 14; **99**(10)**:** 6955-6960.
14. Yan XJ, Albesiano E, Zanesi N, Yancopoulos S, Sawyer A, Romano E*, et al.* B cell receptors in TCL1 transgenic mice resemble those of aggressive, treatment-resistant human chronic lymphocytic leukemia. *Proc Natl Acad Sci U S A* 2006 Aug 01; **103**(31)**:** 11713-11718.
15. Ponader S, Chen SS, Buggy JJ, Balakrishnan K, Gandhi V, Wierda WG*, et al.* The Bruton tyrosine kinase inhibitor PCI-32765 thwarts chronic lymphocytic leukemia cell survival and tissue homing in vitro and in vivo. *Blood* 2012 Feb 02; **119**(5)**:** 1182-1189.
16. Suljagic M, Longo PG, Bennardo S, Perlas E, Leone G, Laurenti L*, et al.* The Syk inhibitor fostamatinib disodium (R788) inhibits tumor growth in the Emu- TCL1 transgenic mouse model of CLL by blocking antigen-dependent B-cell receptor signaling. *Blood* 2010 Dec 02; **116**(23)**:** 4894-4905.
17. Byrd JC, Furman RR, Coutre SE, Flinn IW, Burger JA, Blum KA*, et al.* Targeting BTK with ibrutinib in relapsed chronic lymphocytic leukemia. *N Engl J Med* 2013 Jul 04; **369**(1)**:** 32-42.
18. Robak T, Robak P. BCR signaling in chronic lymphocytic leukemia and related inhibitors currently in clinical studies. *International reviews of immunology* 2013 Aug; **32**(4)**:** 358-376.
19. ter Brugge PJ, Ta VB, de Bruijn MJ, Keijzers G, Maas A, van Gent DC*, et al.* A mouse model for chronic lymphocytic leukemia based on expression of the SV40 large T antigen. *Blood* 2009 Jul 02; **114**(1)**:** 119-127.
20. Ahuja D, Saenz-Robles MT, Pipas JM. SV40 large T antigen targets multiple cellular pathways to elicit cellular transformation. *Oncogene* 2005 Nov 21; **24**(52)**:** 7729-7745.
21. Kil LP, de Bruijn MJ, van Hulst JA, Langerak AW, Yuvaraj S, Hendriks RW. Bruton's tyrosine kinase mediated signaling enhances leukemogenesis in a mouse model for chronic lymphocytic leukemia. *Am J Blood Res* 2013; **3**(1)**:** 71-83.
22. Coscia M, Pantaleoni F, Riganti C, Vitale C, Rigoni M, Peola S*, et al.* IGHV unmutated CLL B cells are more prone to spontaneous apoptosis and subject to environmental prosurvival signals than mutated CLL B cells. *Leukemia* 2011 May; **25**(5)**:** 828-837.
23. Smit LA, Hallaert DY, Spijker R, de Goeij B, Jaspers A, Kater AP*, et al.* Differential Noxa/Mcl-1 balance in peripheral versus lymph node chronic lymphocytic leukemia cells correlates with survival capacity. *Blood* 2007 Feb 15; **109**(4)**:** 1660-1668.
24. Willimott S, Baou M, Naresh K, Wagner SD. CD154 induces a switch in pro-survival Bcl-2 family members in chronic lymphocytic leukaemia. *Br J Haematol* 2007 Sep; **138**(6)**:** 721-732.
25. Kater AP, Evers LM, Remmerswaal EB, Jaspers A, Oosterwijk MF, van Lier RA*, et al.* CD40 stimulation of B-cell chronic lymphocytic leukaemia cells enhances the anti-apoptotic profile, but also Bid expression and cells remain susceptible to autologous cytotoxic T-lymphocyte attack. *Br J Haematol* 2004 Nov; **127**(4)**:** 404-415.
26. Tromp JM, Geest CR, Breij EC, Elias JA, van Laar J, Luijks DM*, et al.* Tipping the Noxa/Mcl-1 balance overcomes ABT-737 resistance in chronic lymphocytic leukemia. *Clin Cancer Res* 2012 Jan 15; **18**(2)**:** 487-498.
27. Hallaert DY, Jaspers A, van Noesel CJ, van Oers MH, Kater AP, Eldering E. c-Abl kinase inhibitors overcome CD40-mediated drug resistance in CLL: implications for therapeutic targeting of chemoresistant niches. *Blood* 2008 Dec 15; **112**(13)**:** 5141-5149.
28. Wohner M, Tagoh H, Bilic I, Jaritz M, Poliakova DK, Fischer M*, et al.* Molecular functions of the transcription factors E2A and E2-2 in controlling germinal center B cell and plasma cell development. *J Exp Med* 2016 Jun 27; **213**(7)**:** 1201-1221.
29. Pal Singh S, Dammeijer F, Hendriks RW. Role of Bruton's tyrosine kinase in B cells and malignancies. *Mol Cancer* 2018 Feb 19; **17**(1)**:** 57.
30. Chiorazzi N, Ferrarini M. Cellular origin(s) of chronic lymphocytic leukemia: cautionary notes and additional considerations and possibilities. *Blood* 2011 Feb 10; **117**(6)**:** 1781-1791.
31. Klein U, Tu Y, Stolovitzky GA, Mattioli M, Cattoretti G, Husson H*, et al.* Gene expression profiling of B cell chronic lymphocytic leukemia reveals a homogeneous phenotype related to memory B cells. *J Exp Med* 2001 Dec 3; **194**(11)**:** 1625-1638.
32. Seifert M, Sellmann L, Bloehdorn J, Wein F, Stilgenbauer S, Durig J*, et al.* Cellular origin and pathophysiology of chronic lymphocytic leukemia. *J Exp Med* 2012 Nov 19; **209**(12)**:** 2183-2198.
33. Griffin DO, Holodick NE, Rothstein TL. Human B1 cells in umbilical cord and adult peripheral blood express the novel phenotype CD20+ CD27+ CD43+ CD70. *J Exp Med* 2011 Jan 17; **208**(1)**:** 67-80.
34. DiLillo DJ, Weinberg JB, Yoshizaki A, Horikawa M, Bryant JM, Iwata Y*, et al.* Chronic lymphocytic leukemia and regulatory B cells share IL-10 competence and immunosuppressive function. *Leukemia* 2013 Jan; **27**(1)**:** 170-182.
35. Garcia-Munoz R, Galiacho VR, Llorente L. Immunological aspects in chronic lymphocytic leukemia (CLL) development. *Ann Hematol* 2012 Jul; **91**(7)**:** 981-996.
36. Mockridge CI, Potter KN, Wheatley I, Neville LA, Packham G, Stevenson FK. Reversible anergy of sIgM-mediated signaling in the two subsets of CLL defined by VH-gene mutational status. *Blood* 2007 May 15; **109**(10)**:** 4424-4431.
37. Singh SP, Pillai SY, de Bruijn MJW, Stadhouders R, Corneth OBJ, van den Ham HJ*, et al.* Cell lines generated from a chronic lymphocytic leukemia mouse model exhibit constitutive Btk and Akt signaling. *Oncotarget* 2017 Sep 22; **8**(42)**:** 71981-71995.
38. Duhren-von Minden M, Ubelhart R, Schneider D, Wossning T, Bach MP, Buchner M*, et al.* Chronic lymphocytic leukaemia is driven by antigen-independent cell-autonomous signalling. *Nature* 2012 Sep 13; **489**(7415)**:** 309-312.

39. Muzio M, Apollonio B, Scielzo C, Frenquelli M, Vandoni I, Boussiotis V, *et al.* Constitutive activation of distinct BCR-signaling pathways in a subset of CLL patients: a molecular signature of anergy. *Blood* 2008 Jul 01; **112**(1)**:** 188-195.

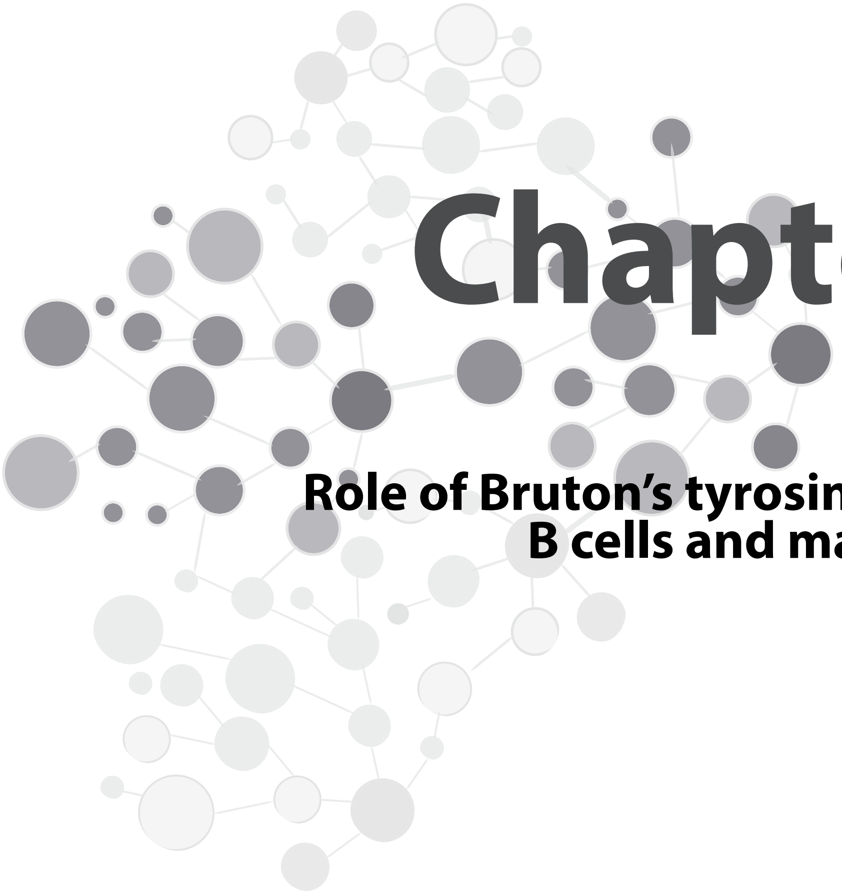

Chapter 2

Role of Bruton's tyrosine kinase in B cells and malignancies

Simar Pal Singh[1,2,3], Floris Dammeijer[1,3,4] and Rudi W. Hendriks[1]

[1]Department of Pulmonary Medicine,
[2]Department of Immunology,
[3]Post graduate school Molecular Medicine,
[4]Erasmus MC Cancer Institute, Erasmus Medical Center, Rotterdam, The Netherlands

Molecular Cancer, Volume 17, Article 57, 2018

ABSTRACT

Bruton's tyrosine kinase (BTK) is a non-receptor kinase that plays a crucial role in oncogenic signaling that is critical for proliferation and survival of leukemic cells in many B cell malignancies. BTK was initially shown to be defective in the primary immunodeficiency X-linked agammaglobulinemia (XLA) and is essential both for B cell development and function of mature B cells. Shortly after its discovery, BTK was placed in the signal transduction pathway downstream of the B cell antigen receptor (BCR). More recently, small-molecule inhibitors of this kinase have shown excellent anti-tumor activity, first in animal models and subsequently in clinical studies. In particular, the orally administered irreversible BTK inhibitor ibrutinib is associated with high response rates in patients with relapsed/refractory chronic lymphocytic leukemia (CLL) and mantle-cell lymphoma (MCL), including patients with high-risk genetic lesions. Because ibrutinib is generally well tolerated and shows durable single-agent efficacy, it was rapidly approved for first-line treatment of patients with CLL in 2016. To date, evidence is accumulating for efficacy of ibrutinib in various other B cell malignancies. BTK inhibition has molecular effects beyond its classic role in BCR signaling. These involve B cell-intrinsic signaling pathways central to cellular survival, proliferation or retention in supportive lymphoid niches. Moreover, BTK functions in several myeloid cell populations representing important components of the tumor microenvironment. As a result, there is currently a considerable interest in BTK inhibition as an anti-cancer therapy, not only in B cell malignancies but also in solid tumors. Efficacy of BTK inhibition as a single agent therapy is strong, but resistance may develop, fueling the development of combination therapies that improve clinical responses. In this review, we discuss the role of BTK in B cell differentiation and B cell malignancies and highlight the importance of BTK inhibition in cancer therapy.

Key words: B cell development, B cell receptor signaling, Bruton's tyrosine kinase, chemokine receptor, chronic lymphocytic leukemia, ibrutinib, leukemia, lymphoma, tumor microenvironment.

INTRODUCTION

Protein kinases represent classes of enzymes that catalyze phosphorylation of proteins and thereby alter their substrate's activity or capacity to interact with other proteins. Kinase signaling pathways represent the most common form of reversible post-translational modifications that control many aspects of cellular function. Aberrant activation of protein kinases drive major hallmarks of malignancies, including alterations in cellular proliferation, survival, motility and metabolism, as well as angiogenesis and evasion of the anti-tumor immune response[1,2].

One such kinase that plays a crucial role in oncogenic signaling is Bruton's tyrosine kinase (BTK), which is critical for the survival of leukemic cells in various B cell malignancies. BTK was initially shown to be mutated in the primary immunodeficiency X-linked agammaglobulinemia (XLA) and is essential at various stages of B lymphocyte development[3,4]. XLA is an inherited immunodeficiency disease originally described by the pediatrician Ogdon Bruton in 1952 and characterized by recurrent bacterial infections. Due to a severe block of B cell development in the bone marrow, XLA patients have very low numbers of B cells in the circulation and antibodies are almost completely absent in the serum. A milder phenotype of the disease is present in CBA/N mice, which harbor the loss-of-function mutation R28C BTK[5,6]. These mice, known as *xid* (X-linked immunodeficiency) mice, manifest only minor defects in B cell development in the bone marrow, but instead the differentiation and survival of mature peripheral B cells is severely impaired[7-10]. Importantly, BTK has received large interest since small-molecule inhibitors of this kinase have shown excellent anti-tumor activity in clinical studies[11,12]. In particular, the orally administered BTK inhibitor ibrutinib, which forms a covalent bond with a cysteine residue in the BTK active site, was also approved for first-line treatment of patients with chronic lymphocytic leukemia (CLL) and small lymphocytic leukemia (SLL) in 2016[13].

Shortly after its discovery as the non-receptor tyrosine kinase defective in XLA[3,4], BTK was placed in the signal transduction pathway downstream of the B cell receptor (BCR). This receptor is expressed on the B cell surface and has the unique capacity to specifically recognize antigens due to hypervariable regions present in the immunoglobulin heavy (IGH) and light (IGL) chains that together form the BCR[14]. BTK is also involved in many other signaling pathways in B cells, including chemokine receptor, Toll-like receptor (TLR) and Fc receptor signaling. Expression of BTK is not restricted to B cells, as also cells of the myeloid lineage express BTK. In these cells, BTK acts also downstream of TLRs and e.g. the FcεR in mast cells[15,16] and the FcγRI in macrophages[17,18]. In addition, BTK is involved in various other pathways, including Receptor activator of nuclear factor-κB (RANK) in osteoclasts[19], collagen and CD32 signaling in platelets[20] and the NLRP3 inflammasome in macrophages and neutrophils[21]. Since myeloid cells are important components of the tumor microenvironment and particularly tumor-associated macrophages contribute to cancer progression[22,23], there is currently a considerable interest in BTK inhibition as an anti-cancer therapy not only in B cell leukemias but also in other hematological malignancies and solid tumors[24-27].

In this review, we describe the importance of BTK in multiple signaling pathways. We discuss the crucial function of BTK in different stages of normal B cell development. In addition, we discuss its role in oncogenic signaling in B cell malignancies associated with genetic events that result in increased BTK activity. We describe clinical benefits of targeting BTK with small molecule inhibitors in B cell malignancies. Finally, we discuss the effects of BTK inhibitors on tumor growth in solid malignancies in the context of the function of myeloid cells in the tumor environment.

BTK structure

BTK is one of the five members of the TEC family of non-receptor tyrosine kinases - along with tyrosine kinase expressed in hepatocellular carcinoma (TEC), interleukin-2-inducible T cell kinase (ITK), resting lymphocyte kinase (RLK) and bone marrow expressed kinase (BMX) - which are strongly conserved throughout evolution[28]. BTK, TEC and ITK are most similar and both contain five different protein interaction domains **(Figure 1A)**. These domains include an amino terminal pleckstrin homology (PH) domain, a proline-rich TEC homology (TH) domain, SRC homology (SH) domains SH2 and SH3, as well as kinase domain with enzymatic activity[28,29]. BTK is essentially cytoplasmic and is only transiently recruited to the membrane through interaction of its PH domain with phosphatidylinositol-3,4,5-triphosphate (PIP$_3$), which is generated by phosphatidylinositol-3 kinase (PI3K) **(Figure 1B)**[14]. BTK activation occurs in two steps upon its recruitment to the cell membrane. First, BTK is phosphorylated at position Y551 in the kinase domain by SYK or SRC family kinases[30]. Phosphorylation of BTK at Y551 promotes its catalytic activity and subsequently results in its autophosphorylation at position Y223 in the SH3 domain[31]. Phosphorylation at Y223 is thought to stabilize the active conformation and fully activate BTK kinase activity[32]. Nevertheless, a Y223F mutation did not significantly affect the function of BTK during B cell development *in vivo*, since B-cell specific transgenic expression of Y223F-BTK could still rescue the *xid* phenotype of Btk-deficient mice[33]. Therefore, the function of the Y223 BTK autophosphorylation site remains unclear in B cells and to date is unexplored *in vivo* in myeloid cells.

BTK in B cell receptor signaling

The IgM BCR is essential for survival of peripheral B cells[34]. In the absence of BTK B cells have a high rate of apoptosis, which correlates with strongly reduced BCR-mediated induction of the anti-apoptotic protein Bcl-xL[35,36]. Upon stimulation with anti-IgM, cell size enlargement and degradation of the cyclin inhibitor p27Kip1 occurs normally, indicating that BTK is not essential for several G1 events[37]. BTK-deficient B cells enter early G1, but not S phase of the cell cycle, because they fail to induce cyclin D2 expression[38]. Apart from B cell survival and proliferation, the BCR controls integrin α4β1 (VLA-4)-mediated adhesion of B cells to vascular cell adhesion molecule-1 (VCAM-1) and fibronectin via BTK[39].

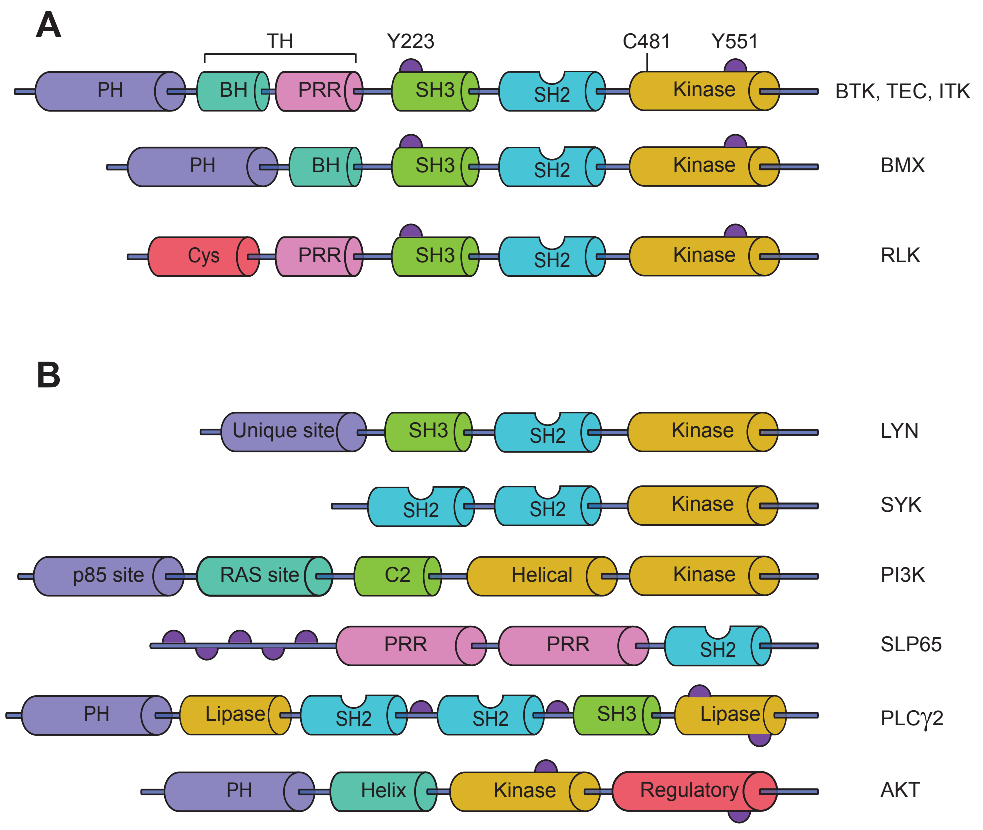

Figure 1. Domain structure of TEC kinase family members and key interacting partners of Bruton's tyrosine kinase.
(A) Schematic overview of the protein structure of BTK and other TEC kinase family members. Shown are five different domains, as explained in text, the Y223 autophosphorylation site, the Y551 phosphorylation site that activates BTK, and the C481 binding site of ibrutinib. (B) Schematic overview of the protein structure of key interacting partners of BTK. PH, pleckstrin homology; TH, TEC homology; BH, BTK homology; PRR, proline rich domain; SH2/SH3, SRC homology domains 2 and 3; Cys, cysteine-string motif.

BCR cross-linking activates four families of non-receptor protein tyrosine kinases and these are transducers of signaling events including phospholipase Cγ (PLCγ), mitogen-activated protein kinase (MAPK) activation, nuclear factor kappa-light-chain-enhancer of activated B cells (NF-κB) pathway components and activation of the serine/threonine kinase AKT (or protein kinase B, PKB).

The IgM BCR has a very short cytoplasmic domain and thus cannot signal directly, but associates with the disulphide-linked Ig-α/Ig-β(CD79a/CD79b) heterodimers. These transmembrane proteins contain immunoreceptor tyrosine based activation motifs (ITAMs) in their cytoplasmic domain **(Figure 2)**. BCR engagement by antigen induces ITAM phosphorylation by Src-family protein tyrosine kinases such as LYN, thereby creating docking sites for spleen tyrosine kinase (SYK)**(Figure 1B)**[40]. In addition, LYN and SYK also phosphorylate tyrosine residues in the cytoplasmic tail of the B-cell co-receptor CD19 and/or the adaptor protein B-cell PI3K adaptor (BCAP), which facilitates recruitment and activation of PI3K and the guanine nucleotide exchange factor VAV[41,42]. VAV further enhances enzymatic activity of PI3K through activation of RAC1, a member of Rho family of GTPases[43]. PI3K phosphorylates PIP2 to generate PIP3, which acts as a critical secondary messenger for activating downstream pathways. PIP3 interacts with the BTK PH-domain, resulting in its recruitment to the plasma membrane[44].

In addition, Ig-α contains a conserved non-ITAM tyrosine residue, Y204, that upon activation by SYK recruits and phosphorylates the central B cell-linker molecule SH2-domain-containing leukocyte protein of 65kDa (SLP65/BLNK)[45]**(Figure 2)**. Hereby, the adaptor molecule Cbl-interacting protein of 85 kD (CIN85) functions to oligomerize SLP65 and assembles intracellular signaling clusters for B cell activation[46]. SLP65 serves as a scaffold for various signaling molecules, including BTK and its substrate PLCγ2[47-50]. In this micro-signalosome BTK is activated through Y551 phosphorylation by SYK or LYN and subsequently at Y223, as described above[30-32]. Fully activated BTK phosphorylates PLCγ2 at Y753 and Y759, which is important for its lipase activity[51]. Activated PLCγ2 hydrolyses PIP2 into inositol triphosphate (IP3) and diacylglycerol (DAG). IP3 regulates intracellular calcium levels and thereby activates nuclear factor of activated T cells (NFAT) transcription, via calcineurin and calmodulin. DAG mediates activation of protein kinase Cβ (PKCβ), which induces activation of several members of the MAPK family, including extracellular signal-regulated kinases 1 and 2 (ERK1/ERK2) and other MAPK targets, such as Jun N-terminal kinase (JNK), p38, and NF-κB pathway components[52]**(Figure 2)**. Hereby, BTK links the BCR to NF-κB activation[53,54].

Another important branching point is induced more upstream in the BCR signaling cascade: in addition to BTK, PIP3 also interacts with PH-domain of AKT, resulting in its recruitment to the plasma membrane. Full activation of AKT requires phosphorylation at position T308, induced by 3-phosphoinositide-dependent protein kinase-1 (PDK1), and at S473, phosphorylated by mechanistic target of rapamycin (mTOR) complex 2 (See Ref[55] for an excellent review). Fully activated AKT then returns to the cytoplasm to enable a pro-survival signaling program that involves NFAT, forkhead transcription factors (FOXOs) and NF-κB-mediated pathways. Importantly, phosphorylation of AKT is positively regulated by BTK[56]. The BTK family member TEC, which can partly compensate for BTK[57], may on the other hand limit the capacity of BTK to activate AKT[58].

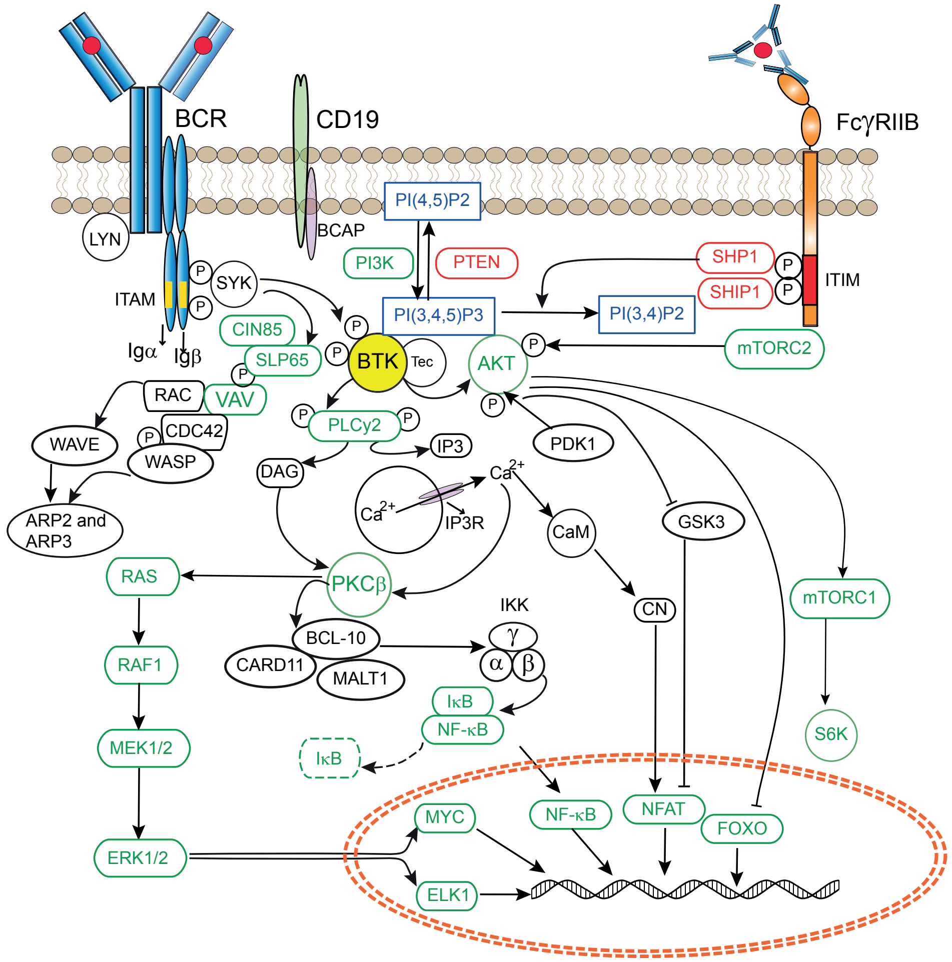

Figure 2. Role of Bruton's tyrosine kinase downstream of the B cell receptor.
Signaling cascade showing important events downstream of B cell receptor (BCR). Antigen engagement by the BCR results in the formation of a micro-signalosome whereby BTK activates four families of non-receptor protein tyrosine kinases that transduce key signaling events including phospholipase Cγ, mitogen-activated protein kinase (MAPK) activation, nuclear factor kappa-light-chain-enhancer of activated B cells (NF-κB) pathway components and activation of the serine/threonine kinase AKT (PKB). In addition, BTK mediated signaling events are regulated by various phosphatases that can be recruited to the cell membrane, following crosslinking of inhibitory receptors, e.g., FcγRIIB that is exclusively expressed on B cells and signals upon immune complex binding. See text for details.

Upon activation in germinal centers (GCs), B cells can perform IGH chain class switching, by which it changes Ig expression from one isotype to another with different effector function, e.g. from IgM to IgG. In this process, the IGH constant (C) region is changed, but the variable (V) region remains the same. Interestingly, in contrast to IgM, the IgG BCR contains a cytoplasmic domain of considerable length with an Ig tail tyrosine (ITT) motif, which amplifies signaling [59]. SYK is required for ITT phosphorylation followed by recruitment of BTK through the adapter protein Grb2, leading to enhancement of IgG BCR-induced calcium mobilization. This amplification loop is thought to represent a cell-intrinsic mechanism for rapid activation of class-switched memory B cells.

Regulation of BTK activity and expression

Consistent with its crucial role in B cell differentiation, proliferation and survival, proper control of BTK activity is important for B cell homeostasis. Several mechanisms for its regulation have been identified to date.

The recruitment of BTK to the plasma membrane and its subsequent activation is regulated by various phosphatases that can be recruited to the cell membrane, similar to BTK. For example, the FcγRIIB is an inhibitory receptor that is exclusively expressed on B cells[60]. In contrast to the Igα/Ig-β ITAM motifs, FcγRIIB has immune tyrosine inhibitory motifs (ITIMs) in its cytoplasmic domain[61,62] **(Figure 2)**. The binding of IgG antibodies to FcγRIIB results in LYN-mediated phosphorylation of ITIMs and recruitment of protein phosphatases such as SH2-domain containing inositol polyphosphate 5'phosphatase-1 (SHIP1) [63-65]. SHIP1 catalyzes the dephosphorylation of PIP3 and thereby inhibits recruitment of PH-domain containing proteins, such as BTK and PLCγ2 to the cell membrane. As a result, the downstream increase in intracellular calcium levels is diminished. Another phosphatase, SH2 domain containing protein tyrosine phosphatase-1 (SHP1), has the capacity to dephosphorylate tyrosine on BTK[65]. SHP1 acts downstream of CD22, a lectin molecule, and the glycoprotein CD5, both of which are on the B cell surface and function as negative regulators of BCR signaling.

In addition, several negative regulators of BTK have been identified. The iBTK protein directly binds to the BTK PH domain and thereby inhibits its activity[66]; PKCβ phosphorylates BTK on residue S180 in TH domain, modulating its membrane localization[67]; microRNA-185 reduces BTK mRNA levels and thereby downregulates BTK expression[68]. Likewise, expression of other microRNAs, including miR-210 and miR-425, significantly reduce BTK expression[69]. In this context, it was shown that treatment of primary CLL samples with histone deacetylase (HDAC) inhibitors resulted in increased expression of these miRs and decreased BTK protein. On the other hand, BTK itself can initiate a proteasome-dependent positive autoregulatory feedback loop by stimulating transcription from its own promoter through a pathway involving NF-κB[70].

BTK in other signaling pathways

Chemokine receptors. These receptors are G-protein coupled receptors that consist of seven transmembrane spanning domains and intracellular hetero-trimeric G-proteins composed of α, β, and γ subunits (Gα, Gβ, and Gγ)[71]. The chemokine receptors CXCR4 and CXCR5 are expressed on B cells in different stages of their development and play important roles in trafficking, homing and homeostasis[72]. Chemokine binding to the extracellular domain of its receptor induces conformational changes that result in dissociation of Gα and Gβγ subunits **(Figure 3A)**. Both Gα and Gβγ subunits can independently activate PI3K, which results in activation of BTK, AKT and MAPK dependent pathways[73,74]. In addition, both Gα and Gβγ subunits can directly bind BTK via the PH and TH domain[74,75]. It has been shown that the Gα subunit directly stimulates the activity of BTK[76]. Due to its function downstream of chemokine receptors including CXCR4 and CXCR5, BTK is important for positioning of B cells in various lymphoid tissue compartments. This was first demonstrated by adoptive transfer experiments with BTK-deficient B cells, which exhibited impaired *in vivo* migration and homing to lymph nodes[77].

Toll-like receptors (TLRs). These extracellular or intracellular pattern recognition receptors are characterized by leucine-rich repeats and Toll/interleukin-1 receptor (TIR) domains **(Figure 3B)**. TLRs, expressed in B cells or myeloid cells, recognize structurally

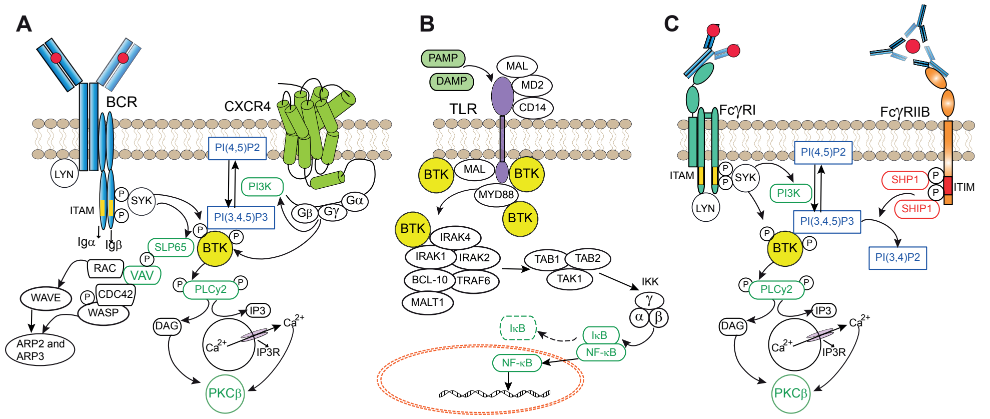

Figure 3. Role of Bruton's tyrosine kinase downstream of chemokine receptors, Toll-like receptors and activating Fcγ receptors.
Signaling cascade showing important events downstream of (A) Chemokine receptors (e.g. CXCR4): upon chemokine binding to the extracellular domain Gα and Gβγ subunits can independently activate PI3K, which results in activation of BTK, AKT and MAPK-dependent pathways. (B) Toll-like receptors: upon ligand recognition TLRs recruit different proteins including TIR, MYD88, IRAK1 and TIRAP/MAL, all of which interact with BTK and induce downstream activation of the transcription factor NF-κB. (C) Activating Fc receptors (e.g. FcγRI): Following FcγRI cross-linking, Src-kinases, SYK, PI3K-γ and BTK are activated. In contrast, inhibitory Fc-receptors (FcγRIIB) containing ITIM domains recruit phosphatases and reduce BTK activation (Figure 2). See text for details.

conserved molecules derived from bacteria and viruses. Upon activation most TLRs recruit the adaptor myeloid differentiation primary response 88 (MYD88)[78]. MYD88 activates interleukin-1 receptor-associated kinase1 (IRAK1), either on its own or in combination with an adaptor molecule, TIR domain containing adaptor protein (TIRAP, also known as MyD88 adapter-like (MAL)). BTK interacts with four different proteins downstream of TLR signaling including TIR, MYD88, IRAK1 and TIRAP/MAL[79-81]. TLR signaling induces transcription factors including NF-κB, activator protein-1 (AP-1) and interferon regulatory factor 3 (IRF3), which results in activation, proliferation, antibody secretion, class switch recombination and pro-inflammatory cytokine production in B cells.

Fc Receptor signaling. BTK is involved in signaling of both activating (ITAM-containing) and inhibitory (ITIM-containing) Fc-receptors, whose balance regulates several myeloid cell processes including activation, polarization and phagocytosis **(Figure 3C)**[60,82]. BTK is rapidly activated upon FcεRI cross-linking in mast cells[15]. In parallel to BCR signaling, following activating Fc-receptor cross-linking, SRC-kinases, SYK, PI3K-γ and BTK are activated[60]. In contrast, inhibitory Fc-receptors (FcγRIIB) containing ITIM domains recruit phosphatases and reduce BTK activation (see above).

BTK and B cell development in the bone marrow

Even before the gene involved in XLA was identified, X-chromosome inactivation studies showed that the defect in XLA patients was intrinsic to the B cell lineage and that myeloid cells had no developmental defects [83,84]. B cells are generated from hematopoietic stem cells in the bone marrow throughout life by the ordered rearrangement of IGH and IGL chain gene segments (**Figure 4**). After productive recombination of the IGH V, D and J genes, the IGH μ protein is expressed on the cell surface in association with the two invariant surrogate light chain (SLC) proteins VpreB and λ5[85,86],as the pre-BCR. Pre-BCR signaling marks a crucial checkpoint (*checkpoint 1*) to test the functionality of the IGH μ protein (**Figure 4**)[87,88]. To date, the mechanisms that initiate pre-BCR-mediated signaling are not fully resolved as both cell-autonomous and ligand-mediated signaling has been described[89-92]. An important function of pre-BCR signaling is to inhibit further IGH VDJ recombination, a phenomenon known as allelic exclusion[88]. Pre-BCR signaling leads to proliferation of pre-B cells and at the same time downregulation of SLC expression[88]. This is important for the exit of pre-B cells from the cell cycle to undergo the transition from large, cycling cells into small resting pre-B cells, in which IGL chain recombination occurs. In XLA patients B cell development is almost completely arrested at the pre-B cell stage. Although pre-B cells expressing intracellular IGH μ are present, they are small in size, indicating that BTK is essential for pre-BCR-dependent proliferation. BTK-deficient mice have only a mild pre-B cell defect, whereby pre-B cells show impaired developmental progression into immature B-cells[9,10]. Nevertheless, an almost complete block is only found in mice that are double-deficient for e.g. BTK and SLP65 or BTK and TEC[57,93,94]. Interestingly SLP65-deficient mice, which also have a mild arrest at the pre-B cell stage, develop pre-B cell leukemia resembling pre-B ALL in humans[93,94]. In this regard, BTK cooperates with SLP65 as a tumor suppressor independent of its kinase activity[95,96]. SLP65 also mediates downregulation of SLC expression[97]. Analyses in wild-type, BTK and SLP65 deficient pre-B cells demonstrated that pre-BCR signaling induces *IGL* κ locus accessibility by functional redistribution of enhancer-mediated chromatin interactions[98]. BTK and SLP65 are important for the induction of *IGL* chain germ-line transcripts that are associated with locus accessibility. Moreover, BTK-deficient mice exhibit a ~50% reduction of *IGL* κ chain usage[98,99]. Transcriptome analyses showed that BTK/SLP65deficient pre-B cells fail to efficiently upregulate many genes involved in *IGL* chain recombination, including *Aiolos, Ikaros, Spib, Irf4, Oct2, polymerase-μ, and Mbp-1*[98].

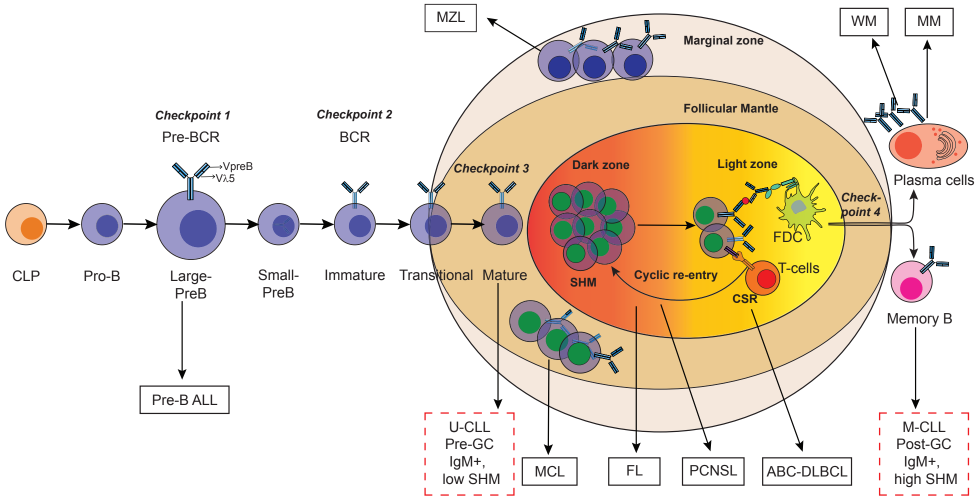

Figure 4. Stages of B cell development and associated malignancies.
Model of B cell development indicating different stages of B cell development and important immune checkpoints where BTK plays a key role. Various B-cell malignancies are indicated, which are associated with abnormal BTK signaling at distinct stages of B-cell development. Note that the cellular origin of U-CLL is still under debate. Somatic hypermutation status of BCR and gene expression profiling indicates pre- and post- germinal center (GC) origin of U-CLL and M-CLL, respectively. See text for detailed information. CLP, common lymphoid progenitor; CSR, class switch recombination; FDC, follicular dendritic cell; SHM, somatic hypermutation.

If *IGL* chain recombination is not productive or the resulting BCR is autoreactive (*checkpoint 2*)(**Figure 4**), developing B cells will undergo secondary *IGL* chain rearrangements, a process termed receptor editing[100-102]. Many autoreactive B cells are lost during development to the immature IgM^{+} B cell stage (central B cell tolerance), but it has been estimated that ~40% of the newly formed B cells that leave the bone marrow have self-reactivity[92].

BTK and peripheral B cell development and activation

Immature B cells from the bone marrow migrate to the spleen, where selection and maturation is continued within the transitional B cell compartment containing T1 and T2 B cells. In mice, T1 B cells, but not T2 B cells, are very sensitive to BCR-mediated apoptosis, indicating that the T1 to T2 differentiation marks a peripheral tolerance checkpoint (*checkpoint 3*)[103,104]. In the absence of BTK, T2 cells do not generate survival responses and peripheral B cells are reduced by ~50%. As a result, BTK-deficient B cells exhibit an impaired transition from $\mathrm{IgM^{high}IgD^{low}}$ into $\mathrm{IgM^{low}IgD^{high}}$ mature B cells. BTK-deficient mice lack the population of innate-like $\mathrm{CD5^+}$ B-1 cells, present in the peritoneal and pleural cavities and in small proportions in the spleen[7-9]. Consistent with the finding that these cells are important for IgM and IgG3 levels in the serum, in BTK-deficient mice IgM and IgG3 levels in serum are severely reduced, but the other isotypes are largely normal.

Marginal zone B cells are present in an area at the outermost portion of the white pulp in the spleen and are phenotypically defined as $\mathrm{IgM^{hi}IgD^{lo}CD21^{high}CD23^{low}}$ B cells that respond to polysaccharide antigens independently of T cell help (**Figure 4**). BCR and NOTCH2 signaling determine whether T1 B cells expressing surface ADAM10 are committed to becoming MZ B cells *in vivo* in the spleen[105,106] . Although contradictory findings on the numbers of MZ B cells in BTK-deficient mice have been reported, it is clear that developing BTK-deficient MZ B cells have a selective disadvantage[107,108].

Upon antigen recognition, activated B cells may either go into an extrafollicular response or develop into GC B cells[109,110]. In the GCs B cells strongly proliferate and undergo somatic hypermutation (SHM) induced by activation induced cytidine deaminase (AID). GC B cells are selected involving follicular dendritic cells (FDCs) and T-follicular helper ($\mathrm{T_{FH}}$) cells (*checkpoint 4*) based on their antigen affinity[109]. Although BTK-deficient mice show normal T-cell dependent responses to model antigens, such as TNP-KLH[7,8], there is a significant reduction in GC B cell numbers in physiological models, e.g. influenza virus infection [108]. In this context, it is of note that mice expressing the constitutively active BTK mutant E41K fail to form GCs[111,112], whereas overexpression of wild-type BTK induces spontaneous GC formation [113,114]. Consequently, BTK-overexpressing mice develop autoimmunity involving B cell-induced disruption of T cell homeostasis[113,114].

BTK in B cell malignancies

BTK activity is crucial for survival and proliferation of leukemic B cells and for their interactions with cells in the tumor microenvironment. Below, we discuss the role of BTK in various B cell malignancies (**Figure 4**).

CLL. This is the most common leukemia in the western world, primarily affecting the elderly, and is characterized by the accumulation of mature circulating $\mathrm{IgM^{low}}$ $\mathrm{CD5^+}$ B cells[115]. Several genetic aberrations with prognostic value and impact on treatment decisions in CLL have been described. These include deletions of the chromosomal regions 17p13 (containing the *TP53* tumor suppressor gene), 11q23 (containing DNA damage checkpoint protein *ATM*), or 13q14 (miR-15a, miR-16-1), and trisomy of chromosome 12[116,117]. Furthermore, >80 % of cases harboring del(17p) also carry *TP53* mutations in the remaining allele[118]. Such patients with *TP53* defects are classified as 'high-risk' and often respond poorly to therapy[119]. Moreover, a significant proportion of CLL patients carry a TP53 mutation in the absence of a 17p deletion [120,121].

On the basis of SHM status of IGHV, CLL can be grouped into mutated CLL (M-CLL) and unmutated CLL (U-CLL). M-CLL have a more favorable prognosis and are derived from post-GC B cells. The origin of U-CLL appeared less clear and several cellular origins of CLL were suggested, including MZ B cells, $\mathrm{CD5^+}$ B cells, and regulatory B cells[122-126]. Although initial gene expression profiling indicated that M-CLL and U-CLL were quite homogeneous and related to memory B cells derived from T cell-dependent and T-cell independent responses, respectively[123], more recent gene expression profiling studies have provided evidence for a different origin [124]. This study by Seifert et al. shows that U-CLL derives from unmutated mature $\mathrm{CD5^+}$ B cells. Moreover, it was concluded that M-CLL originate from a distinct and previously unrecognized post-GC B cell subset with a CD5+CD27+ surface phenotype

Several lines of evidence establish a role of chronic BCR-mediated signaling in CLL pathogenesis[127]. (i) Prognosis is correlated with the BCR SHM status[128]; (ii) The BCR repertoire is highly restricted [129,130], suggesting a role for antigenic selection in the initiation or progression of CLL. Antigens binding to CLL BCRs include self-antigens, such as non-muscle myosin IIA, vimentin, apoptotic cells and oxidized low-density lipoprotein[131-136], as well as foreign antigens (bacterial polysaccharides and β-(1,6)-glucan, a major antigenic determinant on fungi [132-137]); Interestingly, evidence was provided in mice that pathogens may drive CLL pathogenesis by selecting and expanding pathogen-specific B cells that cross-react with self-antigens[138]; (iii) CLL cells were reported to display cell-autonomous $\mathrm{Ca^{2+}}$ mobilization in the absence of exogenous ligands, by virtue of recognizing a single conserved BCR-internal epitope in the IGHV second framework region[139]; very recently, it was found that the internal epitopes recognized by CLL BCRs from distinct subgroups are different[140]. Moreover, the avidity of the BCR-BCR interactions that can lead to receptor declustering influences the clinical course of the disease[139,140].

In line with chronic BCR-mediated signaling, CLL cells show constitutive activation of various BCR pathway associated kinases. Hereby, BTK is essential for constitutively active pathways implicated in CLL cell survival, including AKT, ERK and NF-κB, both in patient cells and mouse models[133,141-143]. CLL cells are thought to interact with the tissue microenvironment and lymph node resident CLL cells show gene expression signatures indicative of BCR activation[144,145]. Moreover, BTK is critical for BCR- and chemokine-controlled integrin-mediated retention and/or homing of CLL B cells in their microenvironment[146].

Mantle cell Lymphoma (MCL). This disease results from malignant transformation of B lymphocytes in the mantle zones surrounding GCs (**Figure 4**) and has a remarkably biased BCR repertoire[147]. Approximately 85% of the patients harbor the hallmark chromosomal translocation t(11:14)(q13;32). This event juxtaposes the *CCND1* gene to an enhancer in the Ig heavy chain locus[148], resulting in constitutively cyclin-D1 expression and abnormal proliferation. In a fraction of MCL patients lymphoma cells express the SOX11 transcription factor, which is associated with minimal Ig SHM, higher genetic instability and a more aggressive clinical course[149,150]. Primary MCL cells show strong expression and Y223-phosphoryation of BTK[151] and in a subset of patients constitutive phosphorylation of LYN, SLP65, SYK and PKCβ[152,153]. Similar to CLL, the tumor microenvironment plays an important role in MCL pathogenesis. BTK is essential for retention of MCL cells in lymphoid tissues, since BTK inhibition induces an egress of malignant cells into peripheral blood[154].

Waldenström's Macroglobulinemia (WM). This indolent B-cell malignancy is characterized by IgM-secreting lymphoma cells in the bone marrow. The majority of WM patients have a somatic leucine to proline substitution at position 265 of MyD88 (MyD88^{L265P})[155]. This activating mutation has also been reported in low frequencies in activated B-cell-like diffuse large B-cell lymphoma (14%-29%) (see below), primary central nervous system lymphoma (PCNSL; 33%), mucosa-associated lymphoid tissue (MALT) lymphoma (9%), and CLL (2.9%) [156-159]. The mutated MyD88^{L265P} protein binds phosphorylated-BTK and triggers NF-κB signaling[160]. In addition, ~30% of WM patients show the CXCR4 S338X somatic mutation, leading to enhanced CXCL12-triggered activation of AKT and ERK[161]. In this regard, CXCR4 and VLA-4 interactions have been shown to regulate trafficking and adhesion of WM cells to the bone marrow[162].

ABC-DLBCL. DLBCL is the most common form of B cell non-Hodgkin lymphomas (B−NHLs) representing ~30-40% of all cases. Patients most often present with a rapidly growing tumor in single or multiple, nodal or extranodal sites. Based on gene expression profiling, three major molecular subtypes have been identified: GC B-cell-like (GCB-DLBLCL), activated-B-cell-like (ABC-DLBCL) and primary mediastinal B-cell lymphoma (PMBL)[163]. Whereas GCB-DLBCL and ABC-DLBCL make up the majority of cases at roughly equal frequency, PMBL accounts for up to 10% of cases of DLBCL[164]. GCB-DLBCL tumors express many genes found in normal GC B cells and have typically switched to an IgG BCR, while gene expression in ABC-DLBCL, which are predominantly IgM^{+}, resembles that of antigen-activated plasmablasts [165,166]. ABC-DLBCL has an inferior clinical outcome than GCB-DLBCL with a three-year overall survival of ~45% [167].

ABC-DLBCL are dependent on constitutive NF-κB signaling for their survival and proliferation[168-170]. Approximately 50% of ABC-DLBCL harbor mutations in CARD11 or other NF-κB pathway components, including the MyD88^{L265P} mutation[169-171]. In addition, ~20% of patients carry an activating mutation in CD79A/B. Consistent with a role of NF-κB downstream of the BCR **(Figure 2)**, it was found that knockdown of BCR components, CD79A/B and downstream signaling molecules, induced cell death in ABC-DLBCL lines with unmutated CARD11[172]. Moreover, RNAi experiments demonstrated that ABC-DLBCL lines are dependent on MyD88 and its associated kinase IRAK1 for their survival in line with NF-kB function in the TLR pathway **(Figure 3B)**. In addition, SYK amplification and deletion of PTEN, a phosphatase that dephosphorylated PIP_3, are also selective genetic alterations identified in ABC-DLBCL[173].

In contrast to ABC-DLBCL, GCB DLBCLs do not acquire highly recurrent mutations in CD79A/B or NF-κB components. Whereas ABC-DLBCL frequently respond to BTK inhibition (see below), GC-DLBCL do not respond and exhibit tonic BCR signaling that does not affect their calcium flux, but acts primarily to activate AKT[174]. Accordingly, forced activation of AKT rescued GCB-DLBCL lines from knockout of the BCR or SYK and CD19, two mediators of tonic BCR signaling[174]. The importance of the oncogenic AKT/PI3K pathway in GCB-DLBCL is evident from the finding that in ~55% of patients the tumor suppressor phosphatase and tensin homolog (PTEN), a negative regulator of PI3K, is inactivated. The mechanisms of PTEN inactivation include mutation, deletion or amplification of the miR17-92 microRNA cluster that downregulates PTEN expression[175,176].

Primary CNS lymphoma (PCNSL), another DLBCL subtype, is an aggressive brain tumor that has a complete response rate of <40% with methotrexate-based regimens and is subject to late recurrences. Patients showed mutations in the *MYD88, CD79B and CARD11* genes in ~58%, ~41% and ~13% of cases, respectively [177].

Other B cell malignancies. The hallmark of follicular lymphoma (FL), the (14;18) translocation resulting in BCL2 overexpression, is found in up to ~85% of patients. The pathogenesis of FL is complex and involves additional cell-intrinsic genetic changes, frequently including mutations in histone-encoding genes (in ~40% of cases), the SWI/SNF complex or the interconnected BCR and CXCR4 chemokine receptor signaling pathways, as well as alterations within the FL microenvironment [178]. The importance of BCR and NF-κB signaling is underscored by the finding of recurrent mutations in the genes encoding

CD22, SLP65/BLNK, PLCγ2, SYK, PKCβ, BCL10,* the NF-κB p100 subunit and the deubiquitinating enzyme A20/*TNFAIP3,* which is a negative regulator of NF-κB signaling. In addition, the *HVCN1* gene (coding for a hydrogen voltage-gated proton channel that acts downstream of the BCR and is downregulated in proliferating B cells) is frequently mutated in FL. Interestingly, BTK mutations were found that suggest activation, e.g. the L528W mutation in the kinase domain, which is associated with resistance to BTK inhibition in CLL (described below), and an in-frame deletion that also alters this amino acid and the adjacent C527. Moreover, two loss-of-function BTK mutations were identified, T117P and R562W, which are also found in XLA patients, but it remains unclear how these mutations contribute to FL pathogenesis [178].

In multiple myeloma (MM), a malignancy of plasma cells in the bone marrow, BTK was shown to be overexpressed, whereby BTK activated AKT signaling, leading to down-regulation of P27 expression and upregulation of key stemness genes [179,180]. MM cells originate from plasma cells, which do not express surface BCR, and rely for their survival and proliferation on signals from the microenvironment in the bone marrow. BTK may be critical in the MM microenvironment, in particular for secretion of cytokines and chemokines by osteoclasts[181].

Finally, BCR and TLR are thought to be key activation pathways in marginal zone lymphoma (MZL), often associated with chronic inflammation in the context of autoimmunity and/or infection[182], implicating BTK as a potential target. In this context, whole exome sequencing identified recurrent inactivating mutations in Kruppel-like factor 2 (KLF2) which impeded its capacity to suppress NF-κB activation. In addition, recurrent mutations in the TLR/NF-κB pathway were found, affecting e.g. the *MYD88, TRAF3, CARD11, A20/TNFAIP3* and *CARD11* genes[183].

The BTK inhibitor ibrutinib in clinical studies

Ibrutinib (PCI-32765) is an oral irreversible BTK inhibitor that covalently binds to cysteine at position 481 in the kinase domain and thereby blocks kinase activity[184]. As a result BTK has lost its kinase activity, but Y551 phosphorylation by SYK is not affected. The *in vivo* effect of ibrutinib was first confirmed in a mouse model of autoimmune disease and in dogs with spontaneous B-cell non-Hodgkin lymphoma, in which it induced objective clinical responses[185].

Efficacy of ibrutinib in a clinical study was first reported in patients with various relapsed/refractory B-cell malignancies, showing clinical safety and promising durable objective responses particularly in CLL and MCL[186]. Responding patients showed sustained reduction in lymphadenopathy, accompanied by transient rise in absolute lymphocyte count, a phenomenon known as lymphocytosis[186]. The next phase Ib/II multicenter trial, with a continuous ibrutinib regimen in relapsed/refractory CLL patients also showed lymphocytosis in the first weeks of treatment, but lymphocyte counts normalized or dropped below baseline after prolonged treatment[11]. Importantly, the overall response rate was ~71%, independent of clinical or genomic risk factors.

In a phase II study, patients with relapsed or refractory MCL were treated orally with ibrutinib, resulting in a response rate of ~68%[187]. It was subsequently demonstrated that Ibrutinib was also highly active and associated with durable responses in pretreated patients with Waldenström's macroglobulinemia, whereby MYD88 and CXCR4 mutation status affected the response[188]. Ibrutinib very rapidly received breakthrough designation and was subsequently approved by the Food and Drug Administration (FDA) for the treatment of MCL, CLL and WM between November 2013 and January 2017.

In addition, ibrutinib has also been tested in other B cell malignancies. In line with the possible role of BTK in FL, 6 out of 16 (38%) relapsed/refractory FL patients show response upon ibrutinib treatment[186]. In a phase II study ibrutinib induced durable remissions in ~50% of the MZL patients[189]. In a phase I study the majority (77%) of patients with PCNSL show clinical responses to ibrutinib [177]. **Table 1** summarizes the data from current clinical trials in various B-cell malignancies.

Several studies were performed to explain the therapeutic mode of action of ibrutinib. In CD40- or BCR-activated CLL cells, ibrutinib reduced survival by abrogating downstream pathways including ERK, PI3K and NF-κB[141]. Ibrutinib inhibited migration of CLL cells towards chemokines such as CXCL12 and CXCL13, suggesting that treatment inhibits homing and retention of malignant cells in their survival niches[77]. Ibrutinib was also found to reduce secretion of BCR-dependent chemokines CCL3 and CCL4[142]. Another key effect was that it inhibited integrin α4β1-mediated adhesion of CLL cells to fibronectin and VCAM1[146] and thus interaction with the tumor microenvironment[146]. Therefore, ibrutinib apparently works by a dual mechanism, by inhibiting intrinsic B cell signaling pathways to compromise their proliferation and survival as well as by disrupting tumor-microenvironment interactions. Importantly, both in CLL and MCL ibrutinib treatment induces a redistribution lymphocytosis, a transient rise of leukemic cells in the circulation and a concomitant rapid reduction of these cells at the affected tissue sites. In contrast to classical cytotoxic chemotherapy, ibrutinib does not cause tumor lysis syndrome, which is a common complication of cancer therapy because of metabolic disturbances when large numbers of tumor cells die quickly. Therefore, most likely the displacement of B cells from nurturing tissue niches because of inhibition of integrin-mediated retention of leukemic cells, is an important mechanism of action of ibrutinib, rather than robust inhibition of survival of malignant B cells[190]. As a result, leukemic cells undergo 'death by neglect', because their mobilization induces 'homelessness' (anoikis), a form of programmed cell death[191,192].

Table 1. Clinical trials with BTK inhibitors in B cell malignancies

Patient population	Therapeutic regimen	Phase	Efficacy	Ref
R/R CLL	Ibrutinib	Ib/II	ORR (71%), PR(20%)	[11]
R/R CLL	Ibrutinib	III	ORR (63%)	[248]
TN CLL	Ibrutinib	Ib/II	ORR (85%), CR(26%)	[199]
TN CLL	Ibrutinib	III	ORR (86%), CR(4%)	[13]
R/R MCL	Ibrutinib	II	ORR (68%), CR(21%)	[187]
R/R MCL	Ibrutinib	III	ORR (72%), CR(19%)	[249]
R/R WM	Ibrutinib	II	ORR(91%), Major response (73%)	[188]
R/R ABC-DLBCL	Ibrutinib	II	ORR (37%)	[196]
R/R CLL	Ibrutinib-Rituximab	II	ORR (95%), CR(8%)	[250]
R/R CLL	Ibrutinib-bendamustine-rituximab	III	ORR (83%), CR(10%)	[251]
R/R MCL	Ibrutinib-Rituximab	II	ORR (88%), CR(44%), PR(44%)	[252]
R/R CLL	Acalabrutinib	I/II	ORR(95%)	[12]
R/R	Acalabrutinib	II	ORR (81%), CR (40%), PR(41%)	[219]
R/R CLL	ONO/GS-4059	I	ORR(96%)	[222]
R/R MCL	ONO/GS-4059	I	ORR(92%)	[222]
R/R non-GCB DLBCL	ONO/GS-4059	I	ORR(35%)	[222]
R/R CLL	BGB-3111	I	ORR(90%)	[253] [221]
R/R MCL	BGB-3111	I	ORR(80%)	[253]
R/R MZL	Ibrutinib	II	ORR(51%)	[254]
R/R FL	Ibrutinib	I	ORR(38%)	[186]

CLL: Chronic Lymphocytic leukemia, MCL: Mantle cell lymphoma, WM: Waldenström's Macroglobulinemia, ABC-DLBCL: Activated B-cell Diffuse large B cell Lymphoma, MZL: Marginal zone lymphoma, FL: Follicular lymphoma, R/R: relapsed or refractory, TN: treatment-naïve, ORR: overall response rate, CR: complete response, PR: partial response, Major response: complete response or at least 50% reduction in serum IgM levels.

Despite impressive clinical success of ibrutinib, its curative potential in B cell malignancies is not established yet, as ibrutinib is often prescribed as life-long therapy. Importantly, continuous therapy may lead to selection or outgrowth of resistant clones, as described in a subset of patients who relapse upon ibrutinib therapy. Two important therapy-associated resistance mechanisms have been identified, involving BTK C481S mutation (the site of action of Ibrutinib) or activating mutations in PLCγ2 (R665W, S707Y and L845F)[193,194]. Recently another BTK mutation, T316A in the SH2 domain, was described, as well as clonal evolution underlying leukemia progression in patients with ibrutinib-relapsed CLL [195]. In addition, missense mutation within the coiled-coil domain of CARD11 (R179Q) have been shown to promote BTK-independent activation of NF-κB and thus ibrutinib resistance in DLBCL, MCL and PCNSL[177,196,197]. Furthermore, an activating mutation in BTK (L528W) that confers resistance to ibrutinib treatment has been found in CLL and FL[178,198].

In clinical trials the adverse events were mostly limited to grade 1 or 2 in severity, but in some cases side-effects led to discontinuation of the therapy [199-201]. Because ibrutinib treatment has a considerable high risk of bleeding in treated patients, concomitant anti-coagulation (~11%) and antiplatelet (~34) use is common and ~3% of the patients were reported to have major bleeding events[202]. Atrial fibrillation has been reported in up to 16% of patients taking ibrutinib, whereby stroke prevention poses a challenge because of the increased bleeding risk. Therefore, close monitoring is recommended, especially during the first 6 months of ibrutinib therapy[203]. Although the occurrence of atrial fibrillation might possibly be related to inhibition of the BTK-regulated PI3K/AKT pathway in cardiac myocytes[204], the mechanisms involved remain largely unidentified.

Three year follow-up of ibrutinib-treated CLL patients showed that prolonged treatment was associated with improvement in response quality (the ORR increased to >90%) and durable remission, while toxicity including cytopenia, fatigue, and infection diminished. Moreover, progression remains uncommon[205]. Findings from the longest follow-up reported to date, evaluating up to 5 years of ibrutinib in CLL patients, show that it is relatively safe and effective, with ~89% of treatment-naïve and relapsed patients experiencing a response to the therapy[206].

Part of the toxicities and side effects of ibrutinib can be explained by its non-specific nature: ibrutinib is not an exclusive inhibitor of BTK and off-target inhibition includes kinases that contain a cysteine residue aligning with Cys-481 in BTK. These include other TEC-family kinases (ITK, BMX, TEC), as well as epidermal growth factor receptor (EGFR), T-cell X chromosome kinase (TXK) and Janus Kinase 3 (JAK3)[12,185,207]. In this context, it is of note that the bleeding risk in patients receiving ibrutinib was thought to relate to off-target inhibition of TEC[12]. BTK is expressed in platelets where it is important for signaling via the collagen receptor glycoprotein VI (GPVI); platelets from XLA patients display diminished aggregation, dense granule secretion and calcium mobilization in response to collagen and C-reactive protein[208]. Nevertheless, XLA patients do not have an increased risk of bleeding[209]. Findings by *Bye et al.* indicated that both BTK and TEC – although required for GPVI-mediated platelet aggregation – are redundant for platelet adhesion to collagen and thrombus formation[210]. Rather, ibrutinib but not the more selective BTK inhibitor acalabrutinib (see below) inhibits SRC family kinases that have a critical role in platelet function[210]. These findings explain why in contrast to ibrutinib, treatment with acalabrutinib was not associated with major bleeding events[12].

A recent systematic review of infectious events with ibrutinib in the treatment of B cell malignancies provided evidence for infection-related complications in ~50% of patients taking ibrutinib, whereby ~20% of patients developed pneumonia due to opportunistic pathogens[211]. Hereby, data suggest that these events may involve inhibition of both BTK and its closely related family member ITK. On the other hand, it was shown that ibrutinib treatment increased the *in vivo* persistence of both $CD4^+$ and $CD8^+$ activated T cells and diminished the immune-suppressive properties of CLL cells. As these effects were not seen with more specific BTK inhibitor acalabrutinib that lacks ITK inhibitory activity (see below), it was concluded that the T cell expansion is unlikely to be caused by BTK inhibition [212]. Rather, ibrutinib treatment of activated T cells diminishes activation-induced cell death by targeting ITK, a finding also reported in murine models of ITK deficiency. However, both inhibitors reduced the expression of the inhibitory co-receptors programmed cell death protein 1 (PD-1) and cytotoxic T-lymphocyte-associated protein 4 (CTLA4) on T cells, as well as expression of the immunosuppressive molecules CD200, B- and T-lymphocyte attenuator (BTLA) and IL-10 by CLL cells [212]. Therefore, ibrutinib likely diminishes the immune-suppressive properties of CLL cells through both BTK-dependent and ITK-dependent mechanisms.

Inhibition of BTK and ITK with ibrutinib was shown to be effective in the prevention of chronic graft-versus-host (GvH) disease following allogeneic hematopoietic stem cell transplantation (SCT) in several mouse models [213,214]. Accordingly, also studies in patients with relapsed CLL following SCT support that ibrutinib augments the GvH versus-leukemia (GVL) benefit likely through ITK inhibition[215]. In particular, it was shown that ibrutinib selectively targeted pre–germinal B cells and depleted Th2 helper cells, whereby these effects persisted after drug discontinuation.

Taken together, these findings provide a rationale for combination immunotherapy approaches with ibrutinib in CLL and other cancers.

Ibrutinib in combination therapies and second generation BTK inhibitors

The finding of ibrutinib resistance, together with multiple modes of action and the microenvironmental dependence of B-cell malignancies, has fueled the development of novel combination strategies. With the aim to achieve deeper remissions within a short treatment time, many ibrutinib combination therapies are currently considered (**Table 2**). Hereby, ibrutinib treatment forces egress of malignant B cells out of their protective niches into circulation, where they become vulnerable to direct cytotoxic activity of either chemotherapy, an inhibitor of the pro-survival protein Bcl-2, or antibody mediated cytotoxicity (ADCC) of anti-CD20 antibody therapy.

Side-effects associated with off-target kinase inhibition may limit the use of ibrutinib as therapeutic agent (as discussed above). Ibrutinib can antagonize rituximab-induced ADCC due to inhibition of its family member ITK in NK cells, further limiting its use in combination regimens[216]. Therefore, many efforts have focused on developing highly selective BTK inhibitors, of which three have reached advanced stages of clinical development[217].

Acalabrutinib (ACP-196). This highly selective irreversible BTK inhibitor has significantly less off-target kinase activity[207]. Acalabrutinib also binds C481 and lacks irreversible targeting to alternative kinases, such as EGFR, ITK, TXK, SRC family kinases and JAK3. The first pre-clinical study in canine models of Non-Hodgkin B-cell lymphoma demonstrated enhanced *in vivo* potency compared to ibrutinib[218]. In a phase I/II clinical trial in patients with relapsed/refractory CLL the overall response rate was ~95% and in patients with del(17)(p13.1) this was 100%, with a median follow-up up ~14 months[12]. No dose-limiting toxicities, episodes of atrial fibrillation, or bleeding-related events have been reported to date. To investigate the superiority of either inhibitor, a phase III trial for direct comparison of ibrutinib with acalabrutinib in R/R CLL patients is currently ongoing (NCT02477696). Additionally, in a phase II trial in patients with relapsed/refractory MCL, acalabrutinib induced an overall response of ~81% with ~40% patients achieving a complete response[219]. This led to accelerated FDA approval of acalabrutinib in MCL [220].

BGB-3111. Another selective inhibitor of BTK kinase activity with superior oral bioavailability and higher selectivity than ibrutinib is BGB-3111, which was shown to inhibit proliferation of several MCL and DLBCL cell lines. Due to weaker ITK inhibition, BGB-3111 was at least 10-fold weaker than ibrutinib in inhibiting rituximab induced ADCC. When 45 CLL patients were treated on a phase I/II study, therapy was well tolerated and was associated with a response rate of ~90% after a follow-up of 7.5 months and no cases of disease progression or Richter's transformation[221] (see also Table 1).

Ono/GS-4059. *In vivo* efficacy of this compound was initially described in an ABC-DLBCL xenograft model and *in vitro* anti-proliferative effects in DLBCL, FL, MCL and CLL cell lines were described[222]. Early-phase clinical trial data in patients with several B-cell malignancies include clinical responses in patients with high-risk CLL genetics (**Table 1**).

Role of BTK in the tumor microenvironment

Inhibition of BTK has now also extended into the field of solid tumors, following insights into the role of BTK in various cells of the tumor microenvironment and in

Table 2. Overview of Ibrutinib in combination therapies

Combination	Disease	Model	Rationale	Effect	Reference
γ-secretase inhibitors (crucial protease in Notch signaling)	CLL	CLL patient cells	NOTCH1 signaling is related to resistance to therapy in B-CLL.	Combination therapy showed enhanced cytotoxicity and reduced CXCR4 expression and functions (response to SDF-1α)	[255]
Histone Deacetylase (HDACs) Inhibitor	CLL	- MCL cell line - mice engrafted with TCL-1 splenocytes	HDACs increase transcription of miRNA that repress BTK	HDAC induced increase in target miRNA and a decrease in BTK RNA; combination exhibited higher cytotoxicity than either drug alone; reduction of p-BTK and total BTK protein.	[69]
Anti-CD19 CAR T Cells (CART19)	MCL	MCL Xenograph model	Efficient B cell depletion	Long-term remission in 80-100% of mice (treated with CART19 only: 0-20% of mice)	[245]
Ethacridine (Poly(ADP-ribose) glycohydrolase inhibitor)	AML	SCID mice injected s.c. with OCI-AML2 cells	Result of a drug screening	High decrease of OCI-AML2 cell growth (more than with either drug alone). Suggested mechanism: increased intracellular ROS production in cells treated with combination.	[256]
ND-2158 (IRAK4 inhibitor)	ABC-DLBCL	- ABC-DLBCL cell lines OCI-Ly10 and TMD8 - OCI-Ly10 xenografts	MYD88-IRAK4 signaling is important for ABC- DLBCL viability	Combination was more effective than ND-2158 alone in inhibiting IKK activity, enhancing apoptosis, and blocking tumor growth in mice.	[257]
PU-H71 (Binds to tumor enhanced HSP90 complexes)	ABC-DLBCL	DLBCL cell lines (HBL-1 and TMD8)	teHSP90 complexes are associated with tumor survival.	PU-H71 disrupts teHSPP90 (but not house-keeping fractions associated with HSP90). Synergistic effect, with ~95% tumor growth inhibition; decreased NF-kB activity	[258]
TP-0903 (AXL inhibitor)	CLL	Patient CLL cells prior to or after ibrutinib therapy	AXL contributes to oncogenic survival in CLL.	TP-093 disrupts the activity of AXL; Induction of cell-death in a dose-dependent fashion	[259]
B-PAC-1 (pro-caspase activating compound)	CLL	B cells from patients on ibrutinib therapy	B-PAC activates caspases dimers	Induced cytotoxicity in leukemic cells	[259]
Carfilzomib (proteasome inhibitor)	CLL	Primary CLL patient samples MEC-1 and MEC2 cell lines	Upregulation of pro-apoptotic transcription factor CHOP	Combination showed an additive cytotoxic effect; Carfilzomib induced a pro-apoptotic response involving Noxa, MCL-1, Bax, and Bak and intrinsic and extrinsic caspase pathways	[260]
Selinexor (Exportin inhibitor)	CLL	Primary CLL patient samples	Selinexor disrupts BCR signaling via BTK depletion	Combination showed synergistic cytoxicity. Selinexor overcomes resistance to Ibrutinib (also in patient cells with C481S mutation)	[261]
Anti-PDL1 antibody (Negative regulator of T cell function)	B cell lymphoma (A20)	- BALB/c mice inoculated with A20 B cells - A20 B cells are resistant to Ibrutinib	Blocking immune checkpoints can enhance the anti-tumor response	Anti-PDL-1 treatment alone delayed tumor growth and slightly increased mouse survival Combination with anti-PDL-1 cured ~50% of the mice, delayed tumor growth and prolonged survival in the remaining mice, and increased IFN-γ producing T-cells	[243]
ABT-199 (BCL-2 antagonist)	CLL	Ex vivo samples from CLL patients on ibrutinib	CLL samples show enhanced BCL-2 expression	Ibrutinib enhances ABT-199 cytotoxicity, both in unstimulated and in αIgM-stimulated CLL cells from. ABT-199 action correlated with a decline in expression of anti-apoptotic MCL-1	[262]
ABT-199 (BCL-2 antagonist)	MCL	CCMCL1 MCL cell line	MCL cells show enhanced BCL-2 expression	Combination results in decrease of p-BTK and p-AKT. Downregulation of both BCL2 and MCL1. ABT-199 and Ibrutinib target non-overlapping pathway s	[263]
Bortezomib (proteosome inhibitor) and lenalidomide chemotherapy	MM	Cells from MM patients and MM cell lines	Blocking BTK to downregulate NF-kB activation and cell survival	Ibrutinib increased the cytotoxicity of bortezomib and lenalidomide in both patient cells and cell lines	[264]
CpG (TLR9 ligand)	B-cell lymphoma	Murine pre-B cell (H11) and B cell lymphoma lines (BL3750, A20)	CpG activates APCs and thereby induces T cell activation	Combination of ibrutinib and intratumoral CpG resulted in tumor regression and resistance, whereby IFNy-producing CD4 and CD8 T are essential	[265]
Sudemycin D1 (spliceosome modulator)	CLL	Primary CLL cells (from SF3B1-unmutated and mutated cases)	*SF3B1* is frequently mutated in CLL, and correlates with aggressiveness	Combination results in enhanced apoptosis of M-CLL and U-CLL. Effect is related to IBTK splicing. Sudemycin D1 downregulates anti-apoptotic MCL-1 through alternative splicing	[266]
BAY80-6946 (PIK3 inhibitor)	PCNSL	- Xenograft model from	CARD11 domain mutations increase	In cell lines, cell death was induced with both combinations of drugs	[177]

INK128 (mTOR inhibitor)		CD79B-mutant biopsies	the activity of the PI3K-mTOR axis		
Idelalisib (PI3K inhibitor)	DLBCL	- Cell lines. - Mouse TMD8 xenograft model	PI3K is upstream regulator of NF-κB pathway.	Cell lines: combination induced 50% apoptosis and inhibited signaling (more than either drug individually). Mouse xenograft: Significant tumor regression	[267][1]
Idelalisib (PI3K inhibitor)	MCL	MCL cell lines	A more robust blockage of BCR signaling	Inhibition of BCR-stimulated integrin-mediated adhesion; stronger inhibition of adhesion compared to each drug alone	[146][1]

---

1) In this study, also ONO/GS-4059, the phosphoinositide-dependent kinase-1 inhibitor GSK2334470 and the AKT inhibitor MK-2206 were investigated.

CLL: Chronic Lymphocytic leukemia, MCL: Mantle cell lymphoma, AML: Acute Myeloid Leukemia, ABC-DLBCL: Activated B-cell Diffuse large B cell Lymphoma, MM: Multiple Myeloma, PCNSL: Primary central nervous system lymphoma.

non-hematological tumor cells when ectopically expressed. An understanding of the diverse roles of BTK in non-lymphocytic cells will be pivotal in the development of novel treatment combinations for haematopoietic and solid tumors.

BTK is involved in TLR- and Fc-receptor mediated activation, maturation, migration and survival of myeloid cells[223,224]. However, the role of BTK identified is dependent on cell type investigated, the nature of activating stimuli, the model used (*in vivo* or *in vitro*) and the species investigated, i.e. mouse or human. Analyses in various mouse models and *in vitro* studies with myeloid cells from XLA-patients clearly implicate BTK in TLR4/8/9-signaling, and possibly others[79,225-227]. However, data are often conflicting, e.g. TLR8-induced IL-6 production by BTK-deficient DCs were reported to be impaired[226], enhanced[228], or unaffected[229]. Also TLR4/7/8-induced TNFα was reported to be reduced[226,229] or enhanced[228].

Of further relevance in the context of the tumor microenvironment is the polarization status of macrophages, with M1 macrophages displaying a pro-inflammatory anti-tumor phenotype and M2 macrophages being immunosuppressive[22]. Whereas one study indicated an M2-skewing of BTK-deficient macrophages[230], recently in a pancreatic cancer mouse model an M1-skewing of intratumoral macrophages was found following ibrutinib treatment [231]. In contrast, ibrutinib induced M1 to M2-skewing of nurse-like cells, which show properties of tumor-associated macrophages, accompanied by impaired phagocytosis, increased IL-10 production mediating pro-survival signals in CLL[232]. It remains unknown what causes these incongruences in BTK-dependent myeloid polarization, however it is conceivable that the different roles of BTK in a complex ecology of tumor-infiltrating cells and the limited specificity of ibrutinib contribute to the conflicting findings.

In solid tumors, chronic deposition of immune complexes foster carcinogenesis due to chronic inflammation, angiogenesis and M2 macrophage polarization in response to activating Fc-receptor ligation on myeloid cells[231,233,234]. Interestingly, inhibiting BTK during Fc-receptor stimulation of macrophages *in vitro* using ibrutinib prevented M2-skewing[231].

Granulocytes and their immature immune-suppressive counterparts, myeloid derived suppressor cells (MDSC), are strongly implicated in tumor progression, rendering them important candidates for therapy[235]. Although loss of BTK in XLA neutrophils does not impair functional TLR responses[236], the numbers of circulating granulocytes are reduced in XLA-patients and BTK-deficient mice[237-239]. Moreover, BTK-deficient neutrophils manifest increased sensitivity to apoptosis, decreased maturation, differentiation, trafficking and impaired functionality including reactive oxygen species (ROS) production[238-241]. Likewise, ibrutinib treatment inhibited the generation, migration, TNFα and ROS-production of MDSCs both *in vitro* and in solid tumor mouse models[242]. Ibrutinib treatment partially alleviated MDSC-mediated $CD8^+$ T-cell suppression and enhanced

Table 3. Clinical trials with BTK-inhibitors in solid tumors

BTK-inhibitor	Tumor Type	Treatment combination	Phase Trial	Status	NCT#
Ibrutinib	Pancreatic cancer	Nab-paclitaxel and gemcitabine	II/III	Ongoing	NCT02436668
Ibrutinib	Pancreatic cancer	Nab-paclitaxel and gemcitabine	I	Recruiting	NCT02562898
Ibrutinib	Renal/Urethelial/Gastric/Colorectal cancer	Chemotherapy/small molecule	Ib/II	Recruiting	NCT02599324
Ibrutinib	HER2/MYC+ Oesophageal Cancer		I	Recruiting	NCT02884453
Ibrutinib	EGFR+NSCLC		I/II	Ongoing	NCT02321540
Ibrutinib	NSCLC/Breast Cancer/Pancreatic Cancer	Durvalumab (aPD-1)	I/II	Completed	NCT02403271
Ibrutinib	Pancreatic Neuro-endocrine tumors (pNET)/metastatic Carcinoid		II	Recruiting	NCT02575300
Ibrutinib	Stage IV Cutaneous Melanoma		II	Recruiting	NCT02581930
Ibrutinib	Metastatic Renal Cancer	Nevolumab (aPD-1)	Ib/II	Recruiting	NCT02899078
Ibrutinib	Localised Prostate Cancer			Recruiting	NCT02643667
Acalabrutinib	Advanced/Metastatic Pancreatic Cancer	Pembrolizumab (aPD-1)	II	Ongoing	NCT02362048
Acalabrutinib	Recurrent Ovarian Cancer	Pembrolizumab (aPD-1)	II	Ongoing	NCT02537444
Acalabrutinib	Glioblastoma	Pembrolizumab (aPD-1)	Ib/II	Recruiting	NCT02586857
Acalabrutinib	Non-Small Cell Lung Cancer (NSCLC)	Pembrolizumab (aPD-1)	II	Ongoing	NCT02448303
Acalabrutinib	Head and Neck Squamous Cell Carcinoma (HNSCC)	Pembrolizumab (aPD-1)	II	Ongoing	NCT02454179
Acalabrutinib	Platinum-resistant Urethelial (Bladder) Cancer	Pembrolizumab (aPD-1)	II	Ongoing	NCT02351739

anti-PD-L1 therapy efficacy in a breast cancer model. BTK inhibition in granulocytes and MDSCs in solid tumors may therefore be important in the development of effective combination therapies.

BTK inhibition in solid malignancies

Ectopic BTK expression has been observed in various solid tumors, whereby evidence is accumulating for its involvement in oncogenesis[24-27]. These pre-clinical findings have led to the initiation of several early phase I/II clinical trials in which BTK inhibition monotherapy is evaluated in advanced ovarian, colorectal, prostate and brain cancer patients (**Table 3**).

Also in BTK-negative solid tumors that do not express BTK, its inhibition may hold promise as multiple cell types in the tumor microenvironment are regulated by BTK. Inhibition of BTK in pre-clinical models of pancreatic cancer, breast cancer and BTK-negative colon cancer have shown only marginal improvement of survival as monotherapy, but when combined with chemo- or immunotherapy, survival was greatly enhanced[231,242,243]. This has sparked the emergence of several trials investigating the safety and efficacy of ibrutinib or acalabrutinib, in combination with conventional PD-1/PD-L1 checkpoint inhibition therapy (**Table 3**).

Given that ibrutinib shows off-target inhibition of JAK3, ITK and EGFR[185,207], it can be used to target oncogenic pathways other than BTK in tumor cells and as a T-cell modulator in combination immunotherapy[243-246]. Hereby, ibrutinib treatment increased cellular persistence and decreased expression of co-inhibitory surface molecules on Chimeric antigen receptor (CAR) T cells in models of CLL and MCL[245,246]. Whether in these studies ibrutinib acts on ITK in (CAR) T cells, on BTK in the malignant cells or other kinases remains undetermined. Paradoxically, inhibiting ITK in T cells may be efficacious in cancer, as this may enhance Th1-skewing of $CD4^+$ T-cells and thereby improved memory formation and functionality of $CD8^+$ T-cells, potentially leading to improved anti-tumor immunity[243,247]. These potentially beneficial off-target effects of ibrutinib may be lost in the highly specific BTK-inhibitors that are currently being evaluated.

CONCLUDING REMARKS

Targeting of BTK, which has a central role in several signaling pathways in B cells, particularly the BCR, has shown impressive efficacy as therapeutic option for various B cell malignancies in clinical trials. Much progress has been made in recent years in defining the complex mechanisms of action of BTK inhibition. These involve intrinsic signaling pathways in leukemic cells that are central to cellular survival, proliferation and – most importantly - retention in supportive microenvironments. Moreover, BTK inhibition shows promise as a therapy that influences crucial immune cells in the tumor microenvironment. Because data from BTK-deficient or inhibitor-treated myeloid cells in the context of cancer are scarce, it is not clear whether BTK inhibition by e.g. ibrutinib is based on its specificity for BTK in particular myeloid cells and/or due to off-target effects in signaling pathways in $CD4^+$ or $CD8^+$ T cells. Of note, because in CLL ibrutinib treatment diminished the immunosuppressive properties of malignant cells through BTK-dependent and BTK-independent mechanisms (probably via ITK inhibition) [212], it will be interesting to observe whether the same level of anti-tumor efficacy is maintained by specific BTK inhibition alone. It is very well conceivable that for particular malignancies it may be advantageous to use BTK inhibitors that show additional specificity for related kinases.

Although the efficacy of BTK inhibition as a single agent therapy is strong, it has been shown that resistance may develop and now a broad range of studies focus on development of effective combination therapies to improve clinical responses. The identification of differences in efficacy and toxicity profiles between available BTK inhibitors awaits direct comparative studies. In this context, design of treatment strategies will depend on detailed analyses of clinical responses, resistance development, toxicity and quality of life for individual BTK inhibitors in combination therapies in relation to the various malignancies and patient subgroups.

REFERENCES

1. Gross S, Rahal R, Stransky N, Lengauer C, Hoeflich KP: Targeting cancer with kinase inhibitors. *J Clin Invest* 2015, **125:**1780-1789.
2. Hanahan D, Weinberg RA: Hallmarks of cancer: the next generation. *Cell* 2011, **144:**646-674.
3. Vetrie D, Vorechovsky I, Sideras P, Holland J, Davies A, Flinter F, Hammarstrom L, Kinnon C, Levinsky R, Bobrow M, et al.: The gene involved in X-linked agammaglobulinaemia is a member of the src family of protein-tyrosine kinases. *Nature* 1993, **361:**226-233.
4. Tsukada S, Saffran DC, Rawlings DJ, Parolini O, Allen RC, Klisak I, Sparkes RS, Kubagawa H, Mohandas T, Quan S, et al.: Deficient expression of a B cell cytoplasmic tyrosine kinase in human X-linked agammaglobulinemia. *Cell* 1993, **72:**279-290.
5. Rawlings DJ, Saffran DC, Tsukada S, Largaespada DA, Grimaldi JC, Cohen L, Mohr RN, Bazan JF, Howard M, Copeland NG, et al.: Mutation of unique region of Bruton's tyrosine kinase in immunodeficient XID mice. *Science* 1993, **261:**358-361.
6. Thomas JD, Sideras P, Smith CI, Vorechovsky I, Chapman V, Paul WE: Colocalization of X-linked agammaglobulinemia and X-linked immunodeficiency genes. *Science* 1993, **261:**355-358.

7. Scher I: The CBA/N mouse strain: an experimental model illustrating the influence of the X-chromosome on immunity. *Adv Immunol* 1982, **33:**1-71.
8. Khan WN, Alt FW, Gerstein RM, Malynn BA, Larsson I, Rathbun G, Davidson L, Muller S, Kantor AB, Herzenberg LA, et al.: Defective B cell development and function in Btk-deficient mice. *Immunity* 1995, **3:**283-299.
9. Hendriks RW, de Bruijn MF, Maas A, Dingjan GM, Karis A, Grosveld F: Inactivation of Btk by insertion of lacZ reveals defects in B cell development only past the pre-B cell stage. *EMBO J* 1996, **15:**4862-4872.
10. Middendorp S, Dingjan GM, Hendriks RW: Impaired precursor B cell differentiation in Bruton's tyrosine kinase-deficient mice. *J Immunol* 2002, **168:**2695-2703.
11. Byrd JC, Furman RR, Coutre SE, Flinn IW, Burger JA, Blum KA, Grant B, Sharman JP, Coleman M, Wierda WG, et al: Targeting BTK with ibrutinib in relapsed chronic lymphocytic leukemia. *N Engl J Med* 2013, **369:**32-42.
12. Byrd JC, Harrington B, O'Brien S, Jones JA, Schuh A, Devereux S, Chaves J, Wierda WG, Awan FT, Brown JR, et al: Acalabrutinib (ACP-196) in Relapsed Chronic Lymphocytic Leukemia. *N Engl J Med* 2016, **374:**323-332.
13. Burger JA, Tedeschi A, Barr PM, Robak T, Owen C, Ghia P, Bairey O, Hillmen P, Bartlett NL, Li J, et al: Ibrutinib as Initial Therapy for Patients with Chronic Lymphocytic Leukemia. *N Engl J Med* 2015, **373:**2425-2437.
14. Hendriks RW, Yuvaraj S, Kil LP: Targeting Bruton's tyrosine kinase in B cell malignancies. *Nat Rev Cancer* 2014, **14:**219-232.
15. Kawakami Y, Yao L, Miura T, Tsukada S, Witte ON, Kawakami T: Tyrosine phosphorylation and activation of Bruton tyrosine kinase upon Fc epsilon RI cross-linking. *Mol Cell Biol* 1994, **14:**5108-5113.
16. Hata D, Kawakami Y, Inagaki N, Lantz CS, Kitamura T, Khan WN, Maeda-Yamamoto M, Miura T, Han W, Hartman SE, et al: Involvement of Bruton's tyrosine kinase in FcepsilonRI-dependent mast cell degranulation and cytokine production. *J Exp Med* 1998, **187:**1235-1247.
17. Jongstra-Bilen J, Puig Cano A, Hasija M, Xiao H, Smith CI, Cybulsky MI: Dual functions of Bruton's tyrosine kinase and Tec kinase during Fcgamma receptor-induced signaling and phagocytosis. *J Immunol* 2008, **181:**288-298.
18. Wang D, Feng J, Wen R, Marine JC, Sangster MY, Parganas E, Hoffmeyer A, Jackson CW, Cleveland JL, Murray PJ, Ihle JN: Phospholipase Cgamma2 is essential in the functions of B cell and several Fc receptors. *Immunity* 2000, **13:**25-35.
19. Shinohara M, Koga T, Okamoto K, Sakaguchi S, Arai K, Yasuda H, Takai T, Kodama T, Morio T, Geha RS, et al: Tyrosine kinases Btk and Tec regulate osteoclast differentiation by linking RANK and ITAM signals. *Cell* 2008, **132:**794-806.
20. Oda A, Ikeda Y, Ochs HD, Druker BJ, Ozaki K, Handa M, Ariga T, Sakiyama Y, Witte ON, Wahl MI: Rapid tyrosine phosphorylation and activation of Bruton's tyrosine/Tec kinases in platelets induced by collagen binding or CD32 cross-linking. *Blood* 2000, **95:**1663-1670.

21. Ito M, Shichita T, Okada M, Komine R, Noguchi Y, Yoshimura A, Morita R: Bruton's tyrosine kinase is essential for NLRP3 inflammasome activation and contributes to ischaemic brain injury. *Nat Commun* 2015, **6:**7360.
22. Noy R, Pollard JW: Tumor-associated macrophages: from mechanisms to therapy. *Immunity* 2014, **41:**49-61.
23. Mantovani A, Marchesi F, Malesci A, Laghi L, Allavena P: Tumour-associated macrophages as treatment targets in oncology. *Nat Rev Clin Oncol* 2017, **14:**399-416.
24. Kokabee L, Wang X, Sevinsky CJ, Wang WL, Cheu L, Chittur SV, Karimipoor M, Tenniswood M, Conklin DS: Bruton's tyrosine kinase is a potential therapeutic target in prostate cancer. *Cancer Biol Ther* 2015, **16:**1604-1615.
25. Grassilli E, Pisano F, Cialdella A, Bonomo S, Missaglia C, Cerrito MG, Masiero L, Ianzano L, Giordano F, Cicirelli V, et al: A novel oncogenic BTK isoform is overexpressed in colon cancers and required for RAS-mediated transformation. *Oncogene* 2016, **35:**4368-4378.
26. Zucha MA, Wu AT, Lee WH, Wang LS, Lin WW, Yuan CC, Yeh CT: Bruton's tyrosine kinase (Btk) inhibitor ibrutinib suppresses stem-like traits in ovarian cancer. *Oncotarget* 2015, **6:**13255-13268.
27. Wei L, Su YK, Lin CM, Chao TY, Huang SP, Huynh TT, Jan HJ, Whang-Peng J, Chiou JF, Wu AT, Hsiao M: Preclinical investigation of ibrutinib, a Bruton's kinase tyrosine (Btk) inhibitor, in suppressing glioma tumorigenesis and stem cell phenotypes. *Oncotarget* 2016, **7:**69961-69975.
28. Bradshaw JM: The Src, Syk, and Tec family kinases: distinct types of molecular switches. *Cell Signal* 2010, **22:**1175-1184.
29. Hyvonen M, Saraste M: Structure of the PH domain and Btk motif from Bruton's tyrosine kinase: molecular explanations for X-linked agammaglobulinaemia. *EMBO J* 1997, **16:**3396-3404.
30. Rawlings DJ, Scharenberg AM, Park H, Wahl MI, Lin S, Kato RM, Fluckiger AC, Witte ON, Kinet JP: Activation of BTK by a phosphorylation mechanism initiated by SRC family kinases. *Science* 1996, **271:**822-825.
31. Park H, Wahl MI, Afar DE, Turck CW, Rawlings DJ, Tam C, Scharenberg AM, Kinet JP, Witte ON: Regulation of Btk function by a major autophosphorylation site within the SH3 domain. *Immunity* 1996, **4:**515-525.
32. Marcotte DJ, Liu YT, Arduini RM, Hession CA, Miatkowski K, Wildes CP, Cullen PF, Hong V, Hopkins BT, Mertsching E, et al: Structures of human Bruton's tyrosine kinase in active and inactive conformations suggest a mechanism of activation for TEC family kinases. *Protein Sci* 2010, **19:**429-439.
33. Middendorp S, Dingjan GM, Maas A, Dahlenborg K, Hendriks RW: Function of Bruton's tyrosine kinase during B cell development is partially independent of its catalytic activity. *J Immunol* 2003, **171:**5988-5996.
34. Lam KP, Kuhn R, Rajewsky K: In vivo ablation of surface immunoglobulin on mature B cells by inducible gene targeting results in rapid cell death. *Cell* 1997, **90:**1073-1083.
35. Anderson JS, Teutsch M, Dong Z, Wortis HH: An essential role for Bruton's [corrected] tyrosine kinase in the regulation of B-cell apoptosis. *Proc Natl Acad Sci U S A* 1996, **93:**10966-10971.

36. Solvason N, Wu WW, Kabra N, Lund-Johansen F, Roncarolo MG, Behrens TW, Grillot DA, Nunez G, Lees E, Howard M: Transgene expression of bcl-xL permits anti-immunoglobulin (Ig)-induced proliferation in xid B cells. *J Exp Med* 1998, **187:**1081-1091.
37. Brorson K, Brunswick M, Ezhevsky S, Wei DG, Berg R, Scott D, Stein KE: xid affects events leading to B cell cycle entry. *J Immunol* 1997, **159:**135-143.
38. Glassford J, Soeiro I, Skarell SM, Banerji L, Holman M, Klaus GG, Kadowaki T, Koyasu S, Lam EW: BCR targets cyclin D2 via Btk and the p85alpha subunit of PI3-K to induce cell cycle progression in primary mouse B cells. *Oncogene* 2003, **22:**2248-2259.
39. Spaargaren M, Beuling EA, Rurup ML, Meijer HP, Klok MD, Middendorp S, Hendriks RW, Pals ST: The B cell antigen receptor controls integrin activity through Btk and PLCgamma2. *J Exp Med* 2003, **198:**1539-1550.
40. Rolli V, Gallwitz M, Wossning T, Flemming A, Schamel WW, Zurn C, Reth M: Amplification of B cell antigen receptor signaling by a Syk/ITAM positive feedback loop. *Mol Cell* 2002, **10:**1057-1069.
41. O'Rourke LM, Tooze R, Turner M, Sandoval DM, Carter RH, Tybulewicz VL, Fearon DT: CD19 as a membrane-anchored adaptor protein of B lymphocytes: costimulation of lipid and protein kinases by recruitment of Vav. *Immunity* 1998, **8:**635-645.
42. Okada T, Maeda A, Iwamatsu A, Gotoh K, Kurosaki T: BCAP: the tyrosine kinase substrate that connects B cell receptor to phosphoinositide 3-kinase activation. *Immunity* 2000, **13:**817-827.
43. Inabe K, Ishiai M, Scharenberg AM, Freshney N, Downward J, Kurosaki T: Vav3 modulates B cell receptor responses by regulating phosphoinositide 3-kinase activation. *J Exp Med* 2002, **195:**189-200.
44. Saito K, Scharenberg AM, Kinet JP: Interaction between the Btk PH domain and phosphatidylinositol-3,4,5-trisphosphate directly regulates Btk. *J Biol Chem* 2001, **276:**16201-16206.
45. Engels N, Konig LM, Heemann C, Lutz J, Tsubata T, Griep S, Schrader V, Wienands J: Recruitment of the cytoplasmic adaptor Grb2 to surface IgG and IgE provides antigen receptor-intrinsic costimulation to class-switched B cells. *Nat Immunol* 2009, **10:**1018-1025.
46. Kuhn J, Wong LE, Pirkuliyeva S, Schulz K, Schwiegk C, Funfgeld KG, Keppler S, Batista FD, Urlaub H, Habeck M, et al: The adaptor protein CIN85 assembles intracellular signaling clusters for B cell activation. *Sci Signal* 2016, **9:**ra66.
47. Guo B, Kato RM, Garcia-Lloret M, Wahl MI, Rawlings DJ: Engagement of the human pre-B cell receptor generates a lipid raft-dependent calcium signaling complex. *Immunity* 2000, **13:**243-253.
48. Su YW, Zhang Y, Schweikert J, Koretzky GA, Reth M, Wienands J: Interaction of SLP adaptors with the SH2 domain of Tec family kinases. *Eur J Immunol* 1999, **29:**3702-3711.
49. Chiu CW, Dalton M, Ishiai M, Kurosaki T, Chan AC: BLNK: molecular scaffolding through 'cis'-mediated organization of signaling proteins. *EMBO J* 2002, **21:**6461-6472.
50. Weber M, Treanor B, Depoil D, Shinohara H, Harwood NE, Hikida M, Kurosaki T, Batista FD: Phospholipase C-gamma2 and Vav cooperate within signaling microclusters to propagate B cell spreading in response to membrane-bound antigen. *J Exp Med* 2008, **205:**853-868.

51. Kim YJ, Sekiya F, Poulin B, Bae YS, Rhee SG: Mechanism of B-cell receptor-induced phosphorylation and activation of phospholipase C-gamma2. *Mol Cell Biol* 2004, **24:**9986-9999.
52. Hashimoto A, Okada H, Jiang A, Kurosaki M, Greenberg S, Clark EA, Kurosaki T: Involvement of guanosine triphosphatases and phospholipase C-gamma2 in extracellular signal-regulated kinase, c-Jun NH2-terminal kinase, and p38 mitogen-activated protein kinase activation by the B cell antigen receptor. *J Exp Med* 1998, **188:**1287-1295.
53. Petro JB, Rahman SM, Ballard DW, Khan WN: Bruton's tyrosine kinase is required for activation of IkappaB kinase and nuclear factor kappaB in response to B cell receptor engagement. *J Exp Med* 2000, **191:**1745-1754.
54. Bajpai UD, Zhang K, Teutsch M, Sen R, Wortis HH: Bruton's tyrosine kinase links the B cell receptor to nuclear factor kappaB activation. *J Exp Med* 2000, **191:**1735-1744.
55. Manning BD, Toker A: AKT/PKB Signaling: Navigating the Network. *Cell* 2017, **169:**381-405.
56. Craxton A, Jiang A, Kurosaki T, Clark EA: Syk and Bruton's tyrosine kinase are required for B cell antigen receptor-mediated activation of the kinase Akt. *J Biol Chem* 1999, **274:**30644-30650.
57. Ellmeier W, Jung S, Sunshine MJ, Hatam F, Xu Y, Baltimore D, Mano H, Littman DR: Severe B cell deficiency in mice lacking the tec kinase family members Tec and Btk. *J Exp Med* 2000, **192:**1611-1624.
58. de Bruijn MJ, Rip J, van der Ploeg EK, van Greuningen LW, Ta VT, Kil LP, Langerak AW, Rimmelzwaan GF, Ellmeier W, Hendriks RW, Corneth OB: Distinct and Overlapping Functions of TEC Kinase and BTK in B Cell Receptor Signaling. *J Immunol* 2017, **198:**3058-3068.
59. Engels N, Konig LM, Schulze W, Radtke D, Vanshylla K, Lutz J, Winkler TH, Nitschke L, Wienands J: The immunoglobulin tail tyrosine motif upgrades memory-type BCRs by incorporating a Grb2-Btk signalling module. *Nat Commun* 2014, **5:**5456.
60. Nimmerjahn F, Ravetch JV: Fcgamma receptors as regulators of immune responses. *Nat Rev Immunol* 2008, **8:**34-47.
61. Amigorena S, Bonnerot C, Drake JR, Choquet D, Hunziker W, Guillet JG, Webster P, Sautes C, Mellman I, Fridman WH: Cytoplasmic domain heterogeneity and functions of IgG Fc receptors in B lymphocytes. *Science* 1992, **256:**1808-1812.
62. Muta T, Kurosaki T, Misulovin Z, Sanchez M, Nussenzweig MC, Ravetch JV: A 13-amino-acid motif in the cytoplasmic domain of Fc gamma RIIB modulates B-cell receptor signalling. *Nature* 1994, **369:**340.
63. Bolland S, Ravetch JV: Inhibitory pathways triggered by ITIM-containing receptors. *Adv Immunol* 1999, **72:**149-177.
64. Ono M, Bolland S, Tempst P, Ravetch JV: Role of the inositol phosphatase SHIP in negative regulation of the immune system by the receptor Fc(gamma)RIIB. *Nature* 1996, **383:**263-266.
65. Ono M, Okada H, Bolland S, Yanagi S, Kurosaki T, Ravetch JV: Deletion of SHIP or SHP-1 reveals two distinct pathways for inhibitory signaling. *Cell* 1997, **90:**293-301.
66. Liu W, Quinto I, Chen X, Palmieri C, Rabin RL, Schwartz OM, Nelson DL, Scala G: Direct inhibition of Bruton's tyrosine kinase by IBtk, a Btk-binding protein. *Nat Immunol* 2001, **2:**939-946.
67. Kang SW, Wahl MI, Chu J, Kitaura J, Kawakami Y, Kato RM, Tabuchi R, Tarakhovsky A, Kawakami T, Turck CW, et al: PKCbeta modulates antigen receptor signaling via regulation of Btk membrane localization. *EMBO J* 2001, **20:**5692-5702.
68. Belver L, de Yebenes VG, Ramiro AR: MicroRNAs prevent the generation of autoreactive antibodies. *Immunity* 2010, **33:**713-722.
69. Bottoni A, Rizzotto L, Lai TH, Liu C, Smith LL, Mantel R, Reiff S, El-Gamal D, Larkin K, Johnson AJ, et al: Targeting BTK through microRNA in chronic lymphocytic leukemia. *Blood* 2016, **128:**3101-3112.
70. Yu L, Mohamed AJ, Simonson OE, Vargas L, Blomberg KE, Bjorkstrand B, Arteaga HJ, Nore BF, Smith CI: Proteasome-dependent autoregulation of Bruton tyrosine kinase (Btk) promoter via NF-kappaB. *Blood* 2008, **111:**4617-4626.
71. Ritter SL, Hall RA: Fine-tuning of GPCR activity by receptor-interacting proteins. *Nat Rev Mol Cell Biol* 2009, **10:**819-830.
72. Okada T, Ngo VN, Ekland EH, Forster R, Lipp M, Littman DR, Cyster JG: Chemokine requirements for B cell entry to lymph nodes and Peyer's patches. *J Exp Med* 2002, **196:**65-75.
73. Servant G, Weiner OD, Herzmark P, Balla T, Sedat JW, Bourne HR: Polarization of chemoattractant receptor signaling during neutrophil chemotaxis. *Science* 2000, **287:**1037-1040.
74. Lowry WE, Huang XY: G Protein beta gamma subunits act on the catalytic domain to stimulate Bruton's agammaglobulinemia tyrosine kinase. *J Biol Chem* 2002, **277:**1488-1492.
75. Tsukada S, Simon MI, Witte ON, Katz A: Binding of beta gamma subunits of heterotrimeric G proteins to the PH domain of Bruton tyrosine kinase. *Proc Natl Acad Sci U S A* 1994, **91:**11256-11260.
76. Bence K, Ma W, Kozasa T, Huang XY: Direct stimulation of Bruton's tyrosine kinase by G(q)-protein alpha-subunit. *Nature* 1997, **389:**296-299.
77. de Gorter DJ, Beuling EA, Kersseboom R, Middendorp S, van Gils JM, Hendriks RW, Pals ST, Spaargaren M: Bruton's tyrosine kinase and phospholipase Cgamma2 mediate chemokine-controlled B cell migration and homing. *Immunity* 2007, **26:**93-104.
78. Rawlings DJ, Schwartz MA, Jackson SW, Meyer-Bahlburg A: Integration of B cell responses through Toll-like receptors and antigen receptors. *Nat Rev Immunol* 2012, **12:**282-294.
79. Jefferies CA, Doyle S, Brunner C, Dunne A, Brint E, Wietek C, Walch E, Wirth T, O'Neill LA: Bruton's tyrosine kinase is a Toll/interleukin-1 receptor domain-binding protein that participates in nuclear factor kappaB activation by Toll-like receptor 4. *J Biol Chem* 2003, **278:**26258-26264.
80. Liu X, Zhan Z, Li D, Xu L, Ma F, Zhang P, Yao H, Cao X: Intracellular MHC class II molecules promote TLR-triggered innate immune responses by maintaining activation of the kinase Btk. *Nat Immunol* 2011, **12:**416-424.
81. Gray P, Dunne A, Brikos C, Jefferies CA, Doyle SL, O'Neill LA: MyD88 adapter-like (Mal) is phosphorylated by Bruton's tyrosine kinase during TLR2 and TLR4 signal transduction. *J Biol Chem* 2006, **281:**10489-10495.
82. Bournazos S, Wang TT, Ravetch JV: The Role and Function of Fcgamma Receptors on Myeloid Cells. *Microbiol Spectr* 2016, **4**.

83. Fearon ER, Winkelstein JA, Civin CI, Pardoll DM, Vogelstein B: Carrier detection in X-linked agammaglobulinemia by analysis of X-chromosome inactivation. *N Engl J Med* 1987, **316:**427-431.
84. Puck JM, Nussbaum RL, Conley ME: Carrier detection in X-linked severe combined immunodeficiency based on patterns of X chromosome inactivation. *J Clin Invest* 1987, **79:**1395-1400.
85. Melchers F, ten Boekel E, Seidl T, Kong XC, Yamagami T, Onishi K, Shimizu T, Rolink AG, Andersson J: Repertoire selection by pre-B-cell receptors and B-cell receptors, and genetic control of B-cell development from immature to mature B cells. *Immunol Rev* 2000, **175:**33-46.
86. Hendriks RW, Middendorp S: The pre-BCR checkpoint as a cell-autonomous proliferation switch. *Trends Immunol* 2004, **25:**249-256.
87. Hendriks RW, Bredius RG, Pike-Overzet K, Staal FJ: Biology and novel treatment options for XLA, the most common monogenetic immunodeficiency in man. *Expert Opin Ther Targets* 2011, **15:**1003-1021.
88. Herzog S, Reth M, Jumaa H: Regulation of B-cell proliferation and differentiation by pre-B-cell receptor signalling. *Nat Rev Immunol* 2009, **9:**195-205.
89. Ohnishi K, Melchers F: The nonimmunoglobulin portion of lambda5 mediates cell-autonomous pre-B cell receptor signaling. *Nat Immunol* 2003, **4:**849-856.
90. Ubelhart R, Bach MP, Eschbach C, Wossning T, Reth M, Jumaa H: N-linked glycosylation selectively regulates autonomous precursor BCR function. *Nat Immunol* 2010, **11:**759-765.
91. ten Boekel E, Yamagami T, Andersson J, Rolink AG, Melchers F: The formation and selection of cells expressing preB cell receptors and B cell receptors. *Curr Top Microbiol Immunol* 1999, **246:**3-9; discussion 9-10.
92. Wardemann H, Yurasov S, Schaefer A, Young JW, Meffre E, Nussenzweig MC: Predominant autoantibody production by early human B cell precursors. *Science* 2003, **301:**1374-1377.
93. Jumaa H, Mitterer M, Reth M, Nielsen PJ: The absence of SLP65 and Btk blocks B cell development at the preB cell receptor-positive stage. *Eur J Immunol* 2001, **31:**2164-2169.
94. Jumaa H, Bossaller L, Portugal K, Storch B, Lotz M, Flemming A, Schrappe M, Postila V, Riikonen P, Pelkonen J, et al: Deficiency of the adaptor SLP-65 in pre-B-cell acute lymphoblastic leukaemia. *Nature* 2003, **423:**452-456.
95. Middendorp S, Zijlstra AJ, Kersseboom R, Dingjan GM, Jumaa H, Hendriks RW: Tumor suppressor function of Bruton tyrosine kinase is independent of its catalytic activity. *Blood* 2005, **105:**259-265.
96. Kersseboom R, Middendorp S, Dingjan GM, Dahlenborg K, Reth M, Jumaa H, Hendriks RW: Bruton's tyrosine kinase cooperates with the B cell linker protein SLP-65 as a tumor suppressor in Pre-B cells. *J Exp Med* 2003, **198:**91-98.
97. Thompson EC, Cobb BS, Sabbattini P, Meixlsperger S, Parelho V, Liberg D, Taylor B, Dillon N, Georgopoulos K, Jumaa H, et al: Ikaros DNA-binding proteins as integral components of B cell developmental-stage-specific regulatory circuits. *Immunity* 2007, **26:**335-344.

98. Stadhouders R, de Bruijn MJ, Rother MB, Yuvaraj S, Ribeiro de Almeida C, Kolovos P, Van Zelm MC, van Ijcken W, Grosveld F, Soler E, Hendriks RW: Pre-B cell receptor signaling induces immunoglobulin kappa locus accessibility by functional redistribution of enhancer-mediated chromatin interactions. *PLoS Biol* 2014, **12:**e1001791.
99. Dingjan GM, Middendorp S, Dahlenborg K, Maas A, Grosveld F, Hendriks RW: Bruton's tyrosine kinase regulates the activation of gene rearrangements at the lambda light chain locus in precursor B cells in the mouse. *J Exp Med* 2001, **193:**1169-1178.
100. Gay D, Saunders T, Camper S, Weigert M: Receptor editing: an approach by autoreactive B cells to escape tolerance. *J Exp Med* 1993, **177:**999-1008.
101. Nemazee D, Weigert M: Revising B cell receptors. *J Exp Med* 2000, **191:**1813-1817.
102. Rolink A, Grawunder U, Haasner D, Strasser A, Melchers F: Immature surface Ig+ B cells can continue to rearrange kappa and lambda L chain gene loci. *J Exp Med* 1993, **178:**1263-1270.
103. Petro JB, Gerstein RM, Lowe J, Carter RS, Shinners N, Khan WN: Transitional type 1 and 2 B lymphocyte subsets are differentially responsive to antigen receptor signaling. *J Biol Chem* 2002, **277:**48009-48019.
104. Levine MH, Haberman AM, Sant'Angelo DB, Hannum LG, Cancro MP, Janeway CA, Jr., Shlomchik MJ: A B-cell receptor-specific selection step governs immature to mature B cell differentiation. *Proc Natl Acad Sci U S A* 2000, **97:**2743-2748.
105. Hammad H, Vanderkerken M, Pouliot P, Deswarte K, Toussaint W, Vergote K, Vandersarren L, Janssens S, Ramou I, Savvides SN, et al: Transitional B cells commit to marginal zone B cell fate by Taok3-mediated surface expression of ADAM10. *Nat Immunol* 2017, **18:**313-320.
106. Gibb DR, El Shikh M, Kang DJ, Rowe WJ, El Sayed R, Cichy J, Yagita H, Tew JG, Dempsey PJ, Crawford HC, Conrad DH: ADAM10 is essential for Notch2-dependent marginal zone B cell development and CD23 cleavage in vivo. *J Exp Med* 2010, **207:**623-635.
107. Martin F, Kearney JF: Positive selection from newly formed to marginal zone B cells depends on the rate of clonal production, CD19, and btk. *Immunity* 2000, **12:**39-49.
108. Corneth OB, Klein Wolterink RG, Hendriks RW: BTK Signaling in B Cell Differentiation and Autoimmunity. *Curr Top Microbiol Immunol* 2016, **393:**67-105.
109. Victora GD: SnapShot: the germinal center reaction. *Cell* 2014, **159:**700-700 e701.
110. Oropallo MA, Cerutti A: Germinal center reaction: antigen affinity and presentation explain it all. *Trends Immunol* 2014, **35:**287-289.
111. Dingjan GM, Maas A, Nawijn MC, Smit L, Voerman JS, Grosveld F, Hendriks RW: Severe B cell deficiency and disrupted splenic architecture in transgenic mice expressing the E41K mutated form of Bruton's tyrosine kinase. *EMBO J* 1998, **17:**5309-5320.
112. Kersseboom R, Kil L, Flierman R, van der Zee M, Dingjan GM, Middendorp S, Maas A, Hendriks RW: Constitutive activation of Bruton's tyrosine kinase induces the formation of autoreactive IgM plasma cells. *Eur J Immunol* 2010, **40:**2643-2654.

113. Kil LP, de Bruijn MJ, van Nimwegen M, Corneth OB, van Hamburg JP, Dingjan GM, Thaiss F, Rimmelzwaan GF, Elewaut D, Delsing D, et al: Btk levels set the threshold for B-cell activation and negative selection of autoreactive B cells in mice. *Blood* 2012, **119:**3744-3756.
114. Corneth OB, de Bruijn MJ, Rip J, Asmawidjaja PS, Kil LP, Hendriks RW: Enhanced Expression of Bruton's Tyrosine Kinase in B Cells Drives Systemic Autoimmunity by Disrupting T Cell Homeostasis. *J Immunol* 2016, **197:**58-67.
115. Ammann EM, Shanafelt TD, Wright KB, McDowell BD, Link BK, Chrischilles EA: Updating survival estimates in patients with chronic lymphocytic leukemia or small lymphocytic lymphoma (CLL/SLL) based on treatment-free interval length. *Leuk Lymphoma* 2017**:**1-7.
116. Kil LP, Yuvaraj S, Langerak AW, Hendriks RW: The role of B cell receptor stimulation in CLL pathogenesis. *Curr Pharm Des* 2012, **18:**3335-3355.
117. Zenz T, Eichhorst B, Busch R, Denzel T, Habe S, Winkler D, Buhler A, Edelmann J, Bergmann M, Hopfinger G, et al: TP53 mutation and survival in chronic lymphocytic leukemia. *J Clin Oncol* 2010, **28:**4473-4479.
118. Gonzalez D, Martinez P, Wade R, Hockley S, Oscier D, Matutes E, Dearden CE, Richards SM, Catovsky D, Morgan GJ: Mutational status of the TP53 gene as a predictor of response and survival in patients with chronic lymphocytic leukemia: results from the LRF CLL4 trial. *J Clin Oncol* 2011, **29:**2223-2229.
119. Robak P, Robak T: Novel synthetic drugs currently in clinical development for chronic lymphocytic leukemia. *Expert Opin Investig Drugs* 2017, **26:**1249-1265.
120. Malcikova J, Smardova J, Rocnova L, Tichy B, Kuglik P, Vranova V, Cejkova S, Svitakova M, Skuhrova Francova H, Brychtova Y, et al: Monoallelic and biallelic inactivation of TP53 gene in chronic lymphocytic leukemia: selection, impact on survival, and response to DNA damage. *Blood* 2009, **114:**5307-5314.
121. Zenz T, Krober A, Scherer K, Habe S, Buhler A, Benner A, Denzel T, Winkler D, Edelmann J, Schwanen C, et al: Monoallelic TP53 inactivation is associated with poor prognosis in chronic lymphocytic leukemia: results from a detailed genetic characterization with long-term follow-up. *Blood* 2008, **112:**3322-3329.
122. Chiorazzi N, Ferrarini M: Cellular origin(s) of chronic lymphocytic leukemia: cautionary notes and additional considerations and possibilities. *Blood* 2011, **117:**1781-1791.
123. Klein U, Tu Y, Stolovitzky GA, Mattioli M, Cattoretti G, Husson H, Freedman A, Inghirami G, Cro L, Baldini L, et al: Gene expression profiling of B cell chronic lymphocytic leukemia reveals a homogeneous phenotype related to memory B cells. *J Exp Med* 2001, **194:**1625-1638.
124. Seifert M, Sellmann L, Bloehdorn J, Wein F, Stilgenbauer S, Durig J, Kuppers R: Cellular origin and pathophysiology of chronic lymphocytic leukemia. *J Exp Med* 2012, **209:**2183-2198.
125. Griffin DO, Holodick NE, Rothstein TL: Human B1 cells in umbilical cord and adult peripheral blood express the novel phenotype CD20+ CD27+ CD43+ CD70. *J Exp Med* 2011, **208:**67-80.
126. DiLillo DJ, Weinberg JB, Yoshizaki A, Horikawa M, Bryant JM, Iwata Y, Matsushita T, Matta KM, Chen Y, Venturi GM, et al: Chronic lymphocytic leukemia and regulatory B cells share IL-10 competence and immunosuppressive function. *Leukemia* 2013, **27:**170-182.
127. Muggen AF, Singh SP, Hendriks RW, Langerak AW: Targeting Signaling Pathways in Chronic Lymphocytic Leukemia. *Curr Cancer Drug Targets* 2016, **16:**669-688.

128. Damle RN, Wasil T, Fais F, Ghiotto F, Valetto A, Allen SL, Buchbinder A, Budman D, Dittmar K, Kolitz J, et al: Ig V gene mutation status and CD38 expression as novel prognostic indicators in chronic lymphocytic leukemia. *Blood* 1999, **94:**1840-1847.
129. Agathangelidis A, Darzentas N, Hadzidimitriou A, Brochet X, Murray F, Yan XJ, Davis Z, van Gastel-Mol EJ, Tresoldi C, Chu CC, et al: Stereotyped B-cell receptors in one-third of chronic lymphocytic leukemia: a molecular classification with implications for targeted therapies. *Blood* 2012, **119:**4467-4475.
130. Murray F, Darzentas N, Hadzidimitriou A, Tobin G, Boudjogra M, Scielzo C, Laoutaris N, Karlsson K, Baran-Marzsak F, Tsaftaris A, et al: Stereotyped patterns of somatic hypermutation in subsets of patients with chronic lymphocytic leukemia: implications for the role of antigen selection in leukemogenesis. *Blood* 2008, **111:**1524-1533.
131. Hayakawa K, Formica AM, Colombo MJ, Shinton SA, Brill-Dashoff J, Morse Iii HC, Li YS, Hardy RR: Loss of a chromosomal region with synteny to human 13q14 occurs in mouse chronic lymphocytic leukemia that originates from early-generated B-1 B cells. *Leukemia* 2016, **30:**1510-1519.
132. Chen SS, Batliwalla F, Holodick NE, Yan XJ, Yancopoulos S, Croce CM, Rothstein TL, Chiorazzi N: Autoantigen can promote progression to a more aggressive TCL1 leukemia by selecting variants with enhanced B-cell receptor signaling. *Proc Natl Acad Sci U S A* 2013, **110:**E1500-1507.
133. Singh SP, Pillai SY, de Bruijn MJW, Stadhouders R, Corneth OBJ, van den Ham HJ, Muggen A, van IW, Slinger E, Kuil A, et al: Cell lines generated from a chronic lymphocytic leukemia mouse model exhibit constitutive Btk and Akt signaling. *Oncotarget* 2017, **8:**71981-71995.
134. Messmer BT, Albesiano E, Efremov DG, Ghiotto F, Allen SL, Kolitz J, Foa R, Damle RN, Fais F, Messmer D, et al: Multiple distinct sets of stereotyped antigen receptors indicate a role for antigen in promoting chronic lymphocytic leukemia. *J Exp Med* 2004, **200:**519-525.
135. Herve M, Xu K, Ng YS, Wardemann H, Albesiano E, Messmer BT, Chiorazzi N, Meffre E: Unmutated and mutated chronic lymphocytic leukemias derive from self-reactive B cell precursors despite expressing different antibody reactivity. *J Clin Invest* 2005, **115:**1636-1643.
136. Lanemo Myhrinder A, Hellqvist E, Sidorova E, Soderberg A, Baxendale H, Dahle C, Willander K, Tobin G, Backman E, Soderberg O, et al: A new perspective: molecular motifs on oxidized LDL, apoptotic cells, and bacteria are targets for chronic lymphocytic leukemia antibodies. *Blood* 2008, **111:**3838-3848.
137. Hoogeboom R, van Kessel KP, Hochstenbach F, Wormhoudt TA, Reinten RJ, Wagner K, Kater AP, Guikema JE, Bende RJ, van Noesel CJ: A mutated B cell chronic lymphocytic leukemia subset that recognizes and responds to fungi. *J Exp Med* 2013, **210:**59-70.
138. Jimenez de Oya N, De Giovanni M, Fioravanti J, Ubelhart R, Di Lucia P, Fiocchi A, Iacovelli S, Efremov DG, Caligaris-Cappio F, Jumaa H, et al: Pathogen-specific B-cell receptors drive chronic lymphocytic leukemia by light-chain-dependent cross-reaction with autoantigens. *EMBO Mol Med* 2017, **9:**1482-1490.
139. Duhren-von Minden M, Ubelhart R, Schneider D, Wossning T, Bach MP, Buchner M, Hofmann D, Surova E, Follo M, Kohler F, et al: Chronic lymphocytic leukaemia is driven by antigen-independent cell-autonomous signalling. *Nature* 2012, **489:**309-312.

140. Minici C, Gounari M, Ubelhart R, Scarfo L, Duhren-von Minden M, Schneider D, Tasdogan A, Alkhatib A, Agathangelidis A, Ntoufa S, et al: Distinct homotypic B-cell receptor interactions shape the outcome of chronic lymphocytic leukaemia. *Nat Commun* 2017, **8:**15746.
141. Herman SE, Gordon AL, Hertlein E, Ramanunni A, Zhang X, Jaglowski S, Flynn J, Jones J, Blum KA, Buggy JJ, et al: Bruton tyrosine kinase represents a promising therapeutic target for treatment of chronic lymphocytic leukemia and is effectively targeted by PCI-32765. *Blood* 2011, **117:**6287-6296.
142. Ponader S, Chen SS, Buggy JJ, Balakrishnan K, Gandhi V, Wierda WG, Keating MJ, O'Brien S, Chiorazzi N, Burger JA: The Bruton tyrosine kinase inhibitor PCI-32765 thwarts chronic lymphocytic leukemia cell survival and tissue homing in vitro and in vivo. *Blood* 2012, **119:**1182-1189.
143. Kil LP, de Bruijn MJ, van Hulst JA, Langerak AW, Yuvaraj S, Hendriks RW: Bruton's tyrosine kinase mediated signaling enhances leukemogenesis in a mouse model for chronic lymphocytic leukemia. *Am J Blood Res* 2013, **3:**71-83.
144. Ramsay AD, Rodriguez-Justo M: Chronic lymphocytic leukaemia--the role of the microenvironment pathogenesis and therapy. *Br J Haematol* 2013, **162:**15-24.
145. Burger JA, Gribben JG: The microenvironment in chronic lymphocytic leukemia (CLL) and other B cell malignancies: insight into disease biology and new targeted therapies. *Semin Cancer Biol* 2014, **24:**71-81.
146. de Rooij MF, Kuil A, Geest CR, Eldering E, Chang BY, Buggy JJ, Pals ST, Spaargaren M: The clinically active BTK inhibitor PCI-32765 targets B-cell receptor- and chemokine-controlled adhesion and migration in chronic lymphocytic leukemia. *Blood* 2012, **119:**2590-2594.
147. Cheah CY, Seymour JF, Wang ML: Mantle Cell Lymphoma. *J Clin Oncol* 2016, **34:**1256-1269.
148. Bertoni F, Rinaldi A, Zucca E, Cavalli F: Update on the molecular biology of mantle cell lymphoma. *Hematol Oncol* 2006, **24:**22-27.
149. Meggendorfer M, Kern W, Haferlach C, Haferlach T, Schnittger S: SOX11 overexpression is a specific marker for mantle cell lymphoma and correlates with t(11;14) translocation, CCND1 expression and an adverse prognosis. *Leukemia* 2013, **27:**2388-2391.
150. Navarro A, Clot G, Royo C, Jares P, Hadzidimitriou A, Agathangelidis A, Bikos V, Darzentas N, Papadaki T, Salaverria I, et al: Molecular subsets of mantle cell lymphoma defined by the IGHV mutational status and SOX11 expression have distinct biologic and clinical features. *Cancer Res* 2012, **72:**5307-5316.
151. Cinar M, Hamedani F, Mo Z, Cinar B, Amin HM, Alkan S: Bruton tyrosine kinase is commonly overexpressed in mantle cell lymphoma and its attenuation by Ibrutinib induces apoptosis. *Leuk Res* 2013, **37:**1271-1277.
152. Pighi C, Gu TL, Dalai I, Barbi S, Parolini C, Bertolaso A, Pedron S, Parisi A, Ren J, Cecconi D, et al: Phospho-proteomic analysis of mantle cell lymphoma cells suggests a pro-survival role of B-cell receptor signaling. *Cell Oncol (Dordr)* 2011, **34:**141-153.
153. Boyd RS, Jukes-Jones R, Walewska R, Brown D, Dyer MJ, Cain K: Protein profiling of plasma membranes defines aberrant signaling pathways in mantle cell lymphoma. *Mol Cell Proteomics* 2009, **8:**1501-1515.

154. Chang BY, Francesco M, De Rooij MF, Magadala P, Steggerda SM, Huang MM, Kuil A, Herman SE, Chang S, Pals ST, et al: Egress of CD19(+)CD5(+) cells into peripheral blood following treatment with the Bruton tyrosine kinase inhibitor ibrutinib in mantle cell lymphoma patients. *Blood* 2013, **122:**2412-2424.
155. Treon SP, Xu L, Yang G, Zhou Y, Liu X, Cao Y, Sheehy P, Manning RJ, Patterson CJ, Tripsas C, et al: MYD88 L265P somatic mutation in Waldenstrom's macroglobulinemia. *N Engl J Med* 2012, **367:**826-833.
156. Pasqualucci L, Trifonov V, Fabbri G, Ma J, Rossi D, Chiarenza A, Wells VA, Grunn A, Messina M, Elliot O, et al: Analysis of the coding genome of diffuse large B-cell lymphoma. *Nat Genet* 2011, **43:**830-837.
157. Puente XS, Pinyol M, Quesada V, Conde L, Ordonez GR, Villamor N, Escaramis G, Jares P, Bea S, Gonzalez-Diaz M, et al: Whole-genome sequencing identifies recurrent mutations in chronic lymphocytic leukaemia. *Nature* 2011, **475:**101-105.
158. Ngo VN, Young RM, Schmitz R, Jhavar S, Xiao W, Lim KH, Kohlhammer H, Xu W, Yang Y, Zhao H, et al: Oncogenically active MYD88 mutations in human lymphoma. *Nature* 2011, **470:**115-119.
159. Montesinos-Rongen M, Godlewska E, Brunn A, Wiestler OD, Siebert R, Deckert M: Activating L265P mutations of the MYD88 gene are common in primary central nervous system lymphoma. *Acta Neuropathol* 2011, **122:**791-792.
160. Yang G, Zhou Y, Liu X, Xu L, Cao Y, Manning RJ, Patterson CJ, Buhrlage SJ, Gray N, Tai YT, et al: A mutation in MYD88 (L265P) supports the survival of lymphoplasmacytic cells by activation of Bruton tyrosine kinase in Waldenstrom macroglobulinemia. *Blood* 2013, **122:**1222-1232.
161. Hunter ZR, Xu L, Yang G, Zhou Y, Liu X, Cao Y, Manning RJ, Tripsas C, Patterson CJ, Sheehy P, Treon SP: The genomic landscape of Waldenstrom macroglobulinemia is characterized by highly recurring MYD88 and WHIM-like CXCR4 mutations, and small somatic deletions associated with B-cell lymphomagenesis. *Blood* 2014, **123:**1637-1646.
162. Ngo HT, Leleu X, Lee J, Jia X, Melhem M, Runnels J, Moreau AS, Burwick N, Azab AK, Roccaro A, et al: SDF-1/CXCR4 and VLA-4 interaction regulates homing in Waldenstrom macroglobulinemia. *Blood* 2008, **112:**150-158.
163. Iqbal J, Shen Y, Huang X, Liu Y, Wake L, Liu C, Deffenbacher K, Lachel CM, Wang C, Rohr J, et al: Global microRNA expression profiling uncovers molecular markers for classification and prognosis in aggressive B-cell lymphoma. *Blood* 2015, **125:**1137-1145.
164. Dunleavy K, Wilson WH: Primary mediastinal B-cell lymphoma and mediastinal gray zone lymphoma: do they require a unique therapeutic approach? *Blood* 2015, **125:**33-39.
165. Alizadeh AA, Eisen MB, Davis RE, Ma C, Lossos IS, Rosenwald A, Boldrick JC, Sabet H, Tran T, Yu X, et al: Distinct types of diffuse large B-cell lymphoma identified by gene expression profiling. *Nature* 2000, **403:**503-511.
166. Lenz G, Nagel I, Siebert R, Roschke AV, Sanger W, Wright GW, Dave SS, Tan B, Zhao H, Rosenwald A, et al: Aberrant immunoglobulin class switch recombination and switch translocations in activated B cell-like diffuse large B cell lymphoma. *J Exp Med* 2007, **204:**633-643.
167. Roschewski M, Staudt LM, Wilson WH: Diffuse large B-cell lymphoma-treatment approaches in the molecular era. *Nat Rev Clin Oncol* 2014, **11:**12-23.

168. Davis RE, Brown KD, Siebenlist U, Staudt LM: Constitutive nuclear factor kappaB activity is required for survival of activated B cell-like diffuse large B cell lymphoma cells. *J Exp Med* 2001, **194:**1861-1874.
169. Ngo VN, Davis RE, Lamy L, Yu X, Zhao H, Lenz G, Lam LT, Dave S, Yang L, Powell J, Staudt LM: A loss-of-function RNA interference screen for molecular targets in cancer. *Nature* 2006, **441:**106-110.
170. Compagno M, Lim WK, Grunn A, Nandula SV, Brahmachary M, Shen Q, Bertoni F, Ponzoni M, Scandurra M, Califano A, et al: Mutations of multiple genes cause deregulation of NF-kappaB in diffuse large B-cell lymphoma. *Nature* 2009, **459:**717-721.
171. Lenz G, Davis RE, Ngo VN, Lam L, George TC, Wright GW, Dave SS, Zhao H, Xu W, Rosenwald A, et al: Oncogenic CARD11 mutations in human diffuse large B cell lymphoma. *Science* 2008, **319:**1676-1679.
172. Davis RE, Ngo VN, Lenz G, Tolar P, Young RM, Romesser PB, Kohlhammer H, Lamy L, Zhao H, Yang Y, et al: Chronic active B-cell-receptor signalling in diffuse large B-cell lymphoma. *Nature* 2010, **463:**88-92.
173. Chen L, Monti S, Juszczynski P, Ouyang J, Chapuy B, Neuberg D, Doench JG, Bogusz AM, Habermann TM, Dogan A, et al: SYK inhibition modulates distinct PI3K/AKT- dependent survival pathways and cholesterol biosynthesis in diffuse large B cell lymphomas. *Cancer Cell* 2013, **23:**826-838.
174. Havranek O, Xu J, Kohrer S, Wang Z, Becker L, Comer JM, Henderson J, Ma W, Man Chun Ma J, Westin JR, et al: Tonic B-cell receptor signaling in diffuse large B-cell lymphoma. *Blood* 2017, **130:**995-1006.
175. Pfeifer M, Grau M, Lenze D, Wenzel SS, Wolf A, Wollert-Wulf B, Dietze K, Nogai H, Storek B, Madle H, et al: PTEN loss defines a PI3K/AKT pathway-dependent germinal center subtype of diffuse large B-cell lymphoma. *Proc Natl Acad Sci U S A* 2013, **110:**12420-12425.
176. Lenz G, Wright GW, Emre NC, Kohlhammer H, Dave SS, Davis RE, Carty S, Lam LT, Shaffer AL, Xiao W, et al: Molecular subtypes of diffuse large B-cell lymphoma arise by distinct genetic pathways. *Proc Natl Acad Sci U S A* 2008, **105:**13520-13525.
177. Grommes C, Pastore A, Palaskas N, Tang SS, Campos C, Schartz D, Codega P, Nichol D, Clark O, Hsieh WY, et al: Ibrutinib Unmasks Critical Role of Bruton Tyrosine Kinase in Primary CNS Lymphoma. *Cancer Discov* 2017, **7:**1018-1029.
178. Krysiak K, Gomez F, White BS, Matlock M, Miller CA, Trani L, Fronick CC, Fulton RS, Kreisel F, Cashen AF, et al: Recurrent somatic mutations affecting B-cell receptor signaling pathway genes in follicular lymphoma. *Blood* 2017, **129:**473-483.
179. Yang Y, Shi J, Gu Z, Salama ME, Das S, Wendlandt E, Xu H, Huang J, Tao Y, Hao M, et al: Bruton tyrosine kinase is a therapeutic target in stem-like cells from multiple myeloma. *Cancer Res* 2015, **75:**594-604.
180. Gu C, Peng H, Lu Y, Yang H, Tian Z, Yin G, Zhang W, Lu S, Zhang Y, Yang Y: BTK suppresses myeloma cellular senescence through activating AKT/P27/Rb signaling. *Oncotarget* 2017, **8:**56858-56867.
181. Tai YT, Chang BY, Kong SY, Fulciniti M, Yang G, Calle Y, Hu Y, Lin J, Zhao JJ, Cagnetta A, et al: Bruton tyrosine kinase inhibition is a novel therapeutic strategy targeting tumor in the bone marrow microenvironment in multiple myeloma. *Blood* 2012, **120:**1877-1887.
182. Yan Q, Huang Y, Watkins AJ, Kocialkowski S, Zeng N, Hamoudi RA, Isaacson PG, de Leval L, Wotherspoon A, Du MQ: BCR and TLR signaling pathways are recurrently targeted by genetic changes in splenic marginal zone lymphomas. *Haematologica* 2012, **97:**595-598.
183. Clipson A, Wang M, de Leval L, Ashton-Key M, Wotherspoon A, Vassiliou G, Bolli N, Grove C, Moody S, Escudero-Ibarz L, et al: KLF2 mutation is the most frequent somatic change in splenic marginal zone lymphoma and identifies a subset with distinct genotype. *Leukemia* 2015, **29:**1177-1185.
184. Pan Z, Scheerens H, Li SJ, Schultz BE, Sprengeler PA, Burrill LC, Mendonca RV, Sweeney MD, Scott KC, Grothaus PG, et al: Discovery of selective irreversible inhibitors for Bruton's tyrosine kinase. *ChemMedChem* 2007, **2:**58-61.
185. Honigberg LA, Smith AM, Sirisawad M, Verner E, Loury D, Chang B, Li S, Pan Z, Thamm DH, Miller RA, Buggy JJ: The Bruton tyrosine kinase inhibitor PCI-32765 blocks B-cell activation and is efficacious in models of autoimmune disease and B-cell malignancy. *Proc Natl Acad Sci U S A* 2010, **107:**13075-13080.
186. Advani RH, Buggy JJ, Sharman JP, Smith SM, Boyd TE, Grant B, Kolibaba KS, Furman RR, Rodriguez S, Chang BY, et al: Bruton tyrosine kinase inhibitor ibrutinib (PCI-32765) has significant activity in patients with relapsed/refractory B-cell malignancies. *J Clin Oncol* 2013, **31:**88-94.
187. Wang ML, Rule S, Martin P, Goy A, Auer R, Kahl BS, Jurczak W, Advani RH, Romaguera JE, Williams ME, et al: Targeting BTK with ibrutinib in relapsed or refractory mantle-cell lymphoma. *N Engl J Med* 2013, **369:**507-516.
188. Treon SP, Tripsas CK, Meid K, Warren D, Varma G, Green R, Argyropoulos KV, Yang G, Cao Y, Xu L, et al: Ibrutinib in previously treated Waldenstrom's macroglobulinemia. *N Engl J Med* 2015, **372:**1430-1440.
189. Noy A, de Vos S, Thieblemont C, Martin P, Flowers CR, Morschhauser F, Collins GP, Ma S, Coleman M, Peles S, et al: Targeting Bruton tyrosine kinase with ibrutinib in relapsed/refractory marginal zone lymphoma. *Blood* 2017, **129:**2224-2232.
190. Burger JA, Wiestner A: Targeting B cell receptor signalling in cancer: preclinical and clinical advances. *Nat Rev Cancer* 2018.
191. Mason JA, Hagel KR, Hawk MA, Schafer ZT: Metabolism during ECM Detachment: Achilles Heel of Cancer Cells? *Trends Cancer* 2017, **3:**475-481.
192. Pals ST, Kersten MJ, Spaargaren M: Targeting cell adhesion and homing as strategy to cure Waldenstrom's macroglobulinemia. *Best Pract Res Clin Haematol* 2016, **29:**161-168.
193. Woyach JA, Furman RR, Liu TM, Ozer HG, Zapatka M, Ruppert AS, Xue L, Li DH, Steggerda SM, Versele M, et al: Resistance mechanisms for the Bruton's tyrosine kinase inhibitor ibrutinib. *N Engl J Med* 2014, **370:**2286-2294.
194. Furman RR, Cheng S, Lu P, Setty M, Perez AR, Guo A, Racchumi J, Xu G, Wu H, Ma J, et al: Ibrutinib resistance in chronic lymphocytic leukemia. *N Engl J Med* 2014, **370:**2352-2354.
195. Kadri S, Lee J, Fitzpatrick C, Galanina N, Sukhanova M, Venkataraman G, Sharma S, Long B, Petras K, Theissen M, et al: Clonal evolution underlying leukemia progression and Richter transformation in patients with ibrutinib-relapsed CLL. *Blood Adv* 2017, **1:**715-727.
196. Wilson WH, Young RM, Schmitz R, Yang Y, Pittaluga S, Wright G, Lih CJ, Williams PM, Shaffer AL, Gerecitano J, et al: Targeting B cell receptor signaling with ibrutinib in diffuse large B cell lymphoma. *Nat Med* 2015, **21:**922-926.

197. Wu C, de Miranda NF, Chen L, Wasik AM, Mansouri L, Jurczak W, Galazka K, Dlugosz-Danecka M, Machaczka M, Zhang H, et al: Genetic heterogeneity in primary and relapsed mantle cell lymphomas: Impact of recurrent CARD11 mutations. *Oncotarget* 2016, **7:**38180-38190.
198. Maddocks KJ, Ruppert AS, Lozanski G, Heerema NA, Zhao W, Abruzzo L, Lozanski A, Davis M, Gordon A, Smith LL, et al: Etiology of Ibrutinib Therapy Discontinuation and Outcomes in Patients With Chronic Lymphocytic Leukemia. *JAMA Oncol* 2015, **1:**80-87.
199. Coutre SE, Furman RR, Flinn IW, Burger JA, Blum K, Sharman J, Jones J, Wierda W, Zhao W, Heerema NA, et al: Extended Treatment with Single-Agent Ibrutinib at the 420 mg Dose Leads to Durable Responses in Chronic Lymphocytic Leukemia/Small Lymphocytic Lymphoma. *Clin Cancer Res* 2017, **23:**1149-1155.
200. Brown JR, Hillmen P, O'Brien S, Barrientos JC, Reddy NM, Coutre SE, Tam CS, Mulligan SP, Jaeger U, Barr PM, et al: Extended follow-up and impact of high-risk prognostic factors from the phase 3 RESONATE study in patients with previously treated CLL/SLL. *Leukemia* 2017.
201. Mulligan SP, Ward CM, Whalley D, Hilmer SN: Atrial fibrillation, anticoagulant stroke prophylaxis and bleeding risk with ibrutinib therapy for chronic lymphocytic leukaemia and lymphoproliferative disorders. *Br J Haematol* 2016, **175:**359-364.
202. Jones JA, Hillmen P, Coutre S, Tam C, Furman RR, Barr PM, Schuster SJ, Kipps TJ, Flinn IW, Jaeger U, et al: Use of anticoagulants and antiplatelet in patients with chronic lymphocytic leukaemia treated with single-agent ibrutinib. *Br J Haematol* 2017, **178:**286-291.
203. Wiczer TE, Levine LB, Brumbaugh J, Coggins J, Zhao Q, Ruppert AS, Rogers K, McCoy A, Mousa L, Guha A, et al: Cumulative incidence, risk factors, and management of atrial fibrillation in patients receiving ibrutinib. *Blood Adv* 2017, **1:**1739-1748.
204. McMullen JR, Boey EJ, Ooi JY, Seymour JF, Keating MJ, Tam CS: Ibrutinib increases the risk of atrial fibrillation, potentially through inhibition of cardiac PI3K-Akt signaling. *Blood* 2014, **124:**3829-3830.
205. Byrd JC, Furman RR, Coutre SE, Burger JA, Blum KA, Coleman M, Wierda WG, Jones JA, Zhao W, Heerema NA, et al: Three-year follow-up of treatment-naïve and previously treated patients with CLL and SLL receiving single-agent ibrutinib. *Blood* 2015, **125:**2497-2506.
206. O'Brien SM, Furman RR, Coutre SE, Flinn IW, Burger J, Blum K, Sharman J, Wierda WG, Jones J, Zhao W, et al: Five-year experience with single-agent ibrutinib in patients with previously untreated and relapsed/refractory chronic lymphocytic leukemia/small lymphocytic leukemia. *Blood* 2016, **128**.
207. Herman SEM, Montraveta A, Niemann CU, Mora-Jensen H, Gulrajani M, Krantz F, Mantel R, Smith LL, McClanahan F, Harrington BK, et al: The Bruton Tyrosine Kinase (BTK) Inhibitor Acalabrutinib Demonstrates Potent On-Target Effects and Efficacy in Two Mouse Models of Chronic Lymphocytic Leukemia. *Clin Cancer Res* 2017, **23:**2831-2841.
208. Quek LS, Bolen J, Watson SP: A role for Bruton's tyrosine kinase (Btk) in platelet activation by collagen. *Curr Biol* 1998, **8:**1137-1140.
209. Futatani T, Watanabe C, Baba Y, Tsukada S, Ochs HD: Bruton's tyrosine kinase is present in normal platelets and its absence identifies patients with X-linked agammaglobulinaemia and carrier females. *Br J Haematol* 2001, **114:**141-149.

210. Bye AP, Unsworth AJ, Desborough MJ, Hildyard CAT, Appleby N, Bruce D, Kriek N, Nock SH, Sage T, Hughes CE, Gibbins JM: Severe platelet dysfunction in NHL patients receiving ibrutinib is absent in patients receiving acalabrutinib. *Blood Adv* 2017, **1:**2610-2623.
211. Tillman BF, Pauff JM, Satyanarayana G, Talbott M, Warner JL: Systematic review of infectious events with the BTK inhibitor ibrutinib in the treatment of haematologic malignancies. *Eur J Haematol* 2017.
212. Long M, Beckwith K, Do P, Mundy BL, Gordon A, Lehman AM, Maddocks KJ, Cheney C, Jones JA, Flynn JM, et al: Ibrutinib treatment improves T cell number and function in CLL patients. *J Clin Invest* 2017, **127:**3052-3064.
213. Schutt SD, Fu J, Nguyen H, Bastian D, Heinrichs J, Wu Y, Liu C, McDonald DG, Pidala J, Yu XZ: Inhibition of BTK and ITK with Ibrutinib Is Effective in the Prevention of Chronic Graft-versus-Host Disease in Mice. *PLoS One* 2015, **10:**e0137641.
214. Dubovsky JA, Flynn R, Du J, Harrington BK, Zhong Y, Kaffenberger B, Yang C, Towns WH, Lehman A, Johnson AJ, et al: Ibrutinib treatment ameliorates murine chronic graft-versus-host disease. *J Clin Invest* 2014, **124:**4867-4876.
215. Ryan CE, Sahaf B, Logan AC, O'Brien S, Byrd JC, Hillmen P, Brown JR, Dyer MJ, Mato AR, Keating MJ, et al: Ibrutinib efficacy and tolerability in patients with relapsed chronic lymphocytic leukemia following allogeneic HCT. *Blood* 2016, **128:**2899-2908.
216. Kohrt HE, Sagiv-Barfi I, Rafiq S, Herman SE, Butchar JP, Cheney C, Zhang X, Buggy JJ, Muthusamy N, Levy R, et al: Ibrutinib antagonizes rituximab-dependent NK cell-mediated cytotoxicity. *Blood* 2014, **123:**1957-1960.
217. Wu J, Liu C, Tsui ST, Liu D: Second-generation inhibitors of Bruton tyrosine kinase. *J Hematol Oncol* 2016, **9:**80.
218. Harrington BK, Gardner HL, Izumi R, Hamdy A, Rothbaum W, Coombes KR, Covey T, Kaptein A, Gulrajani M, Van Lith B, et al: Preclinical Evaluation of the Novel BTK Inhibitor Acalabrutinib in Canine Models of B-Cell Non-Hodgkin Lymphoma. *PLoS One* 2016, **11:**e0159607.
219. Wang M, Rule S, Zinzani PL, Goy A, Casasnovas O, Smith SD, Damaj G, Doorduijn J, Lamy T, Morschhauser F, et al: Acalabrutinib in relapsed or refractory mantle cell lymphoma (ACE-LY-004): a single-arm, multicentre, phase 2 trial. *Lancet* 2017.
220. Acalabrutinib Approved for MCL. *Cancer Discov* 2018, **8:**OF6.
221. Thompson PA, Burger JA: Bruton's tyrosine kinase inhibitors: first and second generation agents for patients with Chronic Lymphocytic Leukemia (CLL). *Expert Opin Investig Drugs* 2018, **27:**31-42.
222. Walter HS, Rule SA, Dyer MJ, Karlin L, Jones C, Cazin B, Quittet P, Shah N, Hutchinson CV, Honda H, et al: A phase 1 clinical trial of the selective BTK inhibitor ONO/GS-4059 in relapsed and refractory mature B-cell malignancies. *Blood* 2016, **127:**411-419.
223. Koprulu AD, Ellmeier W: The role of Tec family kinases in mononuclear phagocytes. *Crit Rev Immunol* 2009, **29:**317-333.

224. Mirsafian H, Ripen AM, Leong WM, Chear CT, Bin Mohamad S, Merican AF: Transcriptome profiling of monocytes from XLA patients revealed the innate immune function dysregulation due to the BTK gene expression deficiency. *Sci Rep* 2017, **7:**6836.

225. Doyle SL, Jefferies CA, Feighery C, O'Neill LA: Signaling by Toll-like receptors 8 and 9 requires Bruton's tyrosine kinase. *J Biol Chem* 2007, **282:**36953-36960.

226. Sochorova K, Horvath R, Rozkova D, Litzman J, Bartunkova J, Sediva A, Spisek R: Impaired Toll-like receptor 8-mediated IL-6 and TNF-alpha production in antigen-presenting cells from patients with X-linked agammaglobulinemia. *Blood* 2007, **109:**2553-2556.

227. Lougaris V, Baronio M, Vitali M, Tampella G, Cattalini M, Tassone L, Soresina A, Badolato R, Plebani A: Bruton tyrosine kinase mediates TLR9-dependent human dendritic cell activation. *J Allergy Clin Immunol* 2014, **133:**1644-1650 e1644.

228. Marron TU, Martinez-Gallo M, Yu JE, Cunningham-Rundles C: Toll-like receptor 4-, 7-, and 8-activated myeloid cells from patients with X-linked agammaglobulinemia produce enhanced inflammatory cytokines. *J Allergy Clin Immunol* 2012, **129:**184-190 e181-184.

229. Taneichi H, Kanegane H, Sira MM, Futatani T, Agematsu K, Sako M, Kaneko H, Kondo N, Kaisho T, Miyawaki T: Toll-like receptor signaling is impaired in dendritic cells from patients with X-linked agammaglobulinemia. *Clin Immunol* 2008, **126:**148-154.

230. Ni Gabhann J, Hams E, Smith S, Wynne C, Byrne JC, Brennan K, Spence S, Kissenpfennig A, Johnston JA, Fallon PG, Jefferies CA: Btk regulates macrophage polarization in response to lipopolysaccharide. *PLoS One* 2014, **9:**e85834.

231. Gunderson AJ, Kaneda MM, Tsujikawa T, Nguyen AV, Affara NI, Ruffell B, Gorjestani S, Liudahl SM, Truitt M, Olson P, et al: Bruton Tyrosine Kinase-Dependent Immune Cell Cross-talk Drives Pancreas Cancer. *Cancer Discov* 2016, **6:**270-285.

232. Fiorcari S, Maffei R, Audrito V, Martinelli S, Ten Hacken E, Zucchini P, Grisendi G, Potenza L, Luppi M, Burger JA, et al: Ibrutinib modifies the function of monocyte/macrophage population in chronic lymphocytic leukemia. *Oncotarget* 2016, **7:**65968-65981.

233. Andreu P, Johansson M, Affara NI, Pucci F, Tan T, Junankar S, Korets L, Lam J, Tawfik D, DeNardo DG, et al: FcRgamma activation regulates inflammation-associated squamous carcinogenesis. *Cancer Cell* 2010, **17:**121-134.

234. Pucci F, Garris C, Lai CP, Newton A, Pfirschke C, Engblom C, Alvarez D, Sprachman M, Evavold C, Magnuson A, et al: SCS macrophages suppress melanoma by restricting tumor-derived vesicle-B cell interactions. *Science* 2016, **352:**242-246.

235. Coffelt SB, Wellenstein MD, de Visser KE: Neutrophils in cancer: neutral no more. *Nat Rev Cancer* 2016, **16:**431-446.

236. Marron TU, Rohr K, Martinez-Gallo M, Yu J, Cunningham-Rundles C: TLR signaling and effector functions are intact in XLA neutrophils. *Clin Immunol* 2010, **137:**74-80.

237. Farrar JE, Rohrer J, Conley ME: Neutropenia in X-linked agammaglobulinemia. *Clin Immunol Immunopathol* 1996, **81:**271-276.

238. Fiedler K, Sindrilaru A, Terszowski G, Kokai E, Feyerabend TB, Bullinger L, Rodewald HR, Brunner C: Neutrophil development and function critically depend on Bruton tyrosine kinase in a mouse model of X-linked agammaglobulinemia. *Blood* 2011, **117:**1329-1339.

239. Mangla A, Khare A, Vineeth V, Panday NN, Mukhopadhyay A, Ravindran B, Bal V, George A, Rath S: Pleiotropic consequences of Bruton tyrosine kinase deficiency in myeloid lineages lead to poor inflammatory responses. *Blood* 2004, **104:**1191-1197.

240. Mueller H, Stadtmann A, Van Aken H, Hirsch E, Wang D, Ley K, Zarbock A: Tyrosine kinase Btk regulates E-selectin-mediated integrin activation and neutrophil recruitment by controlling phospholipase C (PLC) gamma2 and PI3Kgamma pathways. *Blood* 2010, **115:**3118-3127.

241. Volmering S, Block H, Boras M, Lowell CA, Zarbock A: The Neutrophil Btk Signalosome Regulates Integrin Activation during Sterile Inflammation. *Immunity* 2016, **44:**73-87.

242. Stiff A, Trikha P, Wesolowski R, Kendra K, Hsu V, Uppati S, McMichael E, Duggan M, Campbell A, Keller K, et al: Myeloid-Derived Suppressor Cells Express Bruton's Tyrosine Kinase and Can Be Depleted in Tumor-Bearing Hosts by Ibrutinib Treatment. *Cancer Res* 2016, **76:**2125-2136.

243. Sagiv-Barfi I, Kohrt HE, Czerwinski DK, Ng PP, Chang BY, Levy R: Therapeutic antitumor immunity by checkpoint blockade is enhanced by ibrutinib, an inhibitor of both BTK and ITK. *Proc Natl Acad Sci U S A* 2015, **112:**E966-972.

244. Gao W, Wang M, Wang L, Lu H, Wu S, Dai B, Ou Z, Zhang L, Heymach JV, Gold KA, et al: Selective antitumor activity of ibrutinib in EGFR-mutant non-small cell lung cancer cells. *J Natl Cancer Inst* 2014, **106**.

245. Ruella M, Kenderian SS, Shestova O, Fraietta JA, Qayyum S, Zhang Q, Maus MV, Liu X, Nunez-Cruz S, Klichinsky M, et al: The Addition of the BTK Inhibitor Ibrutinib to Anti-CD19 Chimeric Antigen Receptor T Cells (CART19) Improves Responses against Mantle Cell Lymphoma. *Clin Cancer Res* 2016, **22:**2684-2696.

246. Fraietta JA, Beckwith KA, Patel PR, Ruella M, Zheng Z, Barrett DM, Lacey SF, Melenhorst JJ, McGettigan SE, Cook DR, et al: Ibrutinib enhances chimeric antigen receptor T-cell engraftment and efficacy in leukemia. *Blood* 2016, **127:**1117-1127.

247. Dubovsky JA, Beckwith KA, Natarajan G, Woyach JA, Jaglowski S, Zhong Y, Hessler JD, Liu TM, Chang BY, Larkin KM, et al: Ibrutinib is an irreversible molecular inhibitor of ITK driving a Th1-selective pressure in T lymphocytes. *Blood* 2013, **122:**2539-2549.

248. Byrd JC, Brown JR, O'Brien S, Barrientos JC, Kay NE, Reddy NM, Coutre S, Tam CS, Mulligan SP, Jaeger U, et al: Ibrutinib versus ofatumumab in previously treated chronic lymphoid leukemia. *N Engl J Med* 2014, **371:**213-223.

249. Dreyling M, Jurczak W, Jerkeman M, Silva RS, Rusconi C, Trneny M, Offner F, Caballero D, Joao C, Witzens-Harig M, et al: Ibrutinib versus temsirolimus in patients with relapsed or refractory mantle-cell lymphoma: an international, randomised, open-label, phase 3 study. *Lancet* 2016, **387:**770-778.

250. Burger JA, Keating MJ, Wierda WG, Hartmann E, Hoellenriegel J, Rosin NY, de Weerdt I, Jeyakumar G, Ferrajoli A, Cardenas-Turanzas M, et al: Safety and activity of ibrutinib plus rituximab for patients with high-risk chronic lymphocytic leukaemia: a single-arm, phase 2 study. *Lancet Oncol* 2014, **15:**1090-1099.

251. Chanan-Khan A, Cramer P, Demirkan F, Fraser G, Silva RS, Grosicki S, Pristupa A, Janssens A, Mayer J, Bartlett NL, et al: Ibrutinib combined with bendamustine and rituximab compared with placebo, bendamustine, and rituximab for previously treated chronic lymphocytic leukaemia or small lymphocytic lymphoma (HELIOS): a randomised, double-blind, phase 3 study. *Lancet Oncol* 2016, **17:**200-211.
252. Wang ML, Lee H, Chuang H, Wagner-Bartak N, Hagemeister F, Westin J, Fayad L, Samaniego F, Turturro F, Oki Y, et al: Ibrutinib in combination with rituximab in relapsed or refractory mantle cell lymphoma: a single-centre, open-label, phase 2 trial. *Lancet Oncol* 2016, **17:**48-56.
253. Tam C, Grigg AP, Opat S, Ku M, Gilbertson M, Anderson MA, Seymour JF, Ritchie DS, Dicorleto C, Dimovski B, et al: The BTK Inhibitor, Bgb-3111, Is Safe, Tolerable, and Highly Active in Patients with Relapsed/ Refractory B-Cell Malignancies: Initial Report of a Phase 1 First-in-Human Trial. *Blood* 2015, **126**.
254. Noy A, de Vos S, Thieblemont C, Martin P, Flowers C, Morschhauser F, Collins GP, Ma S, Coleman M, Peles S, et al: Single-Agent Ibrutinib Demonstrates Efficacy and Safety in Patients with Relapsed/Refractory Marginal Zone Lymphoma: A Multicenter, Open-Label, Phase 2 Study. *Blood* 2016, **128**.
255. Secchiero P, Voltan R, Rimondi E, Melloni E, Athanasakis E, Tisato V, Gallo S, Rigolin GM, Zauli G: The gamma-secretase inhibitors enhance the anti-leukemic activity of ibrutinib in B-CLL cells. *Oncotarget* 2017, **8:**59235-59245.
256. Rotin LE, Gronda M, MacLean N, Hurren R, Wang X, Lin FH, Wrana J, Datti A, Barber DL, Minden MD, et al: Ibrutinib synergizes with poly(ADP-ribose) glycohydrolase inhibitors to induce cell death in AML cells via a BTK-independent mechanism. *Oncotarget* 2016, **7:**2765-2779.
257. Kelly PN, Romero DL, Yang Y, Shaffer AL, 3rd, Chaudhary D, Robinson S, Miao W, Rui L, Westlin WF, Kapeller R, Staudt LM: Selective interleukin-1 receptor-associated kinase 4 inhibitors for the treatment of autoimmune disorders and lymphoid malignancy. *J Exp Med* 2015, **212:**2189-2201.
258. Goldstein RL, Yang SN, Taldone T, Chang B, Gerecitano J, Elenitoba-Johnson K, Shaknovich R, Tam W, Leonard JP, Chiosis G, et al: Pharmacoproteomics identifies combinatorial therapy targets for diffuse large B cell lymphoma. *J Clin Invest* 2015, **125:**4559-4571.
259. Patel V, Keating MJ, Wierda WG, Gandhi V: Preclinical combination of TP-0903, an AXL inhibitor and B-PAC-1, a procaspase-activating compound with ibrutinib in chronic lymphocytic leukemia. *Leuk Lymphoma* 2016, **57:**1494-1497.
260. Lamothe B, Cervantes-Gomez F, Sivina M, Wierda WG, Keating MJ, Gandhi V: Proteasome inhibitor carfilzomib complements ibrutinib's action in chronic lymphocytic leukemia. *Blood* 2015, **125:**407-410.
261. Hing ZA, Mantel R, Beckwith KA, Guinn D, Williams E, Smith LL, Williams K, Johnson AJ, Lehman AM, Byrd JC, et al: Selinexor is effective in acquired resistance to ibrutinib and synergizes with ibrutinib in chronic lymphocytic leukemia. *Blood* 2015, **125:**3128-3132.
262. Cervantes-Gomez F, Lamothe B, Woyach JA, Wierda WG, Keating MJ, Balakrishnan K, Gandhi V: Pharmacological and Protein Profiling Suggests Venetoclax (ABT-199) as Optimal Partner with Ibrutinib in Chronic Lymphocytic Leukemia. *Clin Cancer Res* 2015, **21:**3705-3715.
263. Zhao X, Bodo J, Sun D, Durkin L, Lin J, Smith MR, Hsi ED: Combination of ibrutinib with ABT-199: synergistic effects on proliferation inhibition and apoptosis in mantle cell lymphoma cells through perturbation of BTK, AKT and BCL2 pathways. *Br J Haematol* 2015, **168:**765-768.
264. Rushworth SA, Bowles KM, Barrera LN, Murray MY, Zaitseva L, MacEwan DJ: BTK inhibitor ibrutinib is cytotoxic to myeloma and potently enhances bortezomib and lenalidomide activities through NF-kappaB. *Cell Signal* 2013, **25:**106-112.
265. Sagiv-Barfi I, Kohrt HE, Burckhardt L, Czerwinski DK, Levy R: Ibrutinib enhances the antitumor immune response induced by intratumoral injection of a TLR9 ligand in mouse lymphoma. *Blood* 2015, **125:**2079-2086.
266. Xargay-Torrent S, Lopez-Guerra M, Rosich L, Montraveta A, Roldan J, Rodriguez V, Villamor N, Aymerich M, Lagisetti C, Webb TR, et al: The splicing modulator sudemycin induces a specific antitumor response and cooperates with ibrutinib in chronic lymphocytic leukemia. *Oncotarget* 2015, **6:**22734-22749.
267. Yahiaoui A, Meadows SA, Sorensen RA, Cui ZH, Keegan KS, Brockett R, Chen G, Queva C, Li L, Tannheimer SL: PI3Kdelta inhibitor idelalisib in combination with BTK inhibitor ONO/GS-4059 in diffuse large B cell lymphoma with acquired resistance to PI3Kdelta and BTK inhibitors. *PLoS One* 2017, **12:**e0171221.

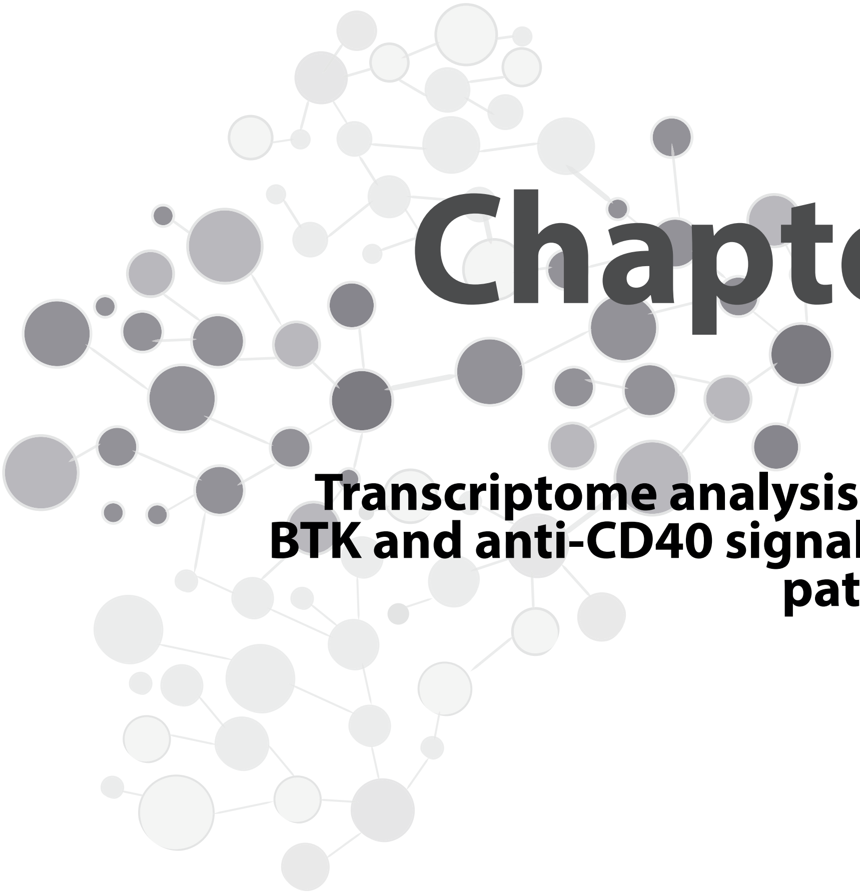

Chapter 3

Transcriptome analysis links BCR, BTK and anti-CD40 signaling to CLL pathogenesis

Simar Pal Singh[1,2,3], Jasper Rip[1], Marjolein J.W. de Bruijn[1],
Anton W. Langerak[2], Wilfred van IJcken[4], Ralph Stadhouders[1,5]
and Rudi W. Hendriks[1]

[1] Department of Pulmonary Medicine,
[2] Department of Immunology,
[3] Post-graduate School Molecular Medicine,
[4] Department of Biomics,
[5] Department of Cell Biology, Erasmus MC Rotterdam, The Netherlands.

In preparation

ABSTRACT

Several reports have implicated clonal selection of B cells by specific antigens in the context of the germinal center reaction in the pathogenesis of CLL. However, the relationship of B cell receptor (BCR)-derived and T-cell dependent signals is largely unknown. Here we analyzed the individual contribution of antigenic stimulation via the BCR, expression of the downstream signaling molecule Bruton's tyrosine kinase (BTK) and signals derived from activated T cells via CD40 to the pathogenesis of CLL. To this end, we performed RNA-Seq analyses in CLL cells from the IgH.TEμ mouse CLL model, which is based on sporadic expression of the SV40 large T oncogene in mature B cells. CLL cell expression profiles were compared to those from normal or BTK-overexpressing naïve splenic B cells, either unstimulated or stimulated via the BCR or to profiles from anti-CD40/IL-4-stimulated B cells. We defined a CLL gene signature comprising 3,611 differentially expressed genes between primary tumor cells from IgH.TEμ mice and naïve splenic B cells from wild type mice (Wt-B). Approximately 48% of these CLL signature genes were modulated by BCR stimulation in Wt-B cells, whereby upregulated and downregulated genes were associated with proliferation and cellular differentiation, respectively. Although Btk overexpression in Wt-B cells induced only a minor fraction of the CLL signature genes, Btk overexpression did enhance the contribution of the BCR stimulation-associated genes to this CLL signature, particularly concerning genes involved in cellular proliferation. Similarly, comparison of α-CD40/IL4 induced genes in follicular B cells with CLL signature genes showed a substantial (~48%) overlap. Hereby, the unique contribution of α-CD40/IL4 induced genes to the CLL signature - in addition to α-IgM stimulation - was ~16%, mainly corresponding to cellular proliferation genes. Since CLL samples included in this study express unmutated BCR, our finding would support a role of T cell help in the origin of unmutated CLL in IgH.TEμ mice. In conclusion, we show that expression profiling allowed us to dissect the importance of both BCR, BTK and CD40-derived stimulatory signals in the pathogenesis of unmutated CLL in IgH.TEμ mice, which may help define targets for therapy strategies in human CLL disease.

Keywords: Chronic lymphocytic leukemia (CLL), Bruton's tyrosine kinase (Btk), B cell receptor (BCR), BCR signaling, CD40, T cell help.

INTRODUCTION

Chronic lymphocytic leukemia (CLL) is the most common leukemia in the Western world[1] and is characterized by accumulation of $CD5^+$ mature B lymphocytes that express low levels of surface immunoglobulin (Ig)[2, 3]. This phenotype suggest a central role of continuous engagement of the B cell receptor (BCR) by antigens in CLL pathogenesis. In support, one-third of CLL samples exhibit highly similar BCR sequence characteristics, known as stereotypic BCRs, pointing to a probably limited set of (auto-)antigens that stimulate these stereotypic BCRs[4]. Several reports have shown that CLL express polyreactive BCRs that bind with low affinity to various auto-antigens generated during apoptosis or oxidation[5, 6]. In contrast to these studies, Dühren-von Minden *et al*. [7] observed that CLL-derived BCRs can be stimulated independently of external antigens, because of the presence of an internal epitope in framework 2 (FR2) of the IGHV domain that is recognized by their CDR3. This recognition induces an increased level of antigen-independent or cell-autonomous signaling of the BCR, as demonstrated by increased cytoplasmic Ca^{2+} levels compared with BCRs from non-malignant B cells. The importance of continuous BCR signaling for CLL cell survival is further demonstrated by constitutive activation of several BCR downstream kinases including Bruton's tyrosine kinase (Btk) increasing CLL cell survival[8]. In support, antitumor activity of the Btk small-molecule inhibitors ibrutinib and acalabrutinib was recently shown in clinical studies of CLL[9, 10].

On the basis of SHM status of the immunoglobulin heavy chain variable (IGHV) genes of the BCR, CLL patients can be grouped into mutated CLL (M-CLL) and unmutated CLL (U-CLL). This division is also clinically relevant because U-CLL have an unfavorable prognosis, with a more aggressive course of the disease and shorter time to first treatment, while M-CLL is associated with a more indolent disease form with a relatively favorable prognosis [11, 12]. Hereby, transcriptome analyses of CLL and normal B cell subsets revealed that unmutated CLL derives from unmutated mature $CD5^+CD27^-$ B cells and mutated CLL derives from a distinct, previously unrecognized, $CD5^+CD27^+$ post-germinal center B cell subset[13]. Thus, in addition to BCR-mediated signaling, CLL cells in particular M-CLL cells are activated via T helper cells during a germinal center (GC) response. However, the impact of such GC interactions on U-CLL cells is debatable because U-CLL cells show an activated B cell phenotype[14] and antigenic specificities of the U-CLL cells seem to include both TI and TD (auto)antigens[6, 15, 16].

To explore the link between Btk expression levels and antigenic stimulation via BCR or T-cell help in CLL pathogenesis we used the IgH.TEμ CLL mouse model previously generated in our lab, which is based on sporadic expression of the SV40 large T oncogene in mature B cells[17]. This was achieved by SV40 large T insertion in opposite transcriptional orientation into the Ig heavy chain locus DH-JH region. Aging IgH.TEμ mice show accumulation of monoclonal CLL-like CD5$^+$CD43$^+$IgM$^+$IgD^{low}CD19$^+$ B cells around nine months of age. Although constitutive Btk signaling was not apparent in primary IgH.TEμ CLL cells, CLL development was dependent on Btk. Btk-overexpression in IgH.TEμ CLL cells enhanced leukemogenesis and Btk-deficiency led to a complete rescue from the disease[18]. This implies that higher BTK protein levels can directly promote CLL development. Therefore, understanding and enhancing mechanisms that regulate BTK protein levels may provide a novel therapeutic strategy for CLL[8, 19].

Here, we compared genome-wide gene expression profiles of IgH.TEμ CLL cells to that induced by *in vitro* stimulation of wild type (Wt) and Btk-overexpressing B cells with anti-IgM (α-IgM), using a total RNA deep sequencing analysis. In addition, we also compared gene expression profiles of IgH.TEμ CLL cells to that induced by *in vitro* stimulation of follicular B cells (Fo-B) with anti-CD40 antibodies and recombinant IL4 (α-CD40/IL4). We found that 3,611 genes were differentially expressed between primary unmutated CLL cells from IgH.TEμ mice and naïve splenic B cells from wild-type mice. While approximately half of this CLL signature is related to BCR signaling, Btk overexpression and α-CD40/IL-4 stimulation additionally contribute to this signature, particularly concerning genes involved in cellular proliferation.

MATERIALS AND METHODS

Mice and genotyping

CD19-hBtk mice have been generated previously [20] and were backcrossed onto the C57bl/6 genetic background for >10 generations. *IgH.TEμ* mice[17] were on a mixed C57BL/6 x 129/Sv background. The mice were genotyped by polymerase chain reaction (PCR) using genomic DNA with the following primers (Life Technologies Europe BV) for the IgH.TEμ construct (forward 5’-GGAAAGTCCTTGGGGTCTTC-3’, reverse 5’-CACTTGTGTGGGTTGATTGC-3’), and the CD19-hBtk transgene (forward 5’-CCTTCCAAGTCCTGGCAT-3’, reverse 5’-CACCAGTCTATTTACAGAGA-3’).

CLL development in IgH.TEμ mice was monitored every 3-6 weeks by screening peripheral blood for a monoclonal B cell expansion using flow cytometry. CLL formation was defined by accumulation of >70% IgMb$^+$ B-cells in the peripheral blood of the mice. All mice were kept and bred at the Erasmus MC experimental animal facility under specified pathogen free conditions. All experimental protocols were reviewed and approved by the Erasmus MC committee for animal experiments.

Naive B cell purification and in vitro stimulation

Splenic single-cell suspensions were prepared in magnetic-activated cell sorting (MACS) buffer (PBS/2mM EDTA/0.5%BSA) and naïve splenic B cells from 8–12 week-old WT C57BL/6 and CD19-hBtk mice were purified by MACS, as previously described[21, 22]. Non-B cells, B-1 cells, GC B cells and plasma cells were first labeled with biotinylated antibodies (BD Biosciences) to CD5 (53–7.3), CD11b (M1-70), CD43 (S7), CD95 (Jo2), CD138 (281-2), Gr-1 (RB6-8C5) and TER-119 (PK136) and subsequently with streptavidin-conjugated magnetic beads (Miltenyi Biotec). Purity of MACS-sorted naïve B cells was confirmed by flow cytometry (typically > 99% CD19+ cells). To obtain activated B cells, purified naïve WT B cells or CD19-hBtk B cells were cultured in culture medium (RPMI 1640 (life technologies)/ 10% FCS (gibco) / 50 μg/mL gentamycin (Life Technologies) / 0.05 mM ß-mercaptoethanol (Sigma)) in the presence of 10 μg/ml F(ab’)2 anti-IgM (Jackson Immunoresearch) for 12h.

RNA sequencing and data analysis

Either directly after purification or following F(ab’)$_2$ α-IgM stimulation, RNA from (cultured) naïve B cells was isolated using the RNeasy Mini Kit (Qiagen) according to the manufacturer’s instructions. Similarly, RNA was extracted from purified (using MACS-purification for CD19+ cells) primary tumors from IgH.TEμ mice. Total mRNA sequencing was performed on a HiSeq 2000 (Illumina), and raw reads were aligned using Bowtie [23] to murine transcripts (RefSeq) corresponding to the University of California at Santa Cruz (UCSC) mouse genome annotation (NCBI37/mm10). Entire genome list (~25,000 genes) was screened for genes with detection limit of ≥1 reads per kilobase of a transcript per million mapped reads (RPKMs) in at least one group on average. Such filtering gave 12,149 genes that were used for subsequent analysis. Gene counts were converted to variance stabilized DEseq values for calculating differentially expressed genes between two groups. Differential gene expression analysis was performed using DESeq2[24] with a false discovery rate (FDR) < 0.05 and a log2-fold change cutoff of 1. Log transformed gene expression levels, quantified as Log$_2$(RPKM+1), were used for generating principle component analysis (PCA), which was performed in R (http://www.r-project.org). Molecular pathway enrichments were obtained from the online Metascape database. Gene expression data for unstimulated and anti-CD40 plus IL-4 stimulated follicular B-cells (FACS sorted CD19$^+$B220$^+$IgD$^+$ B cells) was obtained from previously reported data and downloaded from the Gene Expression Omnibus (GEO; accession number GSE77744)[25]. RNA-seq data used in this study have been deposited in the GEO database (accession number GSE117713)[26].

Statistics

Differential gene expression analysis was performed using DESeq2[24]. To study the correlation between variables, we performed linear regression analysis using GraphPad Prism software (San Diego, CA, USA).

RESULTS

A major fraction of CLL signature genes in *IgH.TEμ* mice is modulated by BCR-stimulation

To determine the *IgH.TEμ* CLL-specific gene signature, we performed genome-wide gene expression profiling on primary *IgH.TEμ* CLL (tumor load >95%, n=6) cells and non-transformed naïve splenic B cells from wild-type mice (Wt-B, n=4). The BCR characteristics of all *IgH.TEμ* CLL included in this study are shown in **Table 1.** Using stringent cut-off levels for significance (p<0.05) and expression levels (≥2-fold differences), we identified 3,611 differentially expressed (DE) genes, referred to as the CLL gene signature. Of these DE genes 2,072 (57%) and 1,539 (~43%) genes were up- and downregulated in CLL cells compared to Wt-B cells, respectively (**Figure 1A**).

We performed principle component analysis (PCA) of Wt-B cells and primary *IgH.TEμ* CLL samples using normalized RPKM values (see Methods for details) of the 3,611 genes in the CLL gene signature. The first principal component (PC1), which represented ~79% of the total variation, identified two separate clusters corresponding to Wt-B cells and the *IgH.TEμ* CLL samples. In PC2 (only ~6% variance) Wt-B cells clustered closely, validating the strong correlation between biological replicates, while CLL samples were scattered, showing heterogeneity across these primary *IgH.TEμ* CLL samples (**Figure 1B**).

Table 1. Characteristics of B cell receptors on CLLs from IgH.TEμ mice.

Tumor code	IgH			HCDR3	Length	% identity	IgL		LCDR3	Length	Mice Background
	VH	DH	JH				VL	JL			
E-29	1-53	2-4	2	CARDYDYDYW	10	100%	6-15	2	CQQYNSYPYTF	11	IgH.TEμ
E-15	9-3	3-1	4	CARYSNYYAMDYW	13	100%	4-59	2	CQQWSSNP#YTF	12	IgH.TEμ
ET-06	3-6	2-5	1	CANSNYVSYWYFDVW	15	100%	5-39	5	CQNGHSFPLTF	11	IgH.TEμ
E-06	11-2	2-5	1	CMRYSNYWYFDVW	13	100%	14-126	2	CLQHGESPYTF	11	IgH.TEμ
EA-02	11-2	2-5	1	CMRYSNYWYFDVW	13	100%	14-126	2	CLQHGESPYTF	11	IgH.TEμ.AICDA$^{-/-}$
EA-04	11-2	2-5	1	CMRYSNYWYFDVW	13	99.63%	14-126	2	CLQHGESPYTF	11	IgH.TEμ.AICDA$^{-/-}$

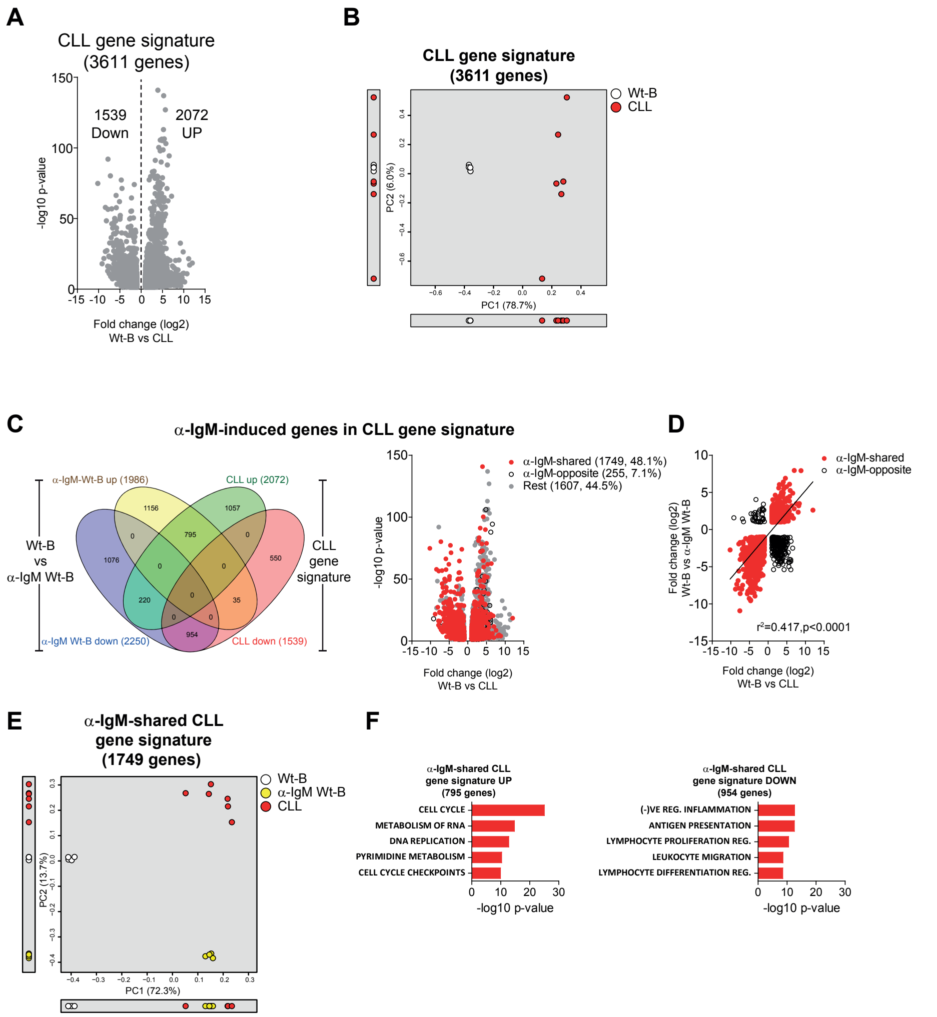

Figure 1. BCR stimulation upregulates proliferation and downregulates differentiation associated IgH.TEμ CLL signature genes.
(A) Volcano plot depicting 3,611 differentially expressed genes (>2fold, q-value<0.05), referred to as CLL gene signature, between naïve wild type B cells (Wt-B, n=4) and *IgH.TEμ* CLL (n=6).
(B) Principle component analysis (PCA) of Wt-B samples (n=4) and *IgH.TEμ* CLL (n=6), using the CLL gene signature.
(C) Venn diagram showing overlap of α-IgM-induced genes in Wt-B cells (α-IgM Wt-B) with the CLL gene signature (*left*) and a Volcano plot showing percentages overlap of α-IgM-induced genes that follow the same or the opposite trends (up or down) as in the CLL gene signature (*right*), depicted as α-IgM-shared (*red dots*) or α-IgM-opposite (*open black dots*), respectively.
(D) Correlation plot comparing fold change (log2) RPKM (Wt-B vs CLL and Wt-B vs α-IgM Wt-B) of 2,004 overlapping genes between the α-IgM Wt-B and CLL gene signatures. Line represents linear regression analysis.
(E) PCA of Wt-B, α-IgM Wt-B and *IgH.TEμ* CLL samples using the 1,749 α-IgM-shared gene signature.
(F) Gene-set enrichment analysis showing pathways enriched by genes either upregulated (*left*) or downregulated (*right*) from the 1,749 α-IgM-shared CLL gene signature.

Next, to be able to determine the extent to which antigenic stimulation via the B cell receptor (BCR) contributes to the malignant transformation of CLL cells, we included samples from naïve splenic B cells that were stimulated with anti-IgM antibodies for 12 hours (α-IgM Wt-B; n=4) in our analysis. Using similar stringent cut-off levels for genome-wide expression differences (≥2-fold, $p<0.05$), we identified 4,236 genes, of which 1,986 (~47%) and 2,250 (53%) genes were up- and downregulated by α-IgM stimulation of Wt-B cells, respectively (**Figure 1C,** *left*). About 41% (1,749/4,236) of these α-IgM-controlled genes were also present in the CLL signature and exhibited a similar trend of up-or down-regulation (referred to as α-IgM-shared; **Figure 1C**, *right*). The α-IgM-shared genes accounted for a major proportion (~48%, 1,749/3,611) of the CLL gene signature, as evidenced by a significant expression correlation ($r^2=0.417$, $p<0.0001$) (**Figure 1D**), as well as by the observed clustering of CLL cells with α-IgM Wt-B cells in PC1 (~72.3%) in a PCA analysis of the α-IgM-shared genes (**Figure 1E**). To identify biological processes associated with the α-IgM-shared CLL gene signature, we performed pathway enrichment analysis using the online Metascape database. Genes upregulated in the α-IgM-shared CLL gene signature were enriched for cell cycle, RNA metabolism, DNA replication, pyrimidine metabolism and cell cycle checkpoints (**Figure 1F**). Genes downregulated in the α-IgM-shared CLL gene signature were involved in quite diverse pathways, including inflammation regulation, antigen presentation, leukocyte migration, lymphocyte proliferation and differentiation (**Figure 1F**).

Taken together, based on comparison of CLL cells from *IgH.TEμ* mice with naïve B cells, we identified a CLL gene signature. Importantly, a major fraction (~48%) of these signature genes is modulated by BCR stimulation in naïve B cells, whereby upregulated and downregulated genes are associated with proliferation and cellular differentiation, respectively.

Additional contribution of Btk overexpression to the BCR stimulation-associated CLL gene signature

Since we have previously shown that Btk-overexpression enhances CLL leukemogenesis in *IgH.TEμ* mice[18], we aimed to identify the contribution of Btk-mediated signaling in the CLL gene signature. To this end, we performed genome-wide gene expression profiling of unstimulated (Btk-Tg-B) and α-IgM stimulated (α-IgM Btk-Tg-B) naïve splenic B cells from CD19-hBtk mice (n=4).

Using similar stringent cut-off levels for significance ($p<0.05$) and differences in expression levels (≥2-fold) between unstimulated Wt-B and Btk-Tg-B cells, we identified 248 Btk-induced genes in B cells, of which 241 genes (97%) were upregulated in Btk-Tg-B B cells and only 7 were downregulated (**Figure 2A,** *left*). Approximately 64% (159/248) of these Btk-induced genes, referred to as Btk-Tg-shared signature, were also present in the CLL gene signature and exhibited a similar trend (up or down) (**Figure 2A,** *right*). The fold-change to Wt-B values of these Btk-Tg-shared genes, which constituted only a minority (4.4%, 159/3,611) of the total CLL gene signature, showed a weak but significant correlation ($r^2=0.169$, $p<0.0001$) with the fold-change to Wt-B values of the CLL gene signature (**Figure 2B**). PCA analysis revealed a clustering of CLL samples that was separate from all Wt-B, α-IgM Wt-B and Btk-Tg-B samples in PC1 (77.1%; **Figure 2C**). While their contribution to CLL gene signature was only minor, pathway enrichment analysis on the group of upregulated Btk-Tg-B-shared genes revealed overrepresentation of genes involved in proliferation, such as cell division, cell cycle regulation, spindle organization, cytokinesis and G2/M checkpoints (**Supplementary Figure 1A**).

Next, to determine if Btk overexpression can modulate BCR-mediated signaling in *IgH.TEμ* CLL, we compared genes that were up- or down-regulated by α-IgM stimulation in Btk-Tg naïve B cells (α-IgM Btk-Tg-B) with the CLL gene signature. Using cut-off levels for genome-wide expression difference of ≥2-fold (and $p<0.05$) between Btk-Tg-B cells and α-IgM Btk-Tg-B cells revealed 4,766 genes, of which 2,207 (~46%) and 2,559 (~54%) genes were up- and downregulated by α-IgM stimulation of CD19-hBtk transgenic B cells, respectively (**Supplementary Figure 1B,** *left*). About 54% (1,960/4,766) of these α-IgM induced genes, referred to as α-IgM-Btk-Tg-shared signature, exhibited a similar trend of up-or downregulation in the CLL gene signature (**Supplementary Figure 1B,** *right*). Unlike Btk-Tg-shared signature, the α-IgM-Btk-Tg-shared signature accounted for a significant proportion (~54%, 1,960/3,611) of the CLL gene signature, as depicted by a significant correlation of the fold-change values of α-IgM-Btk-Tg-B versus Btk-Tg-B and CLL versus Wt-B ($r^2=0.489$, $p<0.0001$) (**Supplementary Figure 1C**). Moreover, the CLL samples clustered with α-IgM Wt-B and α-IgM Btk-Tg-B samples in a PCA analysis using the 1,960 genes of the α-IgM-Btk-Tg-shared signature (PC1=75.7%; **Supplementary Figure 1D**).

Since α-IgM stimulation in Wt-B and Btk-Tg-B cells was associated with a major quantitative (3,913 genes, **Figure 2D**) and qualitative ($r^2=0.954$, $p<0.0001$; **Figure 2E**) overlap of differentially expressed genes, we sought to identify the specific contribution of Btk overexpression to BCR-mediated signaling within the CLL gene signature. Therefore, we focused on 853 genes that were specifically modulated upon α-IgM stimulation in Btk-Tg-B cells, but not in Wt-B cells, referred to as α-IgM-Btk-Tg-B-specific genes (**Figure 2D**). A substantial fraction (~32%, 273/853) of these α-IgM-Btk-Tg-B-specific genes, referred as α-IgM-Btk-Tg-B-specific-shared signature, exhibited a similar trend of up/down-regulation in the CLL gene signature (**Figure 2F**). Hereby, the 273 α-IgM-Btk-Tg-B-specific-shared genes contributed to ~7.6% of the CLL gene signature (273/3611) and their fold-change values versus Btk-Tg-B showed a significant correlation with the CLL versus Wt-B fold-change values ($r^2=0.316$, $p<0.0001$) (**Figure 2G**). Interestingly, the 273 α-IgM-Btk-Tg-B-specific-shared genes represented an additional contribution of Btk overexpression to the BCR stimulation associated gene signature of the CLL that develops in *IgH.TEμ* mice.

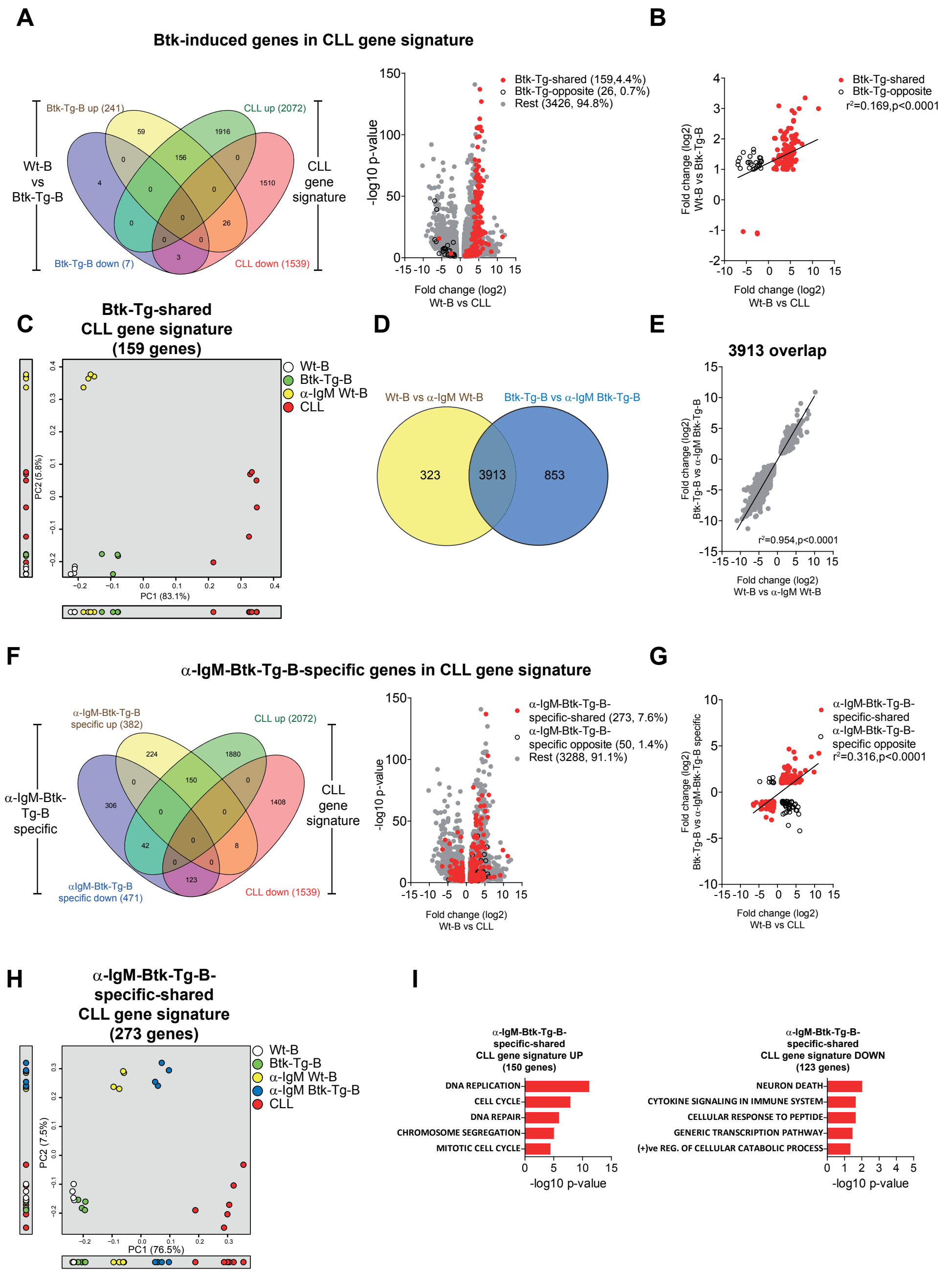

Figure 2 (see left page). Btk overexpression adds to BCR-stimulation associated signature genes of *IgH.TEμ* CLL
(A) Venn diagram showing overlap of genes induced by Btk overexpression in B cells (Btk-Tg-B), referred to as Btk-induced genes, with CLL gene signature from Figure 1A (*left*) and a Volcano plot showing percentages of Btk-induced genes that follow the same or the opposite trend (up or down) as in the CLL gene signature (*right*), depicted as Btk-Tg-shared (*red dots*) or Btk-Tg-opposite (*open black dots*), respectively.
(B) Correlation plot comparing fold change (log2) RPKM (Wt-B vs CLL and Wt-B vs Btk-Tg-B) of 187 overlapping genes between the Btk-Tg-B and CLL gene signatures from panel A. Line represents linear regression analysis.
(C) PCA of Wt-B, α-IgM Wt-B, Btk-Tg-B cells and *IgH.TEμ* CLL samples, using the 159 Btk-Tg-shared gene signature.
(D) Venn diagram showing overlap of α-IgM-induced genes in both Wt-B and Tg-B cells.
(E) Correlation plot comparing fold change (log2) RPKM (Wt-B vs α-IgM-Wt-B and Btk-Tg-B vs α-IgM-Btk-Tg-B) of 3,913 overlapping genes between the α-IgM-Wt-B and α-IgM-Btk-Tg-B signatures from panel D. Line represents linear regression analysis.
(F) Venn diagram showing overlap of 853 α-IgM-induced genes specifically in Btk-Tg-B cells (α-IgM-Btk-Tg-B specific) from panel D with the CLL gene signature (*left*) and Volcano plot showing percentages of 323 α-IgM-Btk-Tg-B specific genes that follow the same or opposite trend (up or down) as in the CLL gene signature (*right*), depicted as α-IgM-Btk-Tg-B-specific-shared (*red dots*) or α-IgM-Btk-Tg-B-specific-opposite (*open black dots*), respectively.
(G) Correlation plot comparing fold change (log2) RPKM (Wt-B vs CLL and Btk-Tg-B vs α-IgM-Btk-Tg-B) of 323 overlapping genes from panel F. Line represents linear regression analysis.
(H) PCA of Wt-B, α-IgM Wt-B, Btk-Tg-B, α-IgM Btk-Tg-B cells and *IgH.TEμ* CLL using 273 α-IgM-Btk-Tg-B-specific-shared genes.
(I) Gene-set enrichment analysis showing pathways enriched by genes either upregulated (*left*) or downregulated (*right*) from the 273 α-IgM-Btk-Tg-B-specific-shared CLL gene signature.

The effect of the 273 α-IgM-Btk-Tg-B-specific-shared genes is also evident from the sequential pattern of clustering in a PCA analysis. In the first component (PC1= 76.5%) constitutive Btk expression clustered the α-IgM activated B cells closer to CLL cells (compare α-IgM Wt-B, α-IgM Btk-Tg-B and CLL; **Figure 2H**). Hereby, α-IgM stimulation segregated resting (Wt-B, Btk-Tg-B) from activated (α-IgM Wt-B and α-IgM Btk-Tg-B) B cells (PC2=~7.5%). Pathway enrichment analysis on the group of upregulated α-IgM-Btk-Tg-B-specific-shared genes revealed overrepresentation of genes involved in proliferation, such as DNA replication, cell cycle, DNA repair, chromosome segregation and mitotic cell cycle pathways (**Figure 2I**). The fewer downregulated α-IgM-Btk-Tg-B-specific-shared genes were enriched for very diverse pathways, with low p values (**Figure 2I**).

In conclusion, our data show that only a minor fraction of the CLL signature genes can be induced by transgenic Btk overexpression in naïve B cells. Nevertheless, Btk overexpression does additionally contribute to the BCR stimulation-associated gene signature of CLL cells in *IgH.TEμ* mice, particularly concerning genes involved in cellular proliferation. This contribution of Btk overexpression may provide a molecular explanation for the early CLL incidence in *IgH.TEμ* mice on the CD19-hBtk transgenic background.

Kinase expression in CLL cells is very different from both resting and activated B cells

Next, to identify additional BCR downstream kinases other than Btk that might play a role in CLL development in *IgH.TEμ* mice, we used a complete list of 478 unique kinase entries in the HGNC database (https://www.genenames.org/tools/search/#!/all?query=Kinases), each belonging to 31 different families. Using a threshold of RPKM≥1, we first identified that 241 (50%) of these 478 kinase genes were expressed in one of more of the sample groups of the total RNA-seq gene expression list. Normalized RPKM values for these 241 kinases were used for PCA analysis (**Supplementary Figure 1E**). The first two principal components, which represented ~79% of the total variation among the kinases in different samples analyzed, identified three separate clusters, corresponding to resting B cells (Wt-B and Btk-Tg-B), activated B cells (α-IgM Wt-B and α-IgM Btk-Tg-B) and primary *IgH.TEμ* CLL samples, validating the strong correlation between biological replicates (**Supplementary Figure 1E**). Moreover, PC1 that explains the majority (~46%) of total variance clustered CLL cells to BCR-activated WT and CD19-hBtk B cells. While expression of kinases clustered CLL together with BCR-activated cells in PC1, in PC2 (~32%) CLL cells were clustered distant from both resting and BCR-activated non-malignant B cells. Interestingly, kinases belonging to MAPK family (Camk2g, Cdk1, Camk2d, Raf1, Rock2, Ryk) and MAPK regulation (Abl2, Epha2, Flt3, Kit, Map3k11) were up and downregulated in CLL, respectively.

Taken together, we conclude that although kinase expression in CLL cells is very different from both resting and activated B cells, kinase expression does cluster CLL closer to BCR-stimulated B cells.

α-CD40/IL4 stimulation enhance CLL cells proliferation in IgH.TEμ mice mutually exclusive of BCR stimulation

In addition to BCR-mediated signaling that supports proliferation and survival, CLL cells interact with the tissue micro-environment whereby their survival is thought to be partly driven by T helper cells through CD40-CD40L interaction and IL-4[27, 28]. Therefore, to investigate the impact of T-cell-dependent stimulatory signals on the CLL gene signature, we included previously reported gene expression values from unstimulated (Fo-B) and 24 hours anti-CD40/IL-4 stimulated follicular B-cells (α-CD40/IL-4 Fo-B)[25].

Using similar stringent cutoff levels for genome-wide expression difference (≥2-fold, $p<0.05$) between Fo-B and α-CD40/IL4 Fo-B cells we identified 4,659 α-CD40/IL4 induced genes, of which 2,356 (~51%) and 2,303 (49%) genes were up- and downregulated by α-CD40/IL-4 stimulation of Fo-B cells, respectively (**Supplementary Figure 2A,** *left*). About 37% (1,718/4,659) of α-CD40/IL-4 induced genes, referred as α-CD40/IL4-shared, exhibited similar trend (up or down) in the CLL gene signature (**Supplementary Figure 2A,** *right*). Importantly, the α-CD40/IL4-shared genes constituted ~48% (1,718/3,611) of the total CLL gene signature as depicted by a significant correlation ($r^2=0.532$, $p<0.0001$) and by clustering of CLL cells with α-CD40/IL4 Fo-B cells in PCA analysis (PC1=62.6%) (**Supplementary Figure 2B, 2C**).

Since, α-IgM stimulation in Wt-B and α-CD40/IL4 stimulation in Fo-B cells resulted in enormous quantitative (2,602 genes, **Figure 3A**) and qualitative ($r^2=0.619$, $p<0.0001$)

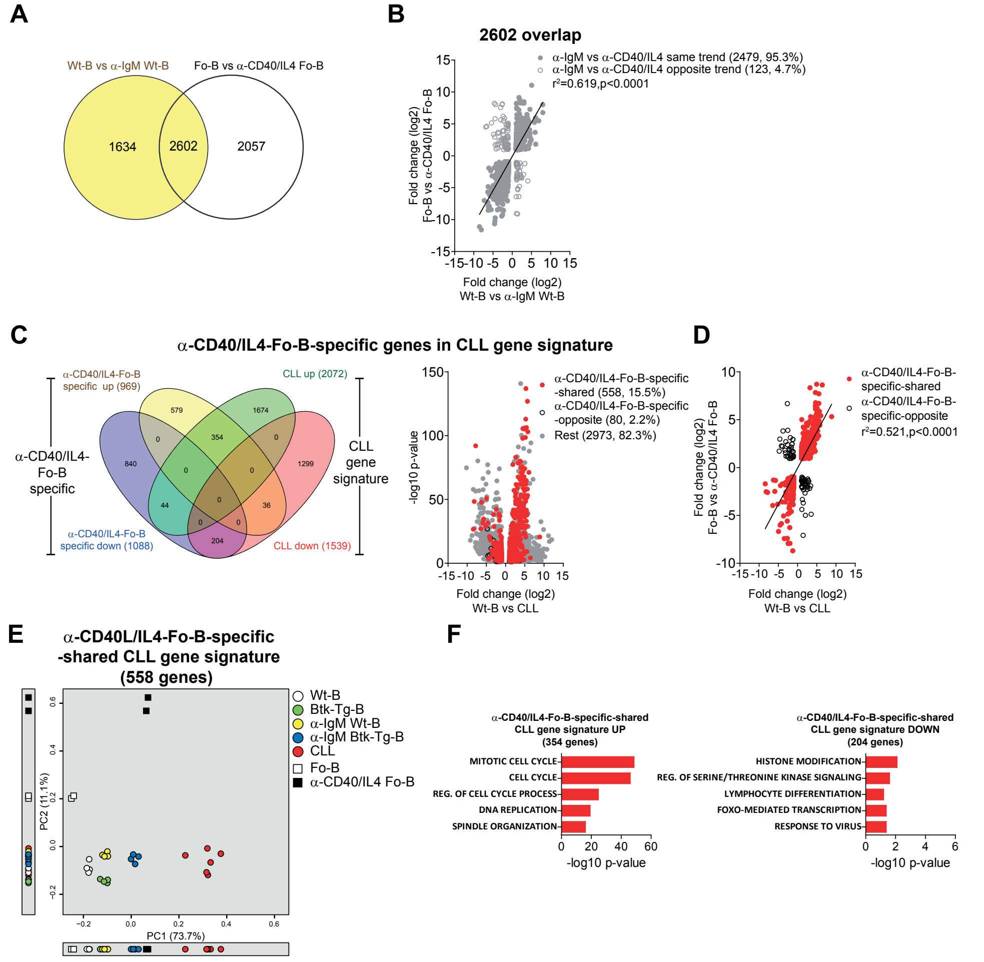

Figure 3. α-CD40/IL-4 stimulation enhances CLL signature proliferation genes in IgH.TEμ mice, independent of BCR-associated genes.
(A) Venn diagram showing overlap of α-IgM induced genes in naïve wild type (Wt-B) and α-CD40/IL4 induced genes in follicular (Fo-B) B cells.
(B) Correlation plot comparing fold change (log2) RPKM (Wt-B vs α-IgM-Wt-B and Fo-B vs α-CD40/IL4 Fo-B) of 2,602 overlapping genes from panel A. Line represents linear regression analysis.
(C) Venn diagram showing overlap of CLL gene signature with α-CD40/IL4-Fo-B-specific genes from panel A (*left*) and Volcano plot showing the percentages of α-CD40/IL4-Fo-B-specific genes that follow the same or the opposite trend (up or down) as in CLL gene signature (*right*), depicted as α-CD40/IL4-Fo-B-specific-shared (*red dots*) or α-CD40/IL4-Fo-B-specific-opposite (*open black dots*), respectively.
(D) Correlation plot comparing fold change (log2) RPKM (Wt-B vs CLL and Fo-B vs α-CD40/IL4 Fo-B) of 638 overlapping genes from panel C. Line represents linear regression analysis.
(E) PCA of Wt-B, α-IgM Wt-B, Btk-Tg-B, α-IgM Btk-Tg-B, Fo-B, α-CD40/IL4 Fo-B cells and *IgH.TEμ* CLL using 558 α-CD40/IL4-Fo-B-specific-shared genes.
(F) Gene-set enrichment analysis showing pathways enriched by genes either upregulated (*left*) or downregulated (*right*) from the 558 α-CD40/IL4-Fo-B-specific-shared gene CLL signature.

overlap (**Figure 3B**), we sought to identify exclusive contribution of α-CD40/IL4 stimulation in addition to BCR-mediated signaling in the CLL gene signature. Therefore, we focused on those 2,057 genes that were specifically modulated upon α-CD40/IL4 stimulation in Fo-B cells, referred as α-CD40/IL4 specific genes (**Figure 3C, 3D**). A substantial proportion (~27%, 558/2,057) of these α-CD40/IL4 specific genes, referred to as α-CD40/IL4-specific-shared genes exhibited a similar trend (up or down) in the CLL gene signature (**Figure 3C,** *right*).

Hereby, the 558 α-CD40/IL4 Fo-B-specific-shared genes contributed to ~16% of the CLL gene signature (558/3,611) and their fold-change values versus Fo-B showed a significant correlation with the CLL versus Wt-B fold-change values (r^2=0.521, $p<0.0001$) (**Figure 3D**). Interestingly, the 558 α-CD40/IL4 Fo-B-specific-shared genes represented an additional contribution of α-CD40/IL4 stimulation to the BCR stimulation associated gene signature of the CLL that develops in *IgH.TEμ* mice. The effect of the α-CD40/IL4 Fo-B-specific-shared genes is also evident from the sequential pattern of clustering in a PCA analysis. In the first component (PC1= 73.7%) α-CD40/IL4 stimulation brought the Fo-B cells closer to CLL cells (compare Fo-B, α-CD40/IL4 Fo-B and CLL; **Figure 3E**). In addition, the analysis of a later time point (48 hours) of α-CD40/IL-4 stimulated follicular B cells[25] identified a similar overlap to CLL gene signature (data not shown). Pathway enrichment analysis of α-CD40/IL4 Fo-B-specific-shared upregulated genes revealed overrepresentation of genes involved in proliferation, such as cell cycle, DNA replication and spindle organization (**Figure 3F**). In contrast, α-CD40/IL4 Fo-B-specific-shared downregulated genes were enriched for diverse pathway again with relatively low p values.

Thus, we identified the importance of α-CD40/IL-4-mediated signaling in malignant transformation of B cells into CLL in *IgH.TEμ* mice. Interestingly, genes modulated by α-CD40/IL-4 additionally contribute to the gene signature of CLL cells in *IgH.TEμ* mice – next to the BCR stimulation-associated genes. This "α-CD40/IL-4-specific" CLL signature particularly consists of genes involved in cellular proliferation.

DISCUSSION

Although evidence for an important role of selection by specific antigens in the pathogenesis of CLL cells is accumulating, the characteristics of these antigenic stimulations have not been addressed in detail. Here we explored the individual contribution of antigenic stimulation via B cell receptor (BCR), the role of Btk expression and co-stimulatory signals via CD40 and IL-4R signaling to the genome-wide CLL gene signature in *IgH.TEμ* mice (**Figure 4**).

We identified 3,611 differentially expressed genes, referred as CLL gene signature, between naïve splenic Wt-B cells and primary *IgH.TEμ* CLL samples. Principle component analysis (total variance ~72%) using CLL gene signature identified three separate clusters, corresponding to resting B cells (Wt-B, Btk-Tg-B and Fo-B), activated B cells (α-IgM Wt-B, α-IgM Btk-Tg-B and α-CD40/IL4 Fo-B cells) and primary *IgH.TEμ* CLL samples, validating the strong correlation between biological replicates (**Figure 4**). Moreover, PC1 that explains the majority (50%) of total variance clustered CLL cells to BCR-activated WT or CD19-hBtk B cells and α-CD40/IL4 activated Fo-B cells. Hereby we observed sequential pattern of clustering in a PCA analysis as, α-IgM or α-CD40/IL4 stimulation segregated resting (Wt-B,

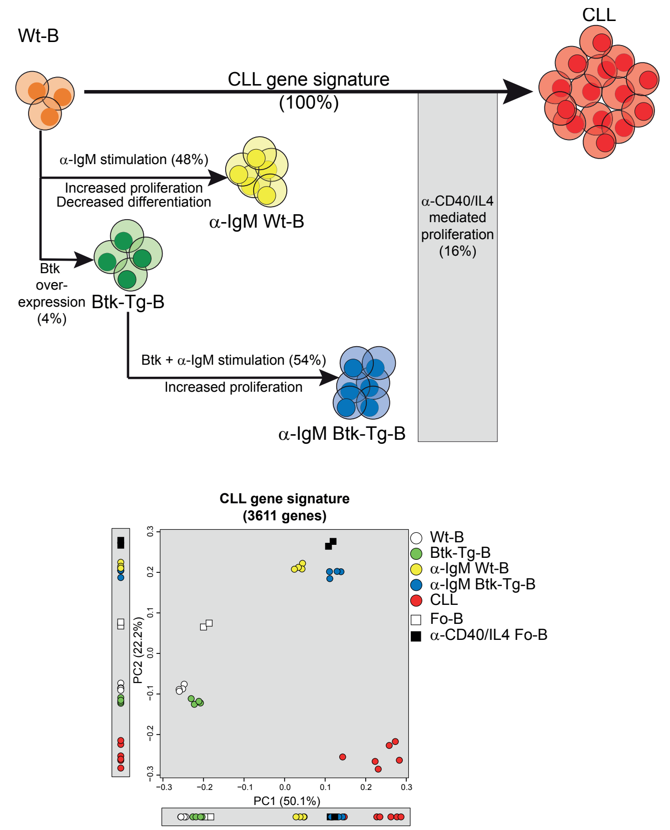

Figure 4. Graphical summary
Total genomic distance, defined as the CLL gene signature, between CLL from IgH.TEμ and naïve splenic wild type B cells (Wt-B) comprising 3,611 differentially expressed genes is shown (*top*). Individual contribution of genes modulated by BCR stimulation (α-IgM), B cell-specific Btk overexpression (Btk-Tg-B) and T cell help (α-CD40L/IL4 stimulation) to the CLL gene signature is depicted (*below*). To quantify such contribution, percentages of genes that follow the same trends (up or downregulated) with the respective modulation are given. PCA analysis of Wt-B, α-IgM Wt-B, Fo-B, α-CD40/IL4 Fo-B cells and *IgH.TEμ* CLL samples of all 3,611 genes from the CLL gene signature is shown at the bottom.

Btk-Tg-B and Fo-B) from activated (α-IgM Wt-B, α-IgM Btk-Tg-B and α-CD40/IL4 Fo-B) B cells and Btk-overexpression further enhanced clustering of the α-IgM activated B cells closer to CLL cells (compare α-IgM Wt-B, α-IgM Btk-Tg-B and CLL; **Figure 4**). While activated B cells clustered together with CLL in PC1, in PC2 (22%) CLL cells were clustered distant from both resting and activated non-malignant B cells.

We demonstrate that a major fraction (~48%) of the CLL signature genes is normally modulated in naïve B cells by BCR antigenic stimulation. Hereby upregulated and downregulated genes are associated with proliferation and cellular differentiation, respectively. Only a minor fraction of the CLL signature genes can be induced by transgenic Btk overexpression in naïve B cells. However, Btk overexpression does increase the fraction of overlapping genes between the BCR stimulation-associated and CLL-associated expression signature. The limited numbers of CLL signature genes that are constitutively induced by Btk independently of BCR signaling indicate that Btk protein overexpression itself does not strongly affect CLL pathogenesis. Instead, it is conceivable that the contribution of Btk to CLL characteristics are dependent on Btk kinase activity, or alternatively that increased Btk protein levels affect CLL characteristics only in the presence of concomitant activation of signaling pathways, e.g. downstream of the BCR, TLR or chemokine receptors.

The substantially larger contribution of Btk to the CLL gene signature in the presence of concomitant BCR stimulation would point to a role for Btk particularly downstream of the BCR in CLL formation. In line, the accelerated development of CLL in CD19-hBtk transgenic *IgH.TEμ* mice, together with their increased frequency of non-stereotypical BCRs harboring longer CDR3s[18], indicates that Btk signaling alters BCR-dependent B cell selection. However, we cannot rule out Btk functions downstream of Toll-like receptors or chemokine receptors[8]. This was affirmed by a transient lymphocytosis, observed in CLL patients and alike diseased mice, upon initiation of treatment with the Btk small molecule inhibitors ibrutinib or acalabrutinib[9, 10, 21, 29]. In addition, an important role for TLR signaling in CLL pathogenesis and in sustaining the viability of CLL cells during ibrutinib therapy has been demonstrated[30]. Therefore, it would be interesting to include expression signatures of TLR-stimulated or chemokine receptor activated B cells in our studies on the CLL gene signature.

Pathway analysis revealed proliferation-related processes to be key downstream of Btk and BCR signaling. In line with this, we previously observed that Btk-mediated signaling enhanced leukemogenesis and Btk-deficiency led to a complete rescue from the disease[18]. Moreover, ibrutinib treatment abrogated proliferation of cultured EMC cell lines obtained from *IgH.TEμ* mice[21]. This is important, as clinical effects of ibrutinib have been mainly attributed to inhibition of proliferation[31-33] and egress of the LN CLL cells from this supportive micro-environment into the blood stream rather than direct cytotoxicity. As a result, a major limitation of ibrutinib therapy is the low rate of complete responses and that MRD-negative CR is rare[34]. This finding necessitates further clinical developments combining ibrutinib with cytotoxic therapies.

Surprisingly, the up- or downregulation of a minority (7.1%, 255 genes) of the BCR-signature genes is found to be inverse compared to their expression trends in CLL gene signature. A possible explanation for such discrepancies could be the different nature of BCR activation *in vivo* versus *in vitro*. Compared to *in vivo* BCR-antigen interaction which are frequently of low affinity, *in vitro* BCR-antigen interactions mimicked by α-IgM stimulation only resemble high-affinity interactions and are thus less intermittent, longer in duration and provoke stronger B cell activation. Indeed, remarkable differences in BCR targets genes following single-round BCR stimulation versus continuous BCR stimulation were demonstrated by Damdinsuren et al. [35]. These authors showed that 9 hours after the onset of single-round versus continuous BCR stimulation of WT B cells only 35-47% of BCR-induced genes were shared between these differentially stimulated cells[35]. This suggests that in CLL cells the 255 BCR target genes exhibiting an inversed expression pattern compared to BCR-stimulated Wt-B cells may reflect true BCR target genes that are nevertheless differentially regulated due to the different nature of BCR engagement *in vivo* versus *in vitro*.

Finally, like α-IgM stimulation, comparison of α-CD40/IL4 induced gene signature also show substantial (~48%) overlap with the CLL gene signature. Hereby, the unique contribution of α-CD40/IL4 induced genes in addition to α-IgM stimulation was ~16%, all corresponding to cellular proliferation. Importantly, the *IgH.TEμ* CLL samples that we included in this study were all expressing an unmutated BCR. However, the nature of α-CD40/IL4 stimulation reflects interaction of B cells with T cells during a GC response. Thus, our finding suggests a possible role of T-cell help in the origin of unmutated CLL in *IgH.TEμ* mice. Studies investigating the effects of the abrogation or the stimulation of GC on BCR repertoire of unmutated CLL in *IgH.TEμ* indeed support the involvement of T cell derived signals in the context of GC formation in the pathogenesis of unmutated CLL[26].

In summary, we have shown that BCR-mediated proliferative signaling plays a key role in malignant growth of naïve B cells in *IgH.TEμ* mice. Although, transgenic Btk-overexpression has only a limited role in inducing CLL-associated genes, Btk-overexpression does accelerate BCR-mediated proliferative signaling in *IgH.TEμ* CLL. Finally, we found an additional role of T-cell help in modulating the CLL genome of unmutated CLL from *IgH.TEμ* mice. These findings show the importance of various B cell autonomous and microenvironmental - T cell-mediated - signals in the pathogenesis of CLL in the *IgH.TEμ* mouse model. They also establish the usefulness of the *IgH.TEμ* CLL mouse model for human CLL, because our studies may help define targets for therapy strategies for CLL patients.

REFERENCES

1. Dores GM, Anderson WF, Curtis RE, Landgren O, Ostroumova E, Bluhm EC, *et al.* Chronic lymphocytic leukaemia and small lymphocytic lymphoma: overview of the descriptive epidemiology. *British journal of haematology* 2007 Dec; **139**(5)**:** 809-819.
2. Zenz T, Mertens D, Kuppers R, Dohner H, Stilgenbauer S. From pathogenesis to treatment of chronic lymphocytic leukaemia. *Nature reviews Cancer* 2010 Jan; **10**(1)**:** 37-50.
3. Dighiero G, Hamblin TJ. Chronic lymphocytic leukaemia. *Lancet* 2008 Mar 22; **371**(9617)**:** 1017-1029.
4. Stamatopoulos K, Belessi C, Moreno C, Boudjograh M, Guida G, Smilevska T, *et al.* Over 20% of patients with chronic lymphocytic leukemia carry stereotyped receptors: Pathogenetic implications and clinical correlations. *Blood* 2007 Jan 1; **109**(1)**:** 259-270.
5. Herve M, Xu K, Ng YS, Wardemann H, Albesiano E, Messmer BT, *et al.* Unmutated and mutated chronic lymphocytic leukemias derive from self-reactive B cell precursors despite expressing different antibody reactivity. *J Clin Invest* 2005 Jun; **115**(6)**:** 1636-1643.
6. Lanemo Myhrinder A, Hellqvist E, Sidorova E, Soderberg A, Baxendale H, Dahle C, *et al.* A new perspective: molecular motifs on oxidized LDL, apoptotic cells, and bacteria are targets for chronic lymphocytic leukemia antibodies. *Blood* 2008 Apr 01; **111**(7)**:** 3838-3848.
7. Duhren-von Minden M, Ubelhart R, Schneider D, Wossning T, Bach MP, Buchner M, *et al.* Chronic lymphocytic leukaemia is driven by antigen-independent cell-autonomous signalling. *Nature* 2012 Sep 13; **489**(7415)**:** 309-312.
8. Pal Singh S, Dammeijer F, Hendriks RW. Role of Bruton's tyrosine kinase in B cells and malignancies. *Mol Cancer* 2018 Feb 19; **17**(1)**:** 57.
9. Byrd JC, Furman RR, Coutre SE, Flinn IW, Burger JA, Blum KA, *et al.* Targeting BTK with ibrutinib in relapsed chronic lymphocytic leukemia. *N Engl J Med* 2013 Jul 04; **369**(1)**:** 32-42.
10. Byrd JC, Harrington B, O'Brien S, Jones JA, Schuh A, Devereux S, *et al.* Acalabrutinib (ACP-196) in Relapsed Chronic Lymphocytic Leukemia. *N Engl J Med* 2016 Jan 28; **374**(4)**:** 323-332.
11. Damle RN, Wasil T, Fais F, Ghiotto F, Valetto A, Allen SL, *et al.* Ig V gene mutation status and CD38 expression as novel prognostic indicators in chronic lymphocytic leukemia. *Blood* 1999 Sep 15; **94**(6)**:** 1840-1847.
12. Hamblin TJ, Davis Z, Gardiner A, Oscier DG, Stevenson FK. Unmutated Ig V(H) genes are associated with a more aggressive form of chronic lymphocytic leukemia. *Blood* 1999 Sep 15; **94**(6)**:** 1848-1854.
13. Seifert M, Sellmann L, Bloehdorn J, Wein F, Stilgenbauer S, Durig J, *et al.* Cellular origin and pathophysiology of chronic lymphocytic leukemia. *The Journal of experimental medicine* 2012 Oct 22.
14. Damle RN, Ghiotto F, Valetto A, Albesiano E, Fais F, Yan XJ, *et al.* B-cell chronic lymphocytic leukemia cells express a surface membrane phenotype of activated, antigen-experienced B lymphocytes. *Blood* 2002 Jun 1; **99**(11)**:** 4087-4093.
15. Catera R, Silverman GJ, Hatzi K, Seiler T, Didier S, Zhang L, *et al.* Chronic lymphocytic leukemia cells recognize conserved epitopes associated with apoptosis and oxidation. *Mol Med* 2008 Nov-Dec; **14**(11-12)**:** 665-674.
16. Chu CC, Catera R, Hatzi K, Yan XJ, Zhang L, Wang XB, *et al.* Chronic lymphocytic leukemia antibodies with a common stereotypic rearrangement recognize nonmuscle myosin heavy chain IIA. *Blood* 2008 Dec 15; **112**(13)**:** 5122-5129.
17. ter Brugge PJ, Ta VB, de Bruijn MJ, Keijzers G, Maas A, van Gent DC, *et al.* A mouse model for chronic lymphocytic leukemia based on expression of the SV40 large T antigen. *Blood* 2009 Jul 02; **114**(1)**:** 119-127.
18. Kil LP, de Bruijn MJ, van Hulst JA, Langerak AW, Yuvaraj S, Hendriks RW. Bruton's tyrosine kinase mediated signaling enhances leukemogenesis in a mouse model for chronic lymphocytic leukemia. *Am J Blood Res* 2013; **3**(1)**:** 71-83.
19. Bottoni A, Rizzotto L, Lai TH, Liu C, Smith LL, Mantel R, *et al.* Targeting BTK through microRNA in chronic lymphocytic leukemia. *Blood* 2016 Dec 29; **128**(26)**:** 3101-3112.
20. Maas A, Dingjan GM, Grosveld F, Hendriks RW. Early arrest in B cell development in transgenic mice that express the E41K Bruton's tyrosine kinase mutant under the control of the CD19 promoter region. *J Immunol* 1999 Jun 01; **162**(11)**:** 6526-6533.
21. Singh SP, Pillai SY, de Bruijn MJW, Stadhouders R, Corneth OBJ, van den Ham HJ, *et al.* Cell lines generated from a chronic lymphocytic leukemia mouse model exhibit constitutive Btk and Akt signaling. *Oncotarget* 2017 Sep 22; **8**(42)**:** 71981-71995.
22. Kil LP, de Bruijn MJ, van Nimwegen M, Corneth OB, van Hamburg JP, Dingjan GM, *et al.* Btk levels set the threshold for B-cell activation and negative selection of autoreactive B cells in mice. *Blood* 2012 Apr 19; **119**(16)**:** 3744-3756.
23. Langmead B, Trapnell C, Pop M, Salzberg SL. Ultrafast and memory-efficient alignment of short DNA sequences to the human genome. *Genome biology* 2009; **10**(3)**:** R25.
24. Love MI, Huber W, Anders S. Moderated estimation of fold change and dispersion for RNA-seq data with DESeq2. *Genome Biol* 2014; **15**(12)**:** 550.
25. Wohner M, Tagoh H, Bilic I, Jaritz M, Poliakova DK, Fischer M, *et al.* Molecular functions of the transcription factors E2A and E2-2 in controlling germinal center B cell and plasma cell development. *J Exp Med* 2016 Jun 27; **213**(7)**:** 1201-1221.
26. Pal Singh S, de Bruijn MJW, de Almeida MP, Meijers RWJ, Nitschke L, Langerak AW, *et al.* Identification of Distinct Unmutated Chronic Lymphocytic Leukemia Subsets in Mice Based on Their T Cell Dependency. *Front Immunol* 2018; **9:** 1996.
27. Coscia M, Pantaleoni F, Riganti C, Vitale C, Rigoni M, Peola S, *et al.* IGHV unmutated CLL B cells are more prone to spontaneous apoptosis and subject to environmental prosurvival signals than mutated CLL B cells. *Leukemia* 2011 May; **25**(5)**:** 828-837.
28. Scielzo C, Apollonio B, Scarfo L, Janus A, Muzio M, Ten Hacken E, *et al.* The functional in vitro response to CD40 ligation reflects a different clinical outcome in patients with chronic lymphocytic leukemia. *Leukemia* 2011 Nov; **25**(11)**:** 1760-1767.

29. Ponader S, Chen SS, Buggy JJ, Balakrishnan K, Gandhi V, Wierda WG, *et al.* The Bruton tyrosine kinase inhibitor PCI-32765 thwarts chronic lymphocytic leukemia cell survival and tissue homing in vitro and in vivo. *Blood* 2012 Feb 02; **119**(5)**:** 1182-1189.
30. Dadashian EL, McAuley EM, Liu D, Shaffer AL, 3rd, Young RM, Iyer JR, *et al.* TLR Signaling Is Activated in Lymph Node-Resident CLL Cells and Is Only Partially Inhibited by Ibrutinib. *Cancer Res* 2019 Jan 15; **79**(2)**:** 360-371.
31. Burger JA, Li KW, Keating MJ, Sivina M, Amer AM, Garg N*, et al.* Leukemia cell proliferation and death in chronic lymphocytic leukemia patients on therapy with the BTK inhibitor ibrutinib. *JCI Insight* 2017 Jan 26; **2**(2)**:** e89904.
32. Herman SE, Mustafa RZ, Gyamfi JA, Pittaluga S, Chang S, Chang B, *et al.* Ibrutinib inhibits BCR and NF-kappaB signaling and reduces tumor proliferation in tissue-resident cells of patients with CLL. *Blood* 2014 May 22; **123**(21)**:** 3286-3295.
33. Herman SE, Niemann CU, Farooqui M, Jones J, Mustafa RZ, Lipsky A, *et al.* Ibrutinib-induced lymphocytosis in patients with chronic lymphocytic leukemia: correlative analyses from a phase II study. *Leukemia* 2014 Nov; **28**(11)**:** 2188-2196.
34. O'Brien SM, Furman RR, Coutre SE, Flinn IW, Burger J, Blum K, *et al.* Five-year experience with single-agent ibrutinib in patients with previously untreated and relapsed/refractory chronic lymphocytic leukemia/small lymphocytic leukemia. Am Soc Hematology; 2016.
35. Damdinsuren B, Zhang Y, Khalil A, Wood WH, 3rd, Becker KG, Shlomchik MJ, *et al.* Single round of antigen receptor signaling programs naive B cells to receive T cell help. *Immunity* 2010 Mar 26; **32**(3)**:** 355-366.

SUPPLEMENTAL DATA

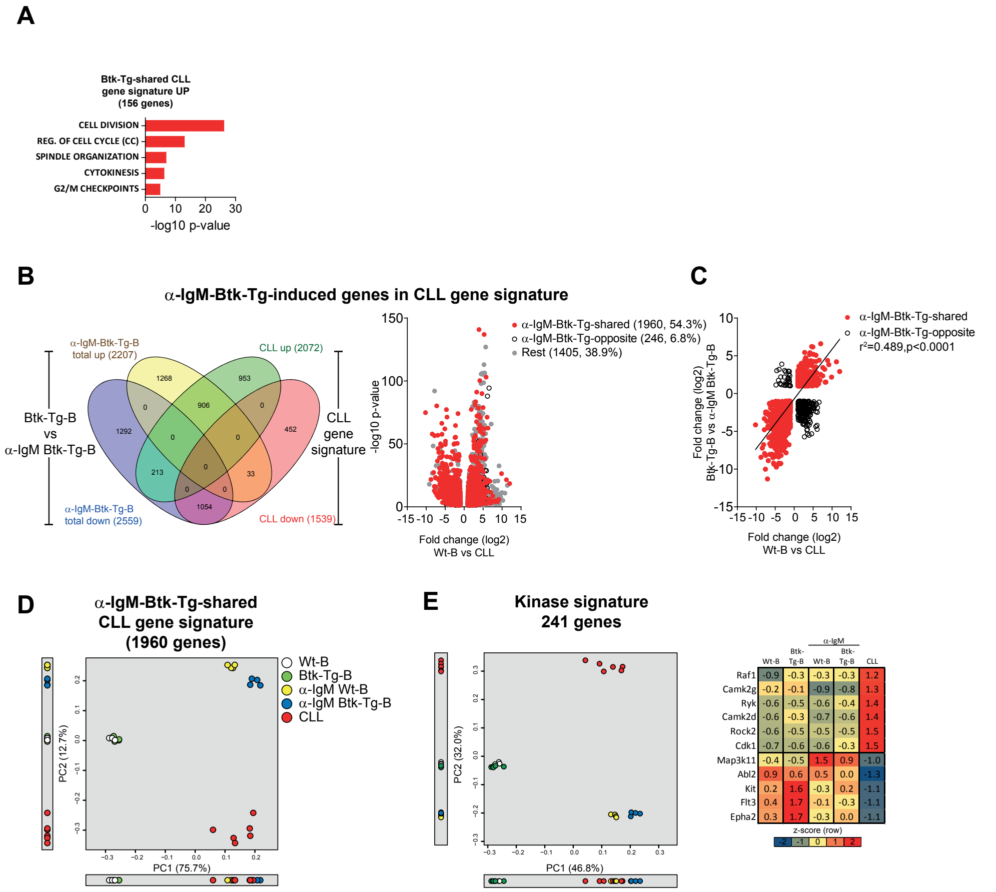

Supplementary Figure 1. Btk overexpression enhances BCR mediated signaling in CLL from IgH.TEμ mice
(A) Pathway enrichment analysis on the group of 156 upregulated Btk-Tg-B-shared genes (from the Venn diagram in Figure 2A) .
(B) Venn diagram showing overlap of α-IgM induced genes in Btk-overexpressing B cells (α-IgM Btk-Tg-B) with the CLL gene signature (Left) and Volcano plot showing percentages of α-IgM-Btk-Tg total genes that follow the same or the opposite trend (up or down) as in the CLL gene signature (right), depicted as α-IgM-Btk-Tg-shared (red dots) or α-IgM-Btk-Tg-opposite (black white circles), respectively.
(C) Correlation plot comparing fold change (log2) RPKM (Wt-B vs CLL and Btk-Tg-B vs α-IgM-Btk-Tg-B) of 2,206 overlapping genes from panel B. Line represents linear regression analysis.
(D) PCA of the indicated sample groups using the 1,960 α-IgM-Btk-Tg-shared gene signature.
(E) PCA of the indicated sample groups using 241 kinase genes from HGNC database (https://www.genenames.org/tools/search/#!/all?query=Kinases) having RPKM>1 in genome-wide RNA-sequencing analysis dataset (left) and heatmap showing row Z-score values of a subset of kinases belonging to the MAPK family which are differentially expressed (>2fold, p<0.05) between CLL and resting (Wt-B, Btk-Tg-B) or activated (α-IgM Wt-B, α-IgM Btk-Tg-B) B cells (right).

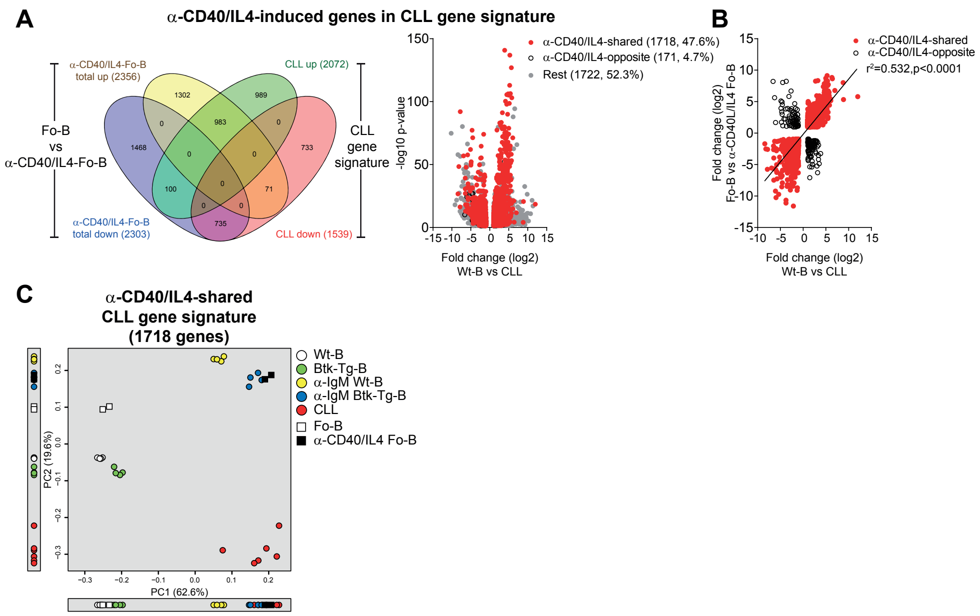

Supplementary Figure 2. α-CD40/IL4 stimulation enhance CLL cells proliferation in IgH.TEμ mice

(A) Venn diagram showing overlap of genes induced by α-CD40/IL4 stimulation of follicular B cells (α-CD40/IL4 Fo-B) with the CLL gene signature (left) and Volcano plot showing percentages of the α-CD40/IL4 Fo-B genes that follow the same or the opposite trend (up-or down) as in the CLL gene signature (right), depicted as α-CD40/IL4-shared (red dots) or α-CD40/IL4-opposite (black open circles), respectively.

(B) Correlation plot comparing fold-change (log2) RPKM (Wt-B vs CLL and Fo-B vs α-CD40/IL4 Fo-B) of overlapping 1,889 genes from panel A. Line represents linear regression analysis.

(C) PCA of indicated sample groups using the 1718 α-CD40/IL4-shared gene signature.

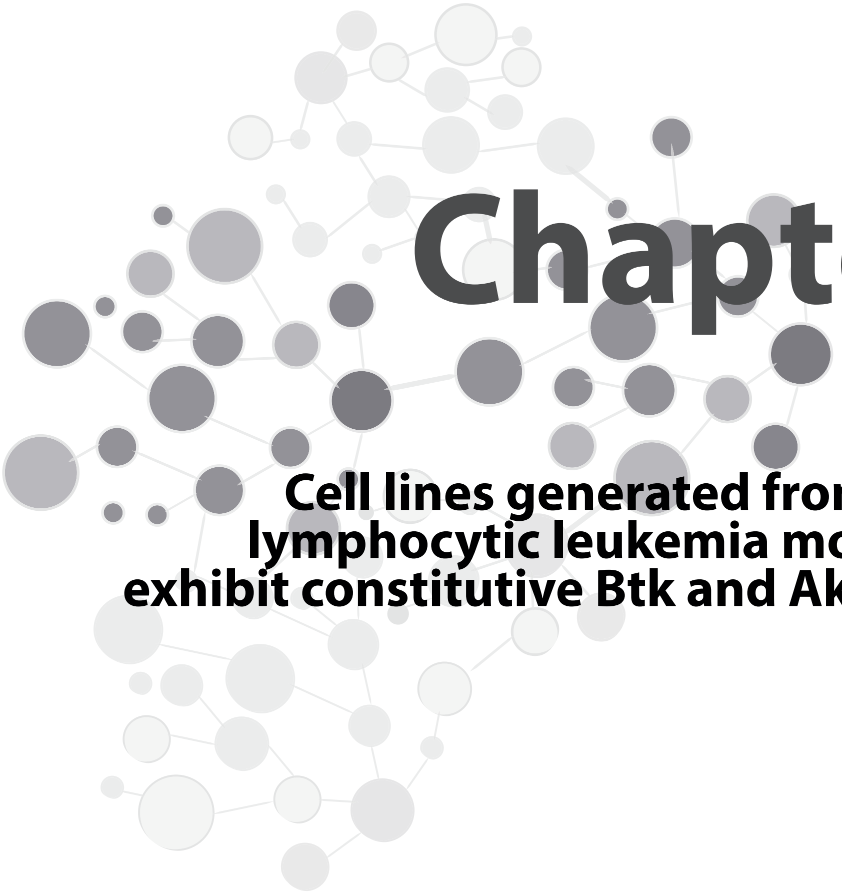

Chapter 4

Cell lines generated from a chronic lymphocytic leukemia mouse model exhibit constitutive Btk and Akt signaling

Simar Pal Singh[1,2,3], Saravanan Y. Pillai[1], Marjolein J.W de Bruijn[1],
Ralph Stadhouders[1,4], Odilia B. J. Corneth[1], Henk Jan van den Ham[5],
Alice Muggen[2], Erik Slinger[6], Annemieke Kuil[7], Marcel Spaargaren[7],
Arnon P. Kater[6], Anton W. Langerak[2] and Rudi W. Hendriks[1]

[1]Department of Pulmonary Medicine,
[2]Department of Immunology,
[3]Post graduate school Molecular Medicine and
[5]Department of Virosciences, Erasmus MC, Rotterdam, The Netherlands;
[4]Centre for Genomic Regulation (CRG), The Barcelona Institute of Science and Technology, Barcelona Spain;
[6]Department of Hematology,
[7]Department of Pathology, Academic Medical Center, Amsterdam, The Netherlands

Oncotarget, Volume 8, Number 42, 2017

ABSTRACT

Chronic lymphocytic leukemia (CLL) is characterized by the accumulation of mature $CD5^+$ B cells in blood. Spontaneous apoptosis of CLL cells in vitro has hampered in-depth investigation of CLL pathogenesis. Here we describe the generation of three monoclonal mouse cell lines, EMC2, EMC4 and EMC6, from the IgH.TEμ CLL mouse model based on sporadic expression of SV40 large T antigen. The cell lines exhibit a stable $CD5^+CD43^+IgM^+CD19^+$ CLL phenotype in culture and can be adoptively transferred into $Rag1^{-/-}$ mice. RNA-seq analysis revealed only minor differences between the cell lines and their primary tumors and suggested that NF-κB and mTOR signaling pathways were involved in cell line outgrowth. *In vitro* survival and proliferation was dependent on constitutive phosphorylation of Bruton's tyrosine kinase (Btk) at Y551/Y223, and Akt(S473). Treatment of the cell lines with small molecule inhibitors specific for Btk (ibrutinib) or PI3K (idelalisib), which is upstream of Akt, resulted in reduced viability, proliferation and fibronectin-dependent cell adhesion. Treatment of cell line-engrafted $Rag1^{-/-}$ mice with ibrutinib was associated with transient lymphocytosis, reduced splenomegaly and increased overall survival. Thus, by generating stable cell lines we established a novel platform for *in vitro* and *in vivo* investigation of CLL signal transduction and treatment modalities.

Keywords: B-cell receptor (BCR), Bruton's tyrosine kinase (Btk), chronic lymphocytic leukemia (CLL), Ibrutinib, Idelalisib.

INTRODUCTION

Chronic lymphocytic leukemia (CLL) is characterized by the accumulation of monoclonal mature B cells with a $CD5^+CD19^+CD20^{dim}Ig^{dim}CD23^+CD43^+CD27^+$ surface phenotype in the circulation[1,2]. Several lines of evidence support a key role for B cell receptor (BCR) signaling in CLL pathogenesis. First, CLL with hypermutated immunoglobulin heavy chain variable (IGHV) genes (M-CLL) show a more favorable prognosis than those with unmutated IGHV genes (U-CLL)[3,4]. Secondly, the IGHV repertoire is highly restricted, whereby stereotypic BCRs are found in multiple CLL patients[5]. Thirdly, CLL B cells often show increased basal activity of protein tyrosine kinases downstream of the BCR[6,7]. Hereby, Bruton's tyrosine kinase (Btk) has been shown to be essential for several constitutively active pathways implicated in CLL cell survival, including the Akt, ERK and NF-κB pathway[8-11]. Antitumor activity of the Btk small-molecule inhibitors ibrutinib and acalabrutinib was recently shown in clinical studies of relapsed/refractory CLL[12,13]. Furthermore, CLL B cells manifest low surface IgM (sIgM) expression and their BCR signaling properties resemble those of anergic B cells. During *in vitro* culture they readily upregulate sIgM expression and regain BCR responsiveness[14-17]. Accordingly, CLL B cells have higher basal, cell-autonomous Ca^{2+} signaling, dependent on an internal BCR epitope[18,19]. Alternatively, the recent identification of antigen-specificity of particular CLL B cells indicates that their proliferation and survival is driven by specific (auto)antigens[20,21].

CLL B cells are thought to interact with the tissue microenvironment[22-24] and lymph node resident CLL cells show gene expression signatures indicative of BCR activation[25]. Btk may be involved in trafficking of CLL B cells to survival niches, because it also functions downstream of chemokine receptors such as CXCR4 and CXCR5[11] and has been implicated in *in vivo* homing to lymphoid organs[26]. Accordingly, treatment of CLL cells with ibrutinib inhibited CXCL12/CXCL13-induced *in vitro* cell adhesion and migration[27,28] and in CLL patients ibrutinib treatment resulted in a transient lymphocytosis, further underscoring the role of Btk in CLL-cell trafficking and homing[12].

Given the importance of intrinsic BCR signaling for survival and progression of CLL as well as support from the tumor microenvironment, research into CLL pathogenesis would benefit from systems that can explore both pathways. However, these approaches have been hampered by the limited *in vitro* survival and non-dividing characteristics of human CLL B cells. Those few available cell lines derived from CLL patients (CD5- MEC1 and MEC2[29], PCL12[30], OSU-CLL[31] and MDA-BM5[32]) may represent EBV+ B-lymphoblastoid cells rather than bonafide B-CLL cells.

Mouse models have provided important insights into CLL pathogenesis. These particularly include the widely studied Eμ-TCL1 model, in which B-cell specific overexpression of the *TCL1* oncogene results in spontaneous development of leukemic $CD5^+IgM^+$

B cells[33-35]. Effects of ibrutinib or the Syk inhibitor fostamatinib (R406) on Eμ-TCL1 leukemias have been tested, whereby the outcome mimicked clinical observations in patients[28,36]. Another mouse model (*IgH.TEμ*) was generated in our lab and is based on sporadic expression of the SV40 large T oncogene in mature B cells[37]. This was achieved by SV40T insertion in opposite transcriptional orientation into the *IgH* locus DH-JH region. Aging *IgH.TEμ* mice show accumulation of monoclonal leukemic $CD5^+CD43^+IgM^+IgD^{low}CD19^+$ B cells, which is dependent on Btk expression and whereby Btk-mediated signaling enhances leukemogenesis[37,38]. Despite their proven usefulness as pre-clinical tools, transgenic mouse models take substantial time (> 6 months) to develop CLL and are not suitable for large-scale screens of novel compounds or combination therapies. Therefore, we aimed to obtain stable CLL cell lines that can be cultured *in vitro* or transferred into mice *in vivo*. In addition, we aimed to explore whether these cell lines could serve as a platform for the investigation of CLL signal transduction and to investigate the efficacy of small molecule inhibitor combinations in CLL. Here, we describe the generation and characterization of three monoclonal $CD5^+CD43^+IgM^+CD19^+$cell lines from *IgH. TE*μ mice. Parallel to human CLL, our cell lines exhibited constitutive activation of BCR downstream kinases.

MATERIALS AND METHODS

EMC cell line culture

Single-cell suspensions (1 × 10^6 cells/ml) obtained from spleen from *IgH. TE*μ mice, which were on a mixed C57Bl/6 × sv129 background (EMC6) or on the $Aicd^{-/-}$ (C57Bl/6 × sv129) background[57] (EMC2 and EMC4). These *IgH. TE*μ mice were diagnosed with leukemia on the basis of a high tumor load (> 90% $CD5^+CD43^+IgM^+CD19^+$ cells) in peripheral blood. Leukemic cells were cultured in medium (RPMI 1640, 10% FCS, 50 ug/ml gentamycin, 50 μM 2-mercapto-ethanol, all components from Life TechnologiesTM), under various conditions, with or without BAFF (25ng/ml, R&D Systems), α-CD40 antibodies (20 ug/ml, R&D Systems), rIL-4 (50 ng/ml, Peprotech) and incubated at 37°C in the presence of 5% CO_2. After initial passages, the EMC cell lines continued to expand in the absence of added growth factors and therefore the cell lines were propagated in culture medium only. For optimum growth, the EMC4 and EMC6 cell lines were propagated in dilution of 0.25 × 10^6 cells/ml and EMC2 cell lines were propagated in dilution of 0.5 × 10^6 cells/ml. Once growing in culture the doubling time for the EMC6 and EMC4 lines were ~36 hours and for EMC2 ~72 hours. The culture media were refreshed twice a week. The cultures were stopped after 12 weeks of the initial culture and vials were frozen. For subsequent experiments, vials were thawed and expanded. All experiments were performed one day after refreshing medium and expanding cell culture. For all *in vitro* assays cells were plated in dilution of 1x10^6 cells/ml.

Adoptive transfer into $Rag1^{-/-}$ mice and ibrutinib treatment

For adoptive transfer, 5 × 10^6 EMC4 cells or 1 × 10^6 EMC6 cells were injected intraperitoneally (i.p.) into $Rag1^{-/-}$ mice[51]. Mice were monitored for leukemia development by regular blood screening for the presence of $CD5^+CD43^+IgM^+CD19^+$ leukemic cells: at day 7, 10 and 14 after engraftment subgroups of mice were tested. Mice were euthanized when they developed signs of sickness, such as lethargy, aversion to activity, shallow or labored breathing and other disabling symptoms.

Ibrutinib (Chiralstar, USA) treatment was initiated 2 weeks following engraftment in mice with > 2% leukemic cells in the circulation, as detected by flow cytometry. Mice were randomized into ibrutinib and vehicle treatment group and ibrutinib (25 mg/kg in water/5%mannitol/0.5%gelatin) or vehicle was orally administered to the mice once daily for 16 days. Mice were euthanized when they developed signs of severe disease, as described above, or at the end of the 16-day treatment cycle.

Mice were housed at the Erasmus MC experimental animal care facility under specific pathogen-free conditions. Animal procedures were reviewed and approved by the Erasmus MC Animal Experiments Committee.

Flow cytometry procedures

Preparation of single-cell suspensions of lymphoid organs and lysis of red blood cells were performed according to standard procedures. Cells were directly stained in the appropriate buffer using the following fluorochrome-conjugated monoclonal antibodies: anti- CD19 (1D3, eBioscience), anti-CD5 (53-7.3, eBioscience), anti-CD43 (S7, BD), anti-IgD (11-26, BD), anti-IgM (Il/41, eBioscience), anti-CD3 (17A2, eBioscience), anti- CD11b (M1/70, eBioscience), anti-MHCII (M5/114.15.3, eBioscience), anti-CD86 (GL1, BD), anti-CD69 (H1.2F3, eBioscience), anti-CD25 (PC61.5, eBioscience), anti- CXCR4 (2B11, BD), anti-CXCR5 (2G8, BD), anti-CCR7 (4B12, eBioscience). All flow cytometric measurements were performed on a LSRII flow cytometer (BD Biosciences) and results were analyzed using FlowJo-V10 software (TreeStar).

For intracellular flow cytometry analysis of phosphorylated proteins (Phosflow), cells were starved for 10 min at 37°C in FCS-free "RPMI-plus" medium (RPMI 1640 from Life TechnologiesTM) and subsequently stimulated with 20 μg/ml goat anti-mouse F(ab')2 anti-IgM fragments (Jackson Immunoresearch) for 5 min (for p-Btk, p-Slp65, p-Plcγ2) or 3 hrs (for p-Akt, p-S6). Unstimulated control cells were treated in parallel without F(ab')2 α-IgM. Following stimulation, cells were fixed in Cytofix fixation buffer (BD Bioscience) for 10 min at 37°C and permeabilized with Perm Buffer III (BD Biosciences) at –20°C for 30 min. The cells were then stained with either with fluorochrome-conjugated anti-p-Btk(Y551), anti-p-Btk(Y223), anti-p-Slp65/BLNK(Y84), anti-p-Plc-y2 (Y759) antibodies (all from BD Biosciences) or with unconjugated anti-p-Akt(S473), anti-p-S6 (all from Cell Signaling

Technology) and PE-conjugated secondary antibody (Jackson ImmunoResearch). WT splenic cell suspensions were stained extracellularly with anti-B220 (RA36B2, eBioscience) and CD3 (145-2c11, BD) before fixation.

Calcium (Ca^{2+}) flux assays

Intracellular Ca^{2+} flux was measured using the Fluo3-AM and Fura Red-AM fluorogenic probes (Life Technologies), as previously detailed[19]. In brief, mouse splenocytes (5×10^6) were incubated with 5 µM Fluo3- AM and 5 µM Fura Red-AM in loading buffer (HBSS medium supplemented with 10 mM HEPES and 5%FCS) at 37°C for 30 min in the dark. To gate for untouched B cells in WT splenocytes, we added biotinylated Abs to NK1.1 (PK136, BD), CD4 (GK1.5, BD), CD8a (53–6.7, BD), Ter119 (BD), CD11c (N418, ebiosciences), Gr-1 (RB6-8C5, ebiosciences), and FcRεI (MAR-1, ebiosciences) for the final 10 min of incubation. Cells were subsequently washed and stained with fluorochrome-conjugated streptavidin at RT for 10 min as a second step for biotin-conjugated antibodies. Cells were then washed, resuspended in buffer (HBSS medium with 10 mM HEPES, 5%FCS and 1 mM $CaCl_2$), filtered and left for at least 30 min at RT. Cells were warmed to 37°C for 5 min before acquisition of events.

Basal intracellular Ca^{2+} levels were measured for 60 s, followed by BCR stimulation with either 20 µg/ml goat anti-mouse F(ab')2 anti-IgM fragments or plain control liposomes (DOPC/CHOL 55:45, Formumax Scientific Inc.) and measured for 5–7 min. At the end of each Ca^{2+} measurement, cells were stimulated with 4 µg/ml ionomycin (Life Technologies, Carlsbad, California, USA) to measure maximum Ca^{2+} signaling.

To determine effects of ibrutinib on Ca^{2+} mobilization, 5×10^6 EMC cells and WT splenocytes were pre-incubated in culture medium with or without ibrutinib (1 µM) at 37°C for 3 h. Staining and Ca^{2+} mobilization measurements were performed as described above.

Cell cycle and viability assays

To evaluate the effect of ibrutinib on survival and proliferation, 1×10^6 EMC cells were placed in culture medium, with or without the appropriate concentration of ibrutinib at 37°C for 24 h. Following treatment, cells were fixed with ethanol and stained with propidium iodide, according to the instructions of the manufacturer (Life TechnologiesTM). Cell cycle analysis was performed as previously described[58].

For testing sensitivity to chemotherapeutic agents, EMC cell lines were incubated with different concentrations of Etoposide, Cisplatin or Fludarabine from Sigma Chemical (St. Louis, MO) for 24 h. Viability was measured by DiOC6/PI staining as described[59]. Relative viability was defined as [% viable cells treated condition/ % viable cells in medium control] × 100.

Adhesion assay

EMC Cells were treated with either ibrutinib (10 nM) or idelalisib (100 nM) or a combination and allowed to adhere to fibronectin-coated surfaces and adhesion to fibronectin-coated plates was measured as described previously[27].

RNA sequencing from naïve, activated and CLL B cells

Splenic single-cell suspensions were prepared in magnetic-activated cell sorting (MACS) buffer (PBS/2 mM EDTA/0.5%BSA) and naïve splenic B cells from 8–12 week-old WT C57BL/6 mice were purified by MACS, as previously described[60]. Non-B cells, B-1 cells, germinal center B cells and plasma cells were first labeled with biotinylated antibodies (BD Biosciences) to CD5 (53–7.3), CD11b (M1-70), CD43 (S7), CD95 (Jo2), CD138 (281-2), Gr-1 (RB6-8C5) and TER-119 (PK136) and subsequently with streptavidin-conjugated magnetic beads (Miltenyi Biotec). Purity of MACS-sorted naïve B cells was confirmed by flow cytometry (typically > 99% CD19+ cells). To obtain activated B cells, purified naïve B cells were cultured in RPMI culture medium in the presence of 10 µg/ml F(ab')2 anti-IgM (Jackson Immunoresearch) for 12 h.

RNA was extracted from naive or activated splenic B cells, as well as from purified EMC2, EMC4 and EMC6 primary tumors (using MACS-purification for $CD19^+$ cells) and from the three EMC cell lines from *IgH.TEμ* mice with Qiagen's RNeasy Mini and Micro kits according to manufacturer's instructions followed by DNase treatment. To facilitate comparisons with resting and activated B cells, MACS purified naïve mature splenic B cells from WT mice, either directly or after 12 hours of stimulation with α-IgM were included. The purity of sorted cells (typically > 99% $CD19^+$ cells) was confirmed by flow cytometry.

Total mRNA sequencing was performed on a HiSeq 2500 (Illumina), and raw reads were aligned using Bowtie to murine transcripts (RefSeq) corresponding to the University of California at Santa Cruz (UCSC) mouse genome annotation (NCBI37/mm9)[61]. Statistical analysis of the RNAseq data was performed using HTseq and edgeR. Gene counts were computed using HTseqCount[62]. Differential gene expression analysis was performed using EdgeR with a false discovery rate (FDR) < 0.05 and a log2-fold change cutoff of 1[61]. Gene counts were converted to logCPM (log counts per million) values for principle component analysis (PCA), which was performed in R, a language for statistical computing (http://www.r-project.org). For generating heatmaps and molecular pathway enrichments the differentially expressed gene list was further filtered for genes with an absolute FPKM value of >1 in at least 2 samples in either group. Molecular pathway enrichments were obtained from the MSigDB[45].

Quantitative real time (RT-) PCR analysis

For quantitative RT-PCR analysis, TaqMan probes were employed. Probe Finder software (Roche Applied Science), the Universal Probe Library (Roche Applied Science) and Ensembl genome browser (http://www. ensembl.org/) were used for primer and probe design. Taqman Universal Master Mix II, was purchased from Thermo Fisher Scientific. For 15 µl RT-PCR reaction, 7.5 µl master mix, 4.15 µl nuclease-free water, 0.6 µl forward and reverse primer (10pmol/ul) and 0.15µl probe was added to the cDNA per reaction. Quantitative RT-PCR was performed by using the 7300 Real Time PCR system (Applied Biosciences) according to manufacturer's instructions. Gene expression was analyzed with an ABI Prism 7300 Sequence Detector and ABI Prism Sequence Detection Software version 1.4 (Applied Biosystems). Cycle-threshold levels were calculated for each gene and housekeeping gene glyceraldehyde-3-phosphate dehydrogenase (Gapdh) was used for normalization of the values. All primer sequences and probe numbers are listed in **Supplementary Table 2**.

Statistical analysis

Statistical analysis was performed using GraphPad Prism software (San Diego, California, USA). For calculating levels of significance, for differences between groups of continuous data we used Mann-Whitney *U* test. To compute synergistic effects of combination treatments we used CompuSyn (version 1.0) software based on Chou and Talalay method[49]. The log rank test was used for calculating the level of significance for survival differences between differently treated mice groups. The one-sample *T*-test was used to determine the significance of differences between means and normalized values (100%).

RESULTS

Generation and characterization of cell lines from IgH.TEµ CLL mice

To obtain stable cell lines, single cell suspensions from spleens of aged *IgH.TE*µ mice [37] with high tumor load (> 90% $CD5^+CD43^+IgM^+CD19^+$ cells) were cultured under various conditions, with or without BAFF, a-CD40 antibodies and rIL-4. After 8 weeks outgrowth was observed in three independent cultures: EMC2, EMC4 and EMC6. The presence of BAFF, a-CD40 or rIL-4 did not appear to be critical and after the initial few passages the EMC cell lines were expanded in culture medium without supplements.

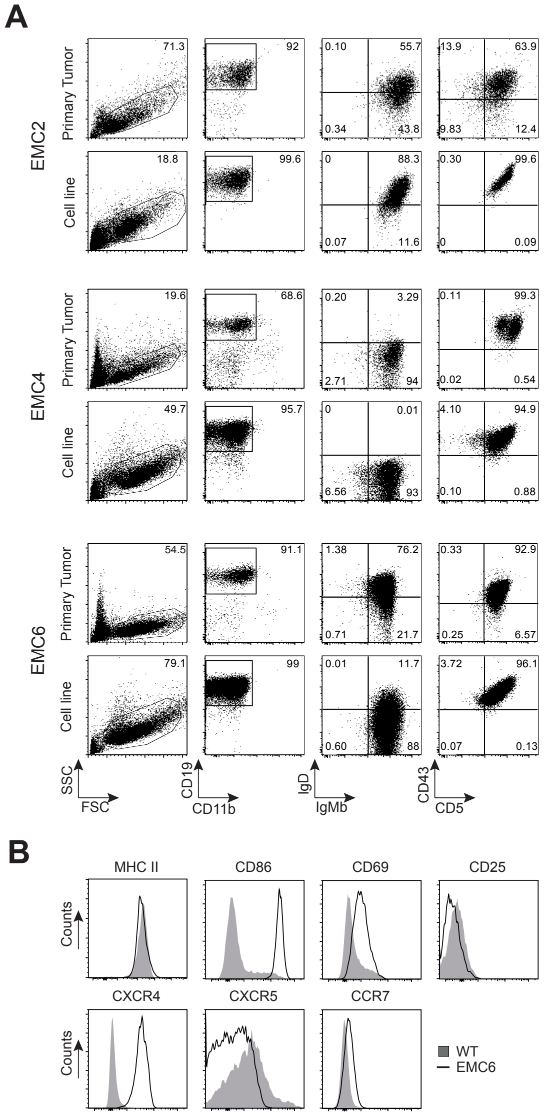

Figure 1. EMC cell lines resemble primary tumors from *IgH.TEµ* mice.
(**A**) Phenotypic comparison of CLL cells from primary splenic tumor cells and established cell lines by flow cytometry. Gated $CD11b^-CD19^+$ (*second column*) were analyzed for IgM/IgD (*third column*) and CD5/CD43 (*fourth column*). (**B**) Histograms showing expression of the indicated markers on gated $CD19^+$ WT splenic cells ($n = 4$) and EMC6 cells, determined by flow cytometry. EMC4 and EMC2 showed similar expression profiles, unless indicated in text.

Flow cytometry analysis showed that the EMC cell lines maintained the $CD5^+CD43^+IgM^+CD19^+$ phenotype of the primary leukemia[37], even after prolonged (at least 22 weeks) *in vitro* culture (**Figure 1A, Supplementary Figure 1A**). Expression levels of the activation markers CD69 and CD86 were higher on the EMC cell lines than on control wild type (WT) splenic B-cells, but surface MHCII or CD25 was similar (shown for EMC6 in **Figure 1B, Supplementary Figure 1A**). Compared with WT B cells, the EMC cell lines exhibited stronger expression of CXCR4 and CCR7, but not CXCR5 (**Figure 1B; Supplementary Figure 1A, 1B**). The expression profiles of activation markers and chemokine receptors of the EMC cell lines resembled those of primary tumors from *IgH.TEμ* mice (*n* = 20), except for CD69 when compared to WT B cells (**Figure 1B ; Supplementary Figure 1C**).

Thus, we generated three stable cell lines that maintained the CD5$^+$CD43$^+$IgM$^+$CD19$^+$ phenotype of the primary CLL, even after prolonged *in vitro* culture.

RNA sequencing reveals limited differences between EMC cell lines and their corresponding primary leukemias

To identify pathways involved in the outgrowth of the three cell lines from the corresponding primary tumors, we compared genome-wide RNA-seq gene expression profiles. We included resting and α-IgM-stimulated WT splenic B cells as controls. A principle component analysis (**Figure 2A**) revealed substantial differences between resting and activated WT splenic B cells and primary CLL. The three EMC cell lines clustered together, close to the primary tumors, with EMC6 showing the smallest difference to its corresponding primary leukemia (**Figure 2A**).

Next, we performed differential gene expression analysis to identify 246 genes that showed more than 2-fold change between primary tumors and EMC cell lines, and from these we subsequently selected genes with FPKMs >1 in at least 2 samples. We identified 34 upregulated and 62 downregulated genes in the EMC cell lines, compared with the primary tumors (**Figure 2B, 2C**; See **Supplementary Table 1A, 1B** for expression values). Expression levels were confirmed by QPCR for a number of key genes, including Tnfsf9, Pim2, CD70 and Egr1, which are also highly expressed in human CLL[39-43] (**Supplementary Figure 2A, 2B**). Interestingly, the glucocorticoid-induced leucine zipper protein (GILZ), encoded by the *Tsc22d3* gene, which inhibits the mTORC/ AKT signaling pathway[44] was amongst the genes downregulated in the EMC cell lines (**Supplementary Figure 2C**). We did not find upregulation of anti-apoptotic genes, including Bcl-2, Bcl-XL or Mcl-1 in the EMC cell lines, compared to primary leukemias. However, expression of these anti-apoptotic genes was increased in both primary tumors and EMC cell lines, when compared to control WT splenic B cells (**Supplementary Figure 2D**).

The top 20 biological processes (Molecular Signatures Database MsigDB)[45] enriched within the differentially expressed genes in the EMC cell lines showed an overrepresentation of cell proliferation, metabolic and tissue development-related pathways (**Figure 2D**). Moreover, pathway analysis revealed a significant overlap with a gene set upregulated in "CLL expressing naturally phosphorylated CD5" (Insig1, Sqle, Tnfsf9, Asns, Pim2, Wnt-10A, IL-10, CD70, Rab39b)[46]. Other prominent signatures emerging from genes upregulated in the EMC cell lines compared to primary CLL tumors were "mTorc1 signaling" and "TNFα signaling via NFkB" (both with $p = \sim 10^{-5}$, FDR<0.05; **Supplementary Figure 2C**).

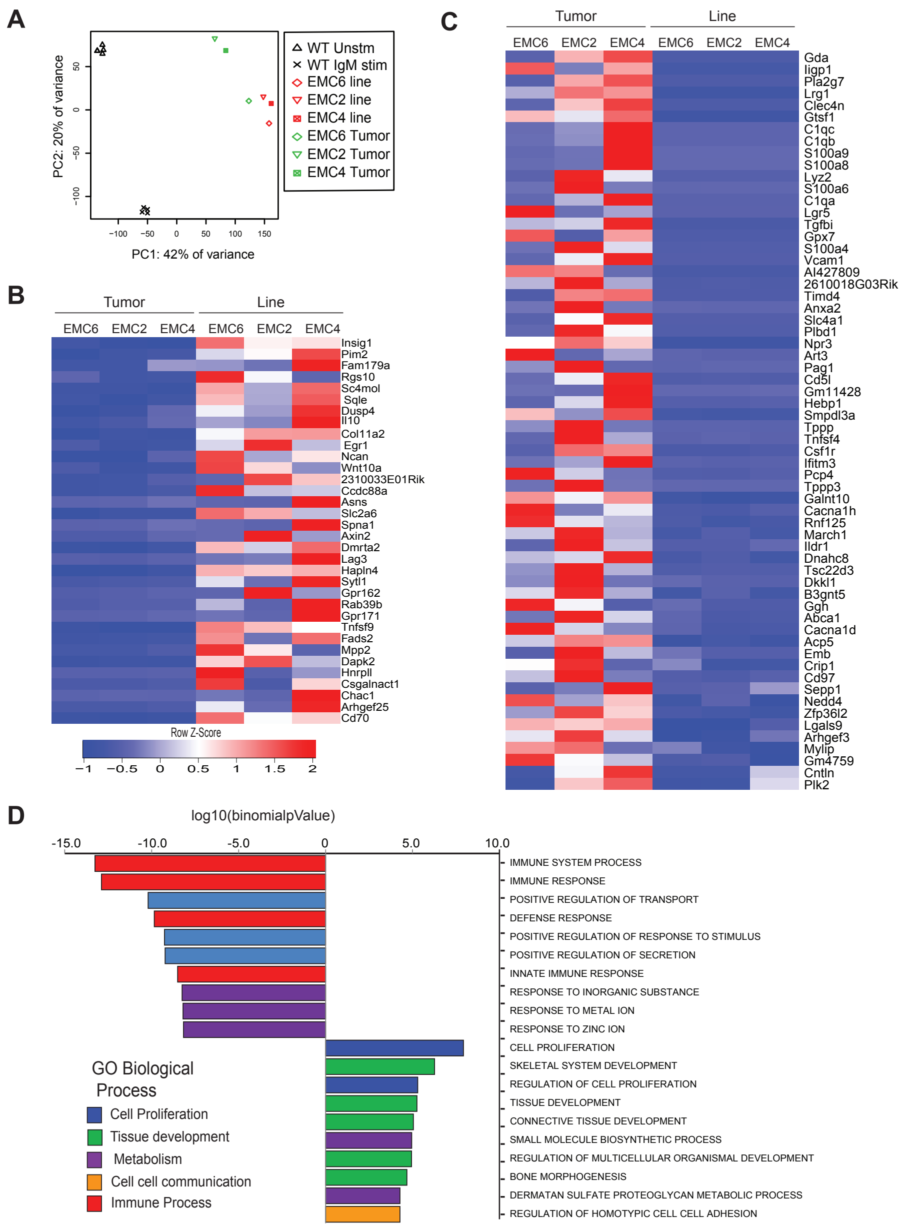

Figure 2. RNA-sequencing reveals limited differences between EMC cell lines and primary leukemias. (**A**) Principle component analysis comparing genome-wide RNA-Seq profiles in resting (Unstim, *n* = 4) or α-IgM-stimulated (IgM stim, *n* = 4) WT splenic B cells, primary tumors (green, *n* = 3) and EMC cell lines (red, *n* = 3). (**B, C**) Heat map showing variation in levels (Z-Score) of 34 upregulated (**B**) and 62 downregulated genes (**C**) in the EMC lines compared to primary tumors, ordered by *p*-value (**Supplementary Table 1**) (**D**) Top 20 biological processes enriched among differentially expressed genes in EMC cells and primary tumors (from MSigDB database).

In conclusion, the genome-wide expression profiles of the three cell lines closely resembled those of the primary tumors and suggest that mTorc1 signaling contributed to cell line outgrowth.

EMC cell lines express a V_H11 BCR recognizing PtC and exhibit constitutive BCR signaling

Next, we determined the rearranged IGHV and IGLV DNA sequence of the EMC cell lines. Even though generated independently from three different mice, all three EMC cell lines expressed V_H11.2*01 (HCDR3: CMRYSNYWYFDVW) together with V_K14-126*01 (LCDR3: CLQHGESPYTF), which was identical to the corresponding primary tumors. This stereotypic V_H11/V_K14 BCR is known to be specific for phosphatidylcholine (PtC)[47] and is the prominent BCR found in both Eμ- TCL1 transgenic CLL[21] and in *IgH.TEμ* transgenic CLL[37,38]. We could confirm uniform PtC binding of EMC cell lines, yielding similar staining intensities as WT peritoneal cavity B-1 cells (**Figure 3A**). Hereby, the signal for EMC6 was lower than for EMC2 and EMC4. PtC also induced Ca^{2+} flux in all three EMC cell lines, indicating that their BCRs did not only bind but also responded to PtC (**Figure 3A**).

Next, we compared the activation status of BCR downstream signaling proteins between the cell lines and WT splenic B cells by intracellular flow cytometry for phosphorylated proteins (Phosflow). In the absence of external stimulation, the EMC cell lines exhibited significant phosphorylation of Btk (Y551/Y223), Slp65(Y84), Akt(S473) and its target S6 (**Figure 3B, Supplementary Figure 3D**). As phosphorylation of these proteins was not observed in resting B cells, these findings provided evidence for constitutively active BCR/Akt signaling in the EMC cell lines, which was corroborated by increased basal Ca^{2+} signals (**Figure 3B, Supplementary Table 3**). Importantly, the constitutive BCR/Akt signaling in the EMC cell lines was stable over 22 weeks of *in vitro* culture (**Supplementary Figure 3E**). In line with our previous report[37,38], constitutively active Btk signaling was not apparent in primary *IgH.TEμ* CLL cells, but these cells had low but detectable expression of p-Akt and substantial levels of p-S6 (**Supplementary Figure 3A**). Anti-IgM stimulation of EMC cell lines further increased p-Btk(Y551/Y223), p-Slp65(Y84), induced p-Plcγ2(Y759), but did not further increase p-Akt(S473) expression (**Figure 3B**). Thus, in the EMC cell lines constitutive Btk activation was suboptimal and did not result in detectable Plcγ2(Y759) phosphorylation, but could be further enhanced by BCR stimulation. In addition, we found that the EMC cell lines had high basal Ca^{2+} and less sustained Ca^{2+} elevation in response to α-IgM stimulation, compared with WT B cells (**Figure 3B**), which represent key features of the anergic phenotype of human CLL B cells[14-17]. Because of the similarities between the EMC cell lines, for most of the experiments described below, we focused on EMC4 and EMC6.

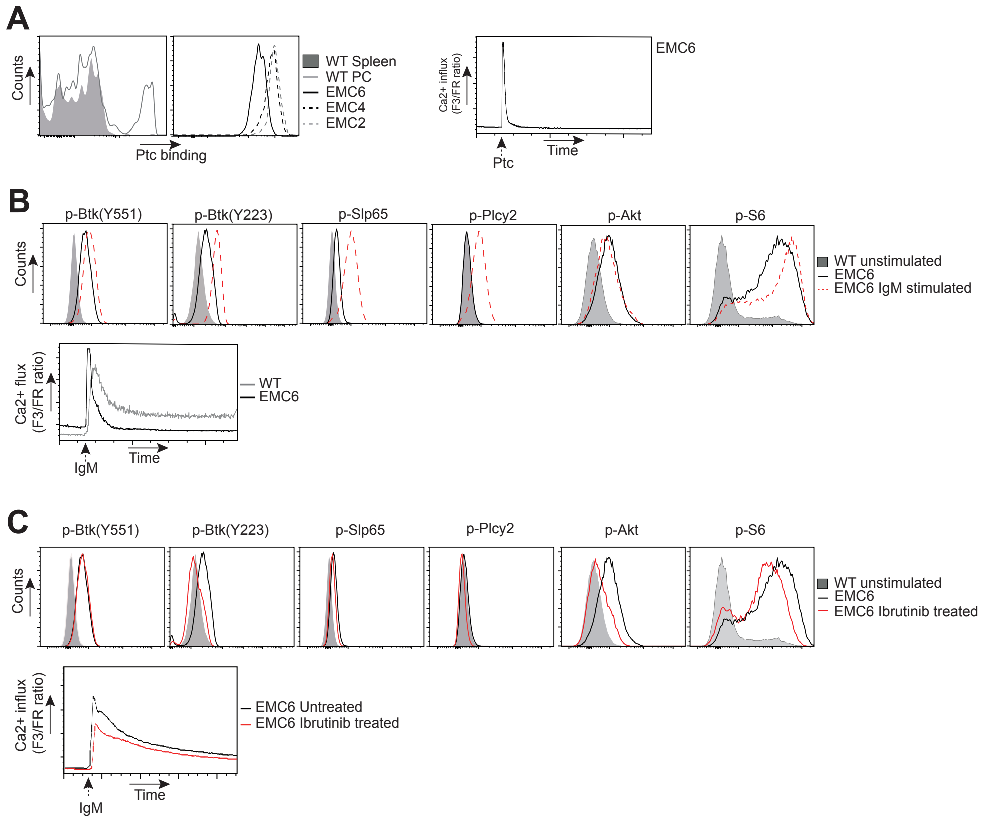

Figure 3. EMC cell lines recognize autoantigens and exhibit constitutive BCR signaling.
(**A**) *Left*: Flow cytometric analysis of gated wildtype (WT) $CD19^+$ splenocytes and $CD19^+CD5^+$ peritoneal cavity (PC) cells, and EMC cell lines stained with phosphatidylcholine (Ptc) liposomes. *Right*: Ca^{2+}-flux analysis of PtC-stimulated EMC6. (**B**) *Top*: PhosFlow analysis of indicated phosphoproteins on gated unstimulated $B220^+CD3^-$ WT splenocytes and EMC6 cells, and α-IgM-stimulated (20 µg/ml) EMC6 cells. *Bottom*: Comparison of basal or α-IgM stimulated Ca^{2+} influx between $B220^+CD3^-$ WT splenic B cells and EMC6. (**C**) *Top*: PhosFlow analysis of indicated phosphoproteins on gated unstimulated $B220^+CD3^-$ WT splenocytes and EMC6 cells and 1µM ibrutinib-treated EMC6 cells. *Bottom*: Comparison of Ca^{2+}-influx between untreated or 1µM ibrutinib-treated EMC6 cells. For all analyses EMC6 cells are shown as representative of the three cell lines.

Next, we investigated whether constitutively active BCR signaling in the EMC cell lines was dependent on Btk kinase activity. We found that in the presence of ibrutinib the signals specific for p-Btk(Y223) but not for p-Btk(Y551) were substantially reduced (**Figure 3C**). Whereas the effect of ibrutinib treatment on lowering basal p-Slp65 was less apparent, it clearly downregulated p-Akt(S473) and pS6. In the presence of ibrutinib, the α-IgM induced Ca^{2+} influx was also slightly reduced (**Figure 3C, Supplementary Figure 3B**). Constitutive Btk(Y551) phosphorylation was Syk kinase independent, because addition of the Syk inhibitor R406 did not affect p-Btk(Y551), nor p-Akt(S473) signals (**Supplementary**

Figure 3C). However, R406 did decrease p-Slp65(Y84), p-Plcγ2(Y759) and α-IgM induced Ca^{2+} influx (**Supplementary Figure 3C**).

Collectively, these findings show that the EMC cell lines are monoclonal, express a PtC-specific V_H11/V_K14 BCR and exhibit stable constitutive Btk and Akt activation. Constitutive Btk(Y551) phosphorylation was Syk-independent and Btk(Y223) autophosphorylation was suboptimal. Whereas upon α-IgM stimulation of the EMC cell lines p-Slp65(Y84) and p-Plcγ2(Y759) were induced, Ca^{2+} influx was limited, congruent with an anergic response to BCR stimulation.

EMC cell lines provide a novel in vitro tool to test therapeutic drugs for CLL

The prolonged stability of the EMC cell lines in culture enabled us to test their sensitivity towards different classes of DNA damaging agents. The cell lines were relatively resistant to Fludarabine (LC_{50}= 17 μM), a purine analogue widely used in combination regimens in CLL. The cells turned out to be highly resistant to cisplatin (LC_{50}= 9.73 μM), which is used in combination regimens in chemorefractory patients. These data are compatible with p53 dysfunction in *IgH.TEμ* mice[37] and lack of induction of the p53 target gene Puma following 24 h of treatment[48]. Interestingly, the EMC cell lines were sensitive to the topoisomerase II inhibitor etoposide (LC_{50}= 0.24 μM) (**Supplementary Figure 4A, 4B**), allowing *in vitro* testing of combination strategies including genotoxic agents. To investigate the role of constitutively active Btk and Akt on EMC cell viability and proliferation, we performed propidium iodide DNA content analyses following overnight treatment with ibrutinib, idelalisib or vehicle as controls. In the presence of ibrutinib and idelalisib the proportions of apoptotic (sub-G1) and cycling (S/G2/M) cells were significantly increased and decreased, respectively (**Figure 4A, 4B**). To quantify the effect of combination treatment, we calculated combination index (CI) values[49] and observed synergistic effects (CI value < 1) on viability and proliferation when the two inhibitors were combined. Interestingly, ibrutinib induced a G1 cell-cycle arrest in EMC6 (**Figure 4A**). Therefore, we evaluated the impact of ibrutinib on different families of apoptosis and proliferation regulators. Ibrutinib treatment alone showed >2 fold downregulation of survivin mRNA expression (**Supplementary Figure 4C–4F**), which was highly expressed in both primary tumors and EMC cell lines, when compared to control WT splenic B cells (**Supplementary Figure 2D**). Since survivin has been shown to be downstream of the PI3K/Akt pathway in CLL[50], it further validates the importance of constitutive Akt signaling in the EMC cell lines. Ibrutinib or idelalisib also significantly inhibited integrin-mediated adhesion to fibronectin *in vitro,* again showing a synergistic effect (CI value < 1) when these inhibitors were combined (**Figure 4C, Supplementary Figure 4G**).

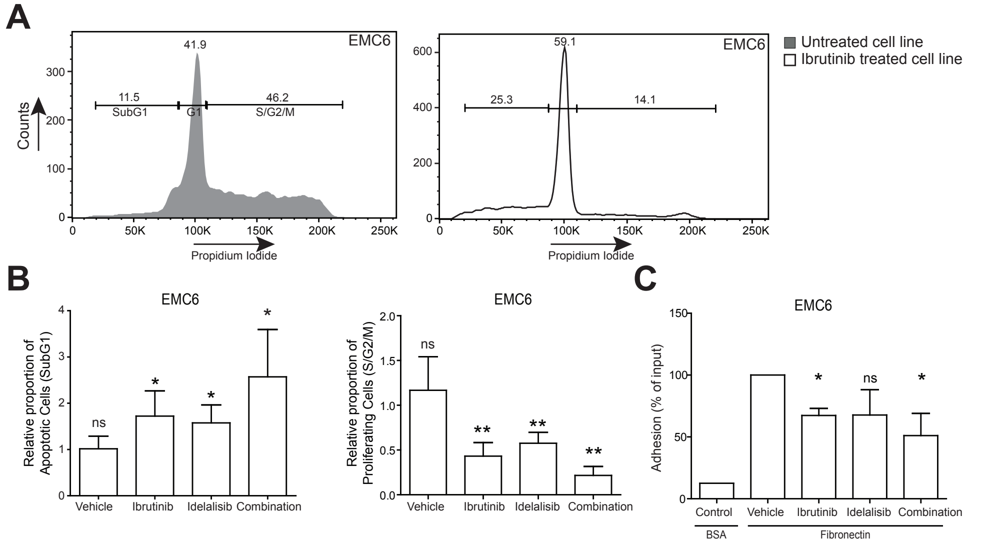

Figure 4. EMC cell lines provide novel *in vitro* tools to test therapeutic drugs for CLL.
(**A**) Gating strategy for DNA content (Propidium Iodide) analysis of EMC6 cells after 24 h culture in the absence or presence of Ibrutinib. Numbers indicate proportions of cells in the respective gates. (**B**) Relative proportions of cycling (S/G2-M) and apoptotic (sub-G1) EMC6 cultured (*n* = 3, in duplicate) in the presence of either ibrutinib (5 nM), idelalisib (100 nM) or in combination. Graphs are presented as normalized mean ± SEM (Untreated EMC6 cells were set to 1). (**C**) *In vitro* adhesion to fibronectin. EMC6 cells were pretreated with ibrutinib (10 nM), idelalisib (100 nM) or a combination (*n* = 3, in triplicate). Graphs are presented as normalized mean ± SD (100%= vehicle-treated EMC6 cells). $^*P < 0.05$, $^{**}P < 0.01$ (paired one-sample *T*-test).

Collectively, these results show the importance of constitutively active Btk and Akt signaling for survival, proliferation and adhesion of the EMC cell lines in *in vitro* cultures.

Engraftment of EMC cell lines into Rag1$^{-/-}$ mice as a tool to study novel CLL therapeutics

To test their tumorigenic potential, we transferred 1–5×10^6 EMC cells into *Rag1*$^{-/-}$ mice[51] by i.p. injection (**Figure 5A**). From 2 weeks post-engraftment onwards, a population of $CD5^+CD43^+IgM^+CD19^+$ B-cells was detectable; these cells were not only present in peripheral blood, but also in various lymphoid organs, including spleen, bone marrow and mesenteric lymph node (shown for EMC4-engrafted mice, 4 weeks after transfer in **Figure 5B**).

To test the effects of ibrutinib *in vivo,* we compared mouse survival in EMC6-engrafted mice that received either ibrutinib or vehicle. Two weeks after engraftment mice were randomized and ibrutinib or vehicle treatment was initiated and continued for 16 days (**Figure 5A**). Whereas in the vehicle group mice had to be euthanized as their condition

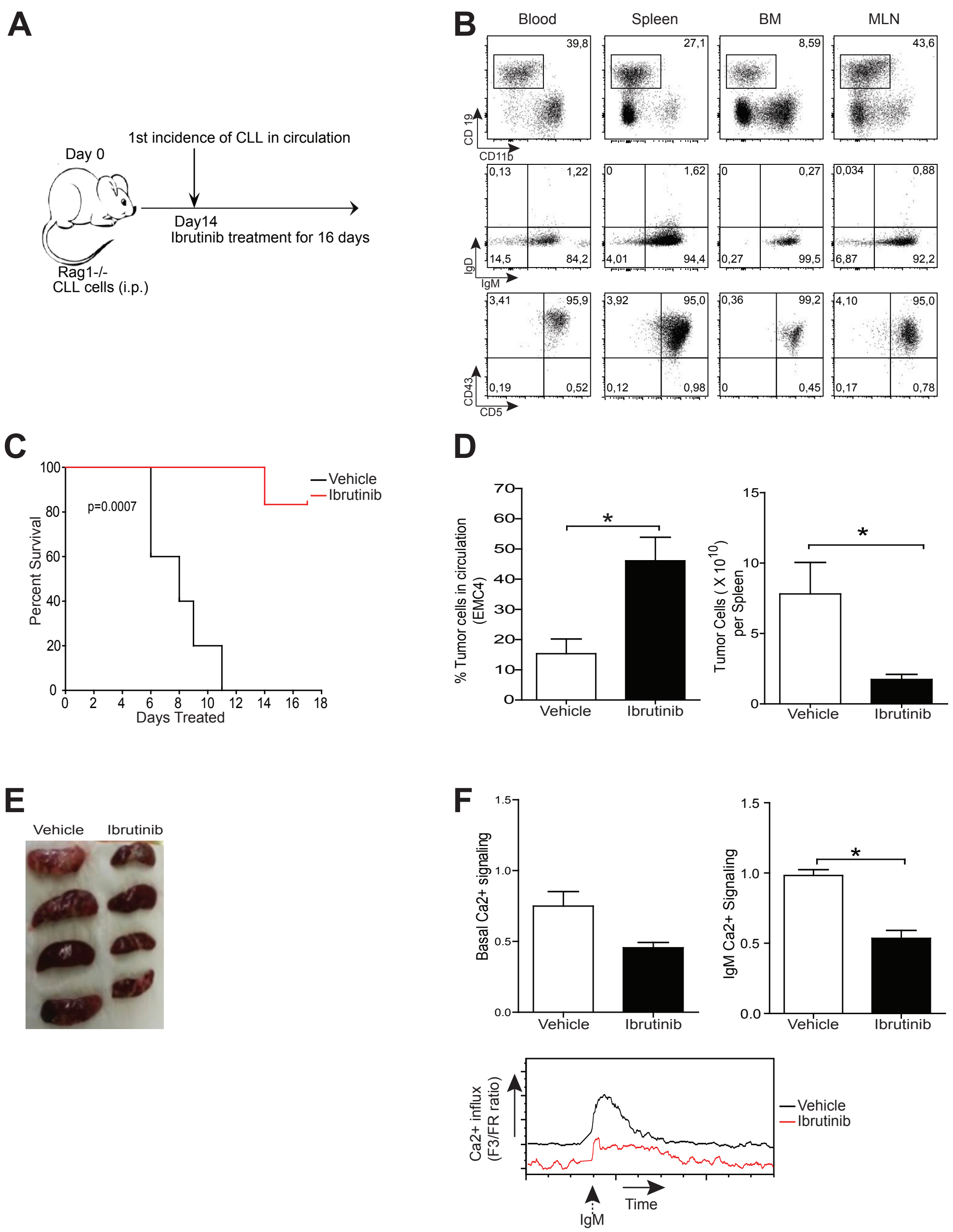

Figure 5 (see left page):.Leukemia induction following EMC cell engraftment as a tool to study therapeutics. (**A**) Experimental timeline of EMC cell transfer. (**B**) Flow cytometric analysis of blood, spleen, bone marrow (BM) and mesenteric lymph node (MLN) of *Rag1*$^{-/-}$ mice after 4 weeks of engraftment of 5x10^{6} EMC4 cells. CD19^{+}CD11b^{-} cells were gated (*left column*) and analyzed for IgM/IgD and CD5/CD43 in the indicated tissues. Dot plots are representative of successful EMC cell engraftment. (**C**) Kaplan-Meier survival curve over 16 days of ibrutinib or vehicle treatment of EMC6- engrafted *Rag1*$^{-/-}$ mice (n = 8 mice/group). (**D**) Proportions of circulating leukemic cells (*left*) and absolute number of leukemic cells in spleen (*right*), 16 days after treatment of EMC4-engrafted mice with vehicle or ibrutinib (n = 4 mice/group). (**E**) Spleens from EMC4-engrafted mice treated for 16 days with vehicle or ibrutinib. (**F**) Comparison of basal and α-IgM-stimulated (20 μg/ml) Ca^{2+}-influx *ex vivo* on splenic tumor cells from EMC4-engrafted mice treated for 16 days with vehicle or ibrutinib. Representative (n = 4) MFI kinetics plot of Ca^{2+} signaling (*bottom*) from each group.*P < 0.05 (n = 4 mice/group, Mann-Whitney U test).

went down rapidly, a major proportion (~80%) of the ibrutinib treatment group was still alive after 16 days of treatment (**Figure 5C**).

Next, we investigated if ibrutinib treatment affected disease progression. EMC4-engrafted mice were randomized to receive either ibrutinib or vehicle. After 3 and 12 days of treatment, the proportions of circulating CD5^{+}CD43^{+}IgM^{+}CD19^{+} B-cells were not different between the two groups (**Supplementary Figure 5**). However, at the end of the 16-day treatment cycle, a major proportion of the control group exhibited lethargy, hunched posture or other disabling symptoms. Therefore, animals from both arms were sacrificed to compare disease progression.

The ibrutinib-treated group had a significant increase of circulating tumor cells, compared with the vehicle-treated group (**Figure 5D**). Vehicle-treated mice had massive splenomegaly, while ibrutinib-treated mice had smaller spleens with significantly lower leukemic CD5^{+}CD43^{+}IgM^{+}CD19^{+} B cell counts (**Figures 5D and 5E**). No significant differences were found in the leukemic cell counts in bone marrow and mesenteric lymph nodes in the two groups (data not shown). Interestingly, ibrutinib-treated mice displayed lower basal Ca^{2+} signaling and significantly reduced Ca^{2+} influx following α-IgM stimulation, compared with vehicle-treated control mice (**Figure 5F**). Thus, our data demonstrate that we have established a novel *in vivo* CLL engraftment model by adoptive transfer of EMC cell lines into *Rag1*$^{-/-}$ mice. Importantly, EMC cells remained sensitive to ibrutinib treatment *in vivo*.

EMC4 Leukemic cells acquire an anergic phenotype when engrafted

Leukemic B cells from the spleens of EMC4- engrafted mice showed only limited induction of Ca^{2+} flux upon α-IgM stimulation *ex vivo* (**Figure 5F**), which was in stark contrast to our previous observation of a substantial α-IgM driven Ca^{2+} flux in cultured EMC4 cells (**Supplementary Figure 3B**).

Therefore, we compared α-IgM-induced Ca^{2+} flux between leukemic cells isolated directly from spleens of EMC4-engrafted mice (*ex vivo*) with long-term *in vitro* cultured EMC4 cells. Unlike *in vitro* cultured EMC4 cells, the *ex vivo* EMC4 cells from engrafted mice showed limited induction of intracellular Ca^{2+} flux upon BCR stimulation (**Figure 6A**).

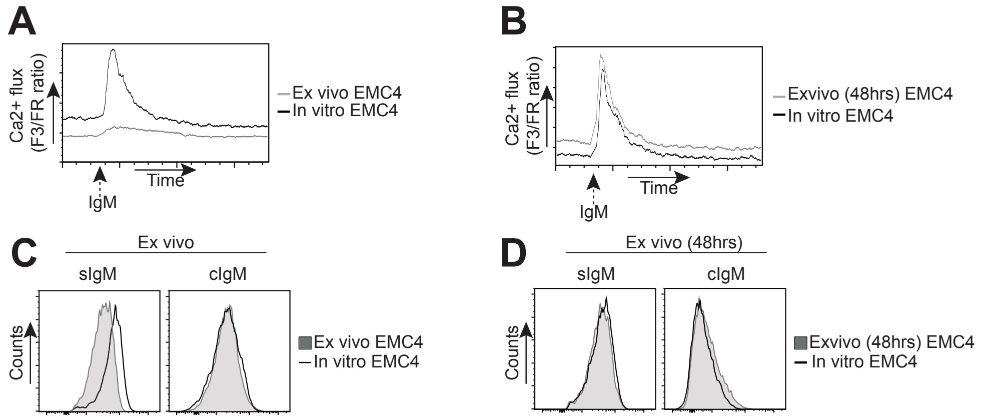

Figure 6. EMC4 cell lines acquire a more anergic phenotype upon engraftment.
(**A, B**) Flow cytometry analysis of α-IgM-stimulated (20 μg/ml) Ca^{2+}-influx between leukemic cells, directly isolated from EMC4-engrafted mice (**A**, *grey line*) or after 48 hours of culture (**B**, *grey line*), compared with *in vitro* cultured (non-transferred) EMC4 cells (**A,B**: *solid black line*). (**C, D**) Expression of surface IgM (sIgM) and cytoplasmic IgM (cIgM) between CD5$^+$CD19$^+$CD43$^+$ splenic leukemic cells from EMC4-engrafted mice analyzed directly after isolation (**C**, *shaded area*) or after 48 hours of culture (**D**, *shaded area*), compared with an *in vitro* cultured (non-transferred) EMC4 cells (*solid black line*).

However, when these EMC4 cells isolated from engrafted mice were cultured for 48h, they regained their BCR responsiveness and Ca^{2+} flux was similar to *in vitro* cultured EMC4 cells (**Figure 6B**).

Interestingly, the freshly isolated leukemic cells from EMC4-engrafted mice showed low sIgM expression compared with *in vitro* cultured EMC4 cells (**Figure 6C, *left***). Upon 48h culturing of the isolated leukemic cells, this difference in sIgM expression with *in vitro* cultured EMC4 cells was no longer detected (**Figure 6D, *left***). The sIgM upregulation was already apparent at 24h (data not shown). We did not see any difference in the cytoplasmic IgM (cIgM) expression (**Figure 6C, 6D, *right***). We therefore conclude that EMC4 cells become anergic to BCR stimulation following engraftment in *Rag1*$^{-/-}$ mice, whereby they downregulate sIgM expression.

DISCUSSION

Proliferation and survival of CLL B-cells are thought to be regulated by intracellular signaling pathways activated by various stimuli from the microenvironment. However, spontaneous apoptosis of CLL cells when cultured *in vitro* has hampered CLL research. Here, we describe the generation of three monoclonal mouse cell lines (EMC2, EMC4 and EMC6) from the SV40 large T antigen-based *IgH.TEμ* CLL mouse model. These cell lines can be cultured *in vitro* for long periods of time and transferred into mice, thus providing a platform to study BCR signaling in CLL and to investigate the efficacy of small molecule inhibitors. The EMC cell lines were remarkably similar to the primary tumors and our analyses indicate that the major pathways associated with their *in vitro* outgrowth are downstream of the BCR (Btk and Akt), CD5 and TNFa/NFkB. Stereotypic BCRs with specific IGHV usage[5] and reactivity towards common antigens[20,21] are characteristic features of CLL. It was remarkable that all three EMC cell lines, even though generated from three different mice, express the stereotypic Ig V$_H$11/Vκ14 genes and recognize PtC. Moreover, we did not see outgrowth of other non-V$_H$11 clones *in vitro*. This may suggest that self-reactivity might drive the selection and outgrowth of these cell lines in *in vitro* cultures. Recently, the usefulness of the stable human CLL cell lines MEC-1 & MEC-2 to test effects of kinase inhibitors such as ibrutinib was shown[52]. Nevertheless, these cell lines are derived from EBV+ B cells and do not stably express surface CD5 and CD43[29]. In contrast, EMC cell lines show stable surface expression of CD5 and intact downstream signaling, as several known downstream CD5 targets were upregulated.

Human CLL cells show aberrant BCR signaling, whereby the downstream Btk/Plcγ2/Ca^{2+} and PI3K/ Akt pathways are thought to be constitutively activated, resulting in increased proliferation and survival[8-10]. We show that our EMC cell lines exhibit *in vitro* - thus in the absence of any stimulatory signals from the microenvironment - constitutive activation of p-Btk(Y551/ Y223) and downstream basal Ca^{2+} signaling, paralleling human CLL. However, constitutive Btk signaling was apparently suboptimal, given the lack of phosphorylation of its main substrate PLCγ2(Y759), and was associated with BCR hyporesponsiveness. BCR anergy was also evident *in vivo*, because EMC4-engrafted cells downregulated sIgM and lacked α-IgM-induced Ca^{2+} influx. Additionally, EMC cells exhibited constitutively active Akt/S6 signaling, possibly because of the ability of SV40T protein to induce cell survival via Akt[53]. This is remarkably similar to the most extensively studied CLL mouse model, Eμ-TCL1, in which TCL-1 expression has also been functionally linked to enhanced Akt signaling[34]. However, to the best of our knowledge stable Eμ-TCL1 leukemia-derived cell lines have not been reported to date.

Evidence is emerging that the efficacy of the novel CLL therapeutics ibrutinib and idelalisib is not only based on their effects on BCR-mediated survival and proliferation, but also on cellular adhesion and migration in the context of the CLL microenvironment[12,27,28,54]. We indeed observed that these inhibitors reduced EMC cell line proliferation and viability, as well as adhesion towards fibronectin. The reduced survival of EMC cell lines was due to inhibition of PI3K/Akt/ Survivin signaling, as also shown for human CLL[50]. Although we did not find evidence for a role of Bcl-2 family members in the outgrowth of the EMC cell lines, upon treatment with the Bcl-2 inhibitor ABT-199 the EMC cell lines also underwent apoptosis (S.P.S. unpublished results). Thus, next to exhibiting a similar phenotype to human CLL, the EMC cell lines also recapitulate key responses to kinase inhibition therapies *in vitro*. We conclude that the EMC cell lines are well suited for high-throughput screening for efficacy or studies on the mechanism of action of novel compounds combinations for CLL treatment. Moreover, due to the transferability of EMC cells into *Rag1*$^{-/-}$ mice *in vivo* responses can be evaluated as well. The rapid CLL development in these engrafted mice facilitates the evaluation of therapeutic strategies within reasonable time schedules and contrasts with the slow disease development in CLL mouse models[33,35,37]. Unfortunately, we have been unsuccessful in establishing EMC cell engraftment in WT mice, which might be related to their mixed C57Bl6x129 background. Nevertheless, ibrutinib treatment of EMC-engrafted *Rag1*$^{-/-}$ mice resulted in increased circulating CLL cell numbers and concurrently decreased tumor load in the spleen, as well as prolonged survival, thus recapitulating key features of ibrutinib therapy in clinical studies of relapsed/ refractory CLL[12].

Patients harboring del(17p13.1) or *TP53* mutations represent a difficult to treat CLL subgroup, warranting development of novel targeted agents. Our EMC cell lines likely reflect a CLL subtype with dysfunctional p53 due to interaction with SV40 large T protein[37,55,56]. This was further supported by a lack of induction of p53 target gene PUMA upon fludarabine treatment. Therefore, EMC cell lines specifically provide a tool to dissect novel treatment options for CLL with a dysfunctional p53 pathway.

In summary, we have generated stable monoclonal cell lines from a CLL mouse model that exhibits constitutive Btk and Akt signaling, presents several features of human CLL and responds to novel targeted therapies. These EMC cell lines thus provide a novel *in vitro* and *in vivo* preclinical platform to study CLL cell biology and to test efficacy of novel targeted therapy combinations.

REFERENCES

1. Miller KD, Siegel RL, Lin CC, Mariotto AB, Kramer JL, Rowland JH, *et al.* Cancer treatment and survivorship statistics, 2016. *CA Cancer J Clin* 2016 Jul; **66**(4)**:** 271-289.
2. Chiorazzi N, Rai KR, Ferrarini M. Chronic lymphocytic leukemia. *N Engl J Med* 2005 Feb 24; **352**(8)**:** 804-815.
3. Damle RN, Wasil T, Fais F, Ghiotto F, Valetto A, Allen SL, *et al.* Ig V gene mutation status and CD38 expression as novel prognostic indicators in chronic lymphocytic leukemia. *Blood* 1999 Sep 15; **94**(6)**:** 1840-1847.
4. Hamblin TJ, Davis Z, Gardiner A, Oscier DG, Stevenson FK. Unmutated Ig V(H) genes are associated with a more aggressive form of chronic lymphocytic leukemia. *Blood* 1999 Sep 15; **94**(6)**:** 1848-1854.
5. Agathangelidis A, Darzentas N, Hadzidimitriou A, Brochet X, Murray F, Yan XJ, *et al.* Stereotyped B-cell receptors in one-third of chronic lymphocytic leukemia: a molecular classification with implications for targeted therapies. *Blood* 2012 May 10; **119**(19)**:** 4467-4475.
6. Contri A, Brunati AM, Trentin L, Cabrelle A, Miorin M, Cesaro L, *et al.* Chronic lymphocytic leukemia B cells contain anomalous Lyn tyrosine kinase, a putative contribution to defective apoptosis. *J Clin Invest* 2005 Feb; **115**(2)**:** 369-378.
7. Buchner M, Fuchs S, Prinz G, Pfeifer D, Bartholome K, Burger M, *et al.* Spleen tyrosine kinase is overexpressed and represents a potential therapeutic target in chronic lymphocytic leukemia. *Cancer Res* 2009 Jul 01; **69**(13)**:** 5424-5432.
8. Cheng S, Ma J, Guo A, Lu P, Leonard JP, Coleman M, *et al.* BTK inhibition targets in vivo CLL proliferation through its effects on B-cell receptor signaling activity. *Leukemia* 2014 Mar; **28**(3)**:** 649-657.
9. Herman SE, Mustafa RZ, Gyamfi JA, Pittaluga S, Chang S, Chang B, *et al.* Ibrutinib inhibits BCR and NF-kappaB signaling and reduces tumor proliferation in tissue-resident cells of patients with CLL. *Blood* 2014 May 22; **123**(21)**:** 3286-3295.
10. Liao W, Jordaan G, Coriaty N, Sharma S. Amplification of B cell receptor-Erk signaling by Rasgrf-1 overexpression in chronic lymphocytic leukemia. *Leuk Lymphoma* 2014 Dec; **55**(12)**:** 2907-2916.
11. Hendriks RW, Yuvaraj S, Kil LP. Targeting Bruton's tyrosine kinase in B cell malignancies. *Nat Rev Cancer* 2014 Apr; **14**(4)**:** 219-232.
12. Byrd JC, Furman RR, Coutre SE, Flinn IW, Burger JA, Blum KA, *et al.* Targeting BTK with ibrutinib in relapsed chronic lymphocytic leukemia. *N Engl J Med* 2013 Jul 04; **369**(1)**:** 32-42.
13. Byrd JC, Harrington B, O'Brien S, Jones JA, Schuh A, Devereux S, *et al.* Acalabrutinib (ACP-196) in Relapsed Chronic Lymphocytic Leukemia. *N Engl J Med* 2016 Jan 28; **374**(4)**:** 323-332.
14. Mockridge CI, Potter KN, Wheatley I, Neville LA, Packham G, Stevenson FK. Reversible anergy of sIgM-mediated signaling in the two subsets of CLL defined by VH-gene mutational status. *Blood* 2007 May 15; **109**(10)**:** 4424-4431.
15. Stevenson FK, Forconi F, Packham G. The meaning and relevance of B-cell receptor structure and function in chronic lymphocytic leukemia. *Semin Hematol* 2014 Jul; **51**(3)**:** 158-167.
16. Muzio M, Apollonio B, Scielzo C, Frenquelli M, Vandoni I, Boussiotis V, *et al.* Constitutive activation of distinct BCR-signaling pathways in a subset of CLL patients: a molecular signature of anergy. *Blood* 2008 Jul 01; **112**(1)**:** 188-195.
17. Packham G, Krysov S, Allen A, Savelyeva N, Steele AJ, Forconi F, *et al.* The outcome of B-cell receptor signaling in chronic lymphocytic leukemia: proliferation or anergy. *Haematologica* 2014 Jul; **99**(7)**:** 1138-1148.
18. Duhren-von Minden M, Ubelhart R, Schneider D, Wossning T, Bach MP, Buchner M, *et al.* Chronic lymphocytic leukaemia is driven by antigen-independent cell-autonomous signalling. *Nature* 2012 Sep 13; **489**(7415)**:** 309-312.
19. Muggen AF, Pillai SY, Kil LP, van Zelm MC, van Dongen JJ, Hendriks RW, *et al.* Basal Ca(2+) signaling is particularly increased in mutated chronic lymphocytic leukemia. *Leukemia* 2015 Feb; **29**(2)**:** 321-328.

20. Hoogeboom R, van Kessel KP, Hochstenbach F, Wormhoudt TA, Reinten RJ, Wagner K, *et al.* A mutated B cell chronic lymphocytic leukemia subset that recognizes and responds to fungi. *J Exp Med* 2013 Jan 14; **210**(1)**:** 59-70.
21. Chen SS, Batliwalla F, Holodick NE, Yan XJ, Yancopoulos S, Croce CM, *et al.* Autoantigen can promote progression to a more aggressive TCL1 leukemia by selecting variants with enhanced B-cell receptor signaling. *Proc Natl Acad Sci U S A* 2013 Apr 16; **110**(16)**:** E1500-1507.
22. Ramsay AD, Rodriguez-Justo M. Chronic lymphocytic leukaemia--the role of the microenvironment pathogenesis and therapy. *Br J Haematol* 2013 Jul; **162**(1)**:** 15-24.
23. Caligaris-Cappio F, Bertilaccio MT, Scielzo C. How the microenvironment wires the natural history of chronic lymphocytic leukemia. *Semin Cancer Biol* 2014 Feb; **24:** 43-48.
24. Burger JA, Gribben JG. The microenvironment in chronic lymphocytic leukemia (CLL) and other B cell malignancies: insight into disease biology and new targeted therapies. *Semin Cancer Biol* 2014 Feb; **24:** 71-81.
25. Herishanu Y, Perez-Galan P, Liu D, Biancotto A, Pittaluga S, Vire B, *et al.* The lymph node microenvironment promotes B-cell receptor signaling, NF-kappaB activation, and tumor proliferation in chronic lymphocytic leukemia. *Blood* 2011 Jan 13; **117**(2)**:** 563-574.
26. de Gorter DJ, Beuling EA, Kersseboom R, Middendorp S, van Gils JM, Hendriks RW, *et al.* Bruton's tyrosine kinase and phospholipase Cgamma2 mediate chemokine-controlled B cell migration and homing. *Immunity* 2007 Jan; **26**(1)**:** 93-104.
27. de Rooij MF, Kuil A, Geest CR, Eldering E, Chang BY, Buggy JJ, *et al.* The clinically active BTK inhibitor PCI-32765 targets B-cell receptor- and chemokine-controlled adhesion and migration in chronic lymphocytic leukemia. *Blood* 2012 Mar 15; **119**(11)**:** 2590-2594.
28. Ponader S, Chen SS, Buggy JJ, Balakrishnan K, Gandhi V, Wierda WG, *et al.* The Bruton tyrosine kinase inhibitor PCI-32765 thwarts chronic lymphocytic leukemia cell survival and tissue homing in vitro and in vivo. *Blood* 2012 Feb 02; **119**(5)**:** 1182-1189.
29. Stacchini A, Aragno M, Vallario A, Alfarano A, Circosta P, Gottardi D, *et al.* MEC1 and MEC2: two new cell lines derived from B-chronic lymphocytic leukaemia in prolymphocytoid transformation. *Leuk Res* 1999 Feb; **23**(2)**:** 127-136.
30. Agathangelidis A, Scarfo L, Barbaglio F, Apollonio B, Bertilaccio MT, Ranghetti P, *et al.* Establishment and Characterization of PCL12, a Novel CD5+ Chronic Lymphocytic Leukaemia Cell Line. *PLoS One* 2015; **10**(6)**:** e0130195.
31. Hertlein E, Beckwith KA, Lozanski G, Chen TL, Towns WH, Johnson AJ, *et al.* Characterization of a new chronic lymphocytic leukemia cell line for mechanistic in vitro and in vivo studies relevant to disease. *PLoS One* 2013; **8**(10)**:** e76607.
32. Kellner J, Wierda W, Shpall E, Keating M, McNiece I. Isolation of a novel chronic lymphocytic leukemic (CLL) cell line and development of an in vivo mouse model of CLL. *Leuk Res* 2016 Jan; **40:** 54-59.

33. Yan XJ, Albesiano E, Zanesi N, Yancopoulos S, Sawyer A, Romano E, *et al.* B cell receptors in TCL1 transgenic mice resemble those of aggressive, treatment-resistant human chronic lymphocytic leukemia. *Proc Natl Acad Sci U S A* 2006 Aug 01; **103**(31)**:** 11713-11718.
34. Simonetti G, Bertilaccio MT, Ghia P, Klein U. Mouse models in the study of chronic lymphocytic leukemia pathogenesis and therapy. *Blood* 2014 Aug 14; **124**(7)**:** 1010-1019.
35. Bichi R, Shinton SA, Martin ES, Koval A, Calin GA, Cesari R, *et al.* Human chronic lymphocytic leukemia modeled in mouse by targeted TCL1 expression. *Proc Natl Acad Sci U S A* 2002 May 14; **99**(10)**:** 6955-6960.
36. Suljagic M, Longo PG, Bennardo S, Perlas E, Leone G, Laurenti L, *et al.* The Syk inhibitor fostamatinib disodium (R788) inhibits tumor growth in the Emu- TCL1 transgenic mouse model of CLL by blocking antigen-dependent B-cell receptor signaling. *Blood* 2010 Dec 02; **116**(23)**:** 4894-4905.
37. ter Brugge PJ, Ta VB, de Bruijn MJ, Keijzers G, Maas A, van Gent DC, *et al.* A mouse model for chronic lymphocytic leukemia based on expression of the SV40 large T antigen. *Blood* 2009 Jul 02; **114**(1)**:** 119-127.
38. Kil LP, de Bruijn MJ, van Hulst JA, Langerak AW, Yuvaraj S, Hendriks RW. Bruton's tyrosine kinase mediated signaling enhances leukemogenesis in a mouse model for chronic lymphocytic leukemia. *Am J Blood Res* 2013; **3**(1)**:** 71-83.
39. Buechele C, Baessler T, Schmiedel BJ, Schumacher CE, Grosse-Hovest L, Rittig K, *et al.* 4-1BB ligand modulates direct and Rituximab-induced NK-cell reactivity in chronic lymphocytic leukemia. *Eur J Immunol* 2012 Mar; **42**(3)**:** 737-748.
40. Chen LS, Redkar S, Bearss D, Wierda WG, Gandhi V. Pim kinase inhibitor, SGI-1776, induces apoptosis in chronic lymphocytic leukemia cells. *Blood* 2009 Nov 05; **114**(19)**:** 4150-4157.
41. Cohen AM, Grinblat B, Bessler H, Kristt D, Kremer A, Schwartz A, *et al.* Increased expression of the hPim-2 gene in human chronic lymphocytic leukemia and non-Hodgkin lymphoma. *Leuk Lymphoma* 2004 May; **45**(5)**:** 951-955.
42. Ranheim EA, Cantwell MJ, Kipps TJ. Expression of CD27 and its ligand, CD70, on chronic lymphocytic leukemia B cells. *Blood* 1995 Jun 15; **85**(12)**:** 3556-3565.
43. Stratowa C, Loffler G, Lichter P, Stilgenbauer S, Haberl P, Schweifer N, *et al.* CDNA microarray gene expression analysis of B-cell chronic lymphocytic leukemia proposes potential new prognostic markers involved in lymphocyte trafficking. *Int J Cancer* 2001 Feb 15; **91**(4)**:** 474-480.
44. Joha S, Nugues AL, Hetuin D, Berthon C, Dezitter X, Dauphin V, *et al.* GILZ inhibits the mTORC2/AKT pathway in BCR-ABL(+) cells. *Oncogene* 2012 Mar 15; **31**(11)**:** 1419-1430.
45. Subramanian A, Tamayo P, Mootha VK, Mukherjee S, Ebert BL, Gillette MA, *et al.* Gene set enrichment analysis: a knowledge-based approach for interpreting genome-wide expression profiles. *Proc Natl Acad Sci U S A* 2005 Oct 25; **102**(43)**:** 15545-15550.
46. Gary-Gouy H, Sainz-Perez A, Marteau JB, Marfaing-Koka A, Delic J, Merle-Beral H, *et al.* Natural phosphorylation of CD5 in chronic lymphocytic leukemia B cells and analysis of CD5-regulated genes in a B cell line suggest a role for CD5 in malignant phenotype. *J Immunol* 2007 Oct 01; **179**(7)**:** 4335-4344.

47. Arnold LW, McCray SK, Tatu C, Clarke SH. Identification of a precursor to phosphatidyl choline-specific B-1 cells suggesting that B-1 cells differentiate from splenic conventional B cells in vivo: cyclosporin A blocks differentiation to B-1. *J Immunol* 2000 Mar 15; **164**(6)**:** 2924-2930.
48. Mackus WJ, Kater AP, Grummels A, Evers LM, Hooijbrink B, Kramer MH*, et al.* Chronic lymphocytic leukemia cells display p53-dependent drug-induced Puma upregulation. *Leukemia* 2005 Mar; **19**(3)**:** 427-434.
49. Chou TC, Talalay P. Quantitative analysis of dose-effect relationships: the combined effects of multiple drugs or enzyme inhibitors. *Adv Enzyme Regul* 1984; **22:** 27-55.
50. Palacios F, Abreu C, Prieto D, Morande P, Ruiz S, Fernandez-Calero T*, et al.* Activation of the PI3K/AKT pathway by microRNA-22 results in CLL B-cell proliferation. *Leukemia* 2015 Jan; **29**(1)**:** 115-125.
51. Mombaerts P, Iacomini J, Johnson RS, Herrup K, Tonegawa S, Papaioannou VE. RAG-1-deficient mice have no mature B and T lymphocytes. *Cell* 1992 Mar 06; **68**(5)**:** 869-877.
52. Voltan R, Rimondi E, Melloni E, Rigolin GM, Casciano F, Arcidiacono MV*, et al.* Ibrutinib synergizes with MDM-2 inhibitors in promoting cytotoxicity in B chronic lymphocytic leukemia. *Oncotarget* 2016 Oct 25; **7**(43)**:** 70623-70638.
53. Cacciotti P, Barbone D, Porta C, Altomare DA, Testa JR, Mutti L*, et al.* SV40-dependent AKT activity drives mesothelial cell transformation after asbestos exposure. *Cancer Res* 2005 Jun 15; **65**(12)**:** 5256-5262.
54. Chang BY, Francesco M, De Rooij MF, Magadala P, Steggerda SM, Huang MM*, et al.* Egress of CD19(+) CD5(+) cells into peripheral blood following treatment with the Bruton tyrosine kinase inhibitor ibrutinib in mantle cell lymphoma patients. *Blood* 2013 Oct 03; **122**(14)**:** 2412-2424.
55. White MK, Khalili K. Polyomaviruses and human cancer: molecular mechanisms underlying patterns of tumorigenesis. *Virology* 2004 Jun 20; **324**(1)**:** 1-16.
56. Ahuja D, Saenz-Robles MT, Pipas JM. SV40 large T antigen targets multiple cellular pathways to elicit cellular transformation. *Oncogene* 2005 Nov 21; **24**(52)**:** 7729-7745.
57. Muramatsu M, Kinoshita K, Fagarasan S, Yamada S, Shinkai Y, Honjo T. Class switch recombination and hypermutation require activation-induced cytidine deaminase (AID), a potential RNA editing enzyme. *Cell* 2000 Sep 01; **102**(5)**:** 553-563.
58. Middendorp S, Dingjan GM, Hendriks RW. Impaired precursor B cell differentiation in Bruton's tyrosine kinase-deficient mice. *J Immunol* 2002 Mar 15; **168**(6)**:** 2695-2703.
59. Thijssen R, Ter Burg J, Garrick B, van Bochove GG, Brown JR, Fernandes SM*, et al.* Dual TORK/DNA-PK inhibition blocks critical signaling pathways in chronic lymphocytic leukemia. *Blood* 2016 Jul 28; **128**(4)**:** 574-583.
60. Kil LP, de Bruijn MJ, van Nimwegen M, Corneth OB, van Hamburg JP, Dingjan GM*, et al.* Btk levels set the threshold for B-cell activation and negative selection of autoreactive B cells in mice. *Blood* 2012 Apr 19; **119**(16)**:** 3744-3756.
61. Robinson MD, McCarthy DJ, Smyth GK. edgeR: a Bioconductor package for differential expression analysis of digital gene expression data. *Bioinformatics* 2010 Jan 01; **26**(1)**:** 139-140.

62. Anders S, Pyl PT, Huber W. HTSeq--a Python framework to work with high-throughput sequencing data. *Bioinformatics* 2015 Jan 15; **31**(2)**:** 166-169.

SUPPLEMENTAL DATA

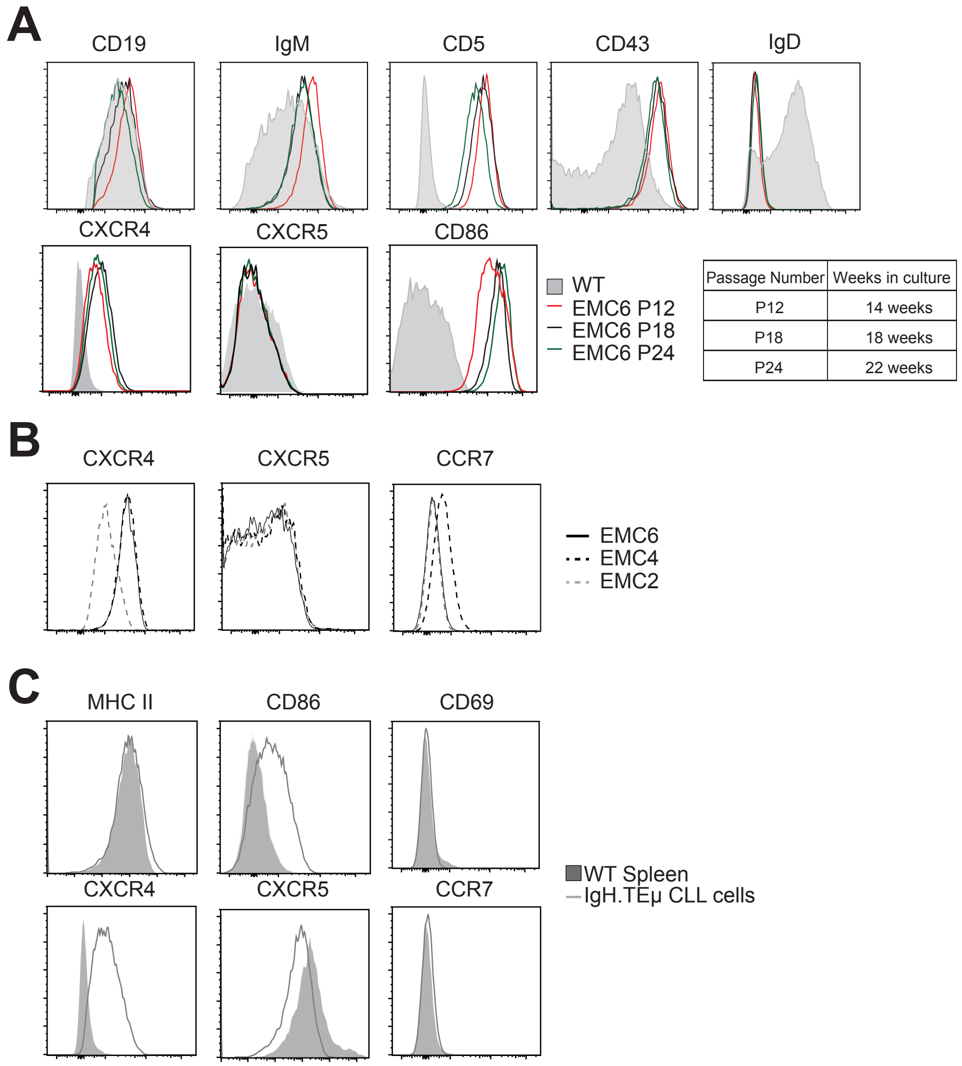

Passage Number	Weeks in culture
P12	14 weeks
P18	18 weeks
P24	22 weeks

Supplementary Figure 1. EMC cell lines resemble primary tumors from IgH.TEμ mice.
(**A**) Histograms showing surface expression of the phenotypic markers on EMC6 cells, as determined by flow cytometry, over the indicated culture period. EMC4 and EMC2 showed similar stable expression profiles. (**B**) Comparison of expression of indicated chemokine receptors on three different EMC cell lines by flow cytometry. (**C**) Representative plot for expression of indicated activation markers and chemokine receptors on gated CD19$^+$ WT splenic B cells and gated CD5$^+$CD19$^+$CD11b$^-$CD43$^+$ CLL B cells from an aged *IgH.TEμ* mouse (representing $n > 20$) as determined by flow cytometry.

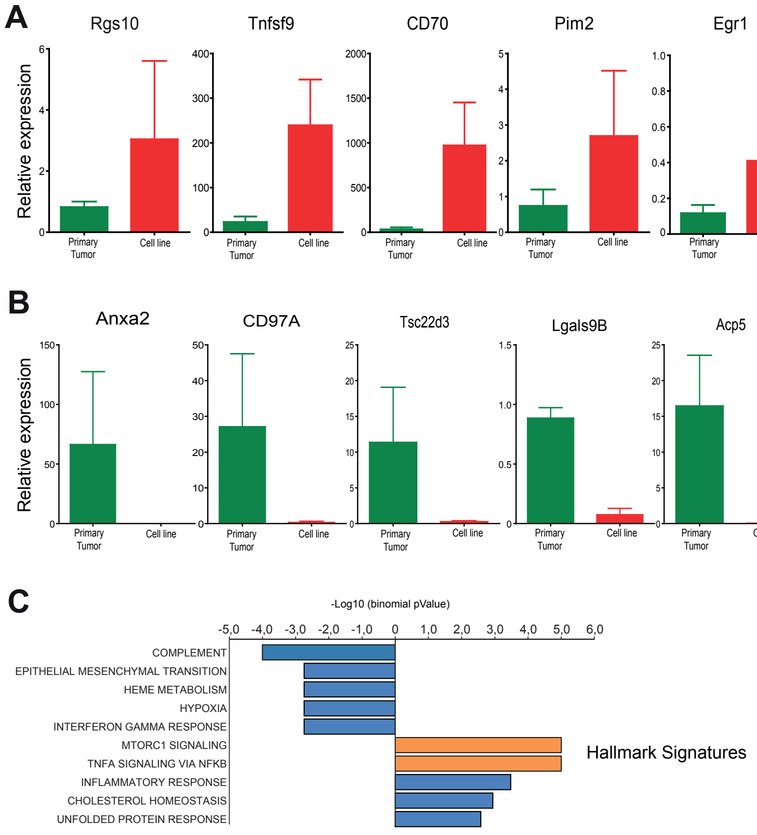

D

Genes	Primary Tumors (n=3)	EMC cell lines (n=3)	Control WT B cells	α -IgM Control WT B cells
Bcl-XL	5.33 ± 2.27	11.03 ± 5.72	2.30 ± 0.30	44.3 ± 1.10
Bcl-2	20.6 ± 3.77	15.37 ± 2.93	19.3 ± 1.68	7.52 ± 0.35
Mcl-1	258.9 ± 2.56	236.5 ± 21.90	130.8 ± 9.77	123.1 ± 3.68
Survivin	79.03 ± 20.05	102.8 ± 14.69	2.90 ± 0.43	3.02 ± 0.34

Supplementary Figure 2. RNA-sequencing reveals active pathways in EMC cell lines.
(**A**, **B**) Validation of RNA-sequencing data by real time quantitative PCR. Bars represents mean values ± SEM expression of indicated genes, either upregulated (**A**) or downregulated (**B**) in cell lines ($n = 3$) compared to original primary tumor ($n = 3$) from *IgH.TEμ* mice. The expression values were calculated relative to expression in splenic B cells from wild type mice ($n = 4$), which were set to 1. (**C**) Hallmark Signature analysis of pathway enrichment for genes that show differential expression in EMC cell lines compared to original primary tumors from *IgH.TEμ* mice. (**D**) Expression values (FPKMs) for indicated anti-apoptotic genes in original primary tumor ($n = 3$) from *IgH.TEμ* mice, EMC cell lines ($n = 3$), unstimulated ($n = 4$) and F(ab')2 anti-IgM stimulated ($n = 4$) control WT splenic B cells compared to corresponding primary tumor.

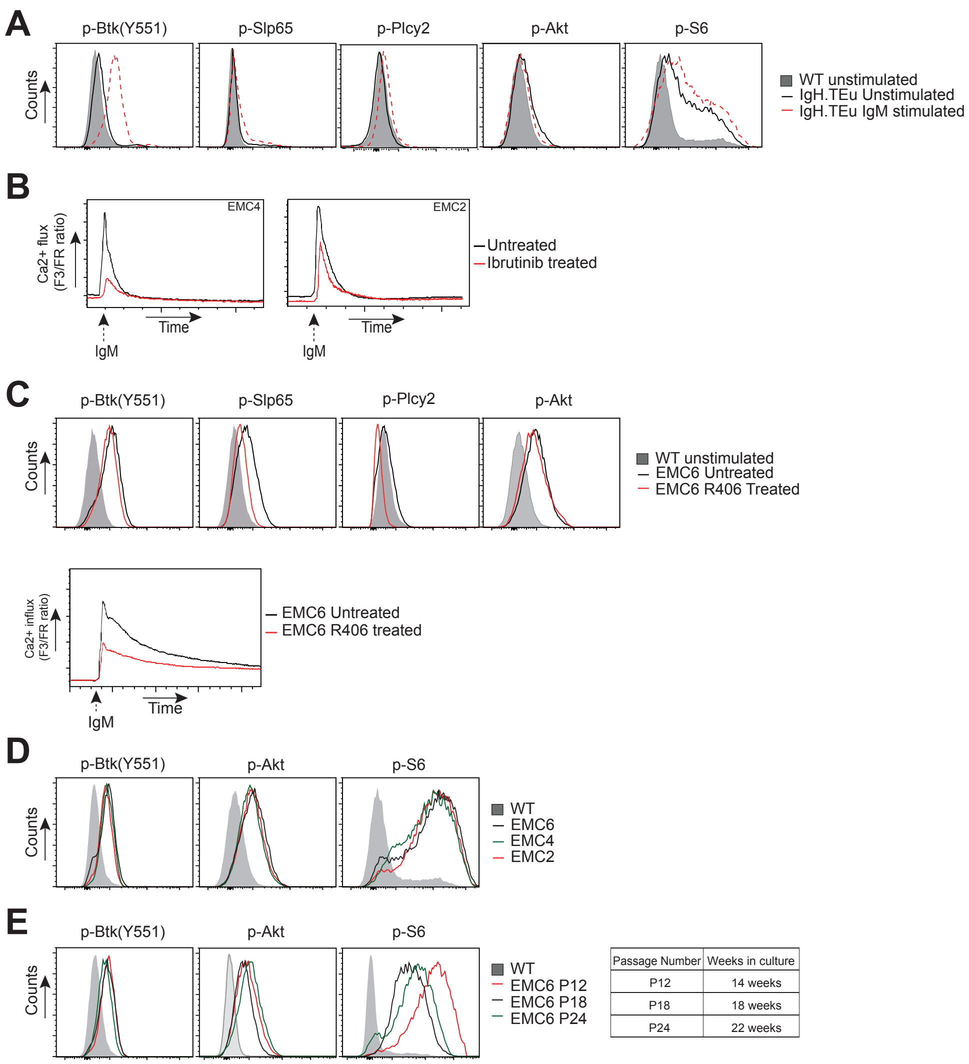

Passage Number	Weeks in culture
P12	14 weeks
P18	18 weeks
P24	22 weeks

Supplementary Figure 3. EMC cell lines and IgH.TEm-derived primary tumor cells exhibit constitutive active BCR signaling.

(**A**) Comparison of Ca^{2+} influx between untreated cells (black) and following 3 hours in-vitro treatment with 1mM Ibrutinib of the indicated EMC cell line. The dotted arrow indicate addition of anti-IgM. (**B**) Flow cytometry analysis of the indicated phosphoproteins on gated B220$^+$CD3$^-$ wild type (WT) splenocytes (shaded area), unstimulated (solid black line) and F(ab')2 anti-IgM stimulated (20 ug/ml, dotted red line) CLL cells from aged *IgH.TEμ* mice. (**C**) *Top*: Flow cytometry analysis of the indicated phosphoproteins on gated B220$^+$CD3$^-$ WT splenocytes (shaded area), untreated EMC6 (solid black line) and R406-treated (4 µM of Syk inhibitor R406, solid red line) EMC6 cells. *Bottom*: Comparison of Ca^{2+} influx between untreated EMC6 cells or EMC6 following *in vitro* treatment with 4 µM Syk inhibitor (R406). The dotted arrow indicates addition of F(ab')2 anti-IgM. (**D**) PhosFlow analysis of the indicated phospho-proteins expressed in the three EMC cell lines, as well as gated unstimulated B220$^+$CD3$^-$ WT splenocytes, as a reference. The histogram plots shown are representative of three independent experiments. (**E**) PhosFlow analysis of the indicated phospho-proteins expressed in the EMC6 cell line, showing its stability over the indicated culture periods. Gated unstimulated B220$^+$CD3$^-$ WT splenocytes serve as a reference.

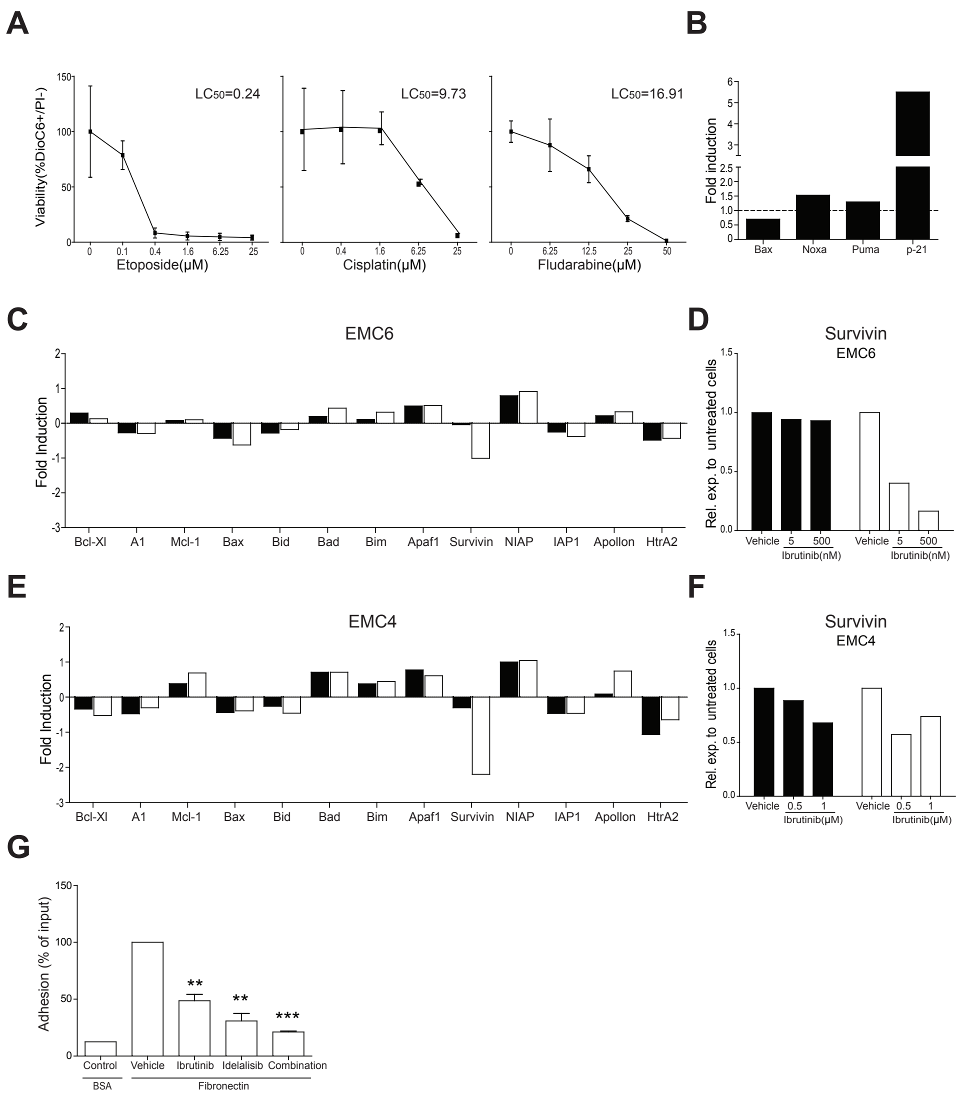

Supplementary Figure 4. CLL cell lines are sensitive to chemotherapeutic drugs.

(**A**) EMC4 cells were cultured in the presence of the indicated concentrations of Etoposide, Cisplatin or Fludarabine for 24 hrs. The sensitivity (LC50) towards individual agent is shown. (**B**) Bar graphs represent Multiplex Ligation-dependent Probe Amplification (MLPA) analysis for respective genes in EMC4 cell line following treatment with Fludarabine for 24 hours. (**C**, **E**) Fold induction (2log) of mRNA levels of indicated pro-/anti-apoptotic mediators in the indicated cell lines upon *in vitro* treatment with Ibrutinib (EMC6 = 5 nM; EMC4 = 500 uM) for 12 hrs (*filled black bars*) or 24 hrs (*clear white bars*). Fold induction was calculated with respect to vehicle treated cell lines. (**D**, **F**) Validation of MLPA result by real time quantitative PCR on survivin upon *in vitro* treatment of the indicated cell line with ibrutinib (dose indicated) for 12 hrs (*filled black bars*) or 24 hrs (*clear white bars*). (**G**) *In vitro* adhesion assay: EMC4 cells pretreated with either ibrutinib (10 nM) or idelalisib (100 nM) or a combination were allowed to adhere to fibronectin-coated surfaces ($n = 3$, in triplicate). Graphs are presented as normalized mean ± SD (100%= EMC4 cells treated with vehicle). $^{**}P < 0.01$ $^{***}P < 0.0001$ (paired one-sample *T*-test).

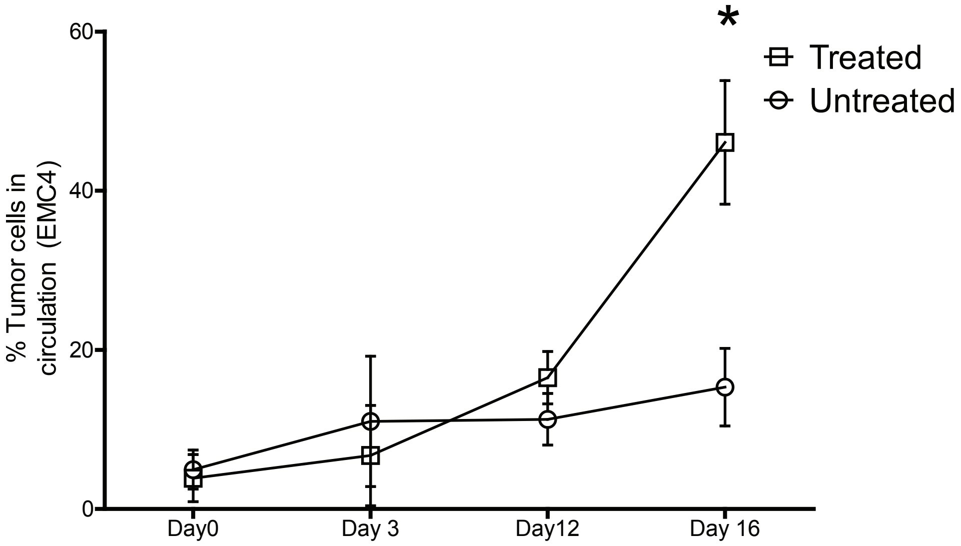

Supplementary Figure 5. Rapid induction of CLL following engraftment of CLL cell line. Proportions of CD5$^+$CD19$^+$CD43$^+$ tumor cells in peripheral blood from EMC4 engrafted *Rag1-/-* mice (*n* = 4 per group) following treatment with either vehicle (open circles) or ibrutinib (open squares) for the indicated time. The treatment was started 14 days following engraftment. Result show mean ± SEM.

Supplementary Table 1: (A) Expression values (FPKMs) for various genes upregulated in EMC cell lines compared to corresponding primary tumor

Genes	EMC6 PT	EMC2 PT	EMC4 PT	EMC6 line	EMC2 line	EMC4 line	*p* Value
Insig1	12,2	9,0	6,9	52,7	38,0	39,5	0,00019069
Pim2	22,1	39,8	43,9	122,9	143,7	229,1	0,0001479
Fam179a	0,3	0,3	5,3	5,1	3,6	20,2	0,00041553
Rgs10	26,2	8,4	9,7	151,5	74,6	26,5	0,00060558
Sc4mol	8,8	8,7	6,6	55,3	29,6	65,1	2,0556E-05
Sqle	8,4	4,4	8,0	46,5	25,7	60,0	1,7405E-05
Dusp4	0,3	0,7	2,8	6,6	4,4	13,1	0,00043918
Il10	10,2	31,5	88,2	155,3	125,4	551,9	2,4666E-06
Col11a2	0,7	1,5	1,4	6,3	8,7	8,8	3,4153E-05
Egr1	53,9	23,0	30,3	179,3	394,6	159,7	1,6531E-05
Ncan	0,1	0,1	1,0	5,1	1,9	3,2	0,00055946
Wnt10a	3,0	0,5	0,9	29,6	18,9	8,7	7,5123E-07
2310033E01Rik	0,0	0,6	2,8	4,0	25,6	17,3	0,00018339
Ccdc88a	0,1	0,2	0,4	5,9	2,2	2,3	1,073E-05
Asns	0,1	2,5	16,8	3,6	1,4	287,3	0,00012651
Slc2a6	1,0	4,1	3,5	58,8	49,1	27,4	2,2787E-08
Spna1	0,0	0,1	1,5	1,1	0,3	24,4	3,9303E-06
Axin2	0,0	0,0	1,5	1,8	19,8	4,1	3,8398E-07
Dmrta2	0,2	0,1	0,6	5,3	3,4	6,7	2,3009E-05
Lag3	1,2	0,5	2,2	5,8	6,8	54,4	6,0572E-05
Hapln4	0,0	0,1	0,3	2,8	2,6	2,8	3,8145E-05
Sytl1	0,4	1,4	2,0	22,4	8,2	57,2	7,5952E-09
Gpr162	0,0	0,2	0,5	0,6	13,1	2,4	4,7813E-05
Rab39b	0,0	0,1	0,1	1,0	0,2	3,7	0,00035858
Gpr171	0,0	0,1	0,4	0,9	0,3	12,0	0,00039336
Tnfsf9	5,4	1,8	1,5	100,4	84,1	66,5	2,1113E-17
Fads2	0,0	0,1	0,2	6,1	1,5	6,7	3,9377E-05
Mpp2	0,0	0,0	0,1	2,2	1,2	0,2	0,00070589
Dapk2	0,1	0,7	0,3	14,4	21,2	8,7	2,2963E-08
Hnrpll	0,2	0,2	0,3	22,6	0,2	3,8	0,00011817
Csgalnact1	0,0	0,0	0,1	4,2	0,0	2,5	0,00054088
Chac1	0,0	0,5	0,3	2,8	0,5	36,8	0,00011808
Arhgef25	0,0	0,0	0,1	1,7	0,5	4,1	6,7117E-05
Cd70	1,2	0,0	1,3	63,9	39,5	47,7	1,7725E-08

Supplementary Table 1: (B) Expression values (FPKMs) for various genes downregulated in EMC cell lines compared to corresponding primary tumor

Genes	EMC6 PT	EMC2 PT	EMC4 PT	EMC6 line	EMC2 line	EMC4 line	*P* value
Gda	0,1	1,2	1,7	0,0	0,0	0,0	7,1799E-08
Iigp1	1,9	0,4	1,5	0,0	0,0	0,0	1,3359E-07
Pla2g7	0,1	1,8	2,4	0,0	0,0	0,0	2,9417E-06
Lrg1	0,8	2,1	1,9	0,0	0,0	0,0	5,015E-07
Clec4n	0,3	2,5	3,9	0,0	0,0	0,0	1,2037E-06
Gtsf1	3,4	2,3	4,4	0,0	0,0	0,0	4,6376E-07
C1qc	0,7	2,3	17,4	0,0	0,0	0,0	4,0055E-08
C1qb	1,0	2,8	22,3	0,0	0,0	0,0	4,9175E-09
S100a9	0,0	1,5	43,0	0,0	0,0	0,0	2,7688E-05
S100a8	0,9	2,1	60,4	0,0	0,0	0,0	9,695E-06
Lyz2	1,9	95,4	34,9	0,0	0,0	0,0	2,3255E-12
S100a6	28,9	724,6	48,2	0,0	0,6	0,1	2,0847E-11
C1qa	0,7	4,2	18,7	0,0	0,0	0,0	7,019E-07
Lgr5	6,6	0,4	1,2	0,0	0,0	0,0	1,1054E-09
Tgfbi	1,3	1,5	4,3	0,0	0,0	0,0	1,4671E-08
Gpx7	7,8	0,2	6,2	0,0	0,0	0,0	4,1037E-06
S100a4	4,2	40,7	14,0	0,0	0,1	0,0	4,8877E-07
Vcam1	0,3	2,2	5,7	0,0	0,0	0,0	7,6093E-07
AI427809	1,9	1,8	0,3	0,0	0,0	0,0	2,0367E-06
2610018G03Rik	3,3	12,1	2,9	0,0	0,1	0,0	8,3176E-09
Timd4	0,0	1,5	1,6	0,0	0,0	0,0	0,000145
Anxa2	12,2	224,3	14,4	1,0	0,1	0,1	3,2995E-11
Slc4a1	0,1	1,9	4,4	0,0	0,0	0,0	1,0717E-06
Plbd1	0,5	7,1	3,0	0,0	0,0	0,0	1,143E-06
Npr3	0,9	1,5	1,1	0,0	0,0	0,0	4,2053E-07
Art3	5,9	0,2	1,1	0,1	0,0	0,0	0,00013629
Pag1	1,4	11,1	0,2	0,0	0,1	0,1	8,929E-07
Cd5l	0,8	3,3	8,3	0,0	0,1	0,0	5,5605E-06
Gm11428	1,6	1,0	51,0	0,0	0,0	0,7	0,00013158
Hebp1	0,3	2,3	7,0	0,0	0,0	0,1	4,4198E-05
Smpdl3a	4,8	1,8	6,9	0,1	0,0	0,1	9,8492E-06
Tppp	2,0	15,3	1,2	0,1	0,1	0,0	3,738E-08
Tnfsf4	0,3	11,6	2,3	0,0	0,2	0,0	0,00019424
Csf1r	0,3	4,4	4,0	0,0	0,0	0,1	7,8117E-07
Ifitm3	1,4	3,4	17,8	0,3	0,1	0,2	0,00021669
Pcp4	57,4	18,2	6,4	0,5	0,2	1,7	0,00068174
Tppp3	3,7	75,4	4,5	0,7	0,8	0,9	2,9088E-05
Galnt10	3,6	2,3	3,6	0,2	0,0	0,1	9,9806E-06
Cacna1h	22,2	3,7	9,1	0,2	0,0	1,1	6,3115E-05
Rnf125	4,3	1,8	1,4	0,2	0,0	0,1	0,0006327
March1	12,5	36,5	10,8	0,1	2,4	0,1	9,8741E-05
Ildr1	0,2	4,6	1,3	0,0	0,0	0,3	0,00018409
Dnahc8	1,7	2,0	5,1	0,1	0,3	0,0	5,6348E-05
Tsc22d3	61,7	304,7	82,3	7,2	11,4	8,2	5,1506E-08
Dkkl1	5,4	38,1	3,3	2,2	0,5	0,3	0,0002477
B3gnt5	17,4	44,0	13,3	0,2	4,4	0,4	0,00022842
Ggh	15,9	6,6	0,4	1,6	0,0	0,0	0,00015714
Abca1	1,8	12,2	4,3	1,1	0,1	0,2	4,5105E-05
Cacna1d	6,1	2,2	1,2	0,6	0,0	0,1	0,00013495
Acp5	44,4	85,3	82,2	2,6	9,4	4,7	9,6697E-08
Emb	0,7	51,8	13,6	5,2	0,3	0,1	0,00030886
Crip1	1479,0	2936,6	396,2	686,8	8,4	57,6	0,00037951
Cd97	129,1	387,3	75,1	31,8	23,4	38,3	0,00017688
Sepp1	0,7	7,0	66,6	0,0	0,8	11,5	1,3934E-05
Nedd4	46,1	17,6	33,3	4,4	10,1	2,1	0,0006947
Zfp36l2	36,4	100,6	68,0	14,4	12,5	9,2	0,00011901
Lgals9	30,6	28,5	31,2	3,8	2,9	9,6	0,00056366
Arhgef3	13,7	26,7	13,1	0,9	1,9	7,5	0,00026268
Mylip	20,2	22,5	6,3	7,3	1,6	0,7	0,0003681
Gm4759	7,1	4,0	3,2	1,3	1,4	0,5	0,00021789
Cntln	0,0	3,2	6,8	0,0	0,0	2,5	0,00056445
Plk2	0,1	10,1	14,1	0,0	0,1	6,7	0,00039975

Supplementary Table 2: List of primers and probes used in real-time quantitative PCR

Gene	Forward primer sequence (5′ to 3′)	Reverse primer sequence (5′ to 3′)	Universal Probe library probe:
Tnfsf9	cgccaagctactggctaaaa	cgtacctcagaccttgagataggt	#33 (cat. no. 04687663001)
Pim2	tcagcgggctcaatatacg	gaaagctgcccgatcctt	#25 (cat. no. 04686993001)
Rgs10	cacaccctctgatgttccaa	gaagcggctgtagctgtcat	#1 (cat. no. 04684974001)
CD70	gtccttcacacacggacca	aggccatcttgatggatacg	#25 (cat. no. 04686993001)
Egr1	cctatgagcacctgaccaca	tcgtttggctgggataactc	#22 (cat. no. 04686969001)
IL-10	actgcacccacttcccagt	tgtccagctggtcctttgtt	#21 (cat. no. 04686942001)
Anxa2	tgtccacgaaatcctgtgc	taggcacttgggggtgtaga	#64 (cat. no. 04688635001)
CD97	ctgcagggcctattcctcta	gcaggcccatttccagta	#13 (cat. no. 04685121001)
Acp5	cgtctctgcacagattgcat	aagcgcaaacggtagtaagg	#60 (cat. no. 04688589001)
Crip1	gctgagagccacactttcaa	ttaaaggcactgagggttcc	#56 (cat. no. 04688538001)
Tsc22d3	ggtggccctagacaacaaga	tcaagcagctcacgaatctg	#10 (cat. no. 04685091001)
Lgals9	ccaggggactaccaagagttt	cttcgtgttgcaaaccacat	#12 (cat. no. 04685113001)

Supplementary Table 3: Basal Calcium flux in the three EMC cell lines

	Basal Ca^{2+} Flux (F3/FR ratio, mean ± SEM)	Mann-Whitney *U* test *P* Value
WT Splenic B cells	0.09 ± 0.01	-
EMC6	0.38 ± 0.17	0.0095
EMC4	0.19 ± 0.06	0.0082
EMC2	0.15 ± 0.01	0.0571

The significance value in the three EMC cell lines is calculated w.r.t. WT splenic B cells in three independent experiments.

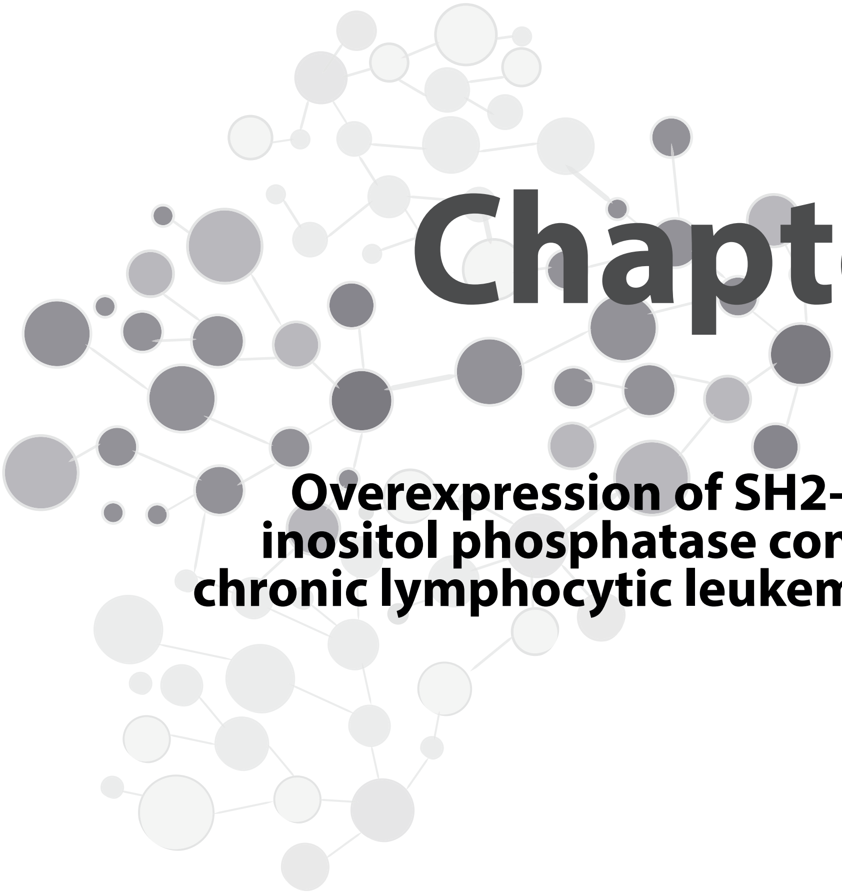

Chapter 5

Overexpression of SH2-containing inositol phosphatase contributes to chronic lymphocytic leukemia survival

Simar Pal Singh,[*,†,‡] Marjolein J.W. de Bruijn,[*]
Catarina Velaso Gago da Graça,[*] Odilia B.J. Corneth,[*] Jasper Rip,[*]
Ralph Stadhouders,[*,§] Ruud W.J. Meijers,[†] Stéphane Schurmans,[¶]
William G. Kerr,[||] Johanna ter Burg,[#] Eric Eldering,[#] Anton W. Langerak,[†]
Saravanan Y. Pillai,[*,**] and Rudi W. Hendriks[*]

[*]Department of Pulmonary Medicine, [†]Department of Immunology,
[‡]Post-graduate School Molecular Medicine, [§]Department of Cell Biology, Erasmus MC, Rotterdam, The Netherlands;
[¶]Laboratoire de Génétique Fonctionnelle, GIGA-Research Centre, Université de Liège (ULiège), Belgium;
[||]Department of Microbiology and Immunology, SUNY Upstate Medical University, Syracuse, NY USA;
[#]Department of Experimental Immunology, Academic Medical Center, University of Amsterdam,
Amsterdam, The Netherlands
[**]Current address: EpiExpressions, Rotterdam, The Netherlands

Under revision

ABSTRACT

Balanced activity of kinases and phosphatases downstream of the B-cell receptor is essential for B-cell differentiation and function and is disturbed in chronic lymphocytic leukemia (CLL). Here, we employed IgH.TEμ mice, which spontaneously develop CLL, and stable EMC CLL cell lines derived from these mice to explore the role of phosphatases in CLL. Genome-wide expression profiling comparing IgH.TEμ CLL cells with wild-type splenic B-cells identified 96 differentially expressed phosphatase genes, including SH2-containing inositol phosphatase (Ship2). B-cell-specific deletion of Ship2 – but not of its close homologue Ship1 – significantly reduced CLL formation in IgH.TEμ mice. Treatment of EMC cell lines with small molecule Ship1/2 inhibitors resulted in the induction of caspase-dependent apoptosis. Using flow cytometry and western blot analysis we observed that blocking Ship1/2 abrogated EMC cell survival by exerting dual effects on the BCR signaling cascade. On one hand, specific Ship1 inhibition enhanced calcium signaling and thereby abrogated an anergic response to BCR stimulation in CLL cells. On the other hand, either concomitant Ship1/Ship2 inhibition or specific Ship2 inhibition reduced constitutive activation of the ribosomal protein S6 pathway and downregulated constitutive expression of the anti-apoptotic protein Mcl-1. Importantly, also in human CLL we found overexpression of many phosphatases including SHIP2. Dual inhibition of SHIP1 and SHIP2 reduced cellular survival in mutated-CLL and unmutated-CLL and was associated with decreased S6 phosphorylation and enhanced basal calcium levels. Taken together, we provide evidence that SHIP2 contributes to CLL pathogenesis in mouse and human, uncovering a novel potential therapeutic target in treating CLL.

Key words: B-cell receptor (BCR) signaling, Bruton's tyrosine kinase (Btk), serine/threonine kinase (Akt), SH2-containing inositol phosphatase (SHIP), chronic lymphocytic leukemia (CLL)

INTRODUCTION

Protein phosphorylation downstream of the B-cell receptor (BCR) represents the most common form of reversible post-translational modification in B-cells. This process is controlled by the coordinated action of specific kinases and phosphatases, which add or remove phosphate groups, respectively(1, 2). The balanced activity of these enzymes determines the optimal BCR signaling threshold that is essential for B-cell selection at various cellular differentiation checkpoints(2). Conversely, aberrant kinase activation is critical for survival of leukemic cells in various B-cell malignancies, including chronic lymphocytic leukemia (CLL)(1).

In CLL, which is characterized by the accumulation of CD5^{+}IgM^{low} monoclonal B-cells, two non-receptor kinases play a crucial role in oncogenic signaling: Bruton's tyrosine kinase (BTK) and the serine/threonine kinase AKT (also known as protein kinase B)(1, 3). Their importance is demonstrated by the exceptional clinical responses of small molecule inhibitors targeting either BTK(4-6) or phosphatidylinositol-3-kinase (PI3K), which is upstream of AKT(7, 8) in relapsed/refractory or treatment-naïve CLL patients. Targeting of PI3K/AKT/mTOR (mammalian target of rapamycin) signaling and its effector ribosomal protein S6 is particularly attractive, because this pathway is activated downstream of both the BCR and various chemokine receptors. Moreover, PI3K/AKT/mTOR/S6 signaling crucially controls protein synthesis, cell growth, proliferation, motility and survival(9).

Despite the impressive clinical advances, it remains largely unexplored how the activity of these kinases is dysregulated in CLL. Constitutive kinase signaling in CLL cells is accompanied by low surface IgM (sIgM) expression, elevated cell-autonomous calcium signaling and unresponsiveness to BCR stimulation(10-12). In these aspects, CLL cells resemble anergic B-cells, but upon *in vitro* culture CLL cells readily upregulate sIgM expression and regain BCR responsiveness. Considering its transient nature, the maintenance of anergy in CLL seems to require continuous BCR occupation by antigen next to dysregulation of intracellular signaling pathways. A key role for BCR signaling is further supported by the finding that CLL with hypermutated Ig heavy chain *(IgH)* variable genes (M-CLL) have a more favorable prognosis than unmutated CLL (U-CLL). Moreover, the BCR repertoire is highly restricted, since one-third of patients can be classified as stereotypic CLL, in which BCRs are highly similar across patients(1, 13).

To investigate the role of phosphatases in CLL, we employed a mouse model established in our laboratory based on sporadic expression of the oncogenic SV40 T antigen (*IgH.TE*μ)(14). This CLL model parallels the commonly employed *Eμ*-Tcl-1 transgenic mouse model in that both SV40 T antigen and Tcl-1 can inhibit apoptosis through activation of Akt(15, 16). In *IgH.TE*μ mice, the SV40 T gene is inserted in anti-sense direction into the *IgH* locus, between the D_H and J_H genes. Consequently, *IgH.TE*μ mice spontaneously develop a CLL-like disease with age, characterized by the accumulation of monoclonal CD5^{+}CD43^{+}IgM^{+}IgD^{low}CD19^{+} B-cells. We have generated EMC cell lines (EMC4 and EMC6) derived from splenocytes of *IgH.TEμ* mice that developed CLL(11). These EMC cells resemble *IgH.TE*μ primary tumors in phenotype and exhibit constitutively active BCR signaling, dependent on Btk, as well as full activation of Akt/S6 signaling.

Transcriptome analysis of primary tumors from *IgH.TE*μ mice and EMC cell lines revealed a unique phosphatase signature. SH2-containing inositol phosphatase (SHIP2) was among the most prominently increased genes in this signature. Here we show by conditional *in vivo* deletion of the *Ship2* gene in *IgH.TE*μ mice and by *in vitro* inhibition experiments with EMC cell lines that Ship2 promotes mouse CLL survival, most likely via the Akt/S6 pathway. Interestingly, SHIP2 expression is also increased in human CLL and *in vitro* SHIP-inhibition reduced AKT/S6-mediated cellular survival.

MATERIALS AND METHODS

Mice

Ship1$^{fl/fl}$ mice(17), *Ship2$^{fl/fl}$* mice(18), *Mb1$^{cre/+}$* mice(19) were kept on a C57BL/6 genetic background and *IgH.TE*μ mice(14) were on a mixed C57BL/6 x 129/Sv background. C57BL/6 mice and 129/Sv were purchased from Charles river. To achieve homozygous deletion of the *Ship1 or Ship2* gene specifically in B-cells, *Ship1 $^{fl/fl}$.Mb1$^{cre/+}$ or Ship2*$^{fl/fl}$.*Mb1$^{cre/+}$* mice were generated, which were crossed with *IgH.TE*μ.*Ship1 $^{fl/fl}$ or IgH.TE*μ.*Ship2$^{fl/fl}$* mice to obtain CLL panels, respectively. All mice were bred and maintained in the animal care facility at the Erasmus Medical Center, Rotterdam (The Netherlands). All animal studies were reviewed and approved by an ErasmusMC Committee of animal experiments (DEC).

CLL samples from human patients

Primary patient material was obtained from peripheral blood of CLL patients, while peripheral blood from healthy controls (>50 years of age) was obtained via Erasmus MC and via Sanquin blood bank (Rotterdam). Diagnostic and control samples were collected upon informed consent and anonymized for further use, following the guidelines of the Institutional Review Board MEC2015-741 (for CLL) and MEC2016-202 (healthy controls), and in accordance with the declaration of Helsinki. The BCR characteristics of CLL patients are included in **Table 1**. Peripheral blood mononuclear cells (PBMCs) were isolated using Ficoll Hypaque (GE Healthcare, Little Chalfont, UK) according to the manufacturer's instructions. Naïve mature B-cells were isolated from healthy control PBMCs using FACS-purification for CD19^{+}CD27^{-}IgD^{+} cells. The purity of naïve mature healthy B-cell samples was >95%, as determined by flow cytometry.

Table 1: B-cell receptor characteristics of CLL patients.

CLL ID	Sample inclusion	% BCR germline identity	IGHV gene	IGHD gene	IGHJ gene	VH CDR3 length	VH CDR3 Sequence AA	Gender	Mutation status	Age
KL2015-240	$, #	89.73	IGHV3-30*03	IGHD6-13*01	IGHJ6*02	19	AKVGRPAAFEEYYYYGMDV	Female	M-CLL	54
KL2015-134	$, #	90.6	IGHV4-61*02	IGHD5-18*01	IGHJ4*02	12	ARDPDTYGYVDC	Male	M-CLL	58
KL2017-070	$, #	91.03	IGHV3-30*03	IGHD3-9*01	IGHJ4*02	18	AKPGSVFRYFDWISGLWYW	Male	M-CLL	71
KL2014-413	$, #	91.9	IGHV3-30*03	IGHD5-12*01	IGHJ3*02	14	ANELVTSSYDGIDIW	Male	M-CLL	66
KL2015-241	$, #	92.02	IGHV3-48*03	IGHD2-15*01	IGHJ1*01	9	ARDGGSYPL	Male	M-CLL	74
KL2010-250	$, #	94.05	IGHV3-72*01	IGHD2-8*01	IGHJ6*02	20	GRIYCTLSRCSIDQYYGMDV	Male	M-CLL	52
KL2010-510	$	94.6	IGHV3-74*01	IGHD2-15*01	IGHJ5*02	18	AREVCIGDNCYSRGWFDP	Male	M-CLL	82
KL2015-555	$	95	IGHV3-53*01	IGHD5-18*01	IGHJ4*02	16	ARDRGGGYSYGGGFDY	Male	M-CLL	61
KL2013-007	$, #	96.02	IGHV4-30*01	IGHD2-2*01	IGHJ6*03	16	ARDAGVVPVHYYYMDV	Male	M-CLL	66
KL2016-263	#	96.85	IGHV5-10-1*01	IGHD2-15*01	IGHJ6*02	28	ATGEGGLGWNPRYCSGGSCYEVGYGMDV	Male	M-CLL	67
KL2010-168	$	97.31	IGHV3-11*03	IGHD2-15*01	IGHJ4*02	13	ARGGEVMVSPLDR	Male	M-CLL	66
KL2011-589	$, #	100.00	IGHV1-69*06	IGHD3-3*01	IGHJ6*03	21	ASGSIFGVVIGSYYYYYYMDVW	Male	U-CLL	57
KL2014-260	$, #	100.00	IGHV3-20*01	IGHD3-3*01	IGHJ4*02	21	ARGTGITIFGVVHTTEYYFDYW	Male	U-CLL	85
KL2014-372	$, #	100.00	IGHV1-69*01	IGHD3-16*02	IGHJ5*02	22	ARDPPFDYIWGSYRYRANWFDPW	Female	U-CLL	61
KL2015-035	$	100.00	IGHV1-69*01	IGHD2-2*01	IGHJ6*02	24	ARDSPHKQDIVVVPAAMVFYSMDV	Male	U-CLL	68
KL2013-006	$, #	100.00	IGHV4-39*01	IGHD3-3*01	IGHJ6*02	26	ARHASPRDFWSGYPELIYYYYYGMDVW	Male	U-CLL	48
KL2014-420	$, #	100.00	IGHV1-69*01	IGHD2-2*01	IGHJ6*02	21	ASLTIVVVPAAMSYYYYGMDVW	Male	U-CLL	61
KL2011-399	$, #	100.00	IGHV4-4*05	IGHD3-16*02	IGHJ6*02	26	ARGRRDDYIWGSYRYTDLGYYYGMDV	Female	U-CLL	73
KL2011-447	$, #	100.00	IGHV1-69*01	IGHD3-3*01	IGHJ4*02	22	ARAAVPYYDFWSGYSLDSGFDY	Male	U-CLL	49
KL2016-025	$	100.00	IGHV4*31*01	IGHD3-22*01	IGHJ6*02	22	ARDSSPRLYYDSSGYYGMGLDV	Male	U-CLL	85
KL2010-451	$	100.00	IGHV4-59*01	IGHD3-22*01	IGHJ6*03	23	ARGNYYDSSGYYYVGYYYYYMDV	Male	U-CLL	57
KL2014-264	#	100.00	IGHV1-24*01	IGHD4-23*01	IGHJ4*02	16	ATLGAARQLGWYYFDYW	Male	U-CLL	68

$, samples included for expression analysis by qRT-PCR

#, samples included for phospho-flow analysis

Treatment of EMC cell lines and human CLL cells with SHIP inhibitors

EMC cell lines were cultured in RPMI medium supplemented with 10% FCS, 50 μg/ml gentamycin, 50 μM 2-mercapto-ethanol (culture medium) at 37°C and 5% CO_2 as previously described(11).

The pan-SHIP1/2 inhibitor 3β-Amino-5α-androstanane hydrochloride (K118) has been described previously was dissolved in MilliQ at 5mM stock concentration(20). The SHIP2-specific inhibitor 3-[(4-Chlorophenyl)methoxy]-N-[(1S)-1-phenylethyl]-2-thiophenecarboxamide (AS1949490)(21) was purchased from Echelon Biosciences Inc. (Salt Lake City, UT, USA) was dissolved in dimethyl sulfoxide (Sigma) at 10mM stock concentration.

All inhibitor treatments were performed in culture medium at 37°C, 5% CO_2, except when otherwise indicated. For the analysis of apoptosis and cell cycle, cells were incubated in the presence/absence of inhibitor or vehicle for 6 hours and 24 hours (EMC cells) or 6 hours (human CLL). For western blot analysis, cells were incubated in the presence/absence of inhibitor for 4 hours. For phospho-flow cytometry and calcium flux assays, cells were cultured in the presence/absence of inhibitor for 3 hours and 24 hours (EMC cell lines) or 1 hours (human CLL). MACS-purified wild-type (WT) C57BL/6 mice splenic B-cells and PBMCs from healthy donors were included as a control.

Caspase apoptosis assay

To detect caspase activation, cells were stained with Caspase-Glo 3/7 (Promega, G8091) assay reagent as described previously(22). Luminescence of the stained cells was measured on an Infinite200 spectrophotometer (Tecan).

Flow cytometry procedures

Apoptosis analysis. Cells were stained for annexin V (PE, BD Biosciences) and 7-Aminoactinomycin D (7-AAD) (PE-Cy5, BD Biosciences) in diluted binding buffer (BD Biosciences) at room temperature in the dark for 15 min. Human CLL samples were additionally stained with anti-CD3 (BV711, Clone UCHT1, BD Biosciences), anti-CD19 (PE-Cy7, Clone SJ25C1/HIB19, BD Biosciences) and anti-CD5 (AF700, Clone UCHT-2, BD Biosciences).

Cell cycle analysis. For DNA content-based cell cycle analysis, cells were fixed with 70% ethanol and stained overnight with 1 mg/mL of propidium iodide (PI, Sigma Aldrich) in the presence of 1%Triton X-100 (Sigma Aldrich) and RNAse (10 mg/mL) (Roche) at 4°C in the dark.

Phospho-flow cytometry. Mouse EMC cells or human CLL samples were stained with a live/dead marker (Invitrogen Probes). Cells were then fixed and permeabilized in FoxP3 staining kit Fix/Perm solution (eBioscience) at 37°C for 10 min as per manufacturer's instructions. For the identification of B lymphocytes in the control WT splenocyte fractions, cell suspensions were additionally stained with anti-B220 (APC, Clone RAS-6B2, BD Biosciences) and anti-CD3 (APCef780, Clone 17-A2, eBioscience) at 4°C for 30 minutes in FoxP3 staining kit wash buffer (eBioscience) after fixation. Similarly, for the identification of B lymphocytes in human CLL samples, the cells were additionally stained with anti-CD5 (BV421, Clone UCHT2, BD Biosciences), anti-CD3 (BV711, Clone UCHT, BD Biosciences), anti-CD19 (FITC, Clone HIB19, BD Biosciences). Following, cells were stained with anti-p-Btk(Y223) (PE, Clone N35-86, BD Phosflow), anti-p-Erk (PE, Clone 20A, BD Phosflow) or with unconjugated anti-p-S6 (Clone D68F8, Cell Signaling Technologies) and PE-conjugated anti-rabbit secondary antibody (Jackson ImmunoResearch).

Calcium flux assay. EMC cells, WT mouse splenocytes or human CLL samples were stained with fluorogenic probes: 1μM of Fluo3-AM and 1 μM of Fura Red-AM (Life Technologies^{TM}) in loading buffer (HBSS medium, supplemented with 10 mM HEPES and 5% FCS) in a water bath at 37°C for 30 min. To gate for untouched B-cells, mouse cells were additionally stained with biotinylated anti-NK1.1 (Clone PK136, BD Biosciences), anti-CD4 (Clone GK1.5, BD Biosciences), anti-CD8α (Clone 53-6.7, BD Biosciences), anti-Ter-119 (BD Biosciences), anti-CD11c (Clone N418, eBioscience), anti-Gr-1(Clone RB6-8C5, eBioscience) and anti-FcεR1(Clone MAR-1, eBioscience) in the final 10 minutes of the Fluo3-AM/FuraRed-AM staining. To gate for untouched B-cells, biotinylated anti-CD3 (BD Biosciences) and anti-CD33 (BD Biosciences) were added in the final 10 minutes of Fluo3-AM/FuraRed-AM staining. For the identification of biotinylated antibodies, WT cells were washed and resuspended in flux buffer (loading buffer supplemented with 1 mM $CaCl_2$) with fluorochrome-conjugated streptavidin in a water bath at 37°C. Subsequently, cells were washed, resuspended in flux buffer, filtered and left at room temperature for at least 30 minutes. Before measurement, cells were placed at 37°C for 5 minutes in a water bath. Basal calcium levels were measured in the first minute. Cells were then stimulated with 20 μg/ml goat anti-mouse $F(ab')_2$ α-IgM (Jackson ImmunoResearch) or anti-human $F(ab')_2$ α-IgM (Southern Biotech) and the calcium flux was measured for another 4 minutes.

Measurements were performed on an LSRII flow cytometer (BD Biosciences) and results were analyzed using FlowJo-V10 software (TreeStar).

MACS-purification and RNA isolation

Splenic single-cell suspensions were prepared in magnetic-activated cell sorting (MACS) buffer (PBS/2mM EDTA/0.5% BSA). Primary tumors from *IgH.TE*μ mice were purified using MACS-purification for $CD19^+$ cells. Naïve splenic B-cells from 8-12-week-old WT C57BL/6 mice were purified by MACS, as previously described(23). Purity of MACS-sorted naïve B-cells was confirmed by flow cytometry (typically > 99% $CD19^+$ cells). To obtain fractions of activated B-cells, purified naïve B-cells were cultured in RPMI/FCS culture medium in the presence of 10 μg/ml $F(ab')_2$ α-IgM (Jackson Immunoresearch) for 12 hours. RNA was extracted with the RNeasy Micro kit (Qiagen) according to manufacturer's instructions.

RNA-sequencing

The TruSeq RNA Library Prep kit (Illumina) was used to construct mRNA sequencing libraries that were sequenced on an Illumina HiSeq 2500 (single read mode, 36 bp read length). Raw reads were aligned using Bowtie to murine transcripts (RefSeq database) from the University of California at Santa Cruz (UCSC) mouse genome annotation (NCBI37/mm9) (24). Normalized gene expression levels quantified as reads per kilobase of a transcript per million mapped reads (RPKMs) were used for various clustering approaches. Unsupervised hierarchical clustering and principal component analysis were performed using R software (R studio version 1.1.383). For visualization of gene clustering analysis, heatmaps depicting row Z-scores of RPKM values were generated using R. RNA-seq data used in this study have been deposited in the GEO database (accession number GSE117713)(25). Gene expression data for Ship1 and Ship2 in various immunological cell types were obtained from the Immunological genome project ULI RNA-seq data (accession number GSE109125)(26).

Quantitative real time PCR (qRT-PCR) analysis

Quantitative RT-PCR analysis was performed with TaqMan probes. Primers and probes were designed using the Ensembl genome browser and Universal Probe Library (Roche Applied Science). cDNA was generated using the RevertAid H-minus first strand cDNA synthesis kit (ThermoFisher) in accordance with the manufacturer instructions. Briefly, each 15 µl of RT-PCR reaction consisted of 7.5 µl of Taqman Universal Mastermix II (ThermoFisher), 4.15 µl of nuclease-free water, 0.6 µl of forward and reverse primers (10 pmol/µl) and 0.15 µl of probe. Quantitative RT-PCR was performed on the 7300 Real Time PCR system (Applied Biosciences). Gene expression was analyzed with an ABI Prism 7300 Sequence Detector and ABI Prism Sequence Detection Software version 1.4 (Applied Biosystems). The housekeeping genes glyceraldehyde-3-phosphate dehydrogenase (*Gapdh*) or ubiquitin were used for normalization of expression of all quantified genes for mouse and human, respectively. Primers and probes used are listed in **Supplementary Table 2, Supplementary Table 3**.

Western Blot

For western blot experiments EMC cells and WT naïve splenic B-cells (purified by MACS as described)(23) were lysed in RIPA lysis buffer (50 mM TrisCl pH7.4, 150 mM NaCl, 1 mM EDTA pH 8, 0.1% SDS, 1% NP-40) containing protease and phosphatase inhibitors (Roche). After sonication, cellular protein content was measured using the BCA protein assay (Pierce, Thermo Fischer). Cellular proteins (30-50 µg) were loaded on an SDS-polyacrylamide gel and separated using a Bio-Rad mini-PROTEAN electrophoresis system(27). Proteins were then transferred onto Immobilon-P polyvinylidene difluoride membranes (Millipore Corporation, Bedford, MA, USA), which were probed with primary antibodies against β -Actin (AB0145-200, SICGEN) and Mcl-1 (ab32087, Abcam). Binding was visualized using IRDye 680 or 800 labeled secondary antibodies and an Odyssey Imager (Li-Cor). Quantification of signal was performed using Odyssey 3.0 software.

Statistical analysis

Statistical analysis was performed using GraphPad Prism software (San Diego, California, USA). The log rank test was used to assess statistical significance in survival between mouse groups. To evaluate differences in the size of various B-cell subsets between two groups we used a Mann-Whitney *U*-test. For evaluation of differences between SHIP-inhibitor or vehicle treated and untreated groups *in vitro* assays, we used Kruskal-Wallis one way ANOVA test corrected with Dunn's Multiple comparison test for comparing multiple pairs. To evaluate differences between human CLL and mature naïve B-cells (after normalization to mature naïve B-cells), and between inhibitor-treated and untreated CLL samples from patients, we used Wilcoxon signed rank test.

RESULTS

CLL from IgH.TEμ mice express a unique phosphatase signature

To identify genome-wide differentially expressed (DE) phosphatase genes in CLL we performed RNA- sequencing (RNA-seq) on primary CLL samples (tumor load >95%, n=6) from *IgH.TEμ* mice. For comparison, unstimulated (Un-B, n=4) and anti-IgM stimulated (αIgM-B stimulated, n=4) naïve splenic B-cells from wild type (WT) mice were included. We used a complete list of 221 unique phosphatase entries (https://www.genenames.org/cgi-bin/genefamilies/set/1076) belonging to 31 different families to identify key phosphatases that were differentially expressed between un-B, αIgM-B and primary *IgH.TE*μ CLL samples.

By applying a threshold of RPKM >1, we first identified 162 of these 221 phosphatase genes (73%) that were expressed in at least one of the three experimental groups. Next, by analyzing differential gene expression (>2-fold change in *IgH.TE*μ CLL compared with Un-B and/or αIgM-B-cells; FDR q<0.05), we identified 96 DE genes (**Figure 1A; Supplementary Table 1**). Hierarchical clustering of expression values revealed that the six CLL samples clustered together, separately from the Un-B and αIgM-B cells, which we confirmed by principal component analysis (**Figure 1B**). Interestingly, *Ptpn22* and *Ptpn11* (*SHP2*), which have already been described to play a role in CLL, were significantly higher in *IgH.TE*μ CLL than in WT B-cells(28, 29). We did not find differential expression of *Inpp5d* (*Ship1*), but the expression of the *Ship1* paralog *Inppl1* (*Ship2*) was ~6-fold higher in *IgH.TE*μ CLL cells compared to un-B and αIgM-B cells (p=0.004). These 96 DE genes were also differentially expressed in stable CLL-like cell lines generated from *IgH.TE*μ mice(11), whereby the expression in the cell lines and primary CLL cells were highly correlated (spearman correlation r^2, ρ=0.836; $p<0.0001$) (**Figure C**).

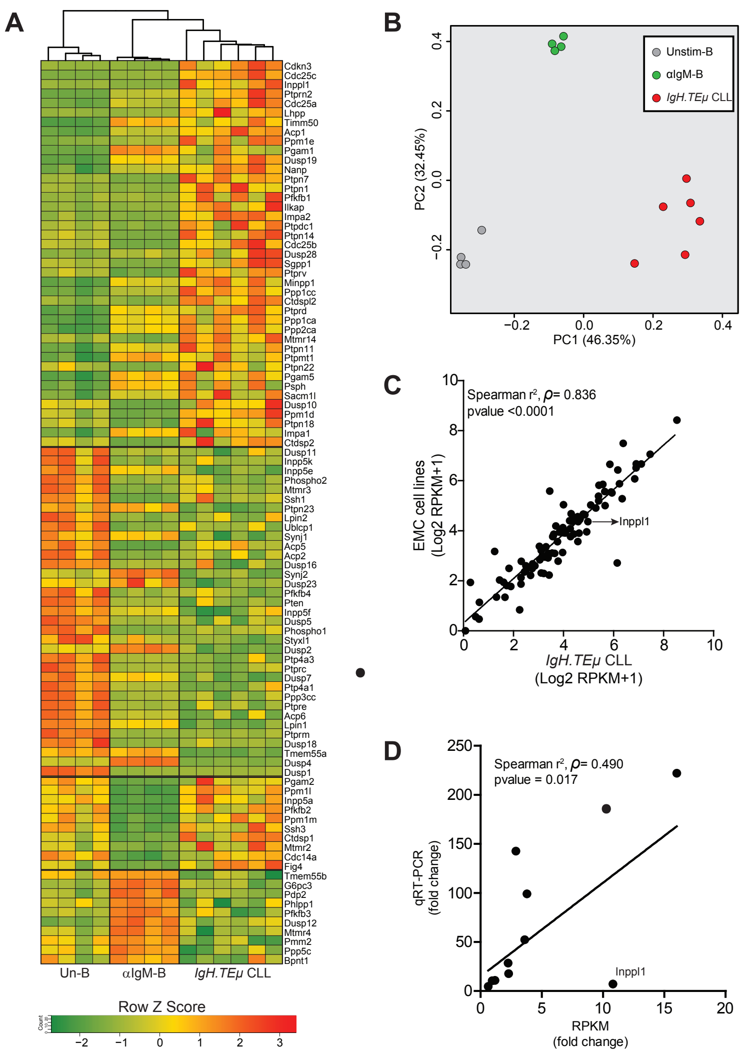

Figure 1. CLL cells from *IgH.TEμ* mice express a unique phosphatase signature.
(**A**) Hierarchical clustering analysis (top) and accompanying heat map showing differences in expression levels (RPKM, depicted as row Z-scores) of the 96 differentially expressed (DE) genes between unstimulated (Un-B, n=4), anti-IgM-stimulated (αIgM-B, n=4) wild-type (WT) splenic B-cells and CLL cells (n=6) from *IgH.TEμ* mice. (**B**) Principle component analysis using the 96 DE genes in Un-B (n=4, *grey*), αIgM-B (n=4, *green*) WT splenic B-cells and CLL cells (n=6, *red*) from *IgH.TEμ* mice. (**C**) Correlation plot comparing gene expression ((log2 RPKM+1) between primary tumor from *IgH.TEμ* mice (mean values of n=6) and EMC cell lines (mean of n=3) for the 96 unique phosphatase genes detected by RNA-seq (spearman r^2, ρ=0.836; $p<0.0001$). (**D**) Correlation plot comparing relative expression to WT splenic B-cells in primary tumor from *IgH.TEμ* mice for 11 genes as measured by RNA-seq (RPKM, n=6) or qRT-PCR (n=30) (spearman r^2, ρ=0.490; p=0.017).

To further strengthen the existence of a unique phosphatase signature in *IgH.TEμ* CLL, we validated DE genes by quantitative real-time PCR (qRT-PCR) in an extended cohort of primary CLL samples (tumor load >95%, n=30) from *IgH.TEμ* mice. Hereby, unstimulated naïve splenic B-cells from WT mice (n=4) served as controls. We selected robustly expressed genes belonging to two families of phosphatases, inositol polyphosphate phosphatases (*Inpp*) and protein tyrosine phosphatases of the non-receptor type (*Ptpn*), as members of these families play a role in B-cell biology or CLL(28-32). Validation by qRT-PCR showed that all selected genes were significantly higher expressed in *IgH.TEμ* CLL than in WT B-cells ($p<0.05$)(**Supplementary Table 2**). Although *Ship1* was not a DE gene in the RNA-seq analysis, qRT-PCR analysis revealed increased expression (~9-fold) in the larger *IgH.TEμ* CLL cohort, when compared with WT splenic B-cells (**Supplementary Table 2**). Comparison of average expression fold-changes as determined by RNA-seq (n= 6) and qRT-PCR (n= 30) for primary CLL samples revealed significantly correlated trends for these 11 genes (spearman correlation r^2, ρ=0.490; p=0.017), validating our RNA-seq analysis when extrapolated to a larger cohort of *IgH.TEμ* CLL (**Figure 1D**).

In summary, these data identified a unique phosphatase signature of 96 DE genes in *IgH.TEμ* CLL. Since particularly Ship1 has been implicated in regulating BCR signaling, maintaining anergy in autoreactive B-cells(33) and survival of multiple myeloma *in vivo*(34) we next focused on Ship1 and its close homologue Ship2 for further studies.

Different effects of conditional Ship1 or Ship2 deletion on B-cell development

To explore expression of *Ship1* and *Ship2* in various hematopoietic cell types, we analyzed previously reported gene expression data(26) (**Supplementary Figure 1**). This revealed that *Ship1* is stably expressed throughout B and T cell development. Expression of *Ship2* is substantially lower than *Ship1*, yet detectable across all B-cell developmental stages and – at a lower level – also in T cells. Likewise, *Ship1* expression was higher than *Ship2* in various innate immune cell types.

To study the role of Ship1 and Ship2 in B-cell development in the context of CLL, we first analyzed a cohort of ~40-week-old mice in which the *Ship1* and *Ship2* genes were targeted specifically in the B-cell lineage using *Mb1*$^{cre/+}$ transgenic mice (n≥5 each group). In these experiments, mice were on a mixed 129/sv x C57BL/6 background and *Mb1*$^{+/+}$ littermates served as controls. Deletion of *Ship1* and *Ship2* had no effect on early B-cell development in the bone marrow, although Ship1-deficiency resulted in a significant reduction of recirculating IgM$^{low/+}$IgD^{+} B-cells, as reported previously for young mice(35) (**Figure 2A, 2B**; see **Supplementary Figure 2A** for the flow cytometry gating strategy). In the spleen, Ship1 or Ship2-deficiency had no effect on transitional or marginal zone (MZ) B-cells, but the absolute numbers of follicular B-cells were significantly reduced in

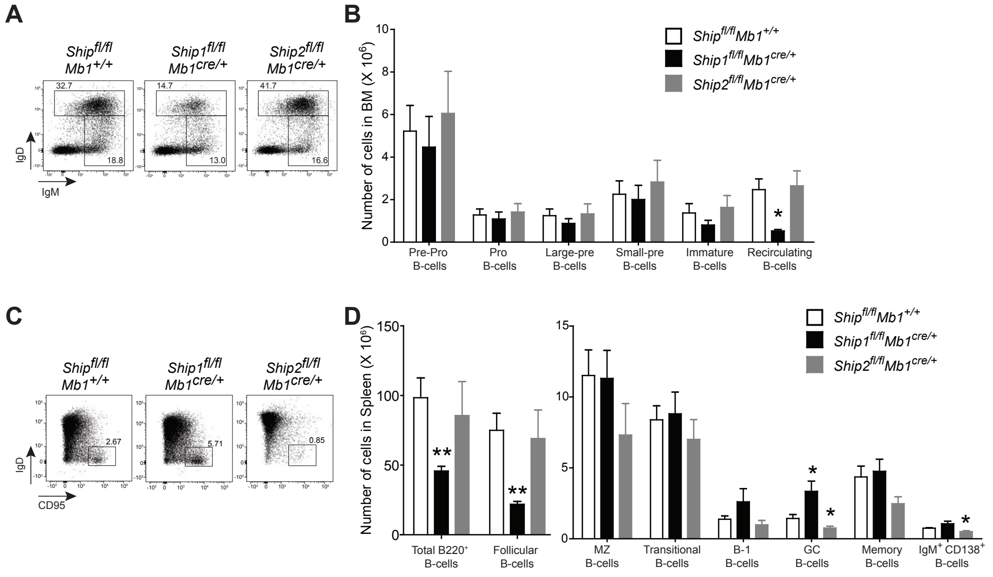

Figure 2. Differential effects of conditional *Ship1* or *Ship2* deletion on B-cell development.
(**A,C**) FACS plots depicting differences in (**A**) recirculating ($IgM^{low/+}IgD^{high}$) and immature ($IgM^{high}IgD^{low/-}$) B-cell subsets in bone marrow or (**C**) germinal center cells ($IgD^{-}CD95^{+}$) in spleen of *$Ship1^{fl/fl}.Mb1^{cre/+}$*mice (n=5), *$Ship2^{fl/fl}.Mb1^{cre/+}$*mice (n=6) and control mice (*$Ship1^{fl/fl}$ or $Ship2^{fl/fl}$* on *$Mb1^{+/+}$*background, n=6). Shown are dot plots on gated $CD19^{+}B220^{high}$ cells, as depicted in **Supplementary Figure 2** (**B, D**) Quantification of various B-cell subsets in (**B**) bone marrow or (**D**) spleen of indicated mice groups. **p* < 0.05, (Mann-Whitney *U* test).

Ship1-deficient mice compared with control littermates (**Figure 2D**). Absolute numbers of splenic B-1 cells were not different (**Figure 2D**), although Ship1-deficient mice had higher proportions of B-1 cells compared with control littermates (**Supplementary Figure 2B**). Interestingly, the two deficiencies had opposite effects on antigen-dependent B-cell subsets: whereas Ship1-deficient mice had significantly higher numbers of germinal center (GC) B-cells, Ship2-deficient mice had significantly lower numbers compared with control littermates (**Figure 2C, D**). Furthermore, Ship2-deficient mice had reduced numbers of memory cells (significance was not reached) and non-switched $IgM^{+}CD138^{+}$ plasma cells, although the total numbers of plasma cells were not different (**Figure 2D**).

In conclusion, these data show that Ship1 and Ship2 have differential effects on mouse B-cell development. While Ship1-deficiency was associated with reduced numbers of follicular B-cells and spontaneous GC formation, the absence of Ship2 resulted in a partial loss of GC B-cells and IgM^{+} plasma cells.

B-cell-specific Ship2 deletion reduces tumor formation in IgH.TEμ mice

We generated *IgH.TEμ* mice with B-cell-specific homozygous deletion of *Ship1* or *Ship2,* referred to as *$IgH.TEμ.Ship1^{-/-}$* and *$IgH.TEμ.Ship2^{-/-}$* mice, respectively. To monitor CLL onset we collected blood every 3-6 weeks. Their mixed 129/sv x C57BL/6 background enabled us to use IgMa/IgMb allotypes to define CLL incidence as an accumulation of >70% $IgMb^{+}CD5^{+}CD43^{+}CD19^{+}$ B cells in peripheral blood, as described previously(14, 25). CLL onset was observed in control *IgH.TEμ* mice and *$IgH.TEμ.Ship1^{-/-}$* mice at median ages of 231 and 201 days, respectively (p=0.55) (**Figure 3A**). In contrast, CLL formation was significantly reduced in *$IgH.TEμ.Ship2^{-/-}$* mice (p<0.001): only two of the 18 mice showed >70% $IgMb^{+}CD5^{+}CD43^{+}CD19^{+}$ cells in peripheral blood (**Figure 3B**).

We analyzed various lymphoid organs in CLL-positive mice within the three groups, either when mice reached the humane end-point or at the age of ~42 weeks in case of *IgH.*

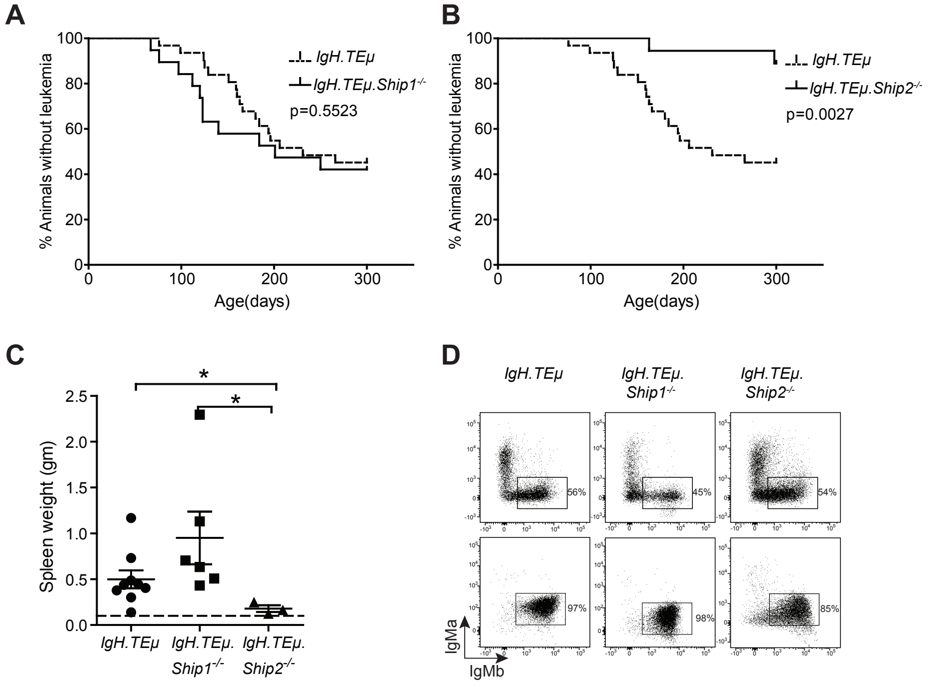

Figure 3. B-cell-specific *Ship2* deletion reduces tumor incidence in *IgH.TEμ* mice.
(**A,B**) Kaplan-Meier CLL incidence curves of (A) *IgH.TEμ* (*dotted line*, n=30) versus *$IgH.TEμ.Ship1^{-/-}$* (*solid line*, n=18) mice or (**B**) *IgH.TEμ* (*dotted line*, n=30) versus *$IgH.TEμ.Ship2^{-/-}$* (*solid line*, n=18) mice. (**C**) Comparison of spleen weight between *IgH.TEμ* and *$IgH.TEμ.Ship1^{-/-}$* mice at end-stage disease (>95% $IgMb^{+}CD5^{+}CD43^{+}CD19^{+}$ CLL-like cells in peripheral blood) or ~42-week-old mice with detectable CLL development in peripheral blood (*IgH. TEμ $Ship2^{-/-}$*). Dotted line represents average spleen weight of 42-week-old WT (C57BL/6) mice. **p*< 0.05 (Mann-Whitney *U* test). (**D**) Flow cytometric profiles for IgMa and IgMb on gated $CD19^{+}$ cell fractions from spleen of non-tumor bearing (*upper row*) and tumor-bearing (*lower row*) mice of the indicated phenotypes. Numbers indicate the proportions of cells within the specified gates.

TEμ.Ship2$^{-/-}$ mice. Both control *IgH.TEμ* mice and *IgH.TEμ.Ship1*$^{-/-}$ mice developed significant splenomegaly and enlarged lymph nodes, compared to age-matched WT control mice (**Figure 3C**). When we compared IgMa/IgMb profiles in splenic B-cells from CLL-positive mice, the *IgH.TEμ* and *IgH.TEμ.Ship1*$^{-/-}$ mice exhibited massive accumulation of a CD19$^+$CD5$^+$ population with exclusive (~97%) expression of the non-targeted IgMb allele (**Figure 3D**). Interestingly, the two CLL-positive *IgH.TEμ.Ship2*$^{-/-}$ mice did not develop splenomegaly, although >95% of the CD19$^+$ cells had the IgMb$^+$CD5$^+$CD43$^+$ CLL phenotype (**Figure 3C, D**). Those *IgH.TEμ.Ship2*$^{-/-}$ mice in which CLL cells were not detected in peripheral blood consistently had close to equal proportions of IgMa- and IgMb-expressing CD19$^+$ B-cells in the spleen (**Figure 3D**), except one animal in which IgMb$^+$CD5$^+$CD43$^+$CD19$^+$ B-cells were abundantly present in the spleen. The CLL phenotype in *IgH.TEμ.Ship2*$^{-/-}$ mice did not appear to differ from that in the other two groups, regarding phosphatidylcholine-specificity of their BCR, S6-phosphorylation, or basal and αIgM-induced calcium flux (data not shown), although statistical analysis was precluded by the low numbers of *IgH.TEμ.Ship2*$^{-/-}$ leukemias.

In conclusion, whereas B-cell-specific deletion of Ship1 did not significantly affect CLL formation, conditional deletion of Ship2 resulted in significantly reduced CLL development and absence of splenomegaly at ~42 weeks. From these findings we conclude that Ship2-mediated signaling in B-cells plays a crucial role in the induction and aggressiveness of CLL in *IgH.TEμ* mice.

Ship inhibition decreases survival of EMC cells in vitro

To investigate the role of *Ship*-mediated signaling in CLL, we employed the *IgH.TE*μ-derived CLL cell lines EMC4 and EMC6(11). Cells were treated either with a pan-Ship1/Ship2 inhibitor K118 (3β-Amino-5α-androstanane, hydrochloride)(20) or with a selective Ship2 inhibitor AS1949490 (3-[(4-Chlorophenyl)-methoxy]-N-[(1S)-1-phenylethyl]-2-thiophene-carboxamide)(21). As a control, vehicle-treated cells were included.

To determine the effect of Ship inhibition on cell survival, K118-, AS1949490- and vehicle-treated EMC cell lines were stained with Annexin V and 7-aminoactinomycin (7-AAD) and analyzed by flow cytometry (**Figure 4A**). Both inhibitors significantly decreased the proportions of alive cells in a dose-dependent manner. However, the kinetics differed between the two inhibitors: whereas the IC$_{50}$ value for K118 was reached after ~6 hours of incubation at 5 μM, the IC$_{50}$ for AS1949490 was only reached following ~24 hours of incubation at 15 μM.

Next, we performed propidium iodide DNA content analysis after ~24 hours of inhibitor treatment to investigate their effects on EMC cell proliferation and apoptosis. AS1949490 induced a significant dose-dependent decrease in the proportions of cycling cells (S/G2/M), whereas K118 had a more moderate effect on the fraction of proliferating EMC cells (**Figure 4B**). However, both inhibitors induced a significant increase (≥4-fold) in the proportions of apoptotic (sub-G1) cells, validating our Annexin V/7-AAD data using a different experimental read-out.

To confirm that the reduced cell viability seen upon incubation with Ship inhibitors was due to the induction of apoptotic pathways, we measured the activity of executioner caspase-3 and caspase-7 following treatment with K118 or AS1949490. We observed up to ~2-fold induction of caspase-3/7 after 6 hours of treatment with K118 in a dose-dependent manner (**Figure 4C**). Treatment with AS1949490 resulted in moderate caspase-3/7 induction after 6 hours (data not shown) and 2-fold induction after 24 hours (**Figure 4C**).

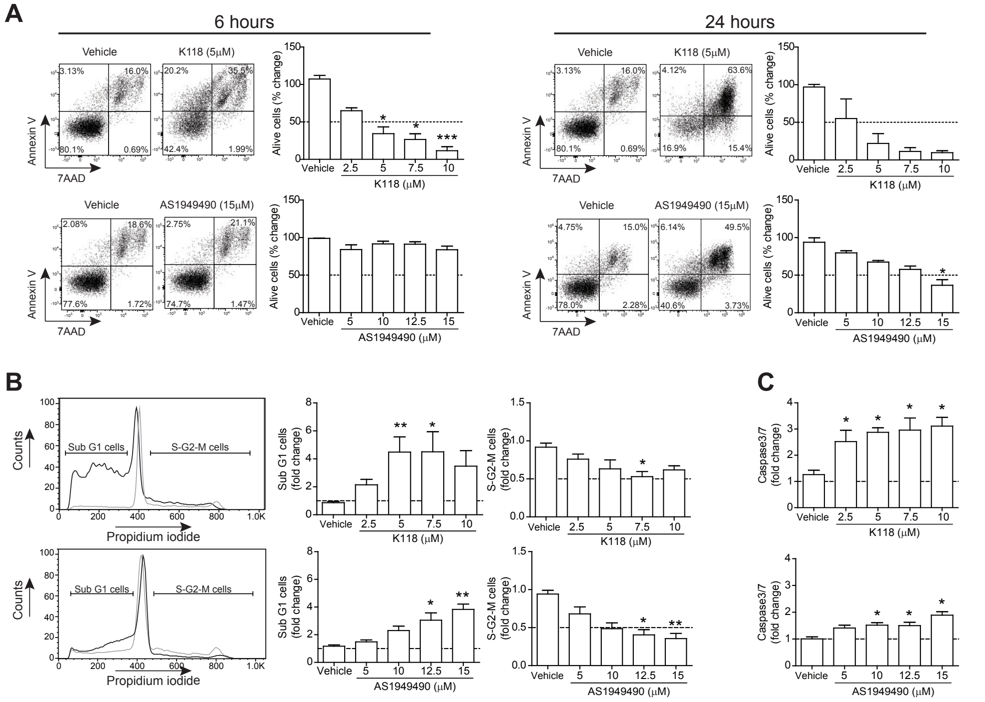

Figure 4. Ship inhibition decreases survival of EMC cells *in vitro*
(**A**) Viable (AnnexinV and 7-AAD negative) cells were determined after 6 hours (*left*) or 24 hours (*right*) of treatment with the indicated concentrations of K118 (*top*) or AS1949490 (*bottom*). Bar graphs represent the proportions of viable cells, normalized to untreated control cells (set to 100%). Dot plot show representative flow cytometric analysis of EMC6 cells. (**B**) Cell cycle profiling in EMC cells after 24h of treatment with the indicated concentrations of K118 (*top*) or AS1949490 (*bottom*). Histogram shows the gating strategy for DNA content (Propidium Iodide) analysis in the absence (*grey*) or presence (*black*) of SHIP inhibitor. Bar graphs represent the proportions of apoptotic (subG1, *left*) and cycling (S-G2-M, *right*) cells normalized to untreated control cells. (**C**) Analysis of caspase activity using the caspase-glo assay in EMC cells treated with the indicated concentrations of K118 for 6h (*top*) or AS1949490 for 24h (*bottom*). Each set of data consists of at least three independent experiments each on EMC4 and EMC6. Statistical analysis was performed by comparing the effect of SHIP inhibitor to the respective vehicle using Dunn's multiple comparison test. *p<0.05, **p<0.01,***p<0.001

Taken together, inhibition of Ship1 and Ship2 induced caspase-mediated apoptosis of EMC cell lines *in vitro*. Nevertheless, the two inhibitors differed in their potency (IC_{50}) and kinetics and Ship2 inhibition in particular resulted in decreased proliferation.

Ship exerts dual effect on the BCR signaling cascade in EMC cells

To investigate if Ship1/2 play a role in regulating constitutive BCR signaling in EMC cells, we measured the effects of Ship1/2 inhibition on phosphorylated Btk(Y223), Erk(T202/Y204) and S6(S240/244), as well as BCR-mediated calcium flux. We used 5 μM of K118 and 15 μM of AS1949490, corresponding to the IC_{50} value of the respective inhibitor.

As reported previously, EMC cells exhibited high basal phosphorylation of Btk(Y223), Erk and S6 in comparison to WT B-cells (**Figure 5A**, **Supplementary Figure 2C**)(11). Both K118 and AS1949490 had minimal effects on constitutive active levels of p-Btk(Y223) and p-Erk in EMC cells (**Figure 5B, 5C, Supplementary Figure 2D, 2E**). However, 3 hours of K118 treatment resulted in substantial downregulation of p-S6 in both EMC cell lines. Similar downregulation of p-S6 levels was seen with AS1949490, but only after 24 hours of treatment. Additionally K118 treatment also resulted in downregulation of p-AKT (S473) in EMC cells (data not shown).

Because p-S6 was shown to be an important regulator of the translation of anti-apoptotic myeloid leukemia cell differentiation protein (Mcl-1) in CLL(36), we investigated the effects of inhibitor treatment on Mcl-1 protein levels in EMC cells by western blot analysis. Both K118 and AS1949490 treatment led to substantial downregulation of Mcl-1 in EMC4 and EMC6 cells (**Figure 5D**). Interestingly, such downregulation was also seen in EMC cells in the presence of caspase inhibitor Quinoline-Val-Asp-Difluorophenoxymethyl Ketone (QVD), suggesting that caspase induction upon Ship1/2 inhibition in EMC cells (**Figure 5D**) occurred as a result of Mcl-1 downregulation. We found that Mcl-1 was constitutively expressed in EMC cells, as Mcl-1 protein levels were higher in EMC cells than in α-IgM+LPS stimulated WT B-cells (**Figure 5D**). Of note, we detected only limited effects of Ship1/2 inhibitors on the protein levels of the pro-apoptotic Bcl-2-like protein 11 (BIM) (data not shown), which interact with Mcl-1(27).

Since Ship1 is a negative regulator of calcium signaling in B lymphocytes(37), we measured αIgM-induced calcium mobilization in untreated or K118 or AS1949490 -treated EMC cells. In contrast to WT B-cells, which display a strong calcium flux upon α-IgM stimulation, EMC cells exhibited low and unsustained calcium flux (**Figure 5E**, **Supplementary Figure 2F)**. This is in agreement with the anergic phenotype of these cell lines(11). Treatment with K118 (5 μM) enhanced basal calcium levels and rendered EMC cells fully unresponsive to BCR stimulation (**Figure 5F, Supplementary Figure 2G**). However, AS1949490 (15 μM) had limited effects on basal and αIgM-induced calcium mobilization in EMC cells, even after 24 hours of exposure (**Figure 5G, Supplementary Figure 2H**).

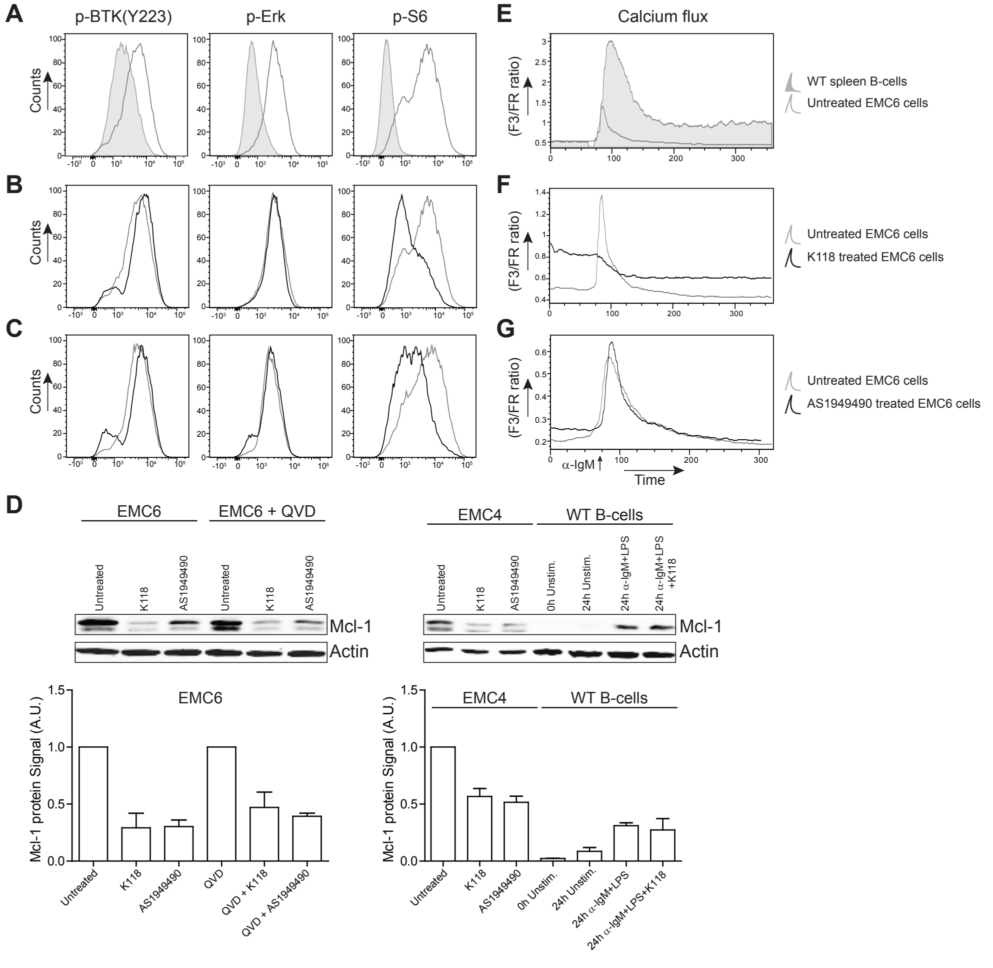

Figure 5. *Ship* inhibition decreases constitutive Akt/p-S6 signaling in EMC cells
(**A-C**) Phospho-flow analysis of the indicated phosphoproteins on (**A**) unstimulated $B220^+CD3^-$ WT splenic B-cells and EMC6 cells; (**B**) EMC cells either untreated or treated with the *pan*-Ship1/2 inhibitor K118 (5μM) for 3 hours or (**C**) the Ship2-specific inhibitor AS1949490 (15μM) for 3 hours (in case of p-Btk Y223 and p-Erk) or 24 hours (for p-S6). Each histogram show representative flow cytometric analysis from at least three independent experiments. (**D**) Western blot analysis for Mcl-1 in the indicated cells (*top*), either untreated or treated with *pan*-Ship1/2 inhibitor K118 (5μM) or the Ship2-specific inhibitor AS1949490 (15μM) for 4 hours. To exclude caspase mediated Mcl-1 breakdown, 5μM Quinoline-Val-Asp-Difluorophenoxymethyl Ketone (QVD) was added to untreated or SHIP-inhibitor treated EMC6 cells. To show constitutive Mcl-1 expression in EMC cells, MACS-purified untouched WT splenic B-cells were included as either uncultured (0h) or cultured for 24 hours (24h) in the presence (α-IgM+LPS) or absence (Unstim.) of stimulation. Bar graph depict quantification of band width normalized to actin in each condition from 2 independent experiments. (**E,F,G**) Histograms depicting basal and αIgM-stimulated calcium influx in (**E**) WT splenic B-cells and EMC6 cells either untreated or treated with (**F**) pan-Ship1/2 inhibitor K118 (5μM) for 3 hours or (**G**) Ship2 specific inhibitor AS1949490 (15μM) for 24 hours.

These findings show that EMC cell lines exhibit constitutive p-S6/Mcl-1 signaling, which is positively regulated – independently of Btk - by the activity of both Ship1 and Ship2.

In addition, Ship1-mediated inhibitory signaling supports the high level of basal calcium signaling in EMC cells and contributes to their anergic phenotype.

SHIP1/2 inhibition decreases AKT/S6 mediated survival of human CLL cells

To translate our findings in *IgH.TEμ* mice to human CLL, we first analyzed the expression of several phosphatases in leukemic cells obtained from a panel of 10 U-CLL and 10 M-CLL patients by qRT-PCR (Details of IGHV sequence are provided in **Table 1**). Expression levels in naïve mature B-cells purified from peripheral blood mono-nuclear cells (PBMCs) of healthy volunteers (n=3) were included as a reference.

Expression of 6 out of 8 selected phosphatase genes was significantly higher in CLL than in naïve resting B-cells from healthy individuals (p<0.05), suggesting a role for these genes in CLL (**Figure 6A, Supplementary Table 3A**). Hereby, *SHIP1* and *SHIP2* showed ~3-fold and ~8-fold higher expression in CLL than in control naïve B-cells, respectively. Although, *INPP5F* was downregulated in CLL from *IgH.TEμ* mice it was expressed ~10-fold higher in our panel of human CLL compared to naïve B-cells, consistent with published findings(30). Because expression levels of *INPP5F* and *PTPN22* were significantly higher in U-CLL than in M-CLL (**Supplementary Table 3B**), it is conceivable that these phosphatases have a unique role in the more aggressive U-CLL subgroup.

We investigated SHIP1/2 inhibition *in vitro* and analyzed survival of CLL cells by incubating them with K118 (2.5μM or 5μM) for 6 hours and subsequent staining with Annexin V and 7-AAD. Treatment resulted in a ~3-fold increase in the proportions of apoptotic cells (p<0.001) and a significant decrease in the proportions of alive cells (**Figure 6B**). These findings support an important role of SHIP1/2 in cellular survival of human CLL cells.

Next, we determined the effect of SHIP1/2 in the regulation of the BCR downstream signaling cascade in CLL cells. Unlike our findings in the EMC cell lines (**Figure 5**), SHIP inhibition by K118 resulted in a moderate downregulation of p-BTK(Y223) and p-ERK levels in human CLL cells (**Figure 6C**). After one hour of K118 treatment, p-S6 levels were substantially downregulated (**Figure 6C**), which was also seen upon AS1949490 treatment (data not shown). These effects were accompanied by upregulation of basal and α-IgM-induced calcium levels for K118 (**Figure 6C**).

In summary, various phosphatases are also highly expressed in human CLL and SHIP1/2 inhibition resulted in downregulation of the AKT/S6 survival pathway and upregulation of basal calcium levels. Thus, these data indicate parallel roles of SHIP1/2 in human CLL and *IgH.TEμ* murine CLL.

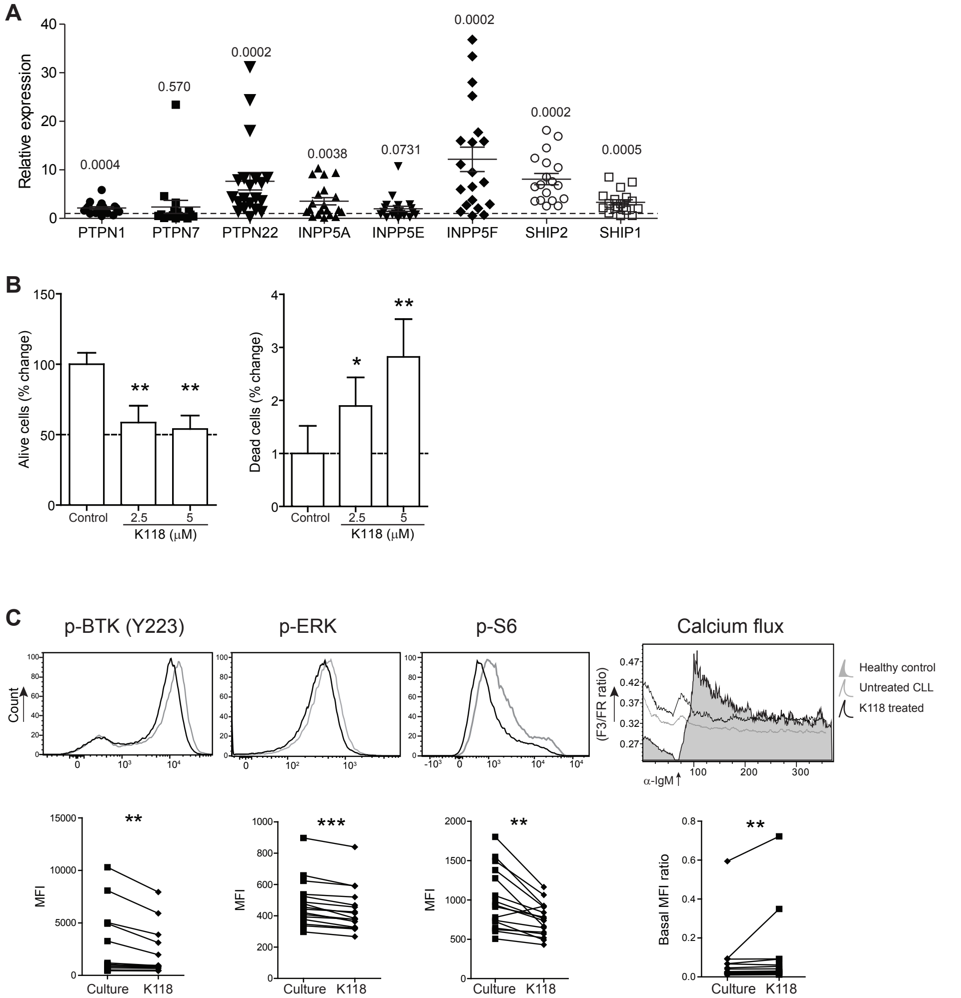

Figure 6. SHIP mediates AKT/S6 dependent survival of CLL cells from patients
(**A**) mRNA expression of the indicated phosphatase genes as measured by qRT-PCR in tumor cells isolated from CLL patients peripheral blood mononuclear cells (PBMCs) (n=20, 10 M-CLL and 10 U-CLL). mRNA expression was normalized to naïve mature B-cells (FACS-purified $CD19^+CD27^-IgD^+$) obtained from healthy donors PBMCs (dashed line, n=3). (**B**) CLL cells were treated with the indicated concentrations of pan-Ship1/2 inhibitor K118 for 6 hours to evaluate cellular survival. Bar graph represents mean ± SEM proportion of viable (Annexin V and 7-AAD negative, *left*) or dead (7-AAD positive, *right*) cells normalized to untreated control. (**C**) Histograms depicting phospho-flow analysis of indicated protein and basal and αIgM-stimulated Calcium influx analysis in CLL cells either left untreated (*grey*) or treated (*black*) with pan-Ship1/2 inhibitor K118 (2.5μM) for 1 hour. Basal and αIgM-stimulated calcium signaling in representative healthy control (*grey shaded*) is also depicted. Each line in the graph below represents a paired analysis from individual patient. (**A-C**) Statistical analysis were performed using wilcoxon signed rank test. *p<0.05, **p<0.01,***p<0.001

DISCUSSION

In this study, we provide compelling evidence that specific phosphatases contribute to malignant B-cell survival in both mouse and human CLL. First, we show that several phosphatases, including *SHIP1* and *SHIP2* are overexpressed in both mouse and human CLL B-cells. Second, in our CLL mouse model we observed that conditional deletion of Ship2 in the B-cell lineage significantly decreased CLL formation. Third, reducing SHIP1/2 activity by the small molecule inhibitor K118 decreased the *in vitro* survival of human and mouse CLL B-cells. Our data further indicate that SHIP1/2 promotes CLL survival by exerting dual effects on the BCR signaling cascade (**Figure 7**). On one hand SHIP1/2 increases Phosphatidylinositol (3,4)-bisphosphate (PI(3,4)P2) levels and thereby enhances the AKT/S6 pathway, resulting in increased Mcl-1 protein expression, which mediates survival of CLL B-cells. On the other hand, SHIP1 maintains optimal calcium levels in the presence of constitutive active kinase signaling, thereby engaging an anergic response to BCR stimulation in CLL B-cells. Because in many tumors PI3K is constitutively active, SHIP1/2 have long been thought to act as tumor suppressors by hydrolyzing Phosphatidylinositol (3,4,5)-trisphosphate (PI(3,4,5)P3). This phospholipid functions to activate downstream signaling pathways, particularly AKT and thereby driving cell growth and survival. However, subsequent studies of SHIP inhibitory molecules showed that both SHIP1 and SHIP2 can have oncogenic roles in hematologic cancers and epithelial cancers through their ability to produce PI(3,4)P2 and activate Akt(38-40). Our data provide additional evidence for a role of SHIP1/2 enzymes as proto-oncogenes that activate AKT through the PI(3,4,5)P3 hydrolysis product PI(3,4)P2 (**Figure 7**) and indicate for the first time that SHIP1/2 can be oncogenic in CLL.

Our *in vitro* studies targeting survival of cultured EMC cells with small molecule inhibitors showed that dual inhibition of Ship1/2 with K118 led to cellular apoptosis at a lower dose, compared with the Ship2-specific inhibitor AS19494940. These findings suggest that in CLL Ship1 and Ship2 have redundant roles: both are able to maintain PI(3,4)P2-mediated activation of the Akt/S6 pathway in the absence of one another, albeit sub-optimally. In agreement with this, pan-SHIP inhibition of multiple myeloma cell lines induced cellular death more efficiently than specific inhibition of SHIP1 by the small molecule 3AC(34). Interestingly, it was also shown that 3AC-resistant tumor cells expressed increased levels of SHIP2, indicating that absence of SHIP1 might lead to increased SHIP2 expression, supporting a redundant function of SHIP1 and SHIP2. Given this redundancy it is conceivable that Ship2 may compensate for the loss of Ship1 function in CLL formation in *IgH.TEμ.Ship1*$^{-/-}$ mice. By contrast, Ship1 did not compensate for Ship2-deficiency (**Figure 3B**) , revealing differential roles for Ship1 and Ship2 in CLL pathogenesis. Taken together, these findings indicate the importance of inhibiting both Ship1 and Ship2 enzymes for optimal decline of CLL cell survival.

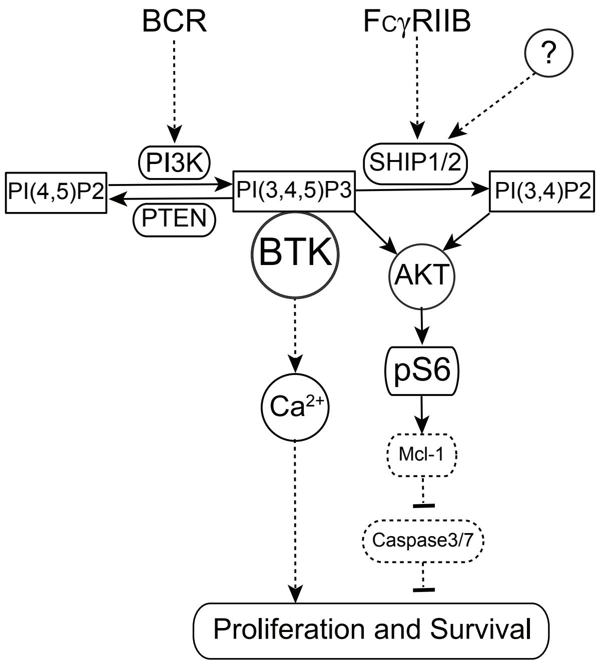

Figure 7. SHIP promotes CLL survival by exerting dual effects on the BCR signaling cascade
Schematic model for SHIP1/2-mediated survival of CLL cells. On one hand SHIP1/2 can increase PI(3,4)P2 levels and thereby enhance the AKT/S6 pathway, associated with increased Mcl-1 protein expression, which promotes survival of CLL B-cells. On the other hand, we hypothesize that SHIP1/2 can maintain optimal calcium levels in the presence of constitutive active kinase signaling, thereby engaging an anergic response to chronic BCR stimulation in CLL B-cells.

Measurement of the phosphorylation status of BCR downstream proteins indicated that apoptosis due to SHIP1/2 inhibition likely relies on downregulation of p-S6 signaling, both in the EMC cell lines and in human CLL. In parallel, inhibition of BTK and PI3K following treatment with ibrutinib and idelalisib, respectively, resulted in downregulation of AKT/S6 in mouse and human CLL cells(7, 11, 41). This dual regulation of the AKT/S6 signaling is in agreement with the proposed “Two PIP hypothesis”, whereby a malignant state results from a balance between the levels of PI(3,4,5)P3 and PI(3,4)P2 (42) (**Figure 7**). Our results indicate that SHIP1/2-mediated generation of PI(3,4)P2 contributes to CLL cell survival by promoting AKT/S6 signaling and Mcl-1 expression at the expense of PI(3,4,5)P3-dependent signals. Therefore, it would be interesting to evaluate the efficacy of combination therapy with a SHIP1/2 inhibitor and either ibrutinib or idelalisib, to achieve complete inhibition of AKT/mTORC1/S6-mediated survival pathways in CLL.

Optimal BCR signaling is essential for B-cell selection, survival and proliferation. Too weak (non-functional BCR) or too high (autoreactive BCR) signaling strength results in cell death (negative selection) of B-cells(2). Such immune checkpoints were suggested to be fully functional in some B-cell malignancies. In autoreactive B-cell acute lymphoblastic leukemia (B-ALL) clones, hyper-activation of BCR signaling has been shown to trigger clonal deletion(43). In addition, knockdown of the PTPN22 phosphatase reduced survival of α-IgM-stimulated CLL cells by abrogating AKT-mediated signaling(28). These observations indicate that malignant B-cells are susceptible to negative selection. In concordance, we observed increased basal calcium levels in SHIP1/2-inhibited EMC and human CLL cells, which are likely to contribute to enhanced cellular apoptosis.

Two independent mechanisms via which SHIP1/2 can regulate intracellular calcium flux have been reported. First, dephosphorylation of PI(3,4,5)P3 by SHIP1/2 inhibits the recruitment of BTK to the plasma membrane and consequently downregulates calcium signaling(44). Second, SHIP was reported to downregulate the levels of Inositol(1,3,4,5) tetraphosphate (IP4) at the endoplasmic reticulum, which in turn diminishes intracellular calcium levels(45, 46). Since we did not observe increased Btk or Erk phosphorylation in the EMC cell lines, increased IP4 levels due to inhibition of Ship1 might be the mechanism responsible for the observed increase in calcium flux, as reported previously in chicken DT40 B-cells(47). Although Ship2 has been reported to dephosphorylate IP4(48), we saw limited changes in basal calcium flux upon Ship2 inhibition in the EMC cell lines, indicating that calcium signaling in EMC cells is exclusively regulated by Ship1. Additional experiments are required to further elucidate the relationship between SHIP1/2, IP4 levels and calcium flux in human and mouse CLL.

Optimal BCR signaling requires a proper balance between kinase and phosphatase activity of several BCR downstream proteins(2). Current therapeutic regimens in CLL focus on blocking the positive kinase signal, which successfully decreases cell survival and proliferation(49). However, phosphatase inhibition may be a valid approach in B-cell malignancies as *in vivo* efficacy of SHIP inhibition was found in a human multiple myeloma SCID xenograft model(34). Increased understanding of the role of phosphatases in regulating the increased kinase signaling will help open new therapeutic avenues for these malignancies. To the best of our knowledge, this is the first study focusing on inhibition of SHIP2 phosphatase in CLL as a therapeutic strategy. Our data indicate that SHIP1/2 activity promotes AKT/S6 signaling and sustains calcium levels at an optimal threshold, thereby contributing to CLL survival. As such regulation is susceptible to the pharmacologic inhibition of SHIP1/2, this may provide a novel therapeutic strategy to target CLL cells. Inhibition of SHIP1/2 may be combined with ibrutinib treatment to target both BTK and AKT-mediated survival signals in CLL. Further experiments should explore whether SHIP1/2 inhibition may have clinical potential in CLL or other tumors(50), since it is currently unknown how well SHIP1/2 inhibition is tolerated in human.

REFERENCES

1. Pal Singh, S., F. Dammeijer, and R. W. Hendriks. 2018. Role of Bruton's tyrosine kinase in B cells and malignancies. *Mol Cancer* 17: 57.
2. Muschen, M. 2018. Autoimmunity checkpoints as therapeutic targets in B cell malignancies. *Nat Rev Cancer* 18: 103-116.
3. Hendriks, R. W., S. Yuvaraj, and L. P. Kil. 2014. Targeting Bruton's tyrosine kinase in B cell malignancies. *Nat Rev Cancer* 14: 219-232.
4. Byrd, J. C., B. Harrington, S. O'Brien, J. A. Jones, A. Schuh, S. Devereux, J. Chaves, W. G. Wierda, F. T. Awan, J. R. Brown, P. Hillmen, D. M. Stephens, P. Ghia, J. C. Barrientos, J. M. Pagel, J. Woyach, D. Johnson, J. Huang, X. Wang, A. Kaptein, B. J. Lannutti, T. Covey, M. Fardis, J. McGreivy, A. Hamdy, W. Rothbaum, R. Izumi, T. G. Diacovo, A. J. Johnson, and R. R. Furman. 2016. Acalabrutinib (ACP-196) in Relapsed Chronic Lymphocytic Leukemia. *N Engl J Med* 374: 323-332.
5. Byrd, J. C., R. R. Furman, S. E. Coutre, I. W. Flinn, J. A. Burger, K. A. Blum, B. Grant, J. P. Sharman, M. Coleman, W. G. Wierda, J. A. Jones, W. Zhao, N. A. Heerema, A. J. Johnson, J. Sukbuntherng, B. Y. Chang, F. Clow, E. Hedrick, J. J. Buggy, D. F. James, and S. O'Brien. 2013. Targeting BTK with ibrutinib in relapsed chronic lymphocytic leukemia. *N Engl J Med* 369: 32-42.
6. Burger, J. A., A. Tedeschi, P. M. Barr, T. Robak, C. Owen, P. Ghia, O. Bairey, P. Hillmen, N. L. Bartlett, J. Li, D. Simpson, S. Grosicki, S. Devereux, H. McCarthy, S. Coutre, H. Quach, G. Gaidano, Z. Maslyak, D. A. Stevens, A. Janssens, F. Offner, J. Mayer, M. O'Dwyer, A. Hellmann, A. Schuh, T. Siddiqi, A. Polliack, C. S. Tam, D. Suri, M. Cheng, F. Clow, L. Styles, D. F. James, T. J. Kipps, and R.-. Investigators. 2015. Ibrutinib as Initial Therapy for Patients with Chronic Lymphocytic Leukemia. *N Engl J Med* 373: 2425-2437.
7. Brown, J. R., J. C. Byrd, S. E. Coutre, D. M. Benson, I. W. Flinn, N. D. Wagner-Johnston, S. E. Spurgeon, B. S. Kahl, C. Bello, H. K. Webb, D. M. Johnson, S. Peterman, D. Li, T. M. Jahn, B. J. Lannutti, R. G. Ulrich, A. S. Yu, L. L. Miller, and R. R. Furman. 2014. Idelalisib, an inhibitor of phosphatidylinositol 3-kinase p110delta, for relapsed/refractory chronic lymphocytic leukemia. *Blood* 123: 3390-3397.
8. Furman, R. R., J. P. Sharman, S. E. Coutre, B. D. Cheson, J. M. Pagel, P. Hillmen, J. C. Barrientos, A. D. Zelenetz, T. J. Kipps, I. Flinn, P. Ghia, H. Eradat, T. Ervin, N. Lamanna, B. Coiffier, A. R. Pettitt, S. Ma, S. Stilgenbauer, P. Cramer, M. Aiello, D. M. Johnson, L. L. Miller, D. Li, T. M. Jahn, R. D. Dansey, M. Hallek, and S. M. O'Brien. 2014. Idelalisib and rituximab in relapsed chronic lymphocytic leukemia. *N Engl J Med* 370: 997-1007.
9. Manning, B. D., and A. Toker. 2017. AKT/PKB Signaling: Navigating the Network. *Cell* 169: 381-405.

10. Mockridge, C. I., K. N. Potter, I. Wheatley, L. A. Neville, G. Packham, and F. K. Stevenson. 2007. Reversible anergy of sIgM-mediated signaling in the two subsets of CLL defined by VH-gene mutational status. *Blood* 109: 4424-4431.
11. Singh, S. P., S. Y. Pillai, M. J. W. de Bruijn, R. Stadhouders, O. B. J. Corneth, H. J. van den Ham, A. Muggen, I. W. van, E. Slinger, A. Kuil, M. Spaargaren, A. P. Kater, A. W. Langerak, and R. W. Hendriks. 2017. Cell lines generated from a chronic lymphocytic leukemia mouse model exhibit constitutive Btk and Akt signaling. *Oncotarget* 8: 71981-71995.
12. Duhren-von Minden, M., R. Ubelhart, D. Schneider, T. Wossning, M. P. Bach, M. Buchner, D. Hofmann, E. Surova, M. Follo, F. Kohler, H. Wardemann, K. Zirlik, H. Veelken, and H. Jumaa. 2012. Chronic lymphocytic leukaemia is driven by antigen-independent cell-autonomous signalling. *Nature* 489: 309-312.
13. Stamatopoulos, K., A. Agathangelidis, R. Rosenquist, and P. Ghia. 2017. Antigen receptor stereotypy in chronic lymphocytic leukemia. *Leukemia* 31: 282-291.
14. ter Brugge, P. J., V. B. Ta, M. J. de Bruijn, G. Keijzers, A. Maas, D. C. van Gent, and R. W. Hendriks. 2009. A mouse model for chronic lymphocytic leukemia based on expression of the SV40 large T antigen. *Blood* 114: 119-127.
15. Yu, Y., and J. C. Alwine. 2002. Human cytomegalovirus major immediate-early proteins and simian virus 40 large T antigen can inhibit apoptosis through activation of the phosphatidylinositide 3'-OH kinase pathway and the cellular kinase Akt. *J Virol* 76: 3731-3738.
16. Laine, J., G. Kunstle, T. Obata, M. Sha, and M. Noguchi. 2000. The protooncogene TCL1 is an Akt kinase coactivator. *Mol Cell* 6: 395-407.
17. Wang, J. W., J. M. Howson, T. Ghansah, C. Desponts, J. M. Ninos, S. L. May, K. H. Nguyen, N. Toyama-Sorimachi, and W. G. Kerr. 2002. Influence of SHIP on the NK repertoire and allogeneic bone marrow transplantation. *Science* 295: 2094-2097.
18. Dubois, E., M. Jacoby, M. Blockmans, E. Pernot, S. N. Schiffmann, L. C. Foukas, J. C. Henquin, B. Vanhaesebroeck, C. Erneux, and S. Schurmans. 2012. Developmental defects and rescue from glucose intolerance of a catalytically-inactive novel Ship2 mutant mouse. *Cell Signal* 24: 1971-1980.
19. Hobeika, E., S. Thiemann, B. Storch, H. Jumaa, P. J. Nielsen, R. Pelanda, and M. Reth. 2006. Testing gene function early in the B cell lineage in mb1-cre mice. *Proc Natl Acad Sci U S A* 103: 13789-13794.
20. Gumbleton, M., R. Sudan, S. Fernandes, R. W. Engelman, C. M. Russo, J. D. Chisholm, and W. G. Kerr. 2017. Dual enhancement of T and NK cell function by pulsatile inhibition of SHIP1 improves antitumor immunity and survival. *Sci Signal* 10.
21. Suwa, A., T. Yamamoto, A. Sawada, K. Minoura, N. Hosogai, A. Tahara, T. Kurama, T. Shimokawa, and I. Aramori. 2009. Discovery and functional characterization of a novel small molecule inhibitor of the intracellular phosphatase, SHIP2. *Br J Pharmacol* 158: 879-887.
22. Ho, T. T., M. R. Warr, E. R. Adelman, O. M. Lansinger, J. Flach, E. V. Verovskaya, M. E. Figueroa, and E. Passegue. 2017. Autophagy maintains the metabolism and function of young and old stem cells. *Nature* 543: 205-210.

23. Kil, L. P., M. J. de Bruijn, M. van Nimwegen, O. B. Corneth, J. P. van Hamburg, G. M. Dingjan, F. Thaiss, G. F. Rimmelzwaan, D. Elewaut, D. Delsing, P. F. van Loo, and R. W. Hendriks. 2012. Btk levels set the threshold for B-cell activation and negative selection of autoreactive B cells in mice. *Blood* 119: 3744-3756.
24. Robinson, M. D., D. J. McCarthy, and G. K. Smyth. 2010. edgeR: a Bioconductor package for differential expression analysis of digital gene expression data. *Bioinformatics* 26: 139-140.
25. Pal Singh, S., M. J. W. de Bruijn, M. P. de Almeida, R. W. J. Meijers, L. Nitschke, A. W. Langerak, S. Y. Pillai, R. Stadhouders, and R. W. Hendriks. 2018. Identification of Distinct Unmutated Chronic Lymphocytic Leukemia Subsets in Mice Based on Their T Cell Dependency. *Front Immunol* 9: 1996.
26. Heng, T. S., M. W. Painter, and C. Immunological Genome Project. 2008. The Immunological Genome Project: networks of gene expression in immune cells. *Nat Immunol* 9: 1091-1094.
27. Hallaert, D. Y., R. Spijker, M. Jak, I. A. Derks, N. L. Alves, F. M. Wensveen, J. P. de Boer, D. de Jong, S. R. Green, M. H. van Oers, and E. Eldering. 2007. Crosstalk among Bcl-2 family members in B-CLL: seliciclib acts via the Mcl-1/Noxa axis and gradual exhaustion of Bcl-2 protection. *Cell Death Differ* 14: 1958-1967.
28. Negro, R., S. Gobessi, P. G. Longo, Y. He, Z. Y. Zhang, L. Laurenti, and D. G. Efremov. 2012. Overexpression of the autoimmunity-associated phosphatase PTPN22 promotes survival of antigen-stimulated CLL cells by selectively activating AKT. *Blood* 119: 6278-6287.
29. Schliffke, S., S. Buhs, S. Bolz, H. Gerull, L. von Wenserski, K. Riecken, B. Fehse, P. Nollau, and M. Binder. 2018. The phosphotyrosine phosphatase SHP2 promotes anergy in chronic lymphocytic leukemia. *Blood* 131: 1755-1758.
30. Johnston, H. E., M. J. Carter, M. Larrayoz, J. Clarke, S. D. Garbis, D. Oscier, J. C. Strefford, A. J. Steele, R. Walewska, and M. S. Cragg. 2018. Proteomics Profiling of CLL Versus Healthy B-cells Identifies Putative Therapeutic Targets and a Subtype-independent Signature of Spliceosome Dysregulation. *Mol Cell Proteomics* 17: 776-791.
31. Li, H., X. Wu, S. Hou, M. Malek, A. Kielkowska, E. Noh, K. J. Makondo, Q. Du, J. A. Wilkins, J. B. Johnston, S. B. Gibson, F. Lin, and A. J. Marshall. 2016. Phosphatidylinositol-3,4-Bisphosphate and Its Binding Protein Lamellipodin Regulate Chemotaxis of Malignant B Lymphocytes. *J Immunol* 196: 586-595.
32. Gabelloni, M. L., M. Borge, J. Galletti, C. Canones, P. Fernandez Calotti, R. F. Bezares, J. S. Avalos, M. Giordano, and R. Gamberale. 2008. SHIP-1 protein level and phosphorylation status differs between CLL cells segregated by ZAP-70 expression. *Br J Haematol* 140: 117-119.
33. Akerlund, J., A. Getahun, and J. C. Cambier. 2015. B cell expression of the SH2-containing inositol 5-phosphatase (SHIP-1) is required to establish anergy to high affinity, proteinacious autoantigens. *J Autoimmun* 62: 45-54.
34. Fuhler, G. M., R. Brooks, B. Toms, S. Iyer, E. A. Gengo, M. Y. Park, M. Gumbleton, D. R. Viernes, J. D. Chisholm, and W. G. Kerr. 2012. Therapeutic potential of SH2 domain-containing inositol-5'-phosphatase 1 (SHIP1) and SHIP2 inhibition in cancer. *Mol Med* 18: 65-75.
35. Leung, W. H., T. Tarasenko, Z. Biesova, H. Kole, E. R. Walsh, and S. Bolland. 2013. Aberrant antibody affinity selection in SHIP-deficient B cells. *Eur J Immunol* 43: 371-381.

36. van Attekum, M. H. A., S. Terpstra, E. Slinger, M. von Lindern, P. D. Moerland, A. Jongejan, A. P. Kater, and E. Eldering. 2017. Macrophages confer survival signals via CCR1-dependent translational MCL-1 induction in chronic lymphocytic leukemia. *Oncogene* 36: 3651-3660.
37. Liu, Q., A. J. Oliveira-Dos-Santos, S. Mariathasan, D. Bouchard, J. Jones, R. Sarao, I. Kozieradzki, P. S. Ohashi, J. M. Penninger, and D. J. Dumont. 1998. The inositol polyphosphate 5-phosphatase ship is a crucial negative regulator of B cell antigen receptor signaling. *J Exp Med* 188: 1333-1342.
38. Brooks, R., G. M. Fuhler, S. Iyer, M. J. Smith, M. Y. Park, K. H. Paraiso, R. W. Engelman, and W. G. Kerr. 2010. SHIP1 inhibition increases immunoregulatory capacity and triggers apoptosis of hematopoietic cancer cells. *J Immunol* 184: 3582-3589.
39. Fuhler, G. M., R. Brooks, B. Toms, S. Iyer, E. A. Gengo, M. Y. Park, M. Gumbleton, D. R. Viernes, J. D. Chisholm, and W. G. Kerr. 2012. Therapeutic potential of SH2 domain-containing inositol-5'-phosphatase 1 (SHIP1) and SHIP2 inhibition in cancer. *Mol Med* 18: 65-75.
40. Hoekstra, E., A. M. Das, M. Willemsen, M. Swets, P. J. Kuppen, C. J. van der Woude, M. J. Bruno, J. P. Shah, T. L. Ten Hagen, J. D. Chisholm, W. G. Kerr, M. P. Peppelenbosch, and G. M. Fuhler. 2016. Lipid phosphatase SHIP2 functions as oncogene in colorectal cancer by regulating PKB activation. *Oncotarget* 7: 73525-73540.
41. Cheng, S., J. Ma, A. Guo, P. Lu, J. P. Leonard, M. Coleman, M. Liu, J. J. Buggy, R. R. Furman, and Y. L. Wang. 2014. BTK inhibition targets in vivo CLL proliferation through its effects on B-cell receptor signaling activity. *Leukemia* 28: 649-657.
42. Kerr, W. G. 2011. Inhibitor and activator: dual functions for SHIP in immunity and cancer. *Ann N Y Acad Sci* 1217: 1-17.
43. Chen, Z., S. Shojaee, M. Buchner, H. Geng, J. W. Lee, L. Klemm, B. Titz, T. G. Graeber, E. Park, Y. X. Tan, A. Satterthwaite, E. Paietta, S. P. Hunger, C. L. Willman, A. Melnick, M. L. Loh, J. U. Jung, J. E. Coligan, S. Bolland, T. W. Mak, A. Limnander, H. Jumaa, M. Reth, A. Weiss, C. A. Lowell, and M. Muschen. 2015. Signalling thresholds and negative B-cell selection in acute lymphoblastic leukaemia. *Nature* 521: 357-361.
44. Bolland, S., R. N. Pearse, T. Kurosaki, and J. V. Ravetch. 1998. SHIP modulates immune receptor responses by regulating membrane association of Btk. *Immunity* 8: 509-516.
45. Damen, J. E., L. Liu, P. Rosten, R. K. Humphries, A. B. Jefferson, P. W. Majerus, and G. Krystal. 1996. The 145-kDa protein induced to associate with Shc by multiple cytokines is an inositol tetraphosphate and phosphatidylinositol 3,4,5-triphosphate 5-phosphatase. *Proc Natl Acad Sci U S A* 93: 1689-1693.
46. Luckhoff, A., and D. E. Clapham. 1992. Inositol 1,3,4,5-tetrakisphosphate activates an endothelial Ca(2+)-permeable channel. *Nature* 355: 356-358.
47. Okada, H., S. Bolland, A. Hashimoto, M. Kurosaki, Y. Kabuyama, M. Iino, J. V. Ravetch, and T. Kurosaki. 1998. Role of the inositol phosphatase SHIP in B cell receptor-induced Ca2+ oscillatory response. *J Immunol* 161: 5129-5132.
48. Pesesse, X., C. Moreau, A. L. Drayer, R. Woscholski, P. Parker, and C. Erneux. 1998. The SH2 domain containing inositol 5-phosphatase SHIP2 displays phosphatidylinositol 3,4,5-trisphosphate and inositol 1,3,4,5-tetrakisphosphate 5-phosphatase activity. *FEBS Lett* 437: 301-303.

49. Jerkeman, M., M. Hallek, M. Dreyling, C. Thieblemont, E. Kimby, and L. Staudt. 2017. Targeting of B-cell receptor signalling in B-cell malignancies. *J Intern Med* 282: 415-428.
50. Kerr, W. G., R. Brooks, M.-Y. Park, M. Gumbleton, S. Iyer, D. Viernes, J. Chisholm, and G. M. Fuhler. 2011. Abstract C81: Therapeutic potential of SHIP1 and SHIP2 inhibitors in cancer. *Molecular Cancer Therapeutics* 10: C81-C81.

SUPPLEMENTAL DATA

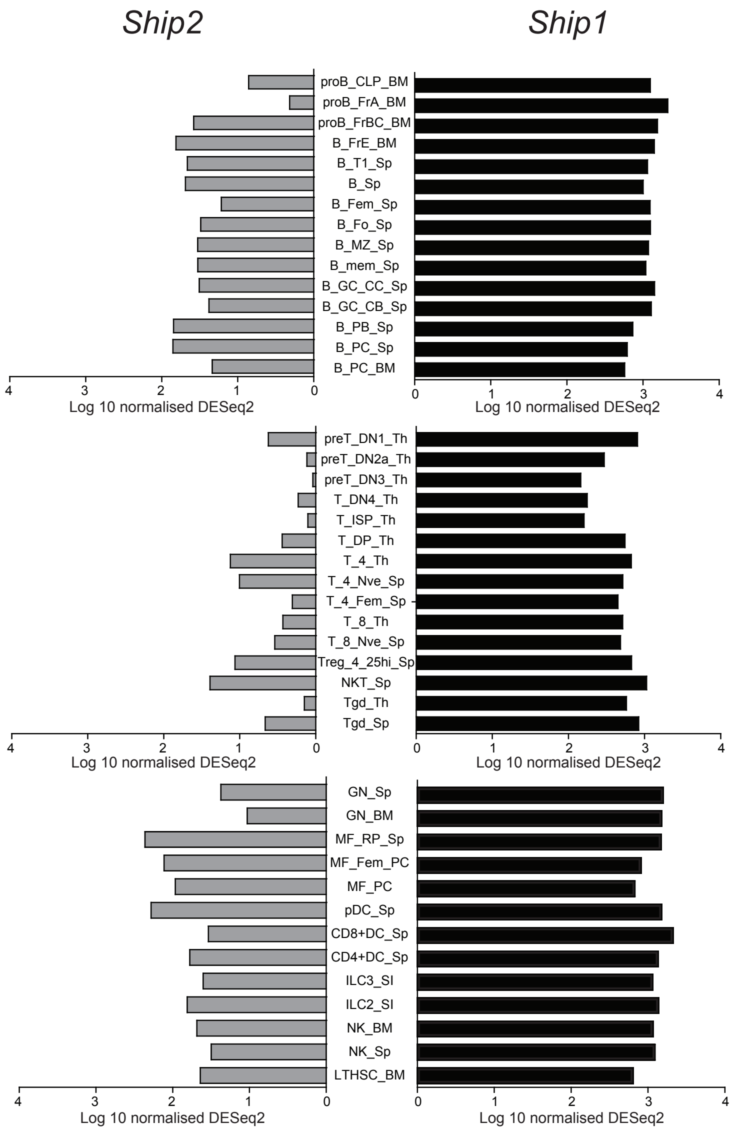

Supplementary Figure 1. Ship1 and Ship2 expression in various hematopoietic cell population
Normalized DE-seq expression values for Ship1 (black) and Ship2 (grey) in various hematopoietic cell populations from C57BL/6J mice (obtained from GSE109125). Bar graphs depict log10 transformed expression values from DE-seq software across all developmental stages in B-cells (top), T cells (middle) and innate immune cells, including dendritic cells, macrophages, granulocytes and innate lymphocytes from various organs. BM, Bone marrow; Sp, Spleen; Th, Thymus; PC, Peritoneal cavity; SI, Small intestine.

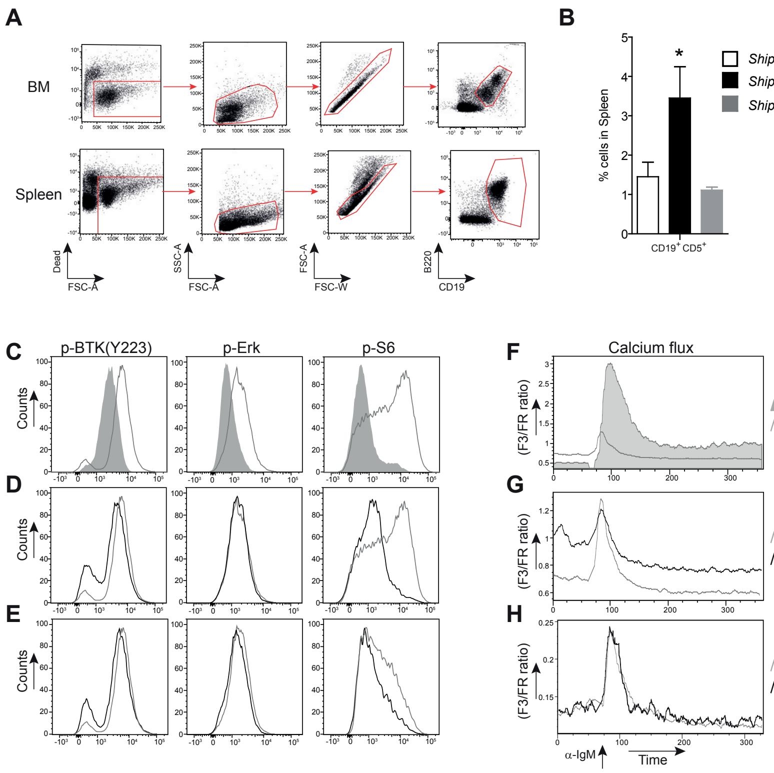

Supplementary Figure 2.
(**A,B**) Differential effects of conditional Ship1 or Ship2 deletion on B-cell development. (**A**) FACS plots depicting representative gating strategy for alive single lymphocytes from total cell suspensions obtained from bone marrow (BM) (top) and spleen (below) of mice depicted in Fig.2. In the bone marrow, Pro (B220^{low}sIgκ/λ^{-}CD2^{-}cIgμ^{-}), Pre-Pro (B220^{low}sIgκ/λ^{-}), Large-pre (B220^{low}sIgκ/λ^{-}CD2^{-}cIgμ^{+}), small-pre (B220^{low}sIgκ/λ^{-}CD2^{+}cIgμ^{+}), immature (B220^{+}CD19^{+}IgM^{high}IgD$^{low/-}$) and recirculating (B220^{+}CD19^{+}IgM$^{low/+}$IgD^{high}) B-cells were gated from alive lymphocytes. In spleen, follicular (CD19^{+}B220^{+}CD21^{-}CD23^{+}), marginal zone (MZ) (CD19^{+}B220^{+}CD21^{high}CD23^{-}), transitional (CD19^{+}B220^{+}CD21^{-}CD23^{-}), B-1 (CD19^{+}B220^{int}CD5^{+}), germinal center (GC) (CD19^{+}B220^{+}IgD^{-}CD95^{+}), memory (CD19^{+}B220^{+}CD80^{+}PDL2^{+}) B-cells and plasma cells (CD19$^{+/-}$IgM^{+}CD138^{+}) were gated from alive lymphocytes. (**B**) Quantification of proportion of B-1 cells (CD19^{+}B220^{int}CD5^{+}) of total B-cells (CD19^{+}CD3^{-}) in spleens of indicated mouse groups. *$p < 0.05$, (Mann-Whitney U test). (**C-H**) Ship inhibition decreases constitutive Akt/p-S6 signaling in EMC cells. (**C-E**) Phospho-flow analysis of the indicated phosphoproteins on (**C**) unstimulated B220^{+}CD3^{-} WT splenic B-cells and EMC4 cells; EMC4 cells either untreated or treated with (**D**) the pan-Ship1/2 inhibitor K118 (5 μM) for 3 hours or (**E**) the Ship2-specific inhibitor AS1949490 (15μM) for 3 hours (in case of p-Btk Y223 and p-Erk) or 24 hours (for p-S6). (**F,G,H**) Histograms depicting basal and αIgM-stimulated Ca^{2+}-influx between (**F**) WT splenic B-cells and EMC4 cells, either (**F**) untreated or treated with (**G**) pan-Ship1/2 inhibitor K118 (5μM) for 3 hours or (H) Ship2 specific inhibitor AS1949490 (15μM) for 24 hours.

Suppl. Table 1: Expression values (RPKM) for 96 differentially expressed phosphatase genes in IgH.TEμ CLL, unstimulated and α-IgM stimulated naïve splenic B cells from wild type (C57/Bl6) mice.

Genes	Unstimulated naïve splenic B cells				anti-IgM stimulated naïve splenic B cells				IgHTEμ CLL						FDR wt
	Un-B1	Un-B2	Un-B3	Un-B4	aIgM1	aIgM2	aIgM3	aIgM4	E-06	EA-02	EA-04	ET-06	E-15	E-29	
Cdkn3	0.97	0.48	0.59	0.77	0.37	0.28	0.31	0.24	11.74	3.09	5.54	11.00	15.38	11.71	0.015644172
Cdc25c	1.39	1.76	1.67	1.55	3.37	2.93	3.73	2.89	12.71	13.99	14.45	16.68	22.31	14.30	0.002760736
Inppl1	4.71	4.51	3.91	4.96	2.12	2.68	2.70	2.42	40.14	17.04	23.64	13.11	29.15	37.55	0.015030675
Ptprn2	5.76	5.82	5.21	5.70	14.24	14.94	15.81	15.46	25.20	16.47	24.72	26.40	42.05	32.32	0.010122699
Cdc25a	2.78	2.57	1.92	2.23	6.03	5.01	5.03	4.40	7.76	5.01	9.73	8.23	13.33	10.68	0.011656442
Lhpp	2.22	2.61	2.21	1.94	2.35	2.65	2.83	2.86	7.59	5.81	14.04	4.60	7.08	8.43	0.017791411
Timm50	20.81	19.75	19.85	23.90	91.39	80.20	86.31	82.66	71.39	43.59	74.65	60.42	105.89	76.62	0.010736196
Acp1	8.61	8.53	6.83	8.34	17.78	16.45	16.95	17.53	23.49	22.04	26.59	36.86	27.57	29.00	0.003374233
Ppm1e	1.90	2.32	2.36	2.49	2.97	3.41	3.00	3.22	9.23	4.19	7.51	3.03	8.52	8.02	0.017484663
Pgam1	38.25	37.83	33.91	37.28	178.39	166.05	173.46	155.61	118.35	51.66	185.38	106.44	83.60	75.98	0.01993865
Dusp19	33.43	31.68	27.54	32.54	77.77	73.26	83.09	73.21	57.99	49.47	95.53	83.71	114.14	90.84	0.014110429
Nanp	4.53	5.70	3.01	4.34	7.68	7.34	7.82	7.84	9.14	9.00	12.67	11.24	14.10	10.42	0.002147239
Ptpn7	19.04	20.05	16.15	19.84	12.07	13.46	14.18	12.43	63.97	39.15	55.24	32.00	48.99	43.34	0.010429448
Ptpn1	51.47	51.28	40.48	47.87	39.90	42.46	39.84	40.08	97.43	156.40	104.36	172.12	88.53	84.82	0.016564417
Pfkfb1	2.94	3.03	2.51	3.79	3.03	3.56	2.75	3.25	5.80	10.45	4.08	9.46	4.11	11.16	0.020552147
Ilkap	23.35	26.45	19.28	25.14	22.70	24.43	23.09	23.44	50.89	57.89	67.81	36.55	47.98	84.28	0.014417178
Impa2	5.75	8.04	5.28	6.44	6.05	5.34	6.02	5.61	12.62	11.42	18.71	17.78	18.83	13.92	0.006748466
Ptpdc1	3.14	4.06	2.60	4.06	1.69	2.42	1.87	2.14	9.42	7.97	1.74	13.03	7.60	10.43	0.021779141
Ptpn14	2.65	3.61	2.15	2.81	0.39	0.49	0.43	0.36	9.96	5.57	1.51	3.49	8.99	10.45	0.023312883
Cdc25b	32.66	30.28	22.64	36.62	3.90	4.44	4.40	4.26	57.10	49.63	40.56	91.21	119.65	62.96	0.021472393
Dusp28	3.30	3.67	3.03	3.39	4.26	4.15	5.12	3.64	5.74	8.37	3.36	6.07	11.36	10.91	0.020858896
Sgpp1	7.32	7.33	5.41	6.37	3.40	3.25	3.80	3.02	10.92	9.58	6.61	15.89	23.55	22.10	0.022699387
Ptprv	1.33	1.88	1.23	1.44	0.42	0.77	0.54	0.60	4.47	2.92	2.76	1.71	3.25	3.45	0.016257669
Minpp1	7.79	7.93	6.71	7.60	13.49	12.32	12.77	11.96	13.61	16.65	18.73	13.03	18.35	12.25	0.00797546
Ppp1cc	87.78	91.58	72.32	91.53	113.72	114.42	119.79	115.00	207.65	158.11	179.75	158.43	185.82	145.10	0.000920245
Ctdspl2	3.04	2.80	2.32	2.89	2.76	2.44	2.50	2.83	5.84	6.05	3.93	4.52	6.59	5.85	0.007055215
Ptprd	0.71	0.80	0.66	0.76	1.32	1.20	1.34	1.20	1.19	1.01	1.49	1.62	1.75	1.36	0.009815951
Ppp1ca	191.58	188.63	166.86	188.99	300.89	297.17	315.21	303.62	382.26	243.82	382.98	309.01	413.52	332.06	0.008588957
Ppp2ca	70.26	58.90	59.79	64.47	106.13	101.24	108.76	107.96	130.95	100.64	130.27	101.86	134.87	102.98	0.004601227
Mtmr14	26.51	28.48	19.16	28.17	21.26	19.61	17.99	20.81	53.31	41.79	54.99	33.22	39.98	57.83	0.01196319
Ptpn11	15.75	16.28	12.83	16.22	24.03	24.42	22.43	22.58	35.12	26.65	30.30	23.33	20.98	29.33	0.009202454
Ptpmt1	5.96	6.63	4.55	5.15	10.99	11.39	11.75	10.33	9.97	9.18	13.41	8.88	8.06	10.60	0.009509202
Ptpn22	57.23	90.21	41.59	39.94	23.89	24.98	25.50	31.15	93.33	189.84	109.69	94.29	29.80	82.99	0.025153374
Pgam5	15.86	16.60	13.90	16.38	27.84	26.26	27.66	25.44	31.54	20.82	26.38	22.86	29.93	25.25	0.008282209
Psph	10.05	11.30	8.50	9.76	17.93	17.08	17.21	15.99	20.13	11.82	19.05	13.12	20.87	11.29	0.020245399
Sacm1l	14.55	14.42	11.25	14.03	18.24	18.10	17.69	18.66	24.41	18.80	28.56	16.94	17.11	24.31	0.016871166
Dusp10	20.12	15.49	18.76	17.32	2.44	2.10	2.65	2.17	9.47	35.65	25.03	21.59	22.63	48.78	0.025460123
Ppm1d	13.19	12.69	9.13	12.17	9.00	8.72	9.34	9.29	16.92	15.76	15.14	17.25	17.57	22.50	0.014723926
Ptpn18	35.30	41.05	30.22	36.83	22.62	24.02	27.01	21.13	50.92	72.59	46.77	44.55	41.65	62.76	0.019325153
Impa1	6.94	7.20	5.71	7.09	10.99	9.86	10.54	10.36	13.38	6.27	11.07	10.82	9.35	8.81	0.021165644
Ctdsp2	23.67	26.40	18.15	24.28	12.80	14.35	13.79	15.28	24.52	49.30	20.99	33.09	38.05	37.37	0.023619632
Dusp11	43.60	43.98	31.49	43.51	27.33	29.16	27.41	30.00	27.31	26.73	19.74	25.61	36.34	28.75	0.018711656
Inpp5k	22.99	23.65	17.16	24.46	13.03	13.86	12.52	14.42	13.95	18.71	13.96	14.00	14.27	14.25	0.019018405
Inpp5e	9.18	9.93	7.24	9.85	8.24	7.91	7.60	8.51	6.61	4.96	5.49	6.55	6.34	5.39	0.01809816
Phospho2	7.27	6.93	6.23	7.41	4.31	4.12	4.50	4.19	5.29	5.30	3.68	4.16	3.73	4.47	0.003680982
Mtmr3	18.23	17.65	14.18	18.47	8.83	9.29	8.63	9.90	12.05	13.55	9.52	10.30	9.46	10.42	0.012576687
Ssh1	18.18	17.73	13.40	17.99	3.59	3.72	4.13	4.14	10.43	19.76	6.45	8.68	7.24	10.48	0.02208589
Ptpn23	15.33	16.12	12.60	16.55	15.46	15.76	13.90	16.03	8.80	10.87	8.42	8.75	9.32	10.43	0.013803681
Lpin2	6.91	6.41	5.16	6.07	3.21	3.29	2.77	3.31	2.75	3.58	4.75	2.86	2.97	5.26	0.012883436
Ublcp1	18.06	19.50	14.93	20.49	6.79	8.17	7.93	8.53	13.16	9.45	8.80	8.93	13.40	7.75	0.011349693
Synj1	5.33	4.68	4.16	5.52	4.40	4.60	4.09	4.91	2.52	3.53	1.89	3.06	2.19	3.22	0.008895706
Acp5	105.22	123.79	87.21	108.21	6.71	5.53	5.25	7.07	36.38	70.91	65.45	95.01	41.02	39.14	0.015337423
Acp2	9.89	9.75	7.26	9.87	3.60	3.78	3.66	4.26	4.54	5.69	3.61	6.93	2.99	5.64	0.011042945
Dusp16	5.41	5.23	4.85	5.11	2.58	2.84	2.60	2.66	2.51	5.17	1.62	1.26	3.29	2.23	0.017177914
Synj2	1.15	1.01	0.82	1.26	2.11	2.34	2.05	2.36	0.27	0.77	0.66	0.83	0.28	0.35	0.01595092
Dusp23	1.19	1.29	0.99	1.08	1.46	2.09	1.16	1.62	0.52	0.19	0.43	0.72	0.68	0.77	0.007361963

Pfkfb4	11.54	12.34	8.55	13.02	4.67	5.80	4.64	5.88	5.97	7.98	5.86	5.03	3.37	4.58	0.013496933
Pten	20.50	20.23	16.71	20.07	9.29	9.38	9.51	9.91	5.27	15.01	8.82	7.13	10.18	7.75	0.005214724
Inpp5f	10.59	10.79	8.85	10.23	6.80	7.39	7.04	7.97	3.58	1.95	2.34	4.05	6.95	8.78	0.013190184
Dusp5	28.47	26.22	24.78	22.58	12.35	11.81	12.40	12.81	12.88	6.34	16.28	6.99	14.99	12.09	0.002453988
Phospho1	10.96	11.47	8.87	11.49	2.92	3.13	2.95	3.40	3.71	5.20	3.64	5.14	4.94	6.28	0.005828221
Styxl1	1.15	1.54	1.57	1.06	0.77	1.17	0.83	0.75	0.64	0.66	0.65	0.57	0.44	0.61	0.018404908
Dusp2	121.75	140.16	116.93	131.92	201.86	199.14	213.75	195.20	90.52	29.98	65.37	41.26	62.49	50.08	0.001840491
Ptp4a3	111.91	120.88	96.78	130.30	50.05	51.54	54.77	52.73	46.31	44.52	32.26	39.22	85.49	38.64	0.004294479
Ptprc	197.11	172.04	141.35	179.65	73.93	78.19	75.74	81.22	62.36	69.15	46.96	59.17	88.24	97.89	0.006441718
Dusp7	11.79	12.71	9.85	10.72	8.67	9.42	9.01	8.24	4.46	6.74	3.51	4.63	2.96	3.95	0.001226994
Ptp4a1	40.58	36.93	30.07	36.54	17.40	16.15	16.59	16.96	9.74	9.34	10.41	8.97	16.15	28.69	0.006134969
Ppp3cc	95.27	91.13	70.17	93.90	28.93	34.27	33.09	35.28	28.55	41.59	11.99	34.56	20.65	44.06	0.003067485
Ptpre	6.42	6.20	4.67	6.86	1.86	1.99	1.64	2.09	0.32	3.48	1.54	2.69	0.58	1.88	0.005521472
Acp6	13.60	12.96	10.32	13.26	4.61	5.76	5.21	5.48	1.18	2.06	6.13	0.58	7.88	1.60	0.00398773
Lpin1	2.86	2.81	2.48	2.77	1.76	1.96	1.71	2.02	0.09	0.84	0.38	0.54	0.37	0.93	0.000306748
Ptprm	1.22	1.03	1.04	1.15	0.18	0.16	0.18	0.18	0.14	0.22	0.17	0.22	0.16	0.27	0.000613497
Dusp18	1.64	1.78	1.31	2.35	0.03	0.04	0.08	0.03	0.14	0.75	0.21	0.12	0.24	0.07	0.012269939
Tmem55a	4.00	4.87	4.15	5.13	3.90	4.55	4.72	4.19	0.32	0.54	0.67	0.34	1.14	0.53	0.001533742
Dusp4	19.50	17.86	13.59	19.97	56.52	55.38	58.60	56.18	0.38	0.66	2.99	2.08	0.58	2.54	0.007668712
Dusp1	279.29	279.98	220.30	268.74	4.08	3.65	5.77	6.83	7.56	5.66	9.70	15.79	16.05	26.19	0.004907975
Pgam2	14.13	17.37	12.17	14.49	1.85	2.08	2.22	2.34	4.68	24.50	10.48	7.35	9.96	10.81	0.026380368
Ppm1l	4.60	5.51	4.08	4.88	2.03	2.35	1.86	2.07	4.92	6.19	5.66	4.11	4.36	5.68	0.026993865
Inpp5a	17.65	18.23	21.96	19.03	8.17	9.47	8.62	8.34	19.55	27.13	18.68	18.10	13.67	21.90	0.02791411
Pfkfb2	3.33	3.63	2.62	3.91	1.59	1.63	1.47	1.60	3.17	3.85	2.49	2.67	3.87	3.87	0.028834356
Ppm1m	37.35	45.34	34.07	42.73	21.71	25.71	23.66	21.35	34.54	29.25	37.95	47.43	36.52	46.77	0.028220859
Ssh3	12.58	13.00	9.20	11.77	6.26	7.46	6.54	7.22	12.75	10.19	9.85	9.12	15.11	11.92	0.029141104
Ctdsp1	48.92	48.89	40.15	52.64	33.45	35.65	37.12	36.47	67.69	41.00	45.66	62.26	65.30	65.35	0.024846626
Mtmr2	15.43	15.64	11.92	16.14	11.93	12.13	10.88	12.27	14.31	23.79	14.48	14.09	23.06	18.39	0.025766871
Cdc14a	5.72	5.31	4.77	5.64	3.33	3.13	2.95	3.52	3.96	3.87	5.11	4.66	5.09	5.20	0.02392638
Fig4	18.26	18.24	14.33	18.11	14.13	14.43	14.75	14.10	18.85	15.73	21.81	22.21	20.39	23.63	0.024539877
Tmem55b	57.21	56.95	44.79	60.47	61.50	61.85	61.89	61.49	38.15	37.45	49.32	46.95	41.35	30.40	0.019631902
G6pc3	21.28	22.18	17.50	24.41	49.47	52.18	48.66	53.27	27.63	22.76	22.26	25.16	11.66	18.77	0.029447853
Pdp2	1.97	1.82	0.97	1.87	3.91	3.87	3.34	4.08	1.42	1.94	1.87	1.64	1.41	1.31	0.028527607
Phlpp1	5.48	5.07	6.49	4.62	8.10	8.63	7.89	7.78	3.06	6.08	1.62	4.23	3.40	6.41	0.02607362
Pfkfb3	10.18	11.51	8.61	10.37	18.25	19.01	18.54	16.51	9.08	14.49	11.06	4.55	6.16	10.34	0.027607362
Dusp12	8.53	9.73	8.14	10.73	20.19	21.94	18.22	20.51	13.57	8.87	11.59	10.55	13.66	14.43	0.022392638
Mtmr4	18.69	19.05	14.20	17.68	26.41	26.66	23.47	25.71	18.37	9.30	16.24	15.44	15.44	18.70	0.026687117
Pmm2	28.24	26.21	20.44	28.60	32.16	31.89	29.38	31.54	21.11	17.22	23.03	24.65	15.47	16.01	0.023006135
Ppp5c	59.75	65.86	47.32	61.78	76.95	73.68	69.99	69.95	34.85	39.88	52.96	46.38	59.97	46.35	0.024233129
Bpnt1	12.55	9.79	6.80	8.20	13.20	11.85	11.25	12.34	5.78	7.78	6.93	6.38	13.02	8.73	0.027300613

Supplementary Table 2: Expression values (Mean ± SEM) of indicated genes, as measured by qRT-PCR, in CLL cells from IgHTEμ mice (relative expression to wild type splenic B cells (n=4))

Gene	IgHTEμ CLL		Wilcoxon Signed Rank Test	Primer sequence		Universal Probe library number
	Mean	SEM		Forward (5' to 3')	Reverse (5' to 3')	
Inpp5a	17.73	2.63	<0.0001	GCATCCTCATGTCCCTGTCT	ACCTTCTCCTCGCTCTCTGA	# 17 (cat. no. 04686900001)
Inpp5d/ Ship1	8.85	1.54	<0.0001	TCATCTTCCACAGCCAACC	GCTTCGTCAGCAGCAGGT	# 1 (cat. no. 04684974001)
Inpp5e	6.14	0.74	<0.0001	GCACCAAGGACATCAGAAGC	TTCGGTCTGGGAAGTACCTG	#68 (cat. no. 04688678001)
Inpp5f	4.75	0.56	<0.0001	CGAGTTAATTGCATGGACTGC	GGGGCATCACACCTAGTTTTT	# 64 (cat. no. 04688635001)
Inppl1/Ship2	7.11	1.46	<0.0001	GAGCCTGAAAAGCCACCAC	TCCTTCCTGCTCAGATGTCC	# 52 (cat. no. 04688490001)
Ptpn1	142.68	34.31	<0.0001	GCCAGCTTGATAAAAATGGAAG	GCCCACATGTGTTTGGTAAA	# 82 (cat.no. 04689054001)
Ptpn7	52.35	11.36	<0.0001	TCGTGTGCCAACTTCGACTA	AAGTGTGGTGCAGAAACTGGT	# 82 (cat.no. 04689054001)
Ptpn11	10.91	2.73	<0.0001	TTTAGCAAGGCCCAGTAAGAGT	TGATGTGGGTAACAGCTCCA	#80 (cat. no. 04689038001)
Ptpn14	221.97	32.91	<0.0001	CTCCACCCCCAATTAGACG	GGCAAGATATACGGCTGCTG	# 1 (cat. no. 04684974001)
Ptpn18	19.16	3.68	<0.0001	GGACCCCTCTGTGTCCACT	TAGTCAACAGCGCACAGGAC	# 71 (cat. no. 04688945001)
Ptpn22	75.46	11.65	<0.0001	CAGATCGACATCAGGATGGTT	GAAGTTTGCACGGCTTGG	# 10 (cat. no. 04685091001)

Supplementary Table 3A: Expression values (Mean ± SEM) of indicated genes as measured by qRT-PCR in tumor cells from CLL patients (n=20) patients, relative to naïve circulating B cells from healthy volunteers (n=3).

Gene	Human CLL		Wilcoxon Signed Rank Test	Primer sequence		Universal Probe library number
	Mean	SEM		Forward (5' to 3')	Reverse (5' to 3')	
INPP5A	3.54	0.76	0.0038	CCAGGGTGAGCAGTACATGA	GACAACCTTCTCCTCGCTCTC	#64 (cat. no. 04688635001)
INPP5D/ SHIP1	3.32	0.532	0.0002	ACTTCCAGGGGGAGATCAAG	ATTCATCACGCTCCGTCTTC	#7 (cat. no. 04685059001)
INPP5E	1.99	0.53	0.0731	GAACATGCAGGGCCAGAA	GACATACAGGTCCTGGGCATA	#64 (cat. no. 04688635001)
INPP5F	12.17	2.50	0.0002	CTGGGACAGCTGCTCTGAA	TCCATCTTTCATAACTCCTGCTAAC	#2 (cat. no. 04684982001)
INPPL1/SHIP2	8.10	1.153	0.0005	GAACCGTATCAGCCATGTCA	TGAAGGAGACGCCCACAG	#47 (cat. no. 04688074001)
PTPN1	2.14	0.26	0.0004	CGGTCACTTTTGGGAGATG	GCCAGTATTGTGCGCATTT	#32 (cat. no. 04687655001)
PTPN7	2.37	1.35	0.57	GGAGGACGGAGATTACATCAAT	CCCTGGGTGGCAATGTAG	#12 (cat. no. 04685113001)
PTPN22	7.65	1.80	0.0002	ATGGCATGCATGGAGTATGA	TCCAGCTGCATCTCTCCTG	#26 (cat. no. 04687574001)

Supplementary Table 3B: Expression values (Mean ± SEM) of indicated genes as measured by qRT-PCR in tumor cells from U-CLL (n=10) and M-CLL (n=10) patients, relative to naïve circulating B cells from healthy volunteers (n=3).

Gene	Unmutated CLL		Mutated CLL		Mann Whitney U-Test
	Mean	SEM	Mean	SEM	
INPP5A	4.20	1.19	2.87	0.97	0.5452
INPP5D/ SHIP1	7.92	1.26	8.27	2.01	0.9654
INPP5E	2.67	0.93	1.31	0.45	0.0753
INPP5F	18.78	3.65	5.55	1.84	0.0039
INPPL1	3.32	0.77	3.33	0.77	0.7304
PTPN1	2.61	0.45	1.67	0.21	0.0587
PTPN7	11.34	8.17	1.10	0.53	0.6058
PTPN22	10.01	2.72	5.28	2.25	0.0355

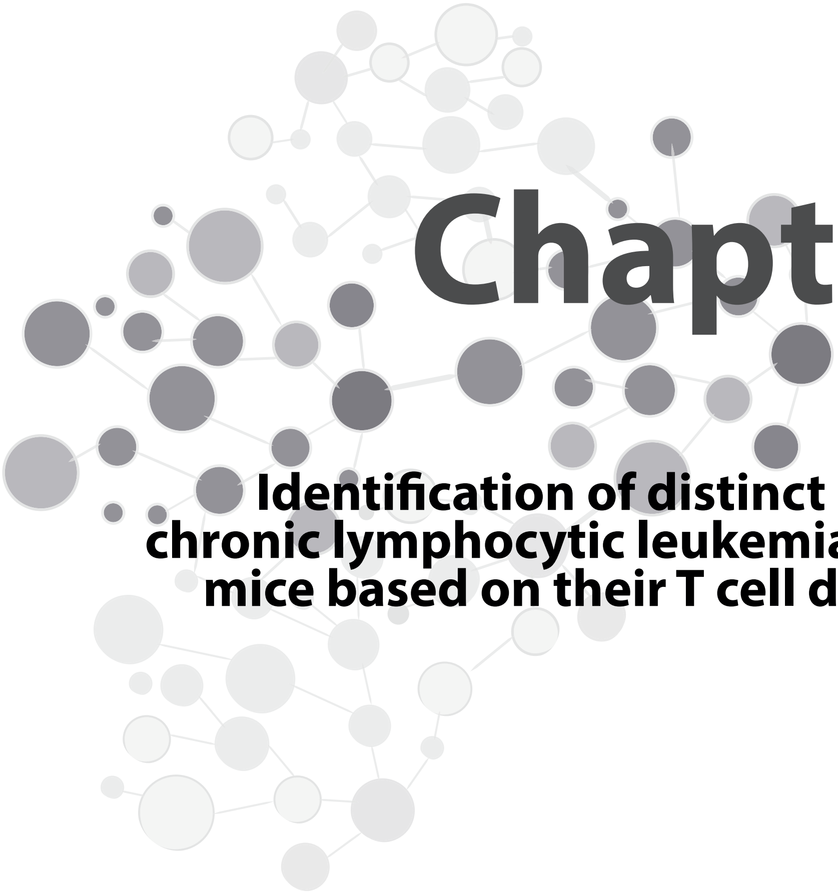

Chapter 6

Identification of distinct unmutated chronic lymphocytic leukemia subsets in mice based on their T cell dependency

Simar P. Singh[1,2,3], Marjolein J.W. de Bruijn[1], Mariana P. de Almeida[1],
Ruud W.J. Meijers[2], Lars Nitschke[4], Anton W. Langerak[2],
Saravanan Y. Pillai[1,5], Ralph Stadhouders[1,6] and Rudi W. Hendriks[1]

[1]Department of Pulmonary Medicine,
[2]Department of Immunology,
[3]Post-graduate School Molecular Medicine, Erasmus MC, Rotterdam, The Netherlands;
[4]Department of Genetics, University of Erlangen, Germany;
[5]Current address: EpiExpressions, Rotterdam, The Netherlands;
[6]Department of Cell Biology, Erasmus MC Rotterdam, The Netherlands.

Frontiers in Immunology, Volume 9, Article 1996, 2018

ABSTRACT

Chronic lymphocytic leukemia (CLL) can be divided into prognostically distinct subsets with stereotyped or non-stereotyped, mutated or unmutated B cell receptors (BCRs). Individual subsets vary in antigen specificity and origin, but the impact of antigenic pressure on the CLL BCR repertoire remains unknown. Here, we employed IgH.TEμ mice that spontaneously develop CLL, expressing mostly unmutated BCRs of which ~35% harbor V_H11-2/Vκ14-126 and recognize phosphatidylcholine. Proportions of V_H11/Vκ14-expressing CLL were increased in the absence of functional germinal centers in IgH.TEμ mice deficient for CD40L or activation-induced cytidine deaminase. Conversely, in vivo T cell-dependent immunization decreased the proportions of V_H11/Vκ14-expressing CLL. Furthermore, CLL onset was accelerated by enhanced BCR signaling in Siglec-G$^{-/-}$ mice or in mice expressing constitutively active Bruton's tyrosine kinase. Transcriptional profiling revealed that V_H11 and non-V_H11 CLL differed in the upregulation of specific pathways implicated in cell signaling and metabolism. Interestingly, principal component analyses using the 148 differentially expressed genes revealed that V_H11 and non-V_H11 CLL clustered with BCR-stimulated and anti-CD40-stimulated B cells, respectively. We identified an expression signature consisting of 13 genes that were differentially expressed in a larger panel of T cell-dependent non-V_H11 CLL compared with T cell-independent V_H11/Vκ14 or mutated IgH.TEμ CLL. Parallel differences in the expression of these 13 signature genes were observed between heterogeneous and stereotypic human unmutated CLL. Our findings provide evidence for two distinct unmutated CLL subsets with a specific transcriptional signature: one is T cell-independent and B-1 cell-derived while the other arises upon antigen stimulation in the context of T-cell help.

Keywords: B cell receptors, T cell help, BCR signaling, Bruton's tyrosine kinase, chronic lymphocytic leukemia

INTRODUCTION

Chronic lymphocytic leukemia (CLL) is the most common adult leukemia characterized by an accumulation of monoclonal CD5$^+$ mature B cells with low surface immunoglobulin (Ig) expression in peripheral blood[1].

CLL is a clinically and molecularly heterogeneous disease whereby progression is influenced by many factors. One-third of patients can be classified as stereotypic CLL, in which BCRs are highly similar between patients[2]. The remaining two-third of CLL either lack or have limited similarity with stereotyped CLL BCRs. This classification provides strong molecular evidence for antigen selection in CLL pathogenesis[2]. CLL can also be grouped based on IGHV mutational status[3,4]. Significant (>2%) somatic hypermutation (SHM) is observed in patients with mutated CLL (M-CLL), who often develop indolent disease. SHM is absent in unmutated CLL (U-CLL) which evolves rapidly and has a less favorable prognosis[4]. The SHM status provides a robust and stable prognostic marker, independently of clinical stage and other markers[5]. Furthermore, it reinforces the role of selection by self-antigens or exogenous antigens in CLL pathogenesis. CLL cells show constitutive activation of several BCR downstream kinases, increasing leukemic cell survival *in vitro*[6]. In support, small molecule inhibitors of BCR–associated kinases including Bruton's tyrosine kinase (Btk) have shown impressive clinical anti-tumor activity[7,8].

Few external antigens that potentially drive CLL *in vivo* have been identified; CLL cells were shown to display antigen-independent, cell-autonomous signaling mediated by auto-recognition[9]. Several reports have shown that U-CLL express polyreactive BCRs that bind with low affinity to various auto-antigens generated during apoptosis or oxidation[10, 11]. In this respect, they resemble natural antibodies secreted by B-1 cells in mice. B-1 cells are a self-renewing CD5$^+$ B cell population with remarkably restricted IGHV gene usage and low or no SHM[12]. B-1 cells are thought to be generated based on positive selection, by virtue of their receptor specificities to self-antigens, independent of T-cell help[12]. Adding to this complexity, the antigen specificity of U-CLL includes both T cell-independent (TI) and T cell-dependent (TD) antigens[11,13,14]. On the other hand, M-CLL express BCRs that are believed to bind with high-affinity to auto-antigens and show activation of pathways associated with anergic B cells[15,16].

Differences regarding BCR reactivity have fueled several theories concerning the cellular origins of CLL. SHM status and transcription profiling indicated that U-CLL and M-CLL are derived from CD5$^+$CD27$^-$ pre- and CD5$^+$CD27$^+$ post-germinal center (GC) B cells, respectively[17,18]. Extrafollicular or marginal zone (MZ) B cell responses, involving the activation of low-affinity B cells to TI antigens with low SHM, could also be relevant for CLL[19]. Direct *in vivo* evidence for the TD or TI origin of CLL subgroups is still missing, mainly due to a lack of mouse models that spontaneously develop both stereotypic and non-stereotypic, mutated and unmutated CLL[20]. In the widely studied *Eμ-TCL1* model, CLL predominantly express unmutated stereotyped *IghV11* or *IghV12* BCRs[21]. The *IgH.TEμ* CLL mouse model that we previously generated is based on sporadic expression of the SV40 large T oncogene in mature B cells[22]. This was achieved by SV40 large T insertion in opposite transcriptional orientation into the *IgH* locus D_H-J_H region. In contrast to the *Eμ-TCL1* model , *IgH.TEμ* mice mainly develop unmutated CLL with a diverse *IghV* repertoire, and at low frequencies mutated CLL[20, 22]. Because of their mixed sv129xC57BL/6 background, IgMa/IgMb allotype expression can be used to define CLL incidence by the accumulation of >70% $IgMb^+$ B-cells[22, 23]. Aging *IgH.TEμ* mice show accumulation of monoclonal CLL-like $CD5^+CD43^+IgM^+IgD^{low}CD19^+$ B cells around nine months of age. Although constitutive Btk signaling is not apparent in primary *IgH.TEμ* CLL cells, CLL development is dependent on Btk. Btk-mediated signaling enhanced leukemogenesis and Btk-deficiency led to a complete rescue from the disease[23]. Moreover, primary CLL cells from *IgH.TEμ* mice or stable cell lines generated from these mice had detectable expression of p-Akt and substantial levels of p-S6, both of which function downstream of the BCR[23,24].

To address the impact of antigenic pressure on BCR selection in CLL, we analyzed the effects of defective T cell help and GC formation, as well as robust antigenic stimulation on CLL development in *IgH.TEμ* mice. We show that there are two distinct unmutated CLL subsets present in the *IgH.TEμ* mouse model. The V_H11-2/Vk14-126-expressing CLL developed independently of T-cell help. Conversely, non-V_H11 CLL was TD and displayed a specific transcriptional signature associated with non-stereotypic U-CLL in human. These findings provide evidence for differential dependence on T cell help in unmutated CLL in mice and suggest that development of human U-CLL can also be T cell-dependent.

MATERIALS AND METHODS

Mice

Mice (C57BL/6) deficient for *Cd40l*[25], *Aicda*[26] *or Siglec-G*[27], and *Cd19-E-Btk-2*[28] transgenic mice were crossed to *IgH.TEμ* mice (F1 sv129xC57BL/6). CLL development was monitored every 3-6 weeks by screening peripheral blood for a monoclonal B cell expansion using flow cytometry. CLL formation was defined by accumulation of >70% $IgMb^+$ B-cells in the peripheral blood of the mice. Mice were sacrificed after detection of CLL. Mice were bred and kept in the Erasmus MC experimental animal facility and experiments were approved by the Erasmus MC committee of animal experiments.

Patients and healthy controls

Primary patient material was obtained from peripheral blood from CLL patients, while peripheral blood from healthy controls (>50 years of age) was obtained via Erasmus MC and via Sanquin blood bank (Rotterdam). Diagnostic and control samples were collected upon informed consent and anonymized for further use, following the guidelines of the Institutional Review Board, and in accordance with the declaration of Helsinki. The BCR characteristics of all CLL patients are included in **Supplementary Table 5**. Peripheral blood mononuclear cells (PBMCs) were isolated using Ficoll Hypaque (GE Healthcare, Little Chalfont, UK) according to the manufacturer's instructions. Naïve mature B cells were isolated from healthy control PBMCs using FACS-purification for $CD19^+CD27IgD^+$ cells. The purity of naïve mature healthy B cell samples was >95% as determined by flow cytometry.

In vivo immunizations

TD immune responses were induced by i.p. immunization. Primary immunizations were induced in 10-12-week-old mice with 100 μg TNP-KLH on alum. After 5 weeks this was followed by a secondary immunization with 100 μg TNP-KLH in PBS[28].

BCR sequencing

Primer sequences and PCR condition were previously described[29]. PCR products were directly sequenced using the BigDye terminator cycle sequencing kit with AmpliTaq DNA polymerase on an ABI 3130xl automated sequencer (Applied Biosystems). Sequences were analyzed using IMGT/V-Quest (http://www.imgt.org, using Ig gene nomenclature as provided by IMGT). All sequences were confirmed in at least one duplicate analysis.

Flow cytometry procedure

Preparation of single-cell suspensions of lymphoid organs and lysis of red blood cells were performed according to standard procedures. Cells were (in)directly stained in flow cytometry buffer (PBS, supplemented with 0.25% BSA, 0.5 mM EDTA and 0.05% sodium azide) using the following fluorochrome or biotin-conjugated monoclonal antibodies or reagents: anti-B220 (RA3-6B2), anti-CD19 (ID3), anti-CD5 (53-7.3), anti-CD43 (R2/60), anti-CD23 (B3B4) all from eBioscience and anti-CD138 (281-2), anti-CD95 (Jo2), anti-IgD (11-26), anti-IgMb (AF6-78), anti-IgMa (DS-1), anti-Igλ (R26-46), anti-Igκ (187.1), anti-CD21 (7G6), all from BD biosciences, using conjugated streptavidin (eBioscience) as a second step for biotin-conjugated antibodies.

Leukemic cells ($CD19^+CD5^+$) were stained with fluorescein-labeled phosphatidylcholine (PtC) liposomes (DOPC/CHOL 55:45, Formumax Scientific Inc.) in flow cytometry buffer. Cells were co-stained with anti-CD19, anti-CD43, or anti-CD5 (BD Biosciences).

MACS cell sorting

Splenic single-cell suspensions were prepared in magnetic-activated cell sorting (MACS) buffer (PBS/2mM EDTA/0.5%BSA) and naïve splenic B cells from 8–12 week-old WT C57BL/6 mice were purified by MACS, as previously described[24,29]. Non-B cells, B-1 cells, GC B cells and plasma cells were first labeled with biotinylated antibodies (BD Biosciences) to CD5 (53–7.3), CD11b (M1-70), CD43 (S7), CD95 (Jo2), CD138 (281-2), Gr-1 (RB6-8C5) and TER-119 (PK136) and subsequently with streptavidin-conjugated magnetic beads (Miltenyi Biotec). Purity of MACS-sorted naïve B cells was confirmed by flow cytometry (typically > 99% CD19$^+$ cells). To obtain activated B cells, purified naïve WT B cells were cultured in culture medium (RPMI 1640 (life technologies)/ 10% FCS (gibco) / 50 µg/mL gentamycin(life technologies) / 0,05 mM ß-mercaptoethanol (Sigma)) in the presence of 10 µg/ml F(ab')2 anti-IgM (Jackson Immunoresearch) for 12h.

RNA-sequencing

RNA was extracted from naive or activated splenic B cells, as well as from purified (using MACS-purification for CD19$^+$ cells) primary tumors from IgH.TEµ mice with the RNeasy Micro kit (Qiagen) according to manufacturer's instructions. The TruSeq RNA Library Prep kit (Illumina) was used to construct mRNA sequencing libraries that were sequenced on an Illumina HiSeq 2500 (single read mode, 36 bp read length). Raw reads were aligned using Bowtie to murine transcripts (RefSeq database) from the University of California at Santa Cruz (UCSC) mouse genome annotation (NCBI37/mm9)[30]. Differential gene expression analysis was performed using DESeq2[31] with an adjusted P-value (false discovery rate; FDR) of P< 0.05. Log2-fold changes and FDR values as calculated by DESeq2 were used to generate a volcano plot using R (R studio version 1.1.383). Normalized gene expression levels quantified as reads per kilobase of a transcript per million mapped reads (RPKMs) were used for various clustering approaches (unsupervised hierarchical clustering, supervised clustering and PCA) that were performed using R and PAST software (https://folk.uio.no/ohammer/past/). Visualization of clustering analysis output was performed using R, PAST and Java TreeView[32]. Molecular pathway enrichments were obtained from the online MSigDB database. Gene expression data for anti-CD40 plus IL-4 stimulated follicular B-cells was obtained from previously reported data and downloaded from the Gene Expression Omnibus (GEO; accession number GSE77744)[33]. RNA-Seq data generated in this study have been deposited in the GEO database (accession number GSE117713).

Quantitative real time PCR analysis

Samples tested in qRT-PCR were from *IgH.TEµ* (7 V_H11 and 15 non-V_H11), from *IgH.TEµ.Aicda*$^{-/-}$ (4 V_H11 and 4 non-V_H11), and from *IgH.TEµ.TD* (4 non-V_H11) mouse groups. For quantitative RT-PCR analysis, TaqMan probes were employed. Probe Finder software (Roche Applied Science), the Universal Probe Library (Roche Applied Science) and Ensembl genome browser (http://www.ensembl.org/) were used for primer and probe design. Taqman Universal Master Mix II, was purchased from Thermo Fisher Scientific. Quantitative RT-PCR was performed by using the 7300 Real Time PCR system (Applied Biosciences) according to manufacturer's instructions. Gene expression was analyzed with an ABI Prism 7300 Sequence Detector and ABI Prism Sequence Detection Software version 1.4 (Applied Biosystems). Cycle-threshold levels were calculated for each gene and the housekeeping gene glyceraldehyde-3-phosphate dehydrogenase (*Gapdh*) was used for normalization of the values. All primer sequences and probe numbers are listed in **Supplementary Table 7**.

Statistical analysis

Statistical analysis was performed using GraphPad Prism software (San Diego, California, USA) or R. The log rank test was used for calculating the level of significance for survival differences between mouse groups. The Chi-square test was used to determine the significance for BCR usage differences between different mouse groups. To evaluate differences in expression levels of different genes by qRT-PCR we used a Mann-Whitney U-test between two groups or a Kruskal-Wallis test corrected with Dunn's multiple comparison test for more than two groups.

RESULTS

Two subsets of unmutated CLL arise in IgH.TEµ mice

To analyze the BCR repertoire, we aged a panel of *IgH.TEµ* mice and collected blood every 3-6 weeks to monitor CLL incidence. Hereby, CLL incidence was defined by the accumulation of >70% IgMb$^+$ B-cells, which displayed a CLL-like CD5$^+$CD43$^+$IgM$^+$IgD^{low}CD19$^+$ phenotype[22, 23]. We performed sequencing analyses of Ig heavy (*Igh*) and light (*Igl*) chain transcripts and found that a substantial proportion (~36%) of CLL in *IgH.TEµ* mice expressed stereotyped BCRs consisting of the V_H11-2 *Igh* chain, with similar *Igh* CDR3 length and amino acid sequences, and the Vk14-126 *Igl* chain[22,23] (**Supplementary Table 1, Figure 1A, 1B**). The V_H11/Vk14 CLL mice exhibited an earlier disease onset compared with *IgH.TEµ* mice with non-stereotypic (non-V_H11) BCR (mean incidence age 184 days and 219 days, respectively, p=0.0175) (**Figure 1C**). In wild-type mice the V_H11-2/Vk14-126 BCR is preferentially expressed by B-1 lymphocytes and shows specificity to phosphatidylcholine (PtC)[12]. We could confirm PtC-binding specificity of V_H11-2 BCRs on CLL cells (**Figure1D**). V_H11 CLL showed decreased surface IgM expression and increased surface IgD expression compared to non-V_H11 CLL (**Figure 1E, 1F**). A major proportion (~65%) of the remaining non-V_H11 CLL expressed a J558 V_H1-family BCR with heterogeneous CDR3 length, amino acid sequence and *Igl* chain usage (**Supplementary Table 1**). V$_H$1 CLL showed delayed disease onset (mean incidence age 231 days), compared with V$_H$11 CLL (**Supplementary Figure 1)**.

In conclusion, based on *Ig* gene usage we could distinguish different subsets of unmutated *IgH.TEμ* CLL displaying differential disease onset.

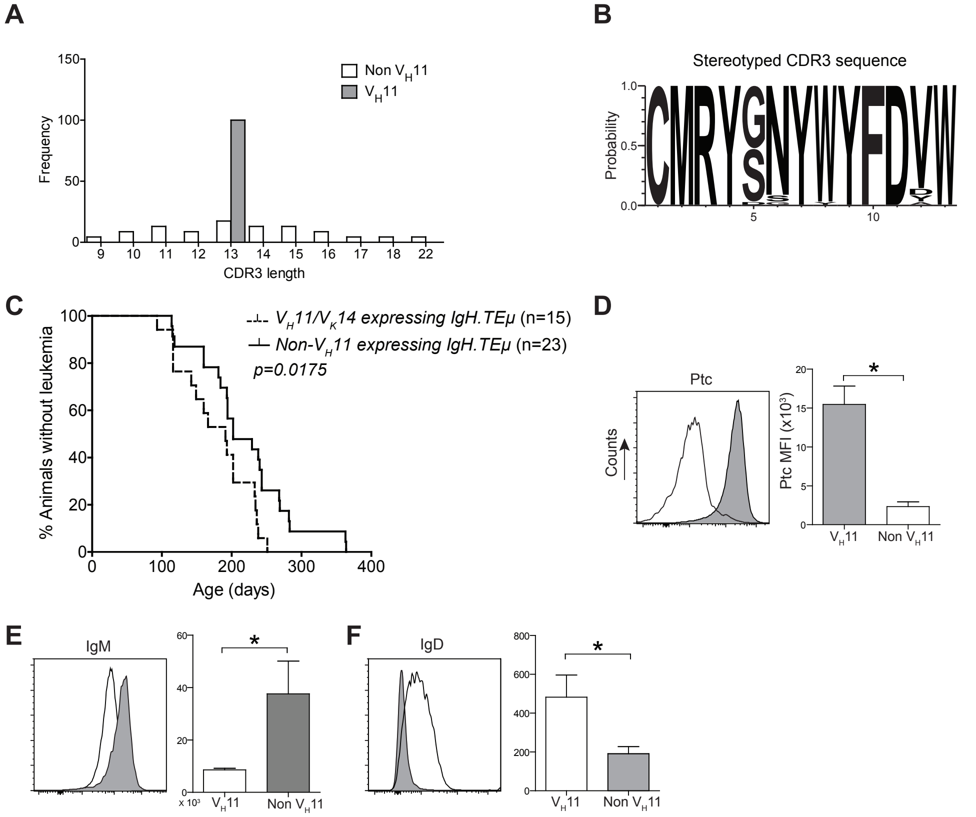

Figure 1. Early onset of disease in CLL expressing PtC-reactive V$_H$11 BCR.
(**A**) Bar graphs summarizing the distribution of CDR3 length in V$_H$11 (*grey,* n=15) versus non-V$_H$11 (*white,* n=23) CLL from *IgH.TEμ* mice. (**B**) Web logo depicting stereotyped CDR3 amino acid sequence of V$_H$11 (n=15) CLL from *IgH. TEμ* mice. (**C**) Retrospective Kaplan-Meier incidence curves including *IgH.TEμ* mice with identified V$_H$11 (*dotted line*) or non-V$_H$11 BCR CLL (*solid line*). (**D,E,F**) Histogram showing flow cytometric analysis of CD19$^+$CD5$^+$CD43$^+$ splenic CLL cells from V$_H$11 (*grey*) versus non-V$_H$11 (*black line*) CLL from *IgH.TEμ* mice, stained with (**D**) phosphatidylcholine (PtC) liposomes or fluorochrome conjugated (**E**) anti-IgM or (**F**) anti-IgD antibodies. Bar graphs summarize mean fluorescence intensity of V$_H$11 (*grey*) and non-V$_H$11 CLL (n=6 per group).

Germinal center defects lead to increased V$_H$11/Vk14 usage in unmutated CLL

Because V$_H$11/Vk14-expressing CLL likely originate from B-1 cells, we hypothesized that they should still develop in the absence of functional GCs. Therefore, we investigated their dependence on functional GCs and T cell help by crossing *IgH.TEμ* mice with *Cd40l$^{-/-}$* or *Aicda$^{-/-}$* mice. *Cd40l $^{-/-}$* or *Aicda$^{-/-}$* mice display a complete lack or aberrant enlargement of GCs, respectively, paralleling the human hyper-IgM syndrome phenotype[26,34]. We monitored CLL incidence, as described above, in cohorts of *Cd40l*-deficient *IgH.TEμ* mice (*IgH. TEμ.Cd40l$^{-/-}$*, n=13), *Aicda*-deficient *IgH.TEμ* mice (*IgH.TEμ.Aicda$^{-/-}$*, n=26) and *IgH.TEμ* control littermates, n=69 or n=56, respectively for ~400 days (**Figure 2**). CLL frequency and onset was not altered in *IgH.TEμ.Cd40l$^{-/-}$*mice (~59%, compared with ~62% in *IgH.TEμ* control littermates; p=0.99) or in *IgH.TEμ.Aicda$^{-/-}$* mice (~62%, compared with ~64% in *IgH.TEμ* control littermates; p=0.78) (**Figure 2A, 2B**).

To explore the impact of CD40L or AID-deficiency on BCR usage in CLL, we performed *IghV* and *IglV* sequence analyses in selected CLL samples with high tumor load (>95%

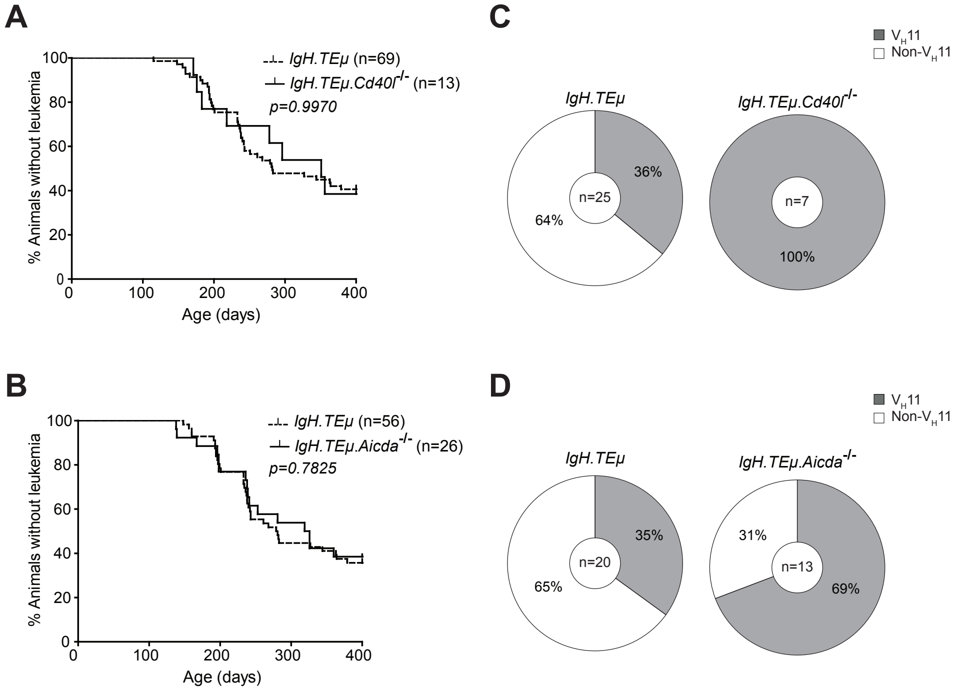

Figure 2. Increased frequency of V$_H$11 usage in CLL from germinal center attenuated *IgH.TE*μ mice.
(**A,B**) Kaplan-Meier incidence curves of (**A**) *IgH.TEμ* (*dotted line*) versus *IgH.TEμ.Cd40l$^{-/-}$* (*solid line*) mice or (**B**) *IgH. TEμ* (*dotted line*) versus *IgH.TEμ.Aicda$^{-/-}$* (*solid line*) mice. (**C,D**) Pie charts summarizing frequencies of V$_H$11 BCR (*grey*) and non- V$_H$11 BCR-expressing CLL in the indicated mouse groups.

IgMb$^+$CD5$^+$CD43$^+$CD19$^+$ CLL-like cells) (**Supplementary Table 1**). Interestingly, usage of the stereotypic V_H11/Vk14 BCR was significantly increased in CLL from *IgH.TEμ.Cd40l*$^{-/-}$ mice (n=7/7, 100%), compared with control *IgH.TEμ* mice (n=9/25, ~36%, Chi-square p<0.001). Also CLL from *IgH.TEμ.Aicda*$^{-/-}$ mice showed increased V_H11/Vk14 usage (n=9/13, ~69%) compared with control littermates (n=7/20, ~35%, Chi-square p<0.01)(**Figure 2C, 2D**). These V_H11 CLL also expressed similar *Igh* CDR3 sequences (**Supplementary Table 1**).

Taken together, these findings indicate that V_H11/Vk14-expressing CLL arise independently of T cell help or GC formation, whereas non-V_H11 CLL is T cell-dependent and reduced in the absence of functional GCs in *IgH.TEμ.Cd40l*$^{-/-}$ and *IgH.TEμ.Aicda*$^{-/-}$ mice.

T-cell dependent antigenic stimulation of B cells in vivo reduces V_H11/Vk14 usage in unmutated IgH.TEμ CLL

To directly investigate whether antigenic stimulation in the context of T cell help affects CLL onset and the CLL BCR repertoire, we immunized *IgH.TEμ* mice with TNP-KLH coupled to alum (*IgH.TEμ.TD,* n=20) to induce a TD B cell response. CLL onset did not differ between immunized and non-immunized littermates (n=56) (**Figure 3A**). At the age of ~400 days, CLL incidence in *IgH.TEμ.TD* mice was ~65% similar to non-immunized control *IgH.TEμ* mice (~62%) (**Figure 3A**).

Next, we analyzed *IghV* and *IglV* sequences in CLL samples with high tumor load (>95% IgMb$^+$CD5$^+$CD43$^+$CD19$^+$ CLL-like cells). In contrast to control *IgH.TEμ* mice, which showed ~35% (n=7/20) V_H11 usage, only 10% (n=1/10) of *IgH.TEμ.TD* CLL expressed a V_H11/Vk14 BCR (Chi-square p=0.09) (**Figure 3B**). The majority (n=6/9, 67%) of CLL in *IgH.TEμ.TD* mice expressed a J558/V_H1-family *IghV* gene and we did not observe mutated CLL (**Supplementary Table 1**).

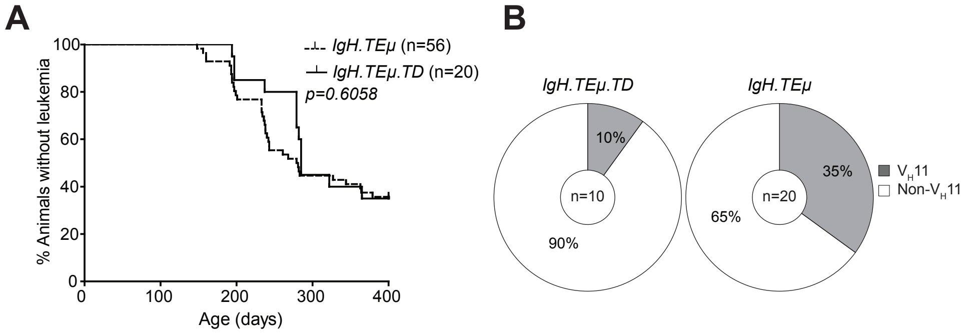

Figure 3. CLL V_H11 usage is dependent on antigenic stimulation.
(**A**) Kaplan-Meier incidence curves of *IgH.TEμ* (*dotted line*) versus *IgH.TEμ.TD* (*solid line*). (**B**) Pie charts summarizing the frequencies of V_H11 (*grey*) and non-V_H11 BCR-expressing CLL in the indicated mouse groups.

In summary, we found that robust TD immunization favors development of non-V_H11 CLL.

Enhanced BCR signaling accelerates disease onset in IgH.TEμ mice

Our findings provide evidence that T cell-derived activation or selection signals, in particular CD40L, shape the BCR repertoire of CLL in *IgH.TEμ* mice, but do not significantly affect disease onset or progression. It is therefore conceivable that in the *IgH.TEμ* mouse model, BCR-derived signals may be more decisive for disease progression.

To monitor the impact of BCR signaling strength on CLL development and *IghV* gene selection, we first crossed *IgH.TEμ* mice with *E-Btk-2* transgenic mice. These mice express the constitutive active E41K-BTK mutant selectively in the B-cell lineage driven by the CD19 promoter[28]. The E41K mutation enhances Btk membrane localization and thereby its activation by Syk or Src-family tyrosine kinases[35]. *E-Btk-2* mice show defective follicular B cell survival and a relative expansion of splenic B-1 cells[28]. Flow cytometry analysis of *E-Btk-2* B-1 cells did not reveal detectable PtC binding, indicating that V_H11 BCR expression was limited (data not shown).

We found that *IgH.TEμ.E-Btk-2* mice (n=21) developed CLL significantly earlier (mean age of onset of ~155 days), compared with control *IgH.TEμ* mice (~279 days; p<0.0001) (**Figure 4A**). In addition, *IgH.TEμ.E-Btk-2* mice appeared to have an increased disease frequency (~90 % at ~400 days, compared with ~71% for control *IgH.TEμ* mice). Sequence analysis of *Igh* revealed that 1 out of 8 (~12%) of tumors from *IgH.TEμ.E-Btk-2* mice expressed a V_H11 BCR, compared with 35% (n=9/26) in the control *IgH.TEμ* group (**Figure 4C, Supplementary Table 1**). This difference was not statistically significant, but the finding of a PtC-reactive V_H11 CLL was surprising, since PtC-binding B-1 cells were not detectable in *E-Btk-2* mice. The majority (~71%; n=5/7) of the non-V_H11 BCRs expressed J558/V_H1-family *IghV* genes.

To confirm that enhanced BCR signaling affects disease onset, we crossed *IgH.TEμ* mice on a *Siglec-G* deficient background (*IgH.TEμ.Siglec-G*$^{-/-}$). *Siglec-G* is a negative regulator of BCR-mediated signaling that is expressed in all B cells[27]. It is a potent inhibitor of BCR-induced Ca^{2+} signaling and a key regulator of survival and selection of B-1 cells[36]. In addition, Siglec-G-deficiency abrogates V_H11 usage in B-1 cells[36].

Similar to *IgH.TEμ.E-Btk-2* mice, also *IgH.TEμ.Siglec-G*$^{-/-}$ mice displayed an increased disease frequency (~93 % at ~400 days, compared with ~70% for IgH.TEμ mice), with significantly accelerated CLL onset (~121 days compared with ~268 days for *IgH.TEμ* mice; p<0.0001)(**Figure 4B**). *IghV* analyses showed a V_H11/Vk14 usage of ~18% (n=2/11) in *IgH.TEμ.Siglec-G*$^{-/-}$ CLL vs. ~35% (9/26) in the control group (Chi-square p<0.242) (**Figure 4C, Supplementary Table 1**). Only 2/11 *IgH.TEμ.Siglec-G*$^{-/-}$ CLL expressed J558/V_H1-family *IghV* genes.

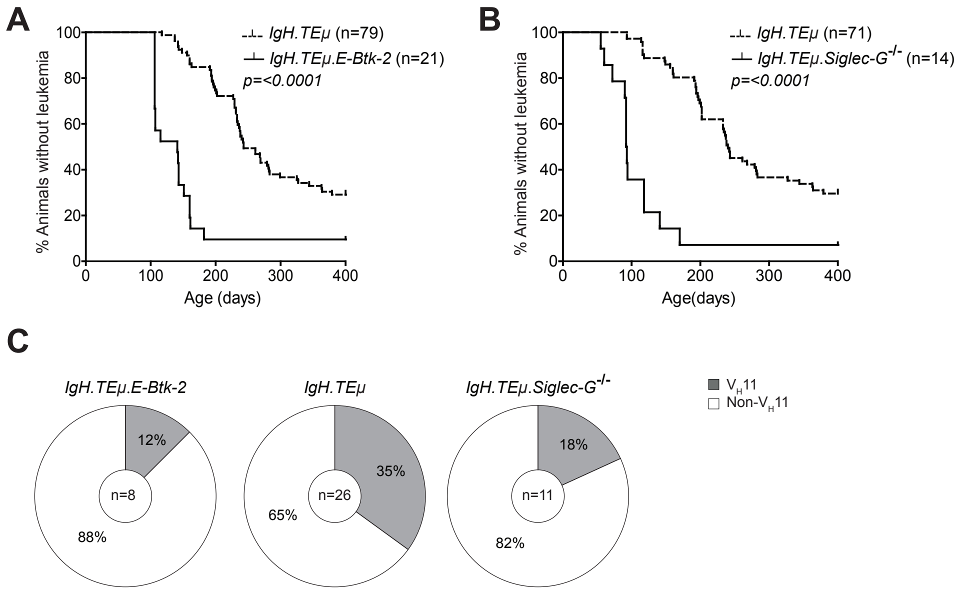

Figure 4. Onset of CLL is dependent on BCR signaling capacity in IgH.TEμ mice.
Kaplan-Meier incidence curves of (**A**) *IgH.TEμ* (*dotted line*) versus *IgH.TEμ.E-Btk-2* (*solid line*) mice or (**B**) *IgH.TEμ* (dotted line) versus *IgH.TEμ.SiglecG$^{-/-}$* (*solid line*) transgenic mice. (**C**) Pie charts summarizing the frequencies of V$_H$11 (*grey*) and non-V$_H$11 BCR-expressing CLL in the indicated mouse groups.

Thus, BCR signaling strength plays an important role in CLL development in *IgH.TEμ* mice, whereby enhanced signaling accelerates disease onset. Because *E-Btk-2* or *Siglec-G$^{-/-}$* B-1 cells do not show detectable PtC expression, our findings suggest that those few V$_H$11 B cells present are efficiently transformed to CLL in *IgH.TEμ.E-Btk-2* or *IgH.TEμ.Siglec-G$^{-/-}$* mice. Thus, BCR signaling strength may also affect the BCR repertoire in CLL.

Transcriptome profiling identifies unique genes and pathway aberrations for V$_H$11/Vk14 and non-V$_H$11 CLL IgH.TEμ mice

To further explore the biological phenotype of the V$_H$11 and non-V$_H$11 CLL subsets, we performed genome-wide gene expression profiling on primary *IgH.TE*μ CLL (tumor load >95%) expressing either a V$_H$11 (n=3) or a non-V$_H$11 (n=3) BCR. As a reference we included resting unstimulated (un-B, n=4) and anti-IgM stimulated (αIgM-B, n=4) naïve splenic B cells from wild-type mice. Normalized gene expression values (see Methods for details) were used for principle component analysis (PCA). The first two principal components, which represented ~70% of the total variation among the different samples analyzed, identified three separate clusters, corresponding to un-B, αIgM-B and primary *IgH.TE*μ CLL samples, indicating a strong correlation between biological replicates (**Supplementary Figure 2**).

When we performed differential gene expression analysis (focusing only on genes passing a stringent statistical filter of Benjamini-Hochberg false discovery rate corrected P<0.05), we found 148 differentially expressed genes (**Figure 5A; Supplementary Table 2**). Of these genes, 59 genes were upregulated in V$_H$11 CLL and 89 genes were upregulated in non-V$_H$11 CLL. To identify biological processes that underlie the transcriptional differences between V$_H$11 and non-V$_H$11 CLL, we performed pathway enrichment analysis using the Molecular Signatures Database (MSigDB)[37]. Genes upregulated in V$_H$11 CLL were functionally enriched for an interferon-mediated response, active Wnt signaling and constitutively active RAF1 signaling (**Figure 5B, Supplementary Table 3A**). On the other hand, genes downregulated in V$_H$11 CLL were involved in quite diverse pathways, including interleukin-, epidermal growth factor receptor (EGFR)-, vascular endothelial growth factor (VEGF)-mediated signaling, metabolic processes, hypoxia and the UV radiation-induced stress response (**Figure 5B, Supplementary Table 3A**).

Taken together, these data suggest that in addition to a different origin, V$_H$11 and non-V$_H$11 CLL subsets display distinct transcriptional signatures, signifying differential activity of key signaling pathways.

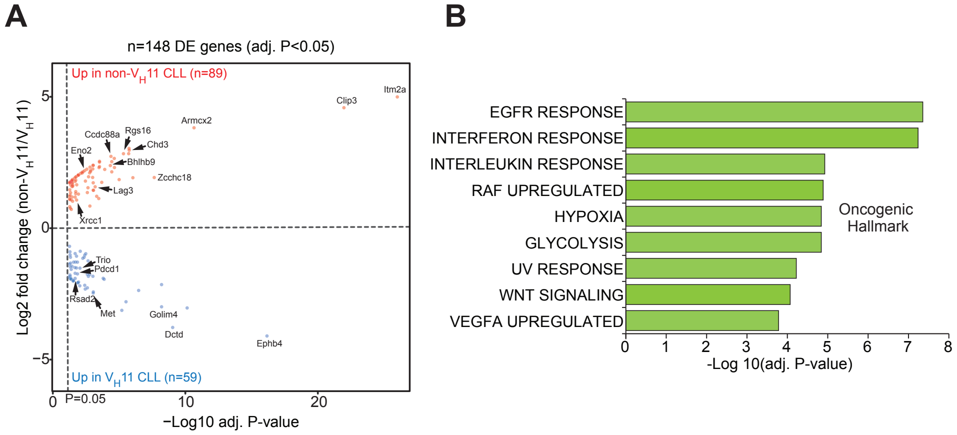

Figure 5. A unique set of genes and pathways is upregulated in V$_H$11 versus non-V$_H$11 CLL in IgH.TEμ mice.
(**A**) Volcano plot showing P-values and fold changes in gene expression levels comparing V$_H$11 and non-V$_H$11 CLL from *IgH.TEμ* mice. Genes upregulated in non-V$_H$11 CLL are indicated in red; genes upregulated in V$_H$11 CLL in blue. Only significantly different genes (Benjamini-Hochberg adjusted p-value <0.05) are shown. Genes indicated represent a subset of the validation gene set analyzed in a larger CLL panel (see **Figure 7**). (**B**) Oncogenic hallmark signatures enriched among differentially expressed genes in V$_H$11 (n=3) versus non-V$_H$11 (n=3) CLL from *IgH.TEμ* mice.

Strong BCR dependence of V_H11/Vk14 CLL in IgH.TEμ mice

Next, we performed a PCA of the 148 differentially expressed genes between V_H11 and non-V_H11 CLL. To investigate the impact of T-cell-independent BCR stimulation and T-cell-dependent CD40 stimulation on differential gene expression, we included RNA-Seq gene expression values of the 148 genes from the unstimulated and αIgM-stimulated B cells described above, as well as previously reported gene expression values from anti-CD40/IL-4 stimulated follicular B-cells (α-CD40/IL4-B)[33].

The first principal component (PC1) separated both CLL groups and the two stimulated B cell subsets from unstimulated B cells, suggesting *IgH.TE*μ CLL cells share a transcriptional signature related to activated B-cell phenotypes. Interestingly, PC2 revealed a strong similarity between αIgM-stimulated B cells and V_H11 CLL on one hand and between α-CD40/IL4-stimulated B cells and non-V_H11 CLL on the other hand (**Figure 6A**). These findings indicate more prominent BCR stimulation in V_H11 than in non-V_H11 CLL B cells *in vivo* and are consistent with a dependence on T-cell help for non-V_H11 CLL.

To identify the gene signature underlying the clustering of αIgM-stimulated B cells and V_H11 CLL, as well as α-CD40/IL-4-stimulated B cells and non-V_H11 CLL, we performed hierarchical clustering analyses to separate the 148 genes into 4 clusters (**Figure 6B, Supplementary Table 3B**). Cluster 1 consists of 17 genes that were highly correlated between αIgM-stimulated B cells and V_H11 CLL and between α-CD40/IL-4-stimulated B cells and non-V_H11 CLL. Pathway enrichment analysis (**Supplementary Table 3C**) on this cluster revealed overrepresentation of genes involved in interferon response and KRAS signaling. Clusters 2 (35 genes) and Cluster 3 (56 genes) consist of genes that were highly correlated only between α-CD40/IL-4-stimulated B cells and non-V_H11 CLL or only between αIgM-stimulated B cells and V_H11 CLL, respectively. These clusters were enriched for interferon response/PI3K-AKT signaling genes (cluster 2) or UV response, epithelial-mesenchymal transition, glycolysis, hypoxia, unfolded protein response genes (cluster 3) (**Supplementary Table 3C**). Finally, cluster 4 (enriched for genes involved in the reactive oxygen species pathway) represents genes with low or anti-correlated expression values between the stimulated B cells and CLL. Thus, genes from clusters 1 and 3 signify the clustering of αIgM-stimulated B cells and V_H11 CLL, while genes from clusters 1 and 2 drive the clustering of α-CD40/IL-4-stimulated B cells and non-V_H11 CLL (**Figure 6B**). This analysis was further validated by computing the average correlation strength for each of the four gene clusters with PC2 from our PCA (**Figure 6B**). Indeed, clusters 1 to 3 underlying the αIgM-B cells and V_H11 CLL and the α-CD40/IL-4-B cells and non-V_H11 CLL segregation - and particularly cluster 1 genes - showed significantly stronger correlation values with PC2 than cluster 4 (**Figure 6C**).

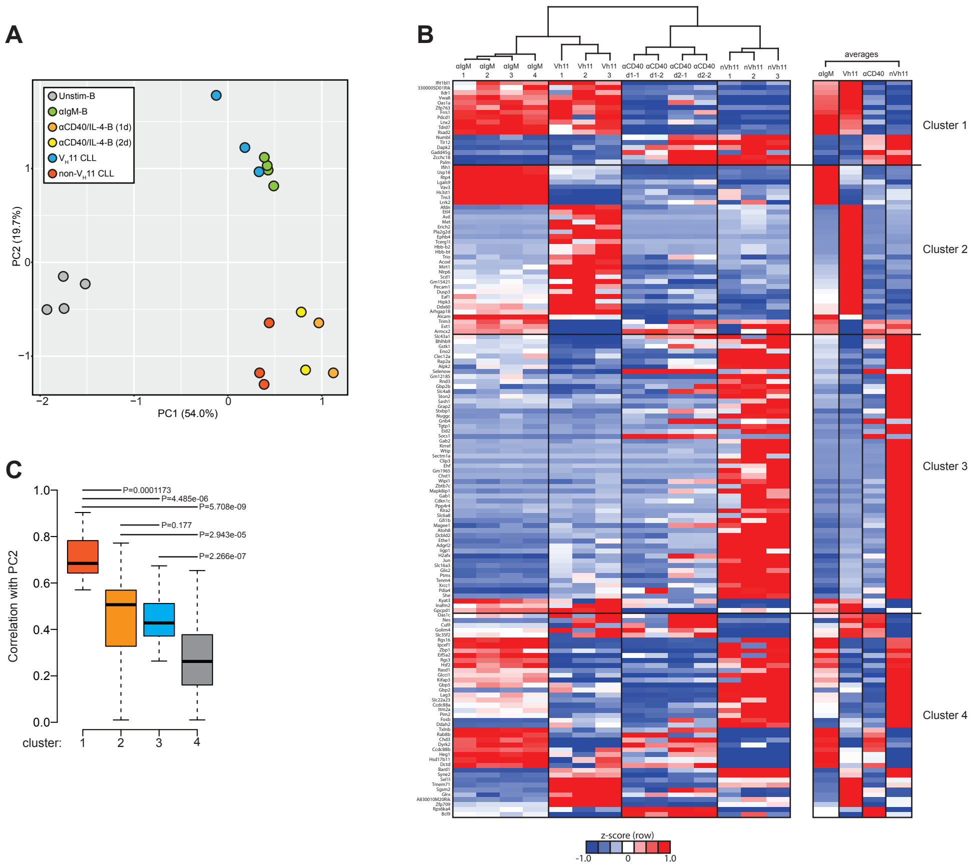

Figure 6. Genes discriminating V_H11 from non-V_H11 CLL show similarly distinct expression profiles in BCR or CD40-stimulated B-cells.
(**A**) Principle component analysis (PCA) using the 148 differentially expressed genes defined in **Figure 5A** in unstimulated (n=4, *black*), anti-IgM-stimulated (n=4, *green*) WT splenic B cells, 1 day (n=2, *orange*) or 2 day (n=2, *yellow*) anti-CD40 plus IL-4 stimulated follicular B-cells (obtained from GSE77744), V_H11-2$^+$/V_k14-126$^+$ BCR (n=3, *blue*) and non-V_H11 (n=3, *red*) BCR-expressing CLL from *IgH.TEμ* mice. (**B**) Hierarchical clustering analysis (top) and accompanying heat map showing differences in expression levels (RPKM, shown as row Z-scores) of the 148 gene signature in anti-IgM-stimulated (n=4) WT splenic B cells, 1 day (n=2) or 2 day (n=2) anti-CD40 plus IL-4 stimulated follicular B-cells, V_H11 and non-V_H11 CLL from *IgH.TEμ* mice. Heatmap shown on the right shows average expression levels for each group. (**C**) Boxplot showing average correlation values of each of the four gene clusters shown in panel B with principal component 2 (PC2) from the PCA shown in panel A. P-values were calculated using a Mann-Whitney U test.

Validation of V_H11/non-V_H11 CLL gene expression differences in mouse and human CLL

To further strengthen the existence of a unique transcriptional signature that differentiates V_H11 and non-V_H11 CLL B cells, we selected 24 robustly differentially expressed genes for validation. Some of these genes have already been shown to play a role in hematologic

malignancies, including CLL (*Pim-2, Met, Rgs16, Ccdc88a, Zcchc18, Clip3*)[38-42], diffuse large B cell lymphoma, follicular lymphoma (*Vav3*)[43], acute lymphoblastic leukemia (ALL) (*Itm2a, Chst1*)[44,45] or acute myeloid leukemia (AML) (*Chd3*)[46].

Expression levels were validated by quantitative real-time PCR (qRT-PCR) in an extended cohort of 15 V_H11 and 23 non-V_H11 primary CLL from *IgH.TEμ* mice. Naïve Splenic B cells from wild type mice (n=4) were included as controls. Comparison of RNA-Seq (RPKM) and qRT-PCR expression fold changes between the two CLL groups revealed highly correlated trends for these 24 genes (spearman correlation r=0.72; p<0.0001), validating our RNA-Seq analysis when extrapolated to a larger *IgH.TEμ* CLL cohort (**Figure 7A**). qRT-PCR validation showed that 11/24 (~46%) of the selected genes were significantly different (p<0.05) between V_H11 and non-V_H11 CLL (**Supplementary Table 4; Figure 7B**). Additionally, 7/24 (~29%) genes were significantly different (p<0.05) between non-V_H11 CLL from *IgH.TEμ* and *IgH.TEμ.Siglec-G*$^{-/-}$ mice, which might be related to the altered V_H usage in *Siglec-G*$^{-/-}$ mice or the early disease onset in *IgH.TEμ.Siglec-G*$^{-/-}$ mice.

Expression of five of these 13 genes that were significantly upregulated in non-V_H11 CLL versus V_H11 CLL (*Ccdc88a, Clip3, Zcchc18, Chd3, Itm2a*) was also evaluated in five mutated *IgH.TEμ* CLL, defined by <97% IghV germline identity (**Supplementary Table 1** and ter Brugge PJ et al[22]). Interestingly, qRT-PCR analysis showed that four out of five tested genes (except *Itm2a*) were expressed at low levels in mutated CLL, similar to V_H11 CLL (**Figure 7B**). Thus, non-V_H11 unmutated CLL in *IgH.TEμ* mice represent a unique subset that can be distinguished from V_H11 unmutated and from mutated CLL by a specific transcriptional signature. Furthermore, correlation analyses indicated that within the non-stereotypic subgroup in particular V_H1 CLL represents the most heterogeneous CLL subgroup in *IgH.TEμ* mice (n=16; average spearman r, ρ=0.280; **Supplementary Figure 3**). In these analyses we also found that expression of these five genes is positively correlated in V_H11 CLL (n=16; average spearman r, ρ=0.537) and in the small non-V_H11/non-V_H1 CLL subgroups (n=6; average spearman r, ρ=0.703) (**Supplementary Figure 3).**

Next, we evaluated the expression of the 13 signature genes in a panel of 44 human CLL samples (15 non-stereotypic U-CLL, 14 stereotypic U-CLL, 15 M-CLL, **Supplementary Table 5**) by qRT-PCR. Hereby, 6/13 (~46%) genes (*CCDC88A, CLIP3, ZCCHC18, CHD3, ITM2A, GOLIM4*) were significantly higher expressed in all three CLL subsets than in naïve B-cells from healthy individuals, suggesting a role for these genes in CLL (**Figure 7C, Supplementary Table 6)**. Expression of CLIP3 was significantly higher in non-stereotypic than M-CLL. Expression of ZCCHC18, CHD3, GOLIM4, BHLH9B and ITM2A was significantly higher in non-stereotypic U-CLL compared to stereotypic U-CLL (**Figure 7C**).

To compute any parallel between stereotypic and heterogeneous U-CLL from patients and *IgH.TEμ* mice, we performed t-SNE clustering analysis on expression values for the 13 signature genes (**Figure 7D, Supplementary Table 6**). We used dCT values obtained by qRT-PCR for non-sterotypic (#U-CLL, n=10) and stereotypic (U-CLL, n=10) U-CLL as well as for non-V_H11 (n=21) and V_H11 (n=14) CLL from *IgH.TEμ* mice. Interestingly, 7/10 stereotypic U-CLL clustered with 10/14 V_H11 CLL (**Figure 7D**). Conversely, non-stereotypic human U-CLL and mouse non-V_H11 CLL showed a more heterogeneous distribution into several clusters largely devoid of stereotypic human U-CLL or mouse V_H11 CLL.

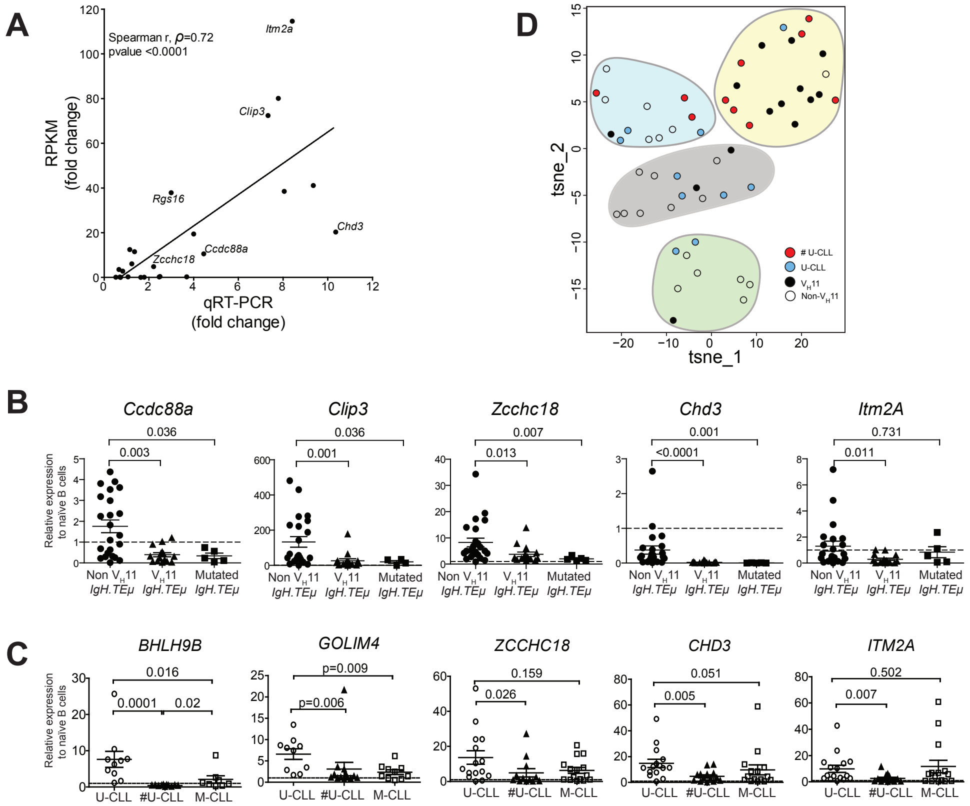

Figure 7. qRT-PCR validation of a subset of differentially expressed genes.
(**A**) Correlation plot comparing fold-changes in expression between V_H11 and non-V_H11 CLL for 24 genes measured by RNA-Seq (RPKM) or qRT-PCR (spearman r, ρ=0.72; p<0.0001). The differentially expressed genes selected for further study are indicated. Characteristics of samples tested in qRT-PCR are provided in the Methods section (**B**) Expression of indicated genes as measured by qRT-PCR in V_H11 (n=15), non-V_H11 (n=23) and mutated (n=5) CLL from *IgH.TEμ* mice. (**C**) Expression of indicated genes as measured by qRT-PCR in CLL cells from non-stereotypic U-CLL (n=15), stereotypic U-CLL (#U-CLL, n=14) and M-CLL (n=15) patients. Bars in panel B and C represent mean ± SEM values. The expression values were calculated relative to expression in (**B**) naïve splenic WT B cells from mice (*n*=4) or (**C**) naïve circulating B cells from healthy controls (*n*=3), both of which were set to 1 (*dashed line*). Numbers indicate p-values (Mann-Whitney U test). (**D**) t-SNE clustering analysis of the expression values for 13 signature genes (from **Supplementary Table 7)** using dCT values obtained by qRT-PCR for non-sterotypic (#U-CLL, n=10) and stereotypic (U-CLL, n=10) human U-CLL and non-V_H11 (n=21) and V_H11 (n=14) CLL from *IgH.TEμ* mice, as indicated. Expression values were converted to Z-scores separately for mouse and human datasets to allow combined t-SNE analysis.

Taken together, we conclude that differences in the expression of these signature genes in heterogeneous U-CLL, stereotyped U-CLL and M-CLL were partly overlapping between human CLL and the corresponding CLL subgroups in our *IgH.TEμ CLL* mouse model.

DISCUSSION

In this report, we investigated the role of antigenic pressure and BCR signaling thresholds on clonal selection of CLL cells in the *IgH.TEμ* CLL mouse model. We found that U-CLL tumors that develop in these mice can be classified into two different groups based on their *IghV* usage. The stereotypic V_H11-2/Vk14-126 CLL subset recognized the PtC self-antigen, developed independently of T cell help or GC formation and represented a somewhat more aggressive type of CLL. Proportions of V_H11/Vκ14-expressing CLL were increased in the absence of functional germinal centers in *IgH.TEμ* mice deficient for CD40L or activation-induced cytidine deaminase. Conversely, *in vivo* T cell-dependent immunization decreased the proportions of V_H11/Vκ14-expressing CLL. Mice were immunized at 10-12 weeks of age, with a secondary immunization at 15-17 weeks of age. In a proportion of mice at these time points, CLL cells become detectable in peripheral blood (**Figure 1**). In our immunization model the onset or frequency of CLL was not altered, but we cannot exclude that there will be effects on CLL onset or disease progression when immunizations are performed at a different age.

Consistent with the observed effects of defective germinal center function or robust T-cell dependent immunization on V_H usage in CLL, PCA of a gene signature comprised of 148 genes differentially expressed between V_H11 and non-V_H11 CLL revealed that V_H11 and non-V_H11 CLL clustered with BCR-stimulated and anti-CD40-stimulated B cells, respectively.

The unmutated V_H11 CLL cells parallel B-1 cells, because these also have a restricted BCR repertoire, may recognize auto-antigens including PtC, and produce natural IgM antibodies in the absence of T cell co-stimulation[12]. In concordance, it was recently shown that peritoneal $CD5^+$ B-1 cells generated early during fetal or neonatal development, increase in number over time and can progress into CLL in aged mice[47,48]. Interestingly, CLL development in these mice was linked to the expression of a restricted BCR repertoire (V_HQ52/Vκ9 or V_H3609/Vk21, reactive towards non-muscle myosin-IIA or Thy-1, respectively) independent of CD40 signaling. Hereby, expression of the *Eμ-TCL1* transgene enhanced aggressiveness of the disease.

Non-V_H11 CLL, on the other hand, consisted of tumors with heterogeneous *IghV/IglV* expression and CDR3 length, lacking affinity for PtC. Although these tumors were T-cell dependent, strongly reduced in the absence of functional GCs, their BCRs were not hypermutated (<3%). This is in line with findings in human U-CLL, indicating that U-CLL cells can recognize both TD and TI autoantigens that have relocated to the external cell surface during apoptosis[11,13,14]. Our observations are also consistent with gene expression profiling studies suggesting that U-CLL reflect memory B cells[49]. In contrast, more recent transcriptome analyses revealed that U-CLL resemble mature pre-GC $CD5^+CD27^-$ B cells, while M-CLL resembles a distinct, previously unrecognized, $CD5^+CD27^+$ post–GC B cell subset[18]. Our findings imply that in mice unmutated CLL can be derived from (i) T cell-independent B-1 cells (e.g. PtC-recognizing V_H11-2/Vκ14-126) or (ii) from B cells that recognize their antigen in the presence of cognate T-cell help and are activated without SHM. This latter group of T cell-dependent unmutated CLL displayed an expression signature, as defined by 13 genes including the *CCDC88A-CLIP3-ZCCHC18-CHD3-ITM2A* module, that is not only different from TI unmutated CLL, but also from mutated CLL in the *IgH.TEμ* mouse model. Moreover, we found evidence that this expression signature may be partly associated with non-stereotypic human U-CLL, suggesting that the development of human U-CLL can also be TD. Such TD U-CLL may derive from B cells involved in an extra-follicular response or alternatively may be related to auto-antibody producing B cells in mice that were shown to recognize TD antigens, mount a rapid IgM response and enter GCs, but do not develop into IgG-expressing plasma cells[50,51]. Although our data suggest a role for T-cell help in human non-stereotypic U-CLL pathophysiology, further investigation is required to translate our findings to human disease. Such studies should include expression profiling of (1) large CLL patient cohorts containing a wide range of stereotypic and non-stereotypic U-CLL samples and (2) activated B cells that received various stimulations including anti-CD40.

Gene expression profiling revealed a set of genes that distinguish V_H11 from non-V_H11 CLL and are similarly regulated in BCR or CD40-stimulated cells, respectively. This observation probably reflects differences in supporting external cues: pathways induced by interleukin or growth factor-mediated signaling were specifically upregulated in non-V_H11 CLL. These include the regulator of G-protein signaling 16, *Rgs16*, which is upregulated in autoimmune B cells of BXD2 mice and enhances GC formation by the canonical NF-κB pathway, signifying the post-GC origin of non-V_H11 CLL[52,53]. Second, the actin-binding protein *Ccdc88a*, which plays a role in cytoskeletal remodeling and cell migration following activation of Akt downstream of EGFR[54] and can also enhance Akt signaling[42,55]. Third, integral membrane protein 2A (*Itm2a*) is a type II integral membrane protein that has been associated with an enhanced GATA3-mediated regulatory network in B ALL[56]. *Chd3* encodes a chromatin remodeler with unexplored function in lymphocytes.

On the other hand, Wnt-associated genes were specifically upregulated in V_H11 tumors, which is interesting because the BTK-inhibitor ibrutinib restrains Wnt signaling in CLL[57]. Although the function of several other upregulated genes is currently unknown, *Zcchc18* has been associated with a CLL-specific transcriptomic signature[42] and *Clip3* was differentially regulated in a CLL patient undergoing spontaneous regression[58]. Notably, many gene sets or pathways were active in both CLL subsets, including high expression levels of MET receptor tyrosine kinase, which prolongs CLL cell survival through STAT3 and AKT phosphorylation[40,59]. This could contribute to the enhanced constitutive activation of the p-Akt/p-S6 pathway in *IgH.TEμ* CLL as reported previously[23,24]. Additionally, genes involved in KRAS signaling were highly expressed in both CLL subsets, consistent with its essential role in B cell lymphopoesis[60], particularly for B-1 cells recognizing PtC[61].

Our data also indicated that availability of T cell help and GC formation did not affect tumor incidence or onset. In contrast, the finding of a significantly earlier CLL incidence of mainly the non-V_H11 type in *IgH.TEμ.Siglec-G*$^{-/-}$ and *IgH.TEμ.E-Btk-2* mice suggests that BCR signaling thresholds are a key factor in determining CLL disease course. Yet, the appearance of V_H11 CLL in these mouse lines may indicate a substantial selective advantage of these clones, because in *Siglec-G*$^{-/-}$ and *E-Btk-2* transgenic mice the frequency of PtC-recognizing cells within the B-1 cell population is very low[28,36].

In conclusion, we found that the formation of a major subset of unmutated CLL in *IgH.TEμ* mice is dependent on T cell signals. Our findings therefore provide a mechanistic explanation for the role of B-cell intrinsic factors, in particular BCR signaling, as well as extrinsic factors such as T cell help and support from the tumor microenvironment, in shaping the repertoire of CLL in mice. These findings are of potential clinical relevance, because B-cell extrinsic signals may reflect effective targets for novel therapeutic strategies in CLL patients.

SUPPLEMENTARY MATERIAL

The Supplementary Tables for this article can be found online at: https://www.frontiersin.org/articles/10.3389/fimmu. 2018.01996/full#supplementary-material

REFERENCES

1. Hallek M. Chronic lymphocytic leukemia: 2015 Update on diagnosis, risk stratification, and treatment. *Am J Hematol* 2015 May; **90**(5)**:** 446-460.
2. Stamatopoulos K, Agathangelidis A, Rosenquist R, Ghia P. Antigen receptor stereotypy in chronic lymphocytic leukemia. *Leukemia* 2017 Feb; **31**(2)**:** 282-291.
3. Damle RN, Wasil T, Fais F, Ghiotto F, Valetto A, Allen SL, *et al.* Ig V gene mutation status and CD38 expression as novel prognostic indicators in chronic lymphocytic leukemia. *Blood* 1999 Sep 15; **94**(6)**:** 1840-1847.
4. Hamblin TJ, Davis Z, Gardiner A, Oscier DG, Stevenson FK. Unmutated Ig V(H) genes are associated with a more aggressive form of chronic lymphocytic leukemia. *Blood* 1999 Sep 15; **94**(6)**:** 1848-1854.
5. Mertens D, Stilgenbauer S. Prognostic and predictive factors in patients with chronic lymphocytic leukemia: relevant in the era of novel treatment approaches? *J Clin Oncol* 2014 Mar 20; **32**(9)**:** 869-872.
6. Pal Singh S, Dammeijer F, Hendriks RW. Role of Bruton's tyrosine kinase in B cells and malignancies. *Mol Cancer* 2018 Feb 19; **17**(1)**:** 57.
7. Byrd JC, Furman RR, Coutre SE, Flinn IW, Burger JA, Blum KA, *et al.* Targeting BTK with ibrutinib in relapsed chronic lymphocytic leukemia. *N Engl J Med* 2013 Jul 04; **369**(1)**:** 32-42.
8. Byrd JC, Harrington B, O'Brien S, Jones JA, Schuh A, Devereux S, *et al.* Acalabrutinib (ACP-196) in Relapsed Chronic Lymphocytic Leukemia. *N Engl J Med* 2016 Jan 28; **374**(4)**:** 323-332.
9. Duhren-von Minden M, Ubelhart R, Schneider D, Wossning T, Bach MP, Buchner M, *et al.* Chronic lymphocytic leukaemia is driven by antigen-independent cell-autonomous signalling. *Nature* 2012 Sep 13; **489**(7415)**:** 309-312.
10. Herve M, Xu K, Ng YS, Wardemann H, Albesiano E, Messmer BT, *et al.* Unmutated and mutated chronic lymphocytic leukemias derive from self-reactive B cell precursors despite expressing different antibody reactivity. *J Clin Invest* 2005 Jun; **115**(6)**:** 1636-1643.
11. Lanemo Myhrinder A, Hellqvist E, Sidorova E, Soderberg A, Baxendale H, Dahle C, *et al.* A new perspective: molecular motifs on oxidized LDL, apoptotic cells, and bacteria are targets for chronic lymphocytic leukemia antibodies. *Blood* 2008 Apr 01; **111**(7)**:** 3838-3848.
12. Baumgarth N. B-1 Cell Heterogeneity and the Regulation of Natural and Antigen-Induced IgM Production. *Front Immunol* 2016; **7:** 324.
13. Catera R, Silverman GJ, Hatzi K, Seiler T, Didier S, Zhang L, *et al.* Chronic lymphocytic leukemia cells recognize conserved epitopes associated with apoptosis and oxidation. *Mol Med* 2008 Nov-Dec; **14**(11-12)**:** 665-674.
14. Chu CC, Catera R, Hatzi K, Yan XJ, Zhang L, Wang XB, *et al.* Chronic lymphocytic leukemia antibodies with a common stereotypic rearrangement recognize nonmuscle myosin heavy chain IIA. *Blood* 2008 Dec 15; **112**(13)**:** 5122-5129.
15. Mockridge CI, Potter KN, Wheatley I, Neville LA, Packham G, Stevenson FK. Reversible anergy of sIgM-mediated signaling in the two subsets of CLL defined by VH-gene mutational status. *Blood* 2007 May 15; **109**(10)**:** 4424-4431.
16. Muzio M, Apollonio B, Scielzo C, Frenquelli M, Vandoni I, Boussiotis V, *et al.* Constitutive activation of distinct BCR-signaling pathways in a subset of CLL patients: a molecular signature of anergy. *Blood* 2008 Jul 01; **112**(1)**:** 188-195.
17. Garcia-Munoz R, Galiacho VR, Llorente L. Immunological aspects in chronic lymphocytic leukemia (CLL) development. *Ann Hematol* 2012 Jul; **91**(7)**:** 981-996.
18. Seifert M, Sellmann L, Bloehdorn J, Wein F, Stilgenbauer S, Durig J, *et al.* Cellular origin and pathophysiology of chronic lymphocytic leukemia. *J Exp Med* 2012 Nov 19; **209**(12)**:** 2183-2198.

19. Chiorazzi N, Rai KR, Ferrarini M. Chronic lymphocytic leukemia. *N Engl J Med* 2005 Feb 24; **352**(8): 804-815.
20. Simonetti G, Bertilaccio MT, Ghia P, Klein U. Mouse models in the study of chronic lymphocytic leukemia pathogenesis and therapy. *Blood* 2014 Aug 14; **124**(7): 1010-1019.
21. Chen SS, Batliwalla F, Holodick NE, Yan XJ, Yancopoulos S, Croce CM, *et al.* Autoantigen can promote progression to a more aggressive TCL1 leukemia by selecting variants with enhanced B-cell receptor signaling. *Proc Natl Acad Sci U S A* 2013 Apr 16; **110**(16): E1500-1507.
22. ter Brugge PJ, Ta VB, de Bruijn MJ, Keijzers G, Maas A, van Gent DC, *et al.* A mouse model for chronic lymphocytic leukemia based on expression of the SV40 large T antigen. *Blood* 2009 Jul 02; **114**(1): 119-127.
23. Kil LP, de Bruijn MJ, van Hulst JA, Langerak AW, Yuvaraj S, Hendriks RW. Bruton's tyrosine kinase mediated signaling enhances leukemogenesis in a mouse model for chronic lymphocytic leukemia. *Am J Blood Res* 2013; **3**(1): 71-83.
24. Singh SP, Pillai SY, de Bruijn MJW, Stadhouders R, Corneth OBJ, van den Ham HJ, *et al.* Cell lines generated from a chronic lymphocytic leukemia mouse model exhibit constitutive Btk and Akt signaling. *Oncotarget* 2017 Sep 22; **8**(42): 71981-71995.
25. Renshaw BR, Fanslow WC, 3rd, Armitage RJ, Campbell KA, Liggitt D, Wright B, *et al.* Humoral immune responses in CD40 ligand-deficient mice. *J Exp Med* 1994 Nov 1; **180**(5): 1889-1900.
26. Muramatsu M, Kinoshita K, Fagarasan S, Yamada S, Shinkai Y, Honjo T. Class switch recombination and hypermutation require activation-induced cytidine deaminase (AID), a potential RNA editing enzyme. *Cell* 2000 Sep 01; **102**(5): 553-563.
27. Hoffmann A, Kerr S, Jellusova J, Zhang J, Weisel F, Wellmann U, *et al.* Siglec-G is a B1 cell-inhibitory receptor that controls expansion and calcium signaling of the B1 cell population. *Nat Immunol* 2007 Jul; **8**(7): 695-704.
28. Kersseboom R, Kil L, Flierman R, van der Zee M, Dingjan GM, Middendorp S, *et al.* Constitutive activation of Bruton's tyrosine kinase induces the formation of autoreactive IgM plasma cells. *Eur J Immunol* 2010 Sep; **40**(9): 2643-2654.
29. Kil LP, de Bruijn MJ, van Nimwegen M, Corneth OB, van Hamburg JP, Dingjan GM, *et al.* Btk levels set the threshold for B-cell activation and negative selection of autoreactive B cells in mice. *Blood* 2012 Apr 19; **119**(16): 3744-3756.
30. Robinson MD, McCarthy DJ, Smyth GK. edgeR: a Bioconductor package for differential expression analysis of digital gene expression data. *Bioinformatics* 2010 Jan 1; **26**(1): 139-140.
31. Love MI, Huber W, Anders S. Moderated estimation of fold change and dispersion for RNA-seq data with DESeq2. *Genome Biol* 2014; **15**(12): 550.
32. Saldanha AJ. Java Treeview--extensible visualization of microarray data. *Bioinformatics* 2004 Nov 22; **20**(17): 3246-3248.
33. Wohner M, Tagoh H, Bilic I, Jaritz M, Poliakova DK, Fischer M, *et al.* Molecular functions of the transcription factors E2A and E2-2 in controlling germinal center B cell and plasma cell development. *J Exp Med* 2016 Jun 27; **213**(7): 1201-1221.

34. Xu J, Foy TM, Laman JD, Elliott EA, Dunn JJ, Waldschmidt TJ, *et al.* Mice deficient for the CD40 ligand. *Immunity* 1994 Aug; **1**(5): 423-431.
35. Park H, Wahl MI, Afar DE, Turck CW, Rawlings DJ, Tam C, *et al.* Regulation of Btk function by a major autophosphorylation site within the SH3 domain. *Immunity* 1996 May; **4**(5): 515-525.
36. Jellusova J, Duber S, Guckel E, Binder CJ, Weiss S, Voll R, *et al.* Siglec-G regulates B1 cell survival and selection. *J Immunol* 2010 Sep 15; **185**(6): 3277-3284.
37. Subramanian A, Tamayo P, Mootha VK, Mukherjee S, Ebert BL, Gillette MA, *et al.* Gene set enrichment analysis: a knowledge-based approach for interpreting genome-wide expression profiles. *Proc Natl Acad Sci U S A* 2005 Oct 25; **102**(43): 15545-15550.
38. Huttmann A, Klein-Hitpass L, Thomale J, Deenen R, Carpinteiro A, Nuckel H, *et al.* Gene expression signatures separate B-cell chronic lymphocytic leukaemia prognostic subgroups defined by ZAP-70 and CD38 expression status. *Leukemia* 2006 Oct; **20**(10): 1774-1782.
39. Wang J, Coombes KR, Highsmith WE, Keating MJ, Abruzzo LV. Differences in gene expression between B-cell chronic lymphocytic leukemia and normal B cells: a meta-analysis of three microarray studies. *Bioinformatics* 2004 Nov 22; **20**(17): 3166-3178.
40. Giannoni P, Scaglione S, Quarto R, Narcisi R, Parodi M, Balleari E, *et al.* An interaction between hepatocyte growth factor and its receptor (c-MET) prolongs the survival of chronic lymphocytic leukemic cells through STAT3 phosphorylation: a potential role of mesenchymal cells in the disease. *Haematologica* 2011 Jul; **96**(7): 1015-1023.
41. Kasar S, Kim J, Improgo R, Tiao G, Polak P, Haradhvala N, *et al.* Whole-genome sequencing reveals activation-induced cytidine deaminase signatures during indolent chronic lymphocytic leukaemia evolution. *Nat Commun* 2015 Dec 07; **6:** 8866.
42. Chadeau-Hyam M, Vermeulen RC, Hebels DG, Castagne R, Campanella G, Portengen L, *et al.* Prediagnostic transcriptomic markers of Chronic lymphocytic leukemia reveal perturbations 10 years before diagnosis. *Ann Oncol* 2014 May; **25**(5): 1065-1072.
43. Bartolome-Izquierdo N, de Yebenes VG, Alvarez-Prado AF, Mur SM, Lopez Del Olmo JA, Roa S, *et al.* miR-28 regulates the germinal center reaction and blocks tumor growth in preclinical models of non-Hodgkin lymphoma. *Blood* 2017 Apr 27; **129**(17): 2408-2419.
44. Pottier N, Paugh SW, Ding C, Pei D, Yang W, Das S, *et al.* Promoter polymorphisms in the beta-2 adrenergic receptor are associated with drug-induced gene expression changes and response in acute lymphoblastic leukemia. *Clin Pharmacol Ther* 2010 Dec; **88**(6): 854-861.
45. Sitthi-Amorn J, Herrington B, Megason G, Pullen J, Gordon C, Hogan S, *et al.* Transcriptome Analysis of Minimal Residual Disease in Subtypes of Pediatric B Cell Acute Lymphoblastic Leukemia. *Clin Med Insights Oncol* 2015; **9:** 51-60.
46. Camos M, Esteve J, Jares P, Colomer D, Rozman M, Villamor N, *et al.* Gene expression profiling of acute myeloid leukemia with translocation t(8;16)(p11;p13) and MYST3-CREBBP rearrangement reveals a distinctive signature with a specific pattern of HOX gene expression. *Cancer Res* 2006 Jul 15; **66**(14): 6947-6954.

47. Hayakawa K, Formica AM, Colombo MJ, Shinton SA, Brill-Dashoff J, Morse Iii HC, *et al.* Loss of a chromosomal region with synteny to human 13q14 occurs in mouse chronic lymphocytic leukemia that originates from early-generated B-1 B cells. *Leukemia* 2016 Jul; **30**(7)**:** 1510-1519.

48. Hayakawa K, Formica AM, Brill-Dashoff J, Shinton SA, Ichikawa D, Zhou Y, *et al.* Early generated B1 B cells with restricted BCRs become chronic lymphocytic leukemia with continued c-Myc and low Bmf expression. *J Exp Med* 2016 Dec 12; **213**(13)**:** 3007-3024.

49. Klein U, Tu Y, Stolovitzky GA, Mattioli M, Cattoretti G, Husson H, *et al.* Gene expression profiling of B cell chronic lymphocytic leukemia reveals a homogeneous phenotype related to memory B cells. *J Exp Med* 2001 Dec 3; **194**(11)**:** 1625-1638.

50. Matejuk A, Beardall M, Xu Y, Tian Q, Phillips D, Alabyev B, *et al.* Exclusion of natural autoantibody-producing B cells from IgG memory B cell compartment during T cell-dependent immune responses. *J Immunol* 2009 Jun 15; **182**(12)**:** 7634-7643.

51. Zenz T, Mertens D, Kuppers R, Dohner H, Stilgenbauer S. From pathogenesis to treatment of chronic lymphocytic leukaemia. *Nat Rev Cancer* 2010 Jan; **10**(1)**:** 37-50.

52. Xie S, Li J, Wang JH, Wu Q, Yang P, Hsu HC, *et al.* IL-17 activates the canonical NF-kappaB signaling pathway in autoimmune B cells of BXD2 mice to upregulate the expression of regulators of G-protein signaling 16. *J Immunol* 2010 Mar 1; **184**(5)**:** 2289-2296.

53. Hsu HC, Yang P, Wang J, Wu Q, Myers R, Chen J, *et al.* Interleukin 17-producing T helper cells and interleukin 17 orchestrate autoreactive germinal center development in autoimmune BXD2 mice. *Nat Immunol* 2008 Feb; **9**(2)**:** 166-175.

54. Enomoto A, Ping J, Takahashi M. Girdin, a novel actin-binding protein, and its family of proteins possess versatile functions in the Akt and Wnt signaling pathways. *Ann N Y Acad Sci* 2006 Nov; **1086:** 169-184.

55. Mayer RL, Schwarzmeier JD, Gerner MC, Bileck A, Mader JC, Meier-Menches SM, *et al.* Proteomics and metabolomics identify molecular mechanisms of aging potentially predisposing for chronic lymphocytic leukemia. *Mol Cell Proteomics* 2017 Dec 1.

56. Hou Q, Liao F, Zhang S, Zhang D, Zhang Y, Zhou X, *et al.* Regulatory network of GATA3 in pediatric acute lymphoblastic leukemia. *Oncotarget* 2017 May 30; **8**(22)**:** 36040-36053.

57. Li PP, Lu K, Geng LY, Zhou XX, Li XY, Wang X. Bruton's tyrosine kinase inhibitor restrains Wnt signaling in chronic lymphocytic leukemia. *Mol Med Rep* 2016 Jun; **13**(6)**:** 4934-4938.

58. Del Giudice I, Chiaretti S, Tavolaro S, De Propris MS, Maggio R, Mancini F, *et al.* Spontaneous regression of chronic lymphocytic leukemia: clinical and biologic features of 9 cases. *Blood* 2009 Jul 16; **114**(3)**:** 638-646.

59. Eksioglu-Demiralp E, Akdeniz T, Bayik M. Aberrant expression of c-met and HGF/c-met pathway provides survival advantage in B-chronic lymphocytic leukemia. *Cytometry B Clin Cytom* 2011 Jan; **80**(1)**:** 1-7.

60. Chen Y, Zheng Y, You X, Yu M, Fu G, Su X, *et al.* Kras Is Critical for B Cell Lymphopoiesis. *J Immunol* 2016 Feb 15; **196**(4)**:** 1678-1685.

61. Guo B, Rothstein TL. RasGRP1 Is an Essential Signaling Molecule for Development of B1a Cells with Autoantigen Receptors. *J Immunol* 2016 Mar 15; **196**(6)**:** 2583-2590.

SUPPLEMENTAL DATA

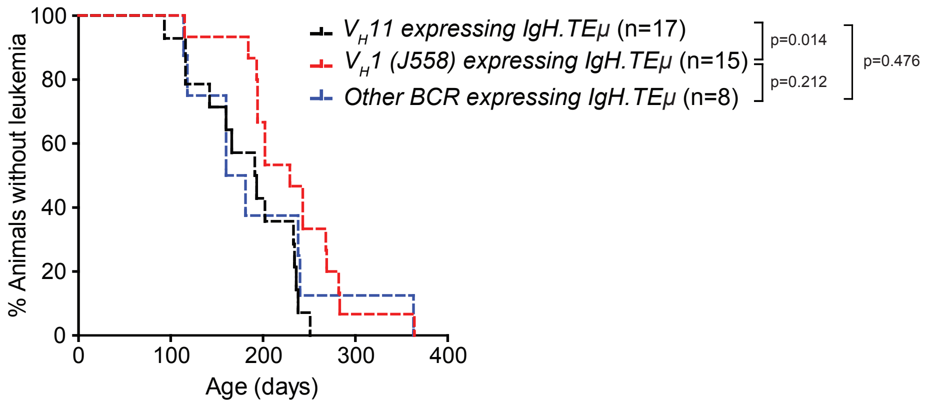

Supplementary Figure 1. Early onset of disease in VH11 expressing CLL from IgH.TEμ mice.
(**A**) Retrospective Kaplan-Meier incidence curve of CLL expressing a VH11 (dotted black line; n=17), a VH1 (J558) (dotted red line; n=15) or another (non- VH11/non-VH1) BCR (dotted blue line; n=8) from IgH.TEμ mice. CLL formation was defined by accumulation of >70% IgMb+ B-cells in peripheral blood of the mice. The log rank test was used for calculating the differences in incidence between different mouse groups.

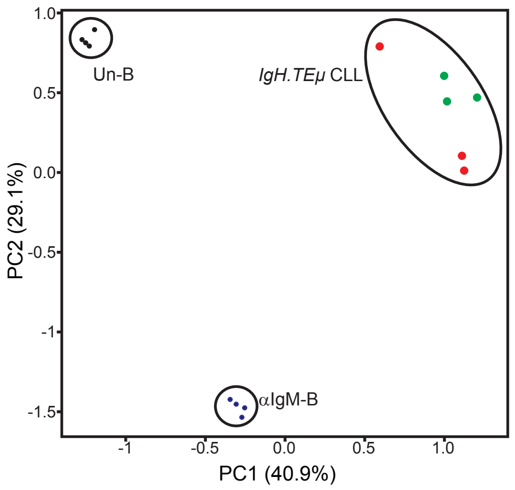

Supplementary Figure 2. RNA-seq analysis reveals an activated B-cell gene signature in CLL from IgH.TEμ mice.
Principle component analysis (PCA) comparing genome wide expression profiles in unstimulated (n=4, black) or anti-IgM-stimulated (n=4, blue) WT splenic B cells, VH11-2+/Vk14-126+ CLL (n=3, red) and non-VH11 (n=3, green) BCR expressing tumors from IgH.TEμ CLL mice.

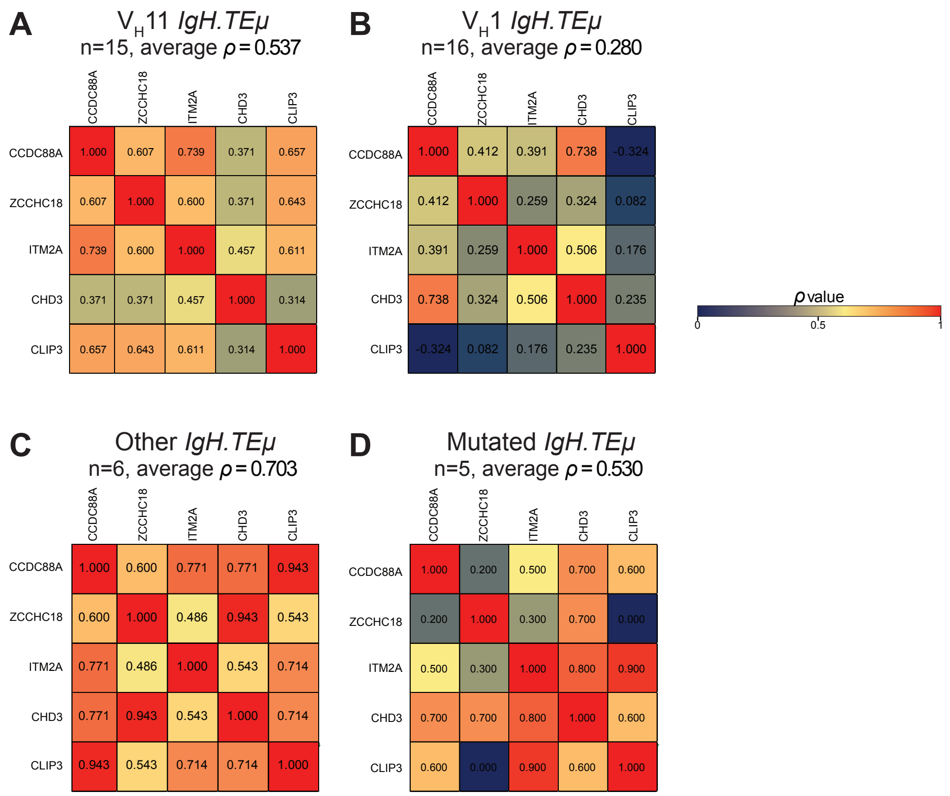

A V_H11 *IgH.TEμ*
n=15, average $\rho = 0.537$

	CCDC88A	ZCCHC18	ITM2A	CHD3	CLIP3
CCDC88A	1.000	0.607	0.739	0.371	0.657
ZCCHC18	0.607	1.000	0.600	0.371	0.643
ITM2A	0.739	0.600	1.000	0.457	0.611
CHD3	0.371	0.371	0.457	1.000	0.314
CLIP3	0.657	0.643	0.611	0.314	1.000

B V_H1 *IgH.TEμ*
n=16, average $\rho = 0.280$

	CCDC88A	ZCCHC18	ITM2A	CHD3	CLIP3
CCDC88A	1.000	0.412	0.391	0.738	-0.324
ZCCHC18	0.412	1.000	0.259	0.324	0.082
ITM2A	0.391	0.259	1.000	0.506	0.176
CHD3	0.738	0.324	0.506	1.000	0.235
CLIP3	-0.324	0.082	0.176	0.235	1.000

C Other *IgH.TEμ*
n=6, average $\rho = 0.703$

	CCDC88A	ZCCHC18	ITM2A	CHD3	CLIP3
CCDC88A	1.000	0.600	0.771	0.771	0.943
ZCCHC18	0.600	1.000	0.486	0.943	0.543
ITM2A	0.771	0.486	1.000	0.543	0.714
CHD3	0.771	0.943	0.543	1.000	0.714
CLIP3	0.943	0.543	0.714	0.714	1.000

D Mutated *IgH.TEμ*
n=5, average $\rho = 0.530$

	CCDC88A	ZCCHC18	ITM2A	CHD3	CLIP3
CCDC88A	1.000	0.200	0.500	0.700	0.600
ZCCHC18	0.200	1.000	0.300	0.700	0.000
ITM2A	0.500	0.300	1.000	0.800	0.900
CHD3	0.700	0.700	0.800	1.000	0.600
CLIP3	0.600	0.000	0.900	0.600	1.000

Supplementary Figure 3. VH1 CLL represent most heterogenous CLL subgroup in IgH.TEμ mice. Heat map depicting correlation between expression level of indicated genes measured by qRT-PCR for (**A**) VH11, (**B**) VH1, (**C**) Others unmutated, and (**D**) mutated BCR expressing CLL from IgH.TEμ mice. Numbers are spearman correlation coefficients (ρ).

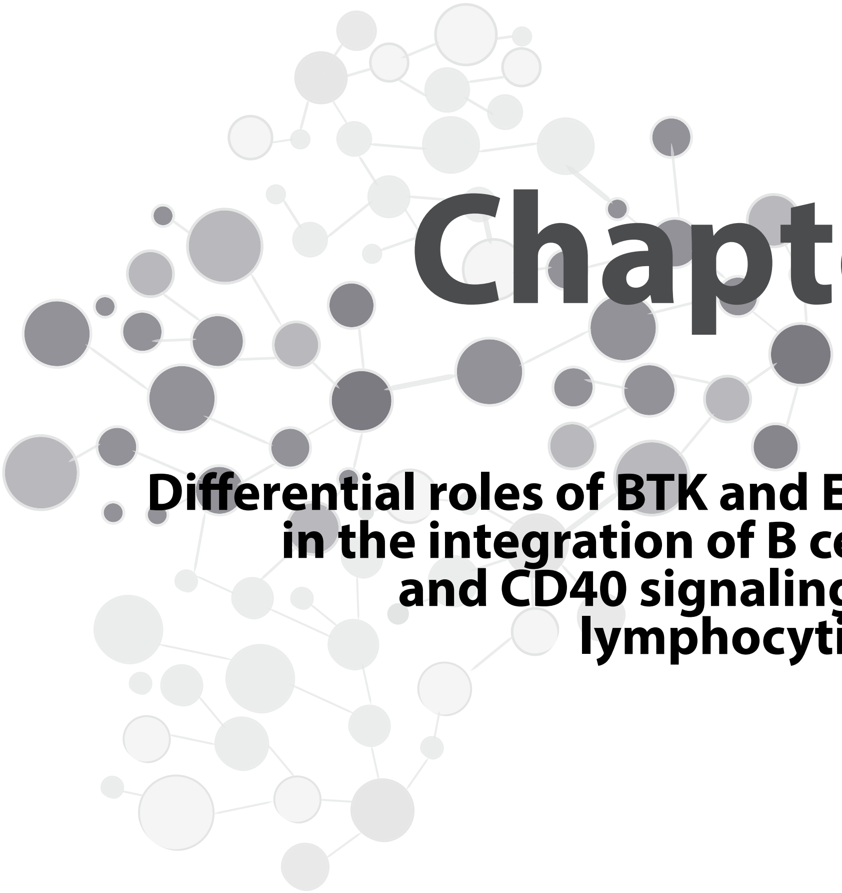

Chapter 7

Differential roles of BTK and ERK activity in the integration of B cell receptor and CD40 signaling in chronic lymphocytic leukemia

Simar Pal Singh[1,2,3], Jasper Rip[1,*], Ruud W.J. Meijers[2,*],
Marjolein J.W. de Bruijn[1], Odilia B.J. Corneth[1],Anton W. Langerak[2,#]
and Rudi W. Hendriks[1,#]

[1]Department of Pulmonary Medicine,
[2]Department of Immunology,
[3]Post-graduate School Molecular Medicine, Erasmus MC, Rotterdam, The Netherlands
[,#]Authors contributed equally*

Submitted

ABSTRACT

Both activated kinase signaling downstream of B-cell receptor (BCR) and interaction with tissue-microenvironment such as CD40L have been implicated in the pathogenesis of chronic lymphocytic leukemia (CLL). However, whether the responsiveness of CLL cells to BCR and CD40 signaling is linked is not fully elucidated. Furthermore, it remains unclear whether the anergic phenotype of CLL cells, characterized by reduced BCR-mediated extracellular signal-regulated kinase (ERK) activation also involves reduced responses to CD40 triggering. Here, we used phospho-specific flow cytometry to study signaling properties of CLL cells. When analyzed directly *ex vivo*, basal phosphorylation of BTK(Y223), PLCγ(Y759) and ribosomal protein S6(S240/S244), which is a downstream target of the PI3K/AKT pathway were correlated, but this was not the case for phospho-ERK(T202/Y204). Phospho-BTK and phospho-ERK were equally induced by BCR and CD40-stimulation in CLL. High basal levels of phospho-ERK correlated with unresponsiveness to BCR and CD40 engagement, as well as apoptosis susceptibility. In contrast, no such correlations were found for phospho-BTK. These findings indicate a differential role for the BTK/PI3K and ERK pathways in CLL. These findings will impact on treatment selection targeting specific kinases and could provide a molecular explanation for disease progression in patients who are currently on targeted kinase therapies.

Keywords: B-cell receptor (BCR) signaling, Bruton's tyrosine kinase (Btk), extracellular signal-regulated kinase (ERK), chronic lymphocytic leukemia (CLL)

INTRODUCTION

Chronic lymphocytic leukemia (CLL) is the most common adult leukemia and is characterized by an accumulation of monoclonal CD5$^+$ mature B-cells with low surface immunoglobulin (sIg) expression in peripheral blood (1). It is a clinically and molecularly heterogeneous disease, subclassified on the basis of Ig heavy chain variable genes (IGHV) mutational status. Whereas patients with mutated CLL (M-CLL, <98% *IGHV* germline identity) often develop indolent disease, unmutated CLL (U-CLL, ≥98% identity) evolves rapidly and has a less favorable prognosis (1). Small molecule inhibitors targeting B-cell receptor (BCR) signaling molecules, such as Bruton's tyrosine kinase (BTK) or phosphatidylinositol-3-kinase (PI3K), which are constitutively active in CLL, have shown impressive clinical anti-tumor activity (2-4). Moreover, extracellular signal-regulated kinase (ERK)1/2 is constitutively active and was found to be associated with NFAT activation and translocation to the nucleus and as a result with a higher anergic state(5, 6). CLL cells interact with the tissue micro-environment and their survival is thought to be driven by T-cell independent BCR signals or by T helper cells through CD40L (7, 8). However, to which extent CLL vary in their dependence on BCR and CD40 signaling is not fully elucidated. Furthermore, it is unclear whether the anergic phenotype of CLL cells, characterized by reduced BCR responsiveness (5), also involves reduced responses to CD40 triggering. Here, we used phospho-specific flow cytometry to study signaling properties of CLL cells. We observed a parallel induction of phospho-BTK (pBTK) and pERK downstream of BCR and CD40-activated pathways in U-CLL. Moreover, basal levels of phosphorylation of ERK – but not BTK – were associated with unresponsiveness to B cell receptor or CD40 stimulation and with increased apoptosis susceptibility of CLL cells.

MATERIALS AND METHODS

Patients and healthy controls

Primary patient material was obtained from peripheral blood of CLL patients, while the peripheral blood from healthy individuals was obtained via Erasmus MC and via Sanquin blood bank (Rotterdam). Diagnostic and control samples were collected upon informed consent and anonymized for further use, following the guidelines of the Institutional Review Board MEC2015-741 (for CLL) and MEC2016-202 (healthy controls), and in accordance with the declaration of Helsinki. Peripheral blood mononuclear cells (PBMCs) were isolated using Ficoll Hypaque (GE Healthcare, Little Chalfont, UK) according to the manufacturer's instructions, and were stored frozen in fetal calf serum (FCS) supplemented with 10% DMSO.

IGHV sequence analysis

Genomic DNA was extracted from PBMCs with use of spin-column kits and QIAcube (Qiagen, Valencia, CA, USA). Primers and protocols for IGHV mutation status analysis were used according to the BIOMED-2 protocol and following ERIC guidelines(29, 30). In brief, PCR products were analyzed by electrophoresis on polyacrylamide gels for monoclonality, followed by direct sequencing. Sequencing results were analyzed online using the IMGT/V-QUEST on the IMGT website (www.imgt.org, version 3.2.32). BCR characteristics of all patients are provided in **Supplementary Table 1**.

Flow cytometry procedures

Phospho-flow cytometry. For intracellular flow cytometry analysis of phosphorylated proteins (Phospho-flow), PBMCs from healthy controls or CLL patients were stimulated with either 20 µg/ml anti-human $F(ab')_2$ α-IgM (Southern Biotech) or 2 µg/ml recombinant human CD40 ligand (R&D Systems) plus 0.25 µg/ml rIL-4 (Peprotech) for 1 min (for pBTK) or 10 min (for pERK). Unstimulated control cells were treated in parallel without stimulus. In addition, unstimulated control cells were separately stained for either pPLCγ2 or pS6 to measure basal levels. PBMCs were stained for life/dead marker (Invitrogen Probes) prior to fixation. Cells were then fixed and permeabilized in FoxP3 staining kit Fix/Perm solution (eBioscience) at 37°C for 10 min. For the identification of CLL cells or B cells (in case of healthy control), cells were additionally stained with anti-CD3 (BV711, Clone UCHT) and anti-CD19 (FITC, Clone HIB19) from BD Biosciences at 4°C for 30 minutes in FoxP3 staining kit wash buffer (eBioscience) after fixation. Following, cells were stained with either anti-pBtk (Y223) (PE, Clone N35-86), anti-pErk (T202/Y204) (PE, Clone 20A), anti-pPLCγ2 (Y759) (AF647, clone K86-689.37) from BD Phosflow for 30 minutes at RT in the dark or with unconjugated anti-pS6 (S240/S244) (Clone D68F8, Cell Signaling Technologies) and subsequently with a PE-conjugated anti-rabbit secondary antibody (Jackson ImmunoResearch) both for 15 minutes at RT in the dark. The measurements were performed on a LSRII flow cytometer (BD Biosciences) and results were analyzed using FlowJo-V10 software (TreeStar).

Apoptosis analysis. CLL cells either uncultured or cultured for 6 hours in RPMI medium supplemented with 10% FCS, 50 µg/ml gentamycin and 50 µM 2-mercapto-ethanol (culture medium) at 37°C and 5% CO_2 were initially stained with anti-CD3 (BV711, Clone UCHT1) and anti-CD19 (PE-Cy7, Clone SJ25C1/HIB19) from BD Biosciences. Cells were subsequently stained for annexin V (PE) and 7-Aminoactinomycin D (7-AAD) (PE-Cy5) in diluted binding buffer (all BD Biosciences) at room temperature (RT) for 15 min in the dark. The measurements were performed within 1 hour of staining on a LSRII flow cytometer (BD Biosciences) and results were analyzed using FlowJo-V10 software (TreeStar).

Statistical analyses

Statistical analysis was performed using GraphPad Prism software (San Diego, CA, USA). For comparing differences between healthy controls and CLL B-cells, the Mann-Whitney *U*-test was used for nonparametric testing. For comparing two paired groups, the Wilcoxon signed rank test was used for nonparametric testing. To study the correlation between variables, we used linear regression analysis.

RESULT AND DISCUSSION

Basal phosphorylation of BTK, PLCγ2 and S6 – but not ERK – are correlated in CLL cells

We applied flow cytometry to investigate the phosphorylation levels of the BCR proximal (BTK and PLCγ2) and distal signaling proteins (ERK and ribosomal protein S6) in peripheral blood B-cell fractions ($CD19^+CD3^-$) of 8 mutated (M-CLL) and 8 unmutated (U-CLL) samples (see Suppl. Table S1 for CLL patient details). $CD19^+CD3^-$ B-cell fractions from peripheral blood mononuclear cells (PBMCs) of healthy controls (HC) served as controls. Compared to HC B-cells, CLL cells showed a trend of lower basal levels of pBTK(Y223) and significantly reduced pPLCγ2(Y759) levels, whereas no differences in pERK(T202/Y204) and pS6(S24/S244) were observed (**Figure 1A**). Basal levels of pBTK and pPLCγ2 were correlated in CLL (R^2= 0.382; p=0.011), particularly in M-CLL (R^2= 0.556; p=0.034; **Figure 1B**). Although pBTK and pS6 were not significantly correlated, a strong correlation between pPLCγ2 and pS6 was observed (R^2= 0.648; p=0.0002; **Figure 1B**). We did not find such a correlation for HC B cells (**Supplementary Figure 1**). This finding pointed to common upstream regulation of PLCγ2 and S6, which would be consistent with aberrant *in vivo* activation of the phosphoinositide 3-kinase (*PI3K*) / AKT kinase pathway in CLL and the observed efficacy of the small molecule PI3Kδ inhibitor idelalisib (4, 9).

In contrast, levels of basal pERK did not correlate with any of the phospho-targets tested (shown for pBTK(Y223) in **Figure 1B**), thus uncoupling pERK activation from PLCγ2 and PI3K-induced signaling. Hence, pERK activation probably occurs downstream of the Ras/Raf/MEK signaling pathway, independently of BTK (10). This is also in line with earlier findings showing that ERK activation in CLL can be independent of PI3K/AKT signaling (5). Likewise, Ringshausen *et al.* found no correlation between NFκB, a BTK downstream target, and p38 MAPK in a subset of CLL patients, further validating that the MAPK and PI3K pathways can be independently activated and have different roles in CLL(11).

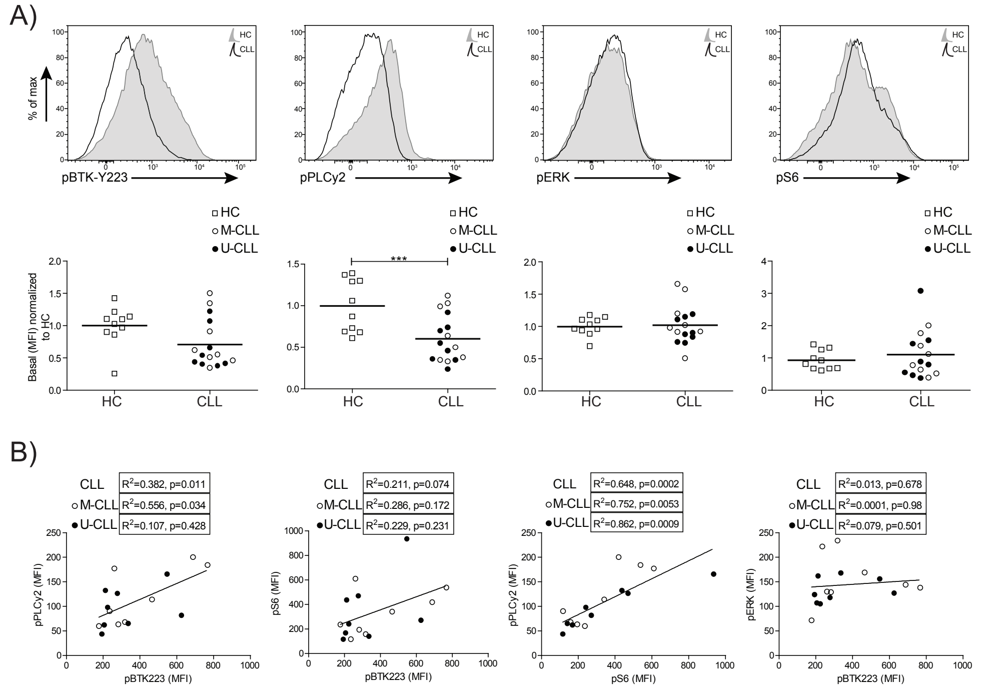

Figure 1. pERK is independently regulated from the BTK and PI3K/AKT signaling pathways in CLL. (**A**, *top*) Flow cytometry histogram overlays showing a comparison of basal (unstimulated) levels of pBTK(Y223), pPLCγ2, pERK and pS6 between representative healthy control (HC, *grey shaded area*) and a CLL patient (*black line*). (**A**, *bottom*) Quantification of median fluorescence intensity (MFI) values for pBTK(Y223), pPLCγ2, pERK and pS6 in unstimulated (basal) B-cells from HC (*square*, n=10), M-CLL (*open circle*, n=8) and U-CLL (*closed circle*, n=8). Each dot represents an individual HC or CLL patient. Data shown is normalized to the mean MFI (median fluorescence intensity) values of the HC group, which was set to 1. Statistical analysis was performed using a Mann-Whitney *U*-test. ***p<0.0001. (**B**) Linear regression analysis comparing basal levels of the indicated phospho-targets in CLL patients (M-CLL, open circles n=8; U-CLL, closed circles n=8). Lines represent regression analyses for the whole CLL group.

Both BTK and ERK show a correlation of BCR-induced and CD40L-induced phosphorylation

To further explore the relation between the PI3K and MAPK pathways in CLL, we decided to focus on BTK(Y223) and ERK phosphorylation. We analyzed the effect of BCR stimulation, using F(ab')2 anti-human IgM (α-IgM), or recombinant CD40L in the presence of recombinant interleukin-4 (rCD40L-IL4) on pBTK(Y223) and pERK levels in U-CLL and M-CLL. Although we noticed heterogeneity in pBTK(Y223) induction in CLL, the responsiveness of pBTK(Y223) and pERK to αIgM or rCD40L-IL4 was significant (**Figure 2A**). Surprisingly, the relative αIgM- or rCD40L-IL4- mediated pBTK(Y223) induction in CLL was higher compared to HC B-cells (**Figure 2A**). This could be related to lower basal pBTK(Y223) levels in CLL (**Figure 1A**). In these analyses, we did not detect significant differences in responsiveness to α-IgM or rCD40L-IL4 between U-CLL and M-CLL.

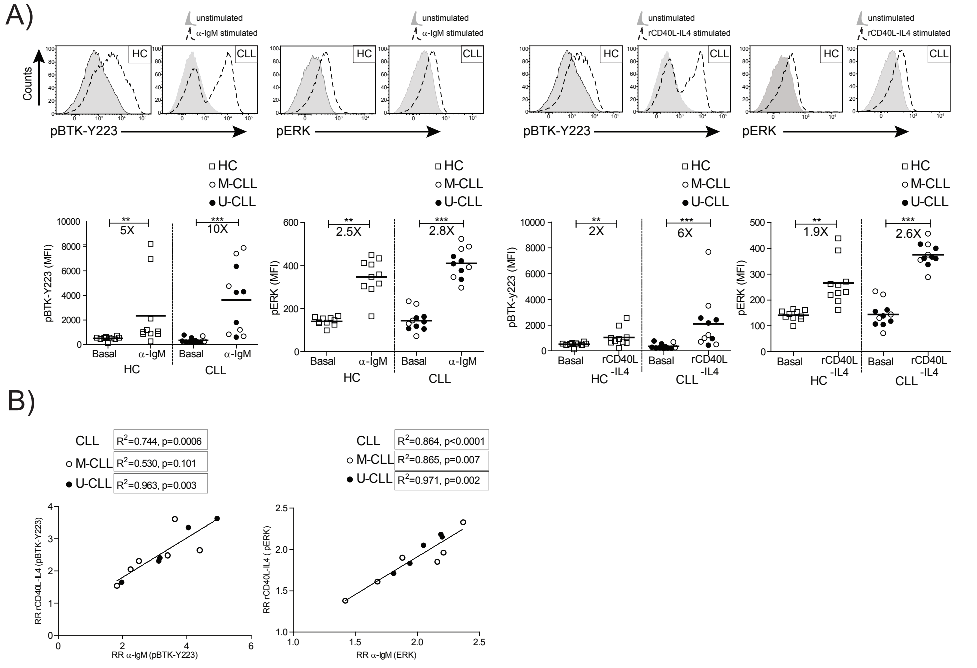

Figure 2. Both BTK and ERK show a correlation of BCR-induced and CD40L-induced phosphorylation (**A**, *top*) Flow cytometry histogram overlays showing a comparison of pBTK(Y223) and pERK signals in unstimulated and (*left*) αIgM-stimulated or (*right*) rCD40L-IL-4-stimulated gated B cells from a healthy control (HC) and a CLL patient. (**A**, *bottom*) Quantification of median fluorescence intensity (MFI) values for pBTK(Y223) and pERK in unstimulated (basal) and (*left*) αIgM-stimulated or (*right*) rCD40L-IL-4-stimulated gated B-cells from HC (*square*), M-CLL (*open circle*) and U-CLL (*closed circle*). (**B**) Linear regression analysis between relative responses (RR, log fold change) upon α-IgM-stimulation or rCD40L-IL4-stimulation of the indicated phospho-targets in M-CLL (*open circle*) and U-CLL (*closed circle*) patients. Lines represent regression analyses for the whole CLL group. Each dot represents an individual HC or CLL patient. Statistical analyses were performed by Wilcoxon-signed rank test. **p<0.001, ***p<0.0001.

Gene expression profiling studies initially suggested that both M-CLL and U-CLL homogeneously reflect memory B cells (12). More recent transcriptome analyses revealed that U-CLL and M-CLL resemble mature pre-germinal center (pre-GC) CD5$^+$CD27$^-$ B cells and a distinct, previously unrecognized, CD5$^+$CD27$^+$ post-GC B cell subset, respectively (13). To investigate the involvement of GC or T-cell help in U-CLL we therefore compared the responsiveness of CLL cells to α-IgM and rCD40L-IL4 stimulation. We found that both for BTK(Y223) and for ERK there was a significant correlation between α-IgM and rCD40L-IL4-induced phosphorylation, particularly in U-CLL (R^2=0.963 and p=0.003 for pBTK and R^2=0.971, p=0.002 for pERK; **Figure 2B**). Interestingly, these findings suggest that U-CLL cells are equally dependent on the BCR and the T-cell or GC-dependent pathway and would be consistent with the reported strong dependency of U-CLL cells on pro-survival signals including CD40 triggering (7). In line, we recently provided *in vivo* evidence for a

T-cell dependent origin of U-CLL. We observed that in the *IgH.TEμ* CLL mouse model a major subset of unmutated CLL was dependent on T cell signals. Hereby, CD40L-mediated signaling played an important role in shaping the CLL BCR repertoire of unmutated CLL (14). However, absence of a significant correlation between α-IgM and rCD40L-IL4-induced pBTK(Y223) levels in M-CLL (**Figure 2B**) suggests differential activation of the PI3K pathway upon BCR or CD40 triggering in this subset, which requires further validation using large CLL patient cohorts.

Basal levels of pERK – but not pBTK – are associated with unresponsiveness and apoptosis susceptibility of CLL cells

CLL cells from subgroup of patients were shown to exhibit constitutive activation of ERK and nuclear factor of activated T cells c1 (NF-ATc1), thereby reducing the ability to further signal through their BCR, and thus resembling anergic B-cells (5, 6). Such a phenotype is thought to require either constant occupancy of the BCR by (self)antigen or cell-autonomous signaling dependent on an internal BCR epitope (15). Accordingly, we found that high basal pERK expression was associated with BCR unresponsiveness, because pERK levels in unstimulated CLL cells showed a strong inverse correlation with the relative pERK induction upon αIgM-stimulation (R^2= 0.788, p=0.0003)(**Figure 3A**). No such inverse correlation was observed for pBTK(Y223)(**Figure 3A**). Importantly, comparison of basal pERK levels and the relative pERK induction upon rCD40L-IL4 stimulation also revealed a strong inverse correlation (R^2= 0.883, p<0.0001), both in M-CLL and U-CLL, which was not seen for pBTK (**Figure 3B**).

Failure to induce pERK in CLL cases with high basal pERK expression by either type of stimulation indicates the strict regulation of this pathway and suggests a role beyond anergy induction in CLL. Activation of ERK can promote both apoptotic and anti-apoptotic events (16, 17). It has been reported that CLL cells with constitutively active ERK are resistant to spontaneous apoptosis upon culture *in vitro* (6). However, CLL cells cultured on mouse fibroblasts were protected from spontaneous apoptosis through the PI3K/AKT but not the RAF–MEK–ERK pathway (18). To explore whether ERK activation in CLL cells is associated with cell death, we compared basal pERK levels to *in vitro* survival of CLL cells and found an inverse correlation (R^2=0.310; p=0.025) (**Figure 3C**). No such inverse correlation was found for pBTK(Y223). Rather for U-CLL, a positive correlation between basal pBTK levels and cellular survival was noticed (R^2=0.660; p=0.014). This finding suggests that specifically pERK signaling – and not pBTK-dependent pathways - can lead to activation of a more apoptotic pathway downstream in CLL and conversely that CLL cells can tightly regulate ERK phosphorylation to promote cell growth. Likewise, constitutive ERK activation has been linked to susceptibility to CD40-mediated cell death in diffuse large B-cell lymphoma cell lines (19, 20).

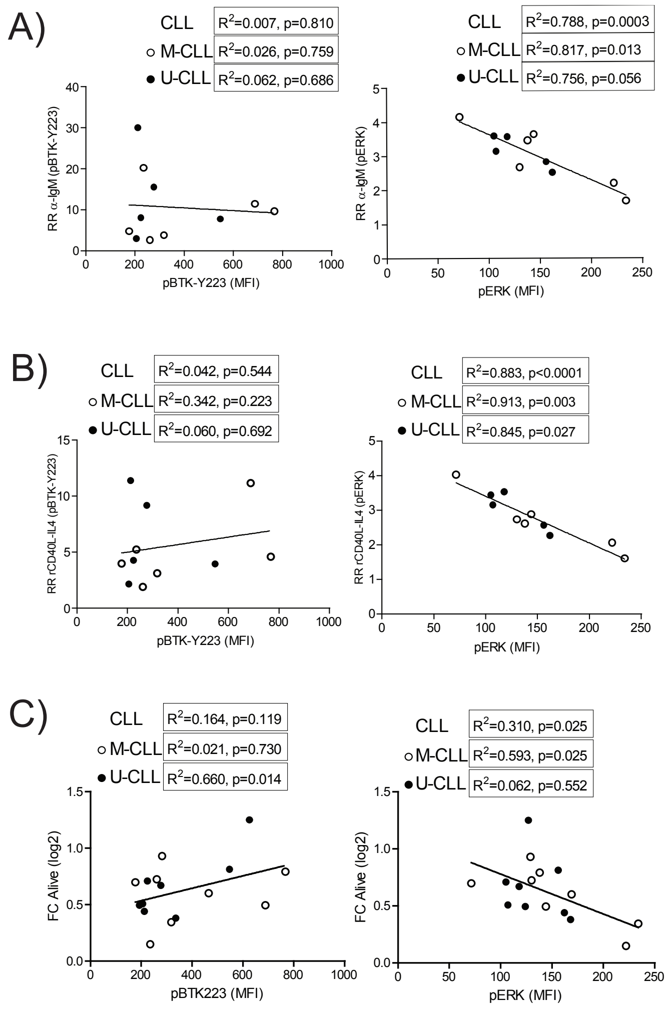

Figure 3. Enhanced pERK activation promotes anergy and apoptosis susceptibility in CLL
(**A,B**) Linear regression analysis comparing basal (unstimulated) and relative response (RR, log fold change) to (**A**) α-IgM stimulation or (**B**) rCD40L-IL4 stimulation of pBTK(Y223) and pERK in M-CLL (open circle) and U-CLL (closed circle) patients. (**C**) Linear regression analysis comparing basal levels of pBTK(Y223) and pERK and spontaneous apoptosis, measured as log2 transformed fraction (FC) of alive cells (annexinV and 7-AAD double negative) following 6hrs of *in vitro* culture. The proportion of alive cells in uncultured samples was set to 1. Lines represent regression analyses for the whole CLL group.

In conclusion, we report here a dual role of ERK activation in CLL (**Figure 4**). On the one hand, ERK activation is known to promote cell survival by enhancing downstream cell death regulators, including BCL-2 and MCL-1, paralleling the role of the PI3K/AKT-mediated pathway. However, to what extent the upstream processes co-operate to feed

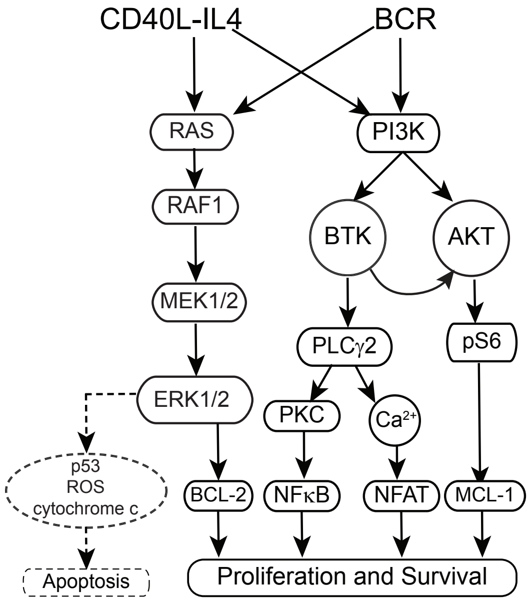

Figure 4. Dual role of pERK activation in CLL.
Schematic of signaling cascade depicting independent activation of the MAPK (RAS/RAF1/MEK/ERK) and PI3K (BTK/PLCγ2/S6) pathways downstream of the BCR and CD40L in CLL cells. The role of ERK activation in the induction of apoptosis in CLL is suggested in dotted lines.

into these common downstream cell-death regulators is not fully elucidated. We observed independent activation of ERK and BTK/PI3K/AKT pathways in CLL (**Figure 1B**), suggesting redundancy in survival signaling in CLL. Such redundancy should be considered while using inhibitors having specificity for certain kinases in cancer therapy. Moreover, our findings indicate that combination therapy with multiple kinase inhibitors and/or BH3-mimetics would be an effective strategy to target CLL. In line, BTK inhibitors, PI3K inhibitors and BCL-2 inhibitors are now approved for CLL therapy in the clinic and ERK pathway inhibition was recently suggested as a target for new antitumor strategies (10, 21). On the other hand, prolonged ERK activation (6-72 hours) has been implicated in DNA-damaging agent-induced cell death, p53 upregulation, cytochrome c release or ROS production in cancers of various origins (17). In support thereof, we show that ERK activation, beyond being a marker of anergy in CLL, was also associated with increased apoptosis susceptibility. Importantly, our finding of a dual role of ERK activation may provide a molecular explanation for the observation that CLL patients show progression despite kinase targeting therapy (22-27). It is conceivable that in such patients ERK-mediated cell death is abrogated, because PI3K and BTK inhibition have been shown to block CD40L-induced ERK signaling in CLL cells (28). Although the crucial biochemical signaling events underlying sensitivity to ERK-mediated cell death in CLL remains to be fully understood, the property of ERK to mediated cell death may be exploited to target CLL cells. Further investigation using large CLL patient cohorts containing a wide range of stereotypic and non-stereotypic U-CLL and M-CLL is required to translate our findings.

ACKNOWLEDGMENTS

The authors would like to thank Alice F Muggen, Otto Bachaus, Mariana P. de Almeida, Catarina Gago da Graça for assistance at various stages of the project. These studies were partly supported by a Dutch Cancer Society grant (KWF 2014-6564), the Netherlands Organization for Scientific Research and by an unrestricted research grant from Roche-Genentech.

REFERENCES

1. Hallek M, Cheson BD, Catovsky D, Caligaris-Cappio F, Dighiero G, Dohner H, et al. iwCLL guidelines for diagnosis, indications for treatment, response assessment, and supportive management of CLL. Blood. 2018;131(25):2745-60.
2. Byrd JC, Furman RR, Coutre SE, Flinn IW, Burger JA, Blum KA, et al. Targeting BTK with ibrutinib in relapsed chronic lymphocytic leukemia. N Engl J Med. 2013;369(1):32-42.
3. Byrd JC, Harrington B, O'Brien S, Jones JA, Schuh A, Devereux S, et al. Acalabrutinib (ACP-196) in Relapsed Chronic Lymphocytic Leukemia. N Engl J Med. 2016;374(4):323-32.
4. Furman RR, Sharman JP, Coutre SE, Cheson BD, Pagel JM, Hillmen P, et al. Idelalisib and rituximab in relapsed chronic lymphocytic leukemia. N Engl J Med. 2014;370(11):997-1007.
5. Muzio M, Apollonio B, Scielzo C, Frenquelli M, Vandoni I, Boussiotis V, et al. Constitutive activation of distinct BCR-signaling pathways in a subset of CLL patients: a molecular signature of anergy. Blood. 2008;112(1):188-95.
6. Apollonio B, Scielzo C, Bertilaccio MT, Ten Hacken E, Scarfo L, Ranghetti P, et al. Targeting B-cell anergy in chronic lymphocytic leukemia. Blood. 2013;121(19):3879-88, S1-8.
7. Coscia M, Pantaleoni F, Riganti C, Vitale C, Rigoni M, Peola S, et al. IGHV unmutated CLL B cells are more prone to spontaneous apoptosis and subject to environmental prosurvival signals than mutated CLL B cells. Leukemia. 2011;25(5):828-37.
8. Scielzo C, Apollonio B, Scarfo L, Janus A, Muzio M, Ten Hacken E, et al. The functional in vitro response to CD40 ligation reflects a different clinical outcome in patients with chronic lymphocytic leukemia. Leukemia. 2011;25(11):1760-7.

9. Brown JR, Byrd JC, Coutre SE, Benson DM, Flinn IW, Wagner-Johnston ND, et al. Idelalisib, an inhibitor of phosphatidylinositol 3-kinase p110delta, for relapsed/refractory chronic lymphocytic leukemia. Blood. 2014;123(22):3390-7.
10. Gimenez N, Martinez-Trillos A, Montraveta A, Lopez-Guerra M, Rosich L, Nadeu F, et al. Mutations in RAS-BRAF-MAPK-ERK pathway define a specific subgroup of patients with adverse clinical features and provide new therapeutic options in chronic lymphocytic leukemia. Haematologica. 2018.
11. Ringshausen I, Dechow T, Schneller F, Weick K, Oelsner M, Peschel C, et al. Constitutive activation of the MAPkinase p38 is critical for MMP-9 production and survival of B-CLL cells on bone marrow stromal cells. Leukemia. 2004;18(12):1964-70.
12. Klein U, Tu Y, Stolovitzky GA, Mattioli M, Cattoretti G, Husson H, et al. Gene expression profiling of B cell chronic lymphocytic leukemia reveals a homogeneous phenotype related to memory B cells. J Exp Med. 2001;194(11):1625-38.
13. Seifert M, Sellmann L, Bloehdorn J, Wein F, Stilgenbauer S, Durig J, et al. Cellular origin and pathophysiology of chronic lymphocytic leukemia. J Exp Med. 2012;209(12):2183-98.
14. Pal Singh S, de Bruijn MJW, de Almeida MP, Meijers RWJ, Nitschke L, Langerak AW, et al. Identification of Distinct Unmutated Chronic Lymphocytic Leukemia Subsets in Mice Based on Their T Cell Dependency. Front Immunol. 2018;9:1996.
15. Muggen AF, Singh SP, Hendriks RW, Langerak AW. Targeting Signaling Pathways in Chronic Lymphocytic Leukemia. Curr Cancer Drug Targets. 2016;16(8):669-88.
16. Balmanno K, Cook SJ. Tumour cell survival signalling by the ERK1/2 pathway. Cell Death Differ. 2009;16(3):368-77.
17. Cagnol S, Chambard JC. ERK and cell death: mechanisms of ERK-induced cell death--apoptosis, autophagy and senescence. FEBS J. 2010;277(1):2-21.
18. Cuni S, Perez-Aciego P, Perez-Chacon G, Vargas JA, Sanchez A, Martin-Saavedra FM, et al. A sustained activation of PI3K/NF-kappaB pathway is critical for the survival of chronic lymphocytic leukemia B cells. Leukemia. 2004;18(8):1391-400.
19. Hollmann CA, Owens T, Nalbantoglu J, Hudson TJ, Sladek R. Constitutive activation of extracellular signal-regulated kinase predisposes diffuse large B-cell lymphoma cell lines to CD40-mediated cell death. Cancer Res. 2006;66(7):3550-7.
20. Alizadeh AA, Eisen MB, Davis RE, Ma C, Lossos IS, Rosenwald A, et al. Distinct types of diffuse large B-cell lymphoma identified by gene expression profiling. Nature. 2000;403(6769):503-11.
21. Brown JR. Relapsed CLL: sequencing, combinations, and novel agents. Hematology Am Soc Hematol Educ Program. 2018;2018(1):248-55.
22. Stephens DM, Byrd JC. How we manage ibrutinib intolerance and complications in patients with chronic lymphocytic leukemia. Blood. 2019.
23. Mato AR, Nabhan C, Barr PM, Ujjani CS, Hill BT, Lamanna N, et al. Outcomes of CLL patients treated with sequential kinase inhibitor therapy: a real world experience. Blood. 2016;128(18):2199-205.

24. Mato AR, Hill BT, Lamanna N, Barr PM, Ujjani CS, Brander DM, et al. Optimal sequencing of ibrutinib, idelalisib, and venetoclax in chronic lymphocytic leukemia: results from a multicenter study of 683 patients. Ann Oncol. 2017;28(5):1050-6.
25. Barrientos JC, Kaur M, Mark A, Chung J, Driscoll N, Bender A, et al. Outcomes of patients with chronic lymphocytic leukemia (CLL) after idelalisib therapy discontinuation. Am Soc Hematology; 2015.
26. Kaur V, Swami A. Ibrutinib in CLL: a focus on adverse events, resistance, and novel approaches beyond ibrutinib. Ann Hematol. 2017;96(7):1175-84.
27. Pal Singh S, Dammeijer F, Hendriks RW. Role of Bruton's tyrosine kinase in B cells and malignancies. Mol Cancer. 2018;17(1):57.
28. Slinger E, Thijssen R, Kater AP, Eldering E. Targeting antigen-independent proliferation in chronic lymphocytic leukemia through differential kinase inhibition. Leukemia. 2017;31(12):2601-7.
29. van Dongen JJ, Langerak AW, Bruggemann M, Evans PA, Hummel M, Lavender FL, et al. Design and standardization of PCR primers and protocols for detection of clonal immunoglobulin and T-cell receptor gene recombinations in suspect lymphoproliferations: report of the BIOMED-2 Concerted Action BMH4-CT98-3936. Leukemia. 2003;17(12):2257-317.
30. Rosenquist R, Ghia P, Hadzidimitriou A, Sutton LA, Agathangelidis A, Baliakas P, et al. Immunoglobulin gene sequence analysis in chronic lymphocytic leukemia: updated ERIC recommendations. Leukemia. 2017;31(7):1477-81.

SUPPLEMENTAL DATA

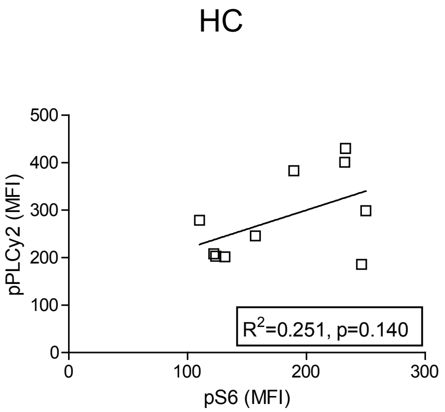

Supplementary Figure 1. No correlation for basal pPLCγ and pS6 in B-cells from healthy controls
Linear regression analysis comparing basal levels of pPLCγ2 and pS6 in healthy controls B-cells (n=10).

Supplementary Table 1 : B-cell receptor characteristics of CLL patients.

CLL ID	Sample ID	% BCR germline identity	IGHV gene	IGHD gene	IGHJ gene	VH CDR3 length	VH CDR3 Sequence AA	gender
KL2013-007	M-CLL	96.02	IGHV4-30*01	IGHD2-2*01	IGHJ6*03	16	ARDAGVVPVHYYYMDV	Male
KL2014-413	M-CLL	91.9	IGHV3-30*03	IGHD5-12*01	IGHJ3*02	14	ANELVTSSYDGIDIW	Male
KL2015-134	M-CLL	90.6	IGHV4-61*02	IGHD5-18*01	IGHJ4*02	12	ARDPDTYGYVDC	Male
KL2015-241*	M-CLL	92.02	IGHV3-48*03	IGHD2-15*01	IGHJ1*01	9	ARDGGSYPL	Male
KL2015-240	M-CLL	89.73	IGHV3-30*03	IGHD6-13*01	IGHJ6*02	19	AKVGRPAAFEEYYYGMDV	Female
KL2016-263	M-CLL	96.85	IGHV5-10-1*01	IGHD2-15*01	IGHJ6*02	28	ATGEGGLGWNPRYCSGGSCYEVGYGMDV	Male
KL2017-070*	M-CLL	91.03	IGHV3-30*03	IGHD3-9*01	IGHJ4*02	18	AKPGSVFRYFDWISGLWYW	Male
KL2010-250	M-CLL	94.05	IGHV3-72*01	IGHD2-8*01	IGHJ6*02	20	GRIYCTLSRCSIDQYYGMDV	Male
KL2011-589	U-CLL	100.00	IGHV1-69*06	IGHD3-3*01	IGHJ6*03	21	ASGSIFGVVIGSYYYYYMDVW	Male
KL2013-006	U-CLL	100.00	IGHV4-39*01	IGHD3-3*01	IGHJ6*02	26	ARHASPRDFWSGYPELIYYYYGMDVW	Male
KL2011-447	U-CLL	100.00	IGHV1-69*01	IGHD3-3*01	IGHJ4*02	22	ARAAVPYYDFWSGYSLDSGFDY	Male
KL2014-420*	U-CLL	100.00	IGHV1-69*01	IGHD2-2*01	IGHJ6*02	21	ASLTIVVVPAAMSYYYYGMDVW	Male
KL2014-260*	U-CLL	100.00	IGHV3-20*01	IGHD3-3*01	IGHJ4*02	21	ARGTGITIFGVVHTTEYYFDYW	Male
KL2014-264	U-CLL	100.00	IGHV1-24*01	IGHD4-23*01	IGHJ4*02	16	ATLGAARQLGWYYFDYW	Male
KL2014-372	U-CLL	100.00	IGHV1-69*01	IGHD3-16*02	IGHJ5*02	22	ARDPPFDYIWGSYRYRANWFDPW	Female
KL2011-399*	U-CLL	100.00	IGHV4-4*05	IGHD3-16*02	IGHJ6*02	26	ARGRRDDYIWGSYRYTDLGYYYGMDV	Female

* No data available upon α-IgM or rCD40L-IL4 stimulation for p-BTK-Y223 and p-ERK.

Chapter 8

General Discussion

Part of this chapter was published in

Muggen A.F. et al., Targeting Signaling Pathways in Chronic Lymphocytic Leukemia, Current Cancer Drug Targets, 2016, 16, 669-688

Pal Singh et al., Targeting Bruton's tyrosine kinase expression levels through microRNAs in chronic lymphocytic leukemia treatment, Translational Cancer Res 2017;6(Suppl 3):S502-S507

GENERAL DISCUSSION

In this thesis we addressed the role of B cell receptor (BCR) signaling and important associated other signal transduction cascades in the pathogenesis of chronic lymphocytic leukemia (CLL). For these studies, we employed the *IgH.TEμ* CLL mouse model previously generated in our laboratory, EMC cell lines derived from the CLL-like leukemic B cells present in aging *IgH.TEμ* mice and panels of human U-CLL and M-CLL samples. The experiments described in this thesis included transcriptome and flow cytometic analyses, *in vivo* experiments involving various mouse crosses, as well as *in vitro* mouse or *ex vivo* human inhibitor studies.

Our main findings are:

1. Antigenic stimulation via the BCR plays a major role in transformation of normal B cells into rapidly proliferating CD19$^+$IgM^{low}CD5$^+$CD43$^+$IgD$^-$ CLL-like cells in *IgH.TEμ* mice. Hereby, Btk overexpression and T-cell help (α-CD40L/IL-4) enhance the BCR-mediated proliferation of CLL cells (**Chapter 3**).
2. Constitutive activation of kinases downstream of the BCR such as Btk and Akt favors antigen-independent outgrowth of EMC cell lines *in vitro* (**Chapter 4**).
3. In addition to kinases downstream of BCR, phosphatases such as Ship1 and Ship2 are also overexpressed and constitutively activated and have an oncogenic role in CLL. Targeted B-cell specific deletion of Ship2 in mice and pharmacologic inhibition of either Ship1 and/or Ship2 in the *IgH.TEμ* mouse model, in EMC cell lines and in human CLL samples reduced cell survival and proliferation, thus providing a novel therapeutic pathway to target CLL (**Chapter 5**).
4. Antigenic stimulation plays an important role in clonal selection of the BCR repertoire in CLL. Hereby, strong BCR stimulation, probably via the self-antigen phosphatidylcholine, favored development of stereotypic (V_H11/Vκ14) U-CLL, while T cell help favored development of non-stereotypic unmutated CLL. Similarly, we found evidence for T-cell dependence of U-CLL in human CLL (**Chapters 6 and 7**).
5. Finally, basal phosphorylation levels of the extracellular signal-regulated kinase (ERK; in the MAP kinase pathway) does not only show a negative correlation with pERK induction upon BCR stimulation, but also with α-CD40L/IL-4-induced pERK levels. These results suggest a tight regulation of ERK activation in CLL. We found that high basal ERK phosphorylation enhanced spontaneous apoptosis of CLL *in vitro*. These findings point to apoptotis-inducing signaling downstream of ERK and support the idea that ERK activation has a role beyond marker of anergy in CLL as an inducer of apoptosis. Such a mechanism may have implications in patients

that show progression on current kinase targeting therapeutic regimens due to abrogation of ERK-mediated cell death (**Chapter 7**).

CRITICAL ROLE OF THE B CELL RECEPTOR IN CLL

CLL is the most frequently occurring type of leukemia in adults in the Western world. CLL is characterized by accumulation of a monoclonal population of small B cells with a typical immunophenotype ($CD19^+$, $CD20^{dim}CD5^+CD23^+CD27^+CD43^+$surface Ig^{dim}) in the blood.

Somatic hypermutation (SHM) of BCR in CLL cells

On the basis of SHM status of the immunoglobulin heavy chain variable (IGHV) genes of the BCR, CLL patients can be grouped into mutated CLL (M-CLL) and unmutated CLL (U-CLL). This division is also clinically relevant because U-CLL have an unfavorable prognosis, with a more aggressive course of the disease and shorter time to first treatment, while M-CLL is associated with a more indolent disease form with a relatively favorable prognosis [1, 2].

Stereotypic BCR in CLL cells

Approximately one-third of all CLL cases can be grouped on the basis of their restricted IGHV, IGHD, and IGHJ gene usage, and similarities in length and amino acid sequence of the heavy and light chain complementarity determining region 3 (CDR3) [3]. These so-called stereotypic BCRs are found in multiple CLL patients and the analyses of large cohorts of CLL patients enabled their clustering into at least 19 major subsets[3]. Recently, it has been shown that BCR stereotypy in CLL not only has biological impact, but also bears clinical significance. Distinct BCR stereotypic subsets appeared to associate with differences in time to first treatment, thus showing added prognostic value over U-CLL/M-CLL status and cytogenetic aberrations[4, 5].

Taken together, these findings demonstrate that important prognostic information resides in the BCR molecules and indicate an important role of the BCR and downstream signaling pathways.

Antigenic stimulation in CLL pathogenesis

For several CLL-derived BCRs a binding antigen has been identified. In general, most U-CLLs were found to express poly-reactive, low affinity BCRs, which bind self- or non-self-antigens, such as DNA, insulin, LPS, apoptotic cells, vimentin, myosin heavy chain 2A (MYH2A), and phosphoryl choline-containing antigens including oxidized low-density lipoprotein (LDL) [6-9]. BCRs from stereotypic subset #1 bind to oxidized LDL [7, 9, 10]. Stereotypic subset #2 recognizes protein L, a cell-wall protein of the commensal gut bacterium *Peptostreptococcus magnus* [11] and in addition binds to cofilin-1 [9]. Several stereotypic CLL subsets, including #3, #6, and #7, are known to use the IGHV1-69 gene, which is very common in CLL and is mostly associated with U-CLL. CLL-derived BCRs containing IGHV1-69 and IGHV3-21 were found to react with the cytomegalovirus protein pUL32 [12]. Recently, two reports demonstrated that two distinct stereotypic M-CLL subsets have specificity for the Fc-tail of IgG, and thereby have so-called rheumatoid factor activity [13, 14]. Stimulation of these specific stereotypic CLL cells with IgG indeed resulted in their proliferation [13]. In addition, Hoogeboom *et al.* [15] identified a stereotypic M-CLL subset with IGHV3-7 gene usage with an extremely short CDR3 of 5-6 amino acids. This stereotypic receptor is highly specific for a potent antigen called β-(1,6)-glucan, which can be found in yeast and filamentous fungi. Antigenic stimulation of CLL cells expressing this particular stereotypic BCR induces proliferation [15]. Collectively, these data provide support for an important role for antigen-driven BCR signaling in CLL pathogenesis. In line with this, we show that ~48% of the genes in the CLL gene signature in *IgH.TEμ* mice is modulated via antigenic stimulation of the BCR (**Chapter 3**). Stimulation via CD40L/IL-4 accounts for an additional ~17% of the gene expression changes supporting malignant transformation of naïve B cells into CLL in *IgH.TEμ* mice.

In contrast to these studies highlighting the role of antigenic stimulation, Dühren-von Minden *et al.* [16] observed that CLL-derived BCRs can be stimulated independently of external antigens, because of the presence of an internal epitope in framework 2 (FR2) of the IGHV domain that is recognized by their CDR3. This recognition induces an increased level of antigen-independent, basal or 'autonomous' signaling of the BCR, as demonstrated by increased cytoplasmic Ca^{2+} levels compared with BCRs from non-malignant B cells. Remarkably, this cell-autonomous BCR signaling was not observed in other B cell malignancies, including multiple myeloma, mantle cell lymphoma, follicular lymphoma, and marginal zone lymphoma.

These findings fueled the controversy whether antigen-dependent or cell-autonomous stimulation would be important in CLL pathogenesis, but at the same time they further underlined the relevance of the BCR in this disease. Importantly, the two contrasting observations may not be mutually exclusive, because it is conceivable that a basic level of autonomous signaling may be enhanced by ligand-dependent, antigen-driven BCR signaling. In support of this hypothesis, Iacovelli et al reported that two types of BCR interactions are positively selected during leukemia development in the *Eμ-TCL1* transgenic mouse model of CLL[17]. The authors showed that signals generated by cell-autonomous BCR interactions are essential for leukemia development, but interactions with external low-affinity autoantigens can modulate the course of the disease and may provide important co-stimulatory signals. Although we did not specifically explore cell-autonomous signaling for our EMC cell lines as described in **Chapter 4**, they do exhibit high basal Ca^{2+} signaling *in vitro,* thus in the absence of any stimulatory signals from the microenvironment. Because the EMC cell lines express the stereotypic Ig $V_H11/V\kappa14$ genes reactive towards self-antigen phosphatidylcholine (PtC), it is likely that both types of BCR interactions play a role in the outgrowth of EMC cell lines.

SIGNALS FROM THE MICRO-ENVIRONMENT IN CLL PATHOGENESIS

In addition to BCR-mediated signaling, CLL cells also interact with the tissue micro-environment and their survival is thought to be driven by T-cell independent (TI) BCR signals or by T helper cells through CD40L [18]. However, the impact of such antigenic interaction on the CLL BCR repertoire remains unknown. In **Chapter 6**, we investigated the role of antigenic pressure and BCR signaling thresholds on clonal selection of CLL cells in the *IgH.TEμ* CLL mouse model. We found that U-CLL tumors that develop in these mice can be classified into two different groups based on their *IghV* usage. The stereotypic $V_H11\text{-}2/V\kappa14\text{-}126$ CLL subset recognized the PtC self-antigen, developed independently of T cell help or GC formation and represented a somewhat more aggressive type of CLL. Proportions of $V_H11/V\kappa14$-expressing CLL were increased in the absence of functional germinal centers in *IgH.TEμ* mice deficient for CD40L or activation-induced cytidine deaminase. Conversely, *in vivo* T cell-dependent (TD) immunization decreased the proportions of $V_H11/V\kappa14$-expressing CLL. Genome-wide gene expression analysis further confirmed that V_H11 and non-V_H11 CLL resemble BCR-stimulated and anti-CD40-stimulated B cells, respectively. Moreover, we found evidence that this "non-V_H11" expression signature may be partly associated with non-stereotypic human U-CLL.

These findings have implication for the origin of CLL and suggest that the development of human U-CLL can also be TD. One such possibility is that U-CLL can derive from post-GC memory B cells to which U-CLL show a surprisingly similar gene expression pattern[19]. In support, there is evidence that GC reactions can generate some memory B cells that lack somatic mutations[20]. Secondly, since U-CLL cells show an activated phenotype[21] and antigenic specificities of the U-CLL cells seem to include both TI and TD (auto)antigens[7, 22, 23], one may speculate that U-CLLs are derived from antigen-stimulated B cells, through both TI and TD mechanisms. Concerning TD antigens, there are some indications that autoreactive B cells are prevented from undergoing full GC reactions[24]. For TI antigens, chronic activation of U-CLL because of their autoreactivity might result in the acquisition of features of antigen-experienced B cells without undergoing a GC reaction.

Taken together, although the cellular origin of CLL cells has not been finally clarified, our findings imply that in mice unmutated CLL can be derived from (i) T cell-independent B-1 cells (e.g. PtC-recognizing VH11-2/Vκ14-126) or (ii) from B cells that recognize their antigen in the presence of cognate T-cell help and are activated in the absence of SHM. Whether U-CLL cells derive from a particular subset of B cells (extra-follicular, aberrant GC response or post-GC) is less clear. Therefore, further investigations using large CLL patient cohorts containing a wide range of stereotypic and non-stereotypic U-CLL samples are required to translate our findings into human disease.

SIGNALING CASCADES IN CLL

Protein phosphorylation and dephosphorylation downstream of the BCR collectively determine the optimal BCR signaling threshold that is essential for B-cell selection at various cellular differentiation checkpoints[25]. This process is controlled by the coordinated action of specific kinases and phosphatases, which add or remove phosphate groups, respectively[25, 26]. The sequential steps of the BCR signaling cascade are described in detail in **Chapter 2** and elsewhere[27].

It is now well known that aberrant kinase activation is critical for survival of leukemic cells in various B-cell malignancies, including CLL[26] (**Figure 1**). The tyrosine kinases LYN and SYK are overexpressed and constitutively phosphorylated[28, 29]. Both expression and phosphorylation of SYK correlate with disease prognosis, being higher in U-CLL than in M-CLL [29, 30]. In addition, there is clear evidence for a role of constitutively activated PI3K, particularly the PI3Kδ isoform, in the survival of CLL B cells [31]. BTK expression levels are 2-3 fold increased in CLL[32], whilst BTK is constitutively phosphorylated in a substantial proportion of CLL cases[32], albeit that its expression or activation cannot be correlated with prognosis[32]. A crucial role for BTK in CLL leukemogenesis was confirmed in CLL mouse models, showing that either CLL-like disease did not develop in the absence of BTK [33], or that BTK inhibition significantly delayed the development of CLL [34]. Aberrant expression of the SYK-related tyrosine kinase ZAP70, which is normally expressed in T cells, where it signals downstream of the T cell receptor (reviewed in [35]), is associated with U-CLL and a more aggressive form of the disease [36]. PLCγ2 phosphorylation levels are increased in CLL, compared with healthy donor B cells [37] and this signal transducer is clearly activated in CLL B cells following BCR stimulation [38]. ZAP70 expression in CLL is known to enhance PLCγ2 phosphorylation upon BCR stimulation [39]. Evidence was provided that primary CLL

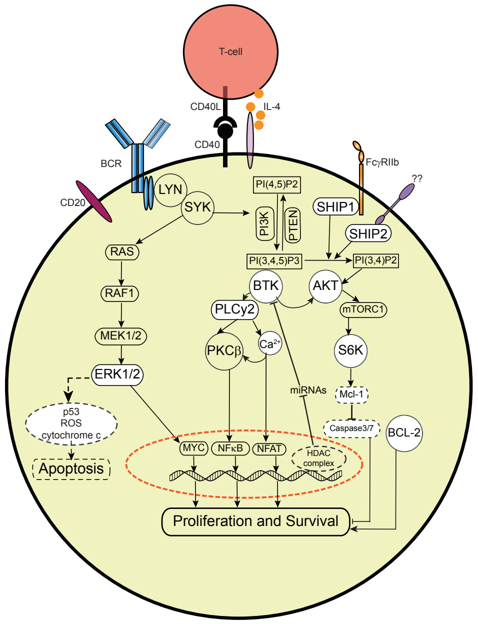

Figure 1. Signaling cascade downstream of the B cell receptor.
Signaling cascade showing important events downstream of B cell receptor (BCR). Antigen engagement by the BCR results in the formation of a micro-signalosome whereby BTK activates four families of non-receptor protein tyrosine kinases that transduce key signaling events including phospholipase C γ, mitogen-activated protein kinase (MAPK) activation, nuclear factor kappa-light-chain-enhancer of activated B cells (NF-κB) pathway components and activation of the serine/threonine kinase AKT (PKB). In addition, BTK mediated signaling events are regulated by: (i) phosphatases that can be recruited to the cell membrane, following crosslinking of inhibitory receptors, e.g., Fc γRIIB that is exclusively expressed on B cells and signals upon immune complex binding recruit SHIP1. (ii) microRNAs (miRNAs) play an important role in the post-translational regulation of BTK expression.

cells generally show a higher basal Ca^{2+} signaling level than B cells derived from peripheral blood of healthy controls [16, 40].

In addition, ERK activation is known to promote cell survival by enhancing downstream cell death regulators, including BCL-2 and MCL-1, paralleling the role of the PI3K/AKT-mediated pathway. However, to what extent the upstream processes co-operate to feed into these common downstream cell-death regulators is not fully elucidated. In **Chapter 7**, we used phospho-specific flow cytometry to study signaling properties of CLL cells. We observed independent activation of ERK and BTK/PI3K/AKT pathways in CLL, suggesting redundancy in survival signaling in CLL. Such redundancy is important to consider when using kinase inhibitors in cancer therapy. Moreover, our findings indicate that combination therapy with multiple kinase inhibitors would be an effective strategy to target CLL. In line, BTK inhibitors and PI3K inhibitors (discussed below) are now approved for CLL therapy in the clinic and the ERK pathway inhibition was recently suggested as a target for new anti-tumor strategies [41, 42].

Despite the well-established function of phosphatases in BCR signaling, their role in CLL pathogenesis remains largely unexplored. In **Chapter 5**, we provide novel evidence that specific phosphatases contribute to malignant B-cell survival in both mouse and human CLL. We demonstrate that several phosphatases, including SHIP1 and SHIP2 are overexpressed in both mouse and human CLL B-cells. Although, SHIP1 is known to function downstream of FcγRIIB in B cells (**Chapter 2, Figure 1**), upstream regulator of SHIP2 is unknown. We observed that conditional deletion of the *Ship2* gene in the B-cell lineage significantly decreased CLL formation in the *IgH.TEμ* CLL mouse model. Our data further indicate that SHIP1/2 promotes CLL survival by exerting dual effects on the BCR signaling cascade. On one hand SHIP1/2 increases PI(3,4)P2 levels and thereby enhances the AKT/S6 pathway, resulting in increased Mcl-1 protein expression, which mediates survival of CLL B-cells. On the other hand, SHIP1 maintains optimal Ca^{2+}levels in the presence of constitutive active kinase signaling, thereby engaging an anergic response to BCR stimulation in CLL B-cells. Importantly, such regulation is susceptible to pharmacologic inhibition of SHIP1/2, and provide a novel therapeutic strategy to target CLL cells. Reducing SHIP1/2 activity by the small molecule inhibitor K118 decreased the *in vitro* survival of human and mouse CLL B-cells.

We also tested the *in vivo* efficacy of K118 in our EMC cell line-engrafted CLL mouse model using a treatment regimen of intraperitoneal injection twice a week. Hereby, we saw that K118 induces significant apoptosis of leukemic cells in peripheral blood, thus recapitulating our *in vitro* data. Nevertheless, we did not see a significant improvement in the overall survival of engrafted mice (data not shown). Part of this lack of efficacy may be explained by *in vivo* toxicity at the injection site. In this regard, we optimized treatment protocol beforehand by determining the safety and tolerability of an intervention with K118 in non-tumor bearing *Rag1-/-* mice. These studies provided evidence that a dose of 10 mg/kg twice a week is safe and tolerable *in vivo* in *Rag1-/-* mice, similar to what is reported in literature[43]. However, when the same dose was used in EMC cell line- engrafted *Rag1-/-* mice, we saw dose-limiting toxic effects at the site of administration after five injections . Therefore, additional dose finding studies are required in EMC-engrafted *Rag1-/-* mice. On the other hand, it will be more interesting to test SHIP2-specific inhibitors in our EMC cell line-engrafted *Rag1-/-* mice. At present, the poor bioavailability of the currently available SHIP2-specific inhibitor (AS1949490) precluded such investigations [44].

Moreover, Ecker et al. recently reported that SHIP1-specific inhibition using the small molecule inhibitor 3AC lead to rapid cell death of CLL cells derived from primary CLL patient samples and *EμTCL1*-driven murine CLL-like cells[45]. This is in contrast with the absence of effects of B-cell specific conditional deletion of the *Ship1* gene on CLL formation in the *IgH.TEμ* CLL mouse model (**Chapter 5**). However, Ecker et al. did not report effects of 3AC on CLL cells *in vivo,* and one might expect different effects *in vivo* compared to the *in vitro* studies described. Secondly, the authors did not mention the concentration of the 3AC compound used in these experiments. When we explored the impact of 3AC on *in vitro* survival of EMC cell lines (**Figure 2**), we saw that 3AC treatment significantly decreased survival of EMC cells *in vitro* by inducing caspase-mediated apoptosis. However, such effects were only seen at EC_{50} of 10 µM, a concentration twice the EC_{50} of K118 (**Chapter 5**). Therefore, it will be interesting to investigate 3AC *in vivo* in EMC cell line-engrafted *Rag1-/-* mice, because of its better tolerability *in vivo*[46].

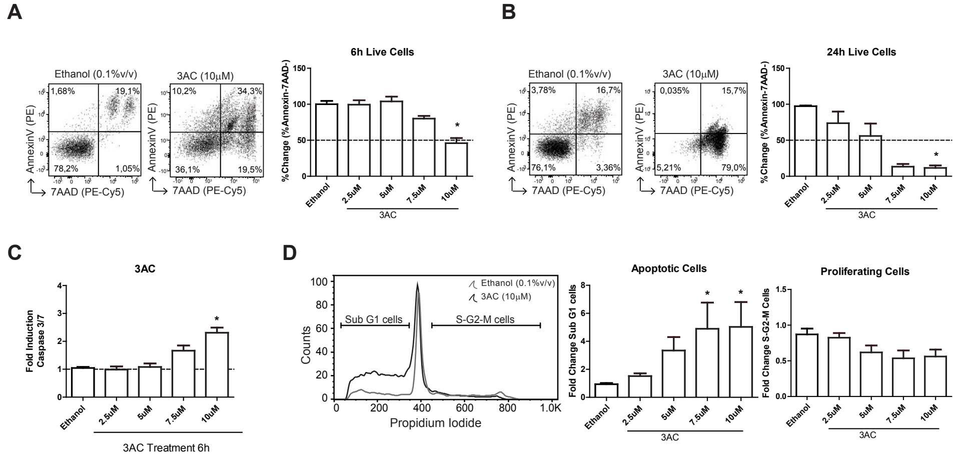

Figure 2. High dose Ship1 inhibition decreases survival of EMC cells *in vitro*.
(A,B) Viable (AnnexinV and 7-AAD negative) cells were determined after (A) 6 hours or (B) 24 hours of treatment with the indicated concentrations of Ship1-specific inhibitor (3AC) or 0.1%v/v of vehicle (Ethanol). The concentration of ethanol used as control corresponds to that used in 10uM of 3AC. Bar graphs represent the proportions of viable cells, normalized to untreated control cells (set to 100%). Dot plots show representative flow cytometric analysis of EMC6 cells. **(C)** Analysis of caspase activity using the caspase-glo assay in EMC cells treated with the indicated concentrations of 3AC or 0.1%v/v of vehicle (Ethanol) for 6h. The concentration of ethanol used as control corresponds to that used in 10uM of 3AC. Each set of data consists of at least three independent experiments, each on EMC4 and EMC6. **(D)** Cell cycle profiling in EMC cells after 24h of treatment with the indicated concentrations of 3AC or 0.1%v/v of vehicle (Ethanol). Histogram shows the gating strategy for DNA content (Propidium Iodide) analysis in the presence of 0.1%v/v of vehicle (Ethanol, grey) or 3AC (red). The concentration of ethanol used as control corresponds to that used in 10uM of 3AC. Bar graphs represent the proportions of apoptotic (subG1, left) and cycling (S-G2-M, right) cells normalized to untreated control cells. Statistical analysis was performed by comparing the effect of 3AC to the respective vehicle using Dunn's multiple comparison test. *p<0.05.

TREATMENT LANDSCAPE OF CLL

The management of CLL patients is rapidly changing from more generalized chemo-(immuno)therapeutic regimens to more personalized treatment using small molecule inhibitors targeting BCR signaling-related kinases. Impressive clinical results obtained for several of these inhibitors have led to FDA approval in the treatment naïve or the relapsed/refractory CLL setting and will be discussed below.

BTK inhibitor (Ibrutinib , Acalabrutinib)

Considering the significant expression levels and the important role of BTK in several signaling pathways implicated in CLL pathogenesis, BTK seemed an important target for CLL therapeutic intervention strategies. In **Chapter 2**, we describe Ibrutinib (PCI-32765, Pharmacyclics), an orally available potent BTK inhibitor that irreversibly and covalently binds to the cysteine at position 481 in the BTK kinase domain and thereby blocks its kinase activity. Although ibrutinib does not prevent Y551 phosphorylation of BTK by SRC-like kinases and SYK, it does prevent BTK autophosphorylation at position Y223[47]. Autophosphorylation of Y223 does not appear to be essential for BTK activity[48], but the phosphorylation status of Y223 reflects the actual kinase activity of BTK.

Despite immense clinical success ibrutinib therapy has some limitations. The major downside to ibrutinib therapy is that it does not achieve minimal residual disease (MRD)-negative complete responses (CRs) and therefore, in the majority of patients, must be given indefinitely. This is associated with considerable cost to patients and society and also a cumulating risk of toxicity, including cardiac arrhythmias, hypertension, and bleeding. Additionally, there is an increased risk of developing resistance to therapy, particularly in high-risk disease such as for patients with del(17p) and/or complex metaphase karyotype. This has led to the search and development of more selective and reversible BTK inhibitors

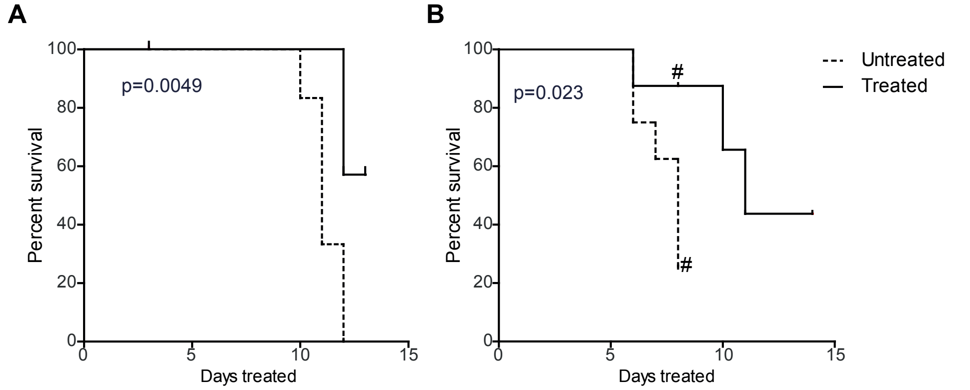

Figure 3, Acalabrutinib treatment improves survival of EMC cell line engrafted *Rag1-/-* mice.
(A,B) Kaplan-Meier survival curve over 16 days of acalabrutinib or vehicle treatment of (A) EMC6- or (B) EMC4-engrafted *Rag1-/-* mice. Mice were randomized into treatment arms 14 days post cell line engraftment following identification of tumor cells in the peripheral blood.
#Three mice from both untreated and treated (randomized) group were sacrificed after 8 days of treatment to compare tumor load in different organs.

such as acalabrutinib (ACP-196), GS-4059 and BGB-3111 described briefly in **Chapter 2**. Of these inhibitors acalabrutinib received specific attention due to high overall response rate of 95%, (85% partial response (PR) and 10% PR with lymphocytosis); the remaining 5% of patients had stable disease[49]. Amongst patients with del(17p), the overall response rate (ORR) was 100%. We also tested the *in vivo* efficacy of acalabrutinib in our EMC cell line-engrafted CLL mouse model (**Figure 3**), similar to our studies on ibrutinib described in this thesis (**Chapter 4**). Hereby, acalabrutinib significantly improved survival of *Rag1-/-* mice engrafted with either of two EMC cell lines. This *in vivo* effect was associated with increased apoptosis and reduced proliferation of EMC cells by acalabrutinib *in vitro*. Thus, acalabrutinib could provide a suitable alternative to ibrutinib for patients who had severe or recurrent adverse events during ibrutinib therapy, leading to permanent treatment cessation and who subsequently progressed. In this regard, a phase II study is evaluating acalabrutinib in chemotherapy/ibrutinib ineligible patients (NCT02717611). Moreover, a pivotal phase III non-inferiority study of ibrutinib vs. acalabrutinib in patients with relapsed/refractory CLL (NCT02477696) is currently underway.

Although optimized kinase monotherapy has a better efficacy and low toxicity profile, it does not provide deep remission and needs to be given indefinitely until progression or toxicity. Therefore, therapeutic combinations aimed at achieving maximal disease elimination with minimal toxicity for a finite treatment duration can be conceived as better treatment strategy. There has been increasing interest in developing rational BTK inhibitor-based combinations, some of which are described in **Table 1.**

Table 1. BTK-inhibitor-based combination therapies for CLL

Patient population	Therapeutic regimen	Phase	Status(results)	Reference
R/R CLL	Ibrutinib + Rituximab	II	Ongoing, not recruiting	NCT02007044
R/R CLL	Ibrutinib + Obinutuzumab	I	Recruiting	NCT02537613
First line	Ibrutinib + Obinutuzumab	IB/II	Ongoing, not recruiting	NCT02315768
First line	Ibrutinib + Obinutuzumab	III	Ongoing, not recruiting	NCT02264574
First line Young	Ibrutinib + Obinutuzumab + Venetoclax	III	Recruiting	NCT03701282
First line Old	Ibrutinib + Obinutuzumab + Venetoclax	III	Recruiting	NCT03737981
First line	Ibrutinib + Venetoclax	III	Recruiting	NCT03462719
First line Old	Acalabrutinib + Obinutuzumab	III	Ongoing, not recruiting	NCT02475681

Targeting BTK protein levels

In addition to BTK kinase activity, BTK protein levels are also decisive for B cell function[50]. This can have direct implications in CLL, as B cell-specific BTK-overexpression accelerated leukemogenesis in the *IgH.TEμ* CLL mouse model[33]. In addition, we showed that BTK overexpression enhances BCR mediated signaling and accounts for ~54% of the CLL gene signature in our mouse model (**Chapter 3**). Thus, targeting BTK protein levels may provide a novel therapeutic strategy. One way to achieve this may be to enhance expression of microRNAs (miRNAs) that regulate BTK expression.

In this regard, Bottoni et al used inhibition of histone deacetylates (HDACs) to increase the expression of miRNAs controlling BTK expression[51]. Treatment of primary CLL samples either with the HDAC inhibitors (HDACi) panobinostat and abexinostat or small interfering RNA-mediated knockdown of HDAC resulted in increased expression of BTK-targeting miRNAs and as a consequence decreased BTK mRNA and protein expression[51]. More importantly, the combination of HDACi with ibrutinib induced synergistic cytotoxicity in primary CLL cells compared to either agent alone. The effect of the ibrutinib and HDACi combination on abrogating BTK-mediated signaling and diminishing CLL cell survival was also confirmed *in vivo* in the *EμTCL-1* mouse model of CLL[52]. Finally, the downregulation of the BTK-targeting miRNAs and response to HDACi was independent of the BTK C481S mutational status. This study provides convincing evidence that effective reduction of BTK expression by HDAC inhibitors and targeting enzymatic activity of BTK may be promising as a therapeutic modality that suppresses survival signals in CLL.

However, there are some potential concerns associated with targeting HDACs in CLL which may limit the usefulness of this approach. First, HDACi's have known toxicity in CLL patients in particular thrombocytopenia[53]. Second, although CLL cells with C481S-mutant BTK can be very well targeted by HDACi, patients with an ibrutinib-induced constitutive active PLCγ2 mutation will not benefit from HDACi because it does not affect PLCγ2 protein expression.

In conclusion, abrogating epigenetic silencing of BTK-targeting miRNAs using HDACi's may remove/reduce BTK overexpression induced survival of CLL and may prevent the emergence of ibrutinib-resistant clones. Thus, there is need to initiate clinical trials to assess HDACi in combination with ibrutinib.

PI3Kδ inhibitor (Idelalisib)

Expression of PI3Kδ is restricted to hematopoietic cells, whereby it plays a key role in proliferation and survival in B cells. As mentioned above, the PI3K pathway is constitutively activated in CLL and this is dependent on PI3Kδ [31]. The highly-selective oral PI3Kδ inhibitor, idelalisib (CAL-101, GS-1101, Calistoga Pharmaceuticals) stimulated apoptosis in primary CLL cells *ex vivo* in a dose- and time-dependent manner, which was shown to be independent of IGHV mutational status or recurrent cytogenetic aberrations. Idelalisib-mediated cytotoxicity induced an increase in caspase activity, which was not rescued by co-culture on stromal cells. Additionally, idelalisib abolished normal CLL cell protection from spontaneous apoptosis induced by B cell-activating factors such as CD40L, or other signals from the microenvironment [31]. Similar to ibrutinib and SYK inhibitors, also idelalisib inhibits CLL cell chemotaxis towards CXCL12 and CXCL13, and induces downregulation of chemokine secretion. CAL-101 was shown to inhibit BCR- and chemokine-receptor-induced AKT phosphorylation, ERK activation and survival signals [54]. In a phase 1 trial idelalisib was evaluated in 54 patients with relapsed/refractory CLL with various adverse prognostic characteristics including unmutated IGHV status (91%), and del17p and/or *TP53* mutations (24%) [55]. The patients were treated with different dosage levels of oral idelalisib and remained on continuous therapy while showing clinical improvement. Similar to what was shown for *ex vivo* CLL cells, inhibition of PI3Kδ abolished AKT phosphorylation in patient CLL cells, and significantly reduced serum levels of chemokines related to CLL such as CCL3, CCL4, CCL17 and CCL22. Idelalisib induced clear reductions in lymph node and spleen size and lymphocytosis was observed in the patients already a few hours after the initiation of the treatment. The most commonly observed adverse events were pneumonia, neutropenic fever and diarrhea. The ORR was ~72%, and a median progression free survival (PFS) for all patients was 15.8 months, demonstrating the clinical efficacy of idelalisib [55].

In a multicenter phase 3 study, which was performed in a randomized, double-blind, and placebo-controlled manner, the efficacy and safety of idelalisib in combination with rituximab was assessed [56]. Two-hundred-and-twenty CLL patients were included, with advanced stage disease of which a part was in a poor condition with renal dysfunction, previous therapy-induced reduced bone marrow function, or major coexisting diseases. The patients received rituximab and either idelalisib or placebo. PFS at 24 weeks after treatment initiation was ~93% in the idelalisib-treated group and ~46% in the placebo group. Because of this large efficacy difference between the two patient groups, the study was stopped before its end-point was reached. The observed ORRs were ~81% in the patients receiving rituximab/idelalisib versus ~13% in the rituximab/placebo group, of which all were considered as partial responses. The idelalisib-related lymphocytosis which was seen in the phase 1 study [55], appeared to be less profound and shorter in duration when combined with rituximab [56], parallel to observations in the study in which ibrutinib was combined with rituximab [57].

In a recently reported multicenter, phase 3, open-label, randomized controlled trial idelalisib was tested in combination with Ofatumumab, a fully humanized anti-CD20 monoclonal antibody in 164 heavily pretreated patients with relapsed or refractory CLL[58]. The ORR was 75.3% with 1(<1%) CRs and 134 (75%) PRs. Interestingly, lymph node response was observed in 93.3% of patients. The median PFS was 16.3 months[58].

Taken together, the reported clinical data convincingly show that idelalisib treatment induces an impressive response in CLL patients, without causing significant toxicity, particularly in a combination therapy strategy with rituximab.

Cytotoxic therapy—BCL-2 inhibitors (Navitoclax, Venetoclax)

Two different apoptotic pathways have been described, the extrinsic and the intrinsic pathways[59]. In the extrinsic pathway, apoptosis occurs via triggering of cell surface death receptors such as CD95 or TNF-related apoptosis-inducing ligand (TRAIL) receptors[60]. Ligation of these receptors leads to downstream formation of the death inducing signaling complex (DISC) that activates caspase 8 and caspase 3mediated cell death[60, 61]. In the intrinsic pathway, numerous cytotoxic stimuli and pro-apoptotic signals induce outer mitochondrial membrane permeabilization followed by cytochrome C release and caspase-mediated cell death[62]. The balance of pro-apoptotic (BAX, BAK and BH3-only members) and anti-apoptotic (BCL-2, BCL-XL, BCL-W, MCL-1) regulators in a cell is a key determinant in the outcome of the intrinsic cell-death pathway[63, 64].

Most CLL patients show overexpression of the anti-apoptotic protein BCL-2, due to deleted or silenced miR-15a and/or miR-16.1, which normally suppress BCL-2 expression[65]. This fueled the development of treatment strategies that aim at targeting BCL-2 in CLL, using BH3 mimetics. The first generation of BH3 mimetics included ABT-737/263 or navitoclax, which efficiently antagonizes BCL-2, BCL-XL, and BCL-W. In a phase 1 study with navitoclax more than 50% patients showed reduction in lymphocytosis compared to baseline and ~35% achieved PR[66]. Median PFS was 25 months. Importantly, a response was observed in patients with fludarabine-refractory disease, bulky adenopathy, and del(17p) CLL. However, platelets also express BCL-XL, and as a consequence treatment resulted in rapid platelet death and dose-limiting thrombocytopenia. This restricted the use of ABT-737 in patients with CLL[67].

Therefore, a second generation BH3-mimetic, named ABT-199/venetoclax, was developed which lacked binding to BCL-XL[68]. Venetoclax is highly cytotoxic for CLL cells and shows improved clinical efficacy with reduced peripheral blood cell counts and diminished lymph nodes size early after treatment. Venetoclax had an ORR of 79% in relapsed-refractory CLL patients[68]. Responses were also seen in subgroups with an adverse prognosis, including those with resistance to fludarabine, chromosome 17p deletions (del17p CLL), or unmutated IGHV status. This led to FDA approval of venetoclax for patients with del(17p) and one prior therapy with BCR inhibitors[68]. Although the ORR with venetoclax was high, CR was only reached in ~20% of patients. The low CR percentage may result from microenvironment-induced resistance. In the CLL lymph node microenvironment, upregulation of other anti-apoptotic proteins such as BCL-XL, Mcl-1 and Bfl-1 can be clearly observed[69, 70]. Since these BCL-2 family members are not targeted by venetoclax, it explains the decreased sensitivity for this compound. Therefore, combination therapy that prevents the microenvironment-induced venetoclax resistance is required. In this regard, venetoclax has been tested in combination with anti-CD20 monoclonal antibodies, such as rituximab, to which CLL cells are sensitive via antibody mediated cellular cytotoxicity (ADCC) mechanisms. After a median follow-up period of 23.8 months, the 2-year PFS was 84.9%. This included the subgroup of patients with chromosome 17p deletion in which the 2-year PFS was 81.5%, compared to 85.9% among those without chromosome 17p deletion[71].

FUTURE PERSPECTIVE

A large number of studies have highlighted the importance of BCR signaling in CLL pathogenesis. These findings have remarkably changed the therapeutic landscape of CLL by the introduction of small molecule inhibitors targeting BCR-associated kinases. However, a fraction of patients receiving long-term targeted kinase therapies developed resistances to these novel agents. It is therefore essential to identify additional molecular mechanisms which contribute to CLL survival and proliferation (**Figure 4**). Which could be these molecular mechanisms?

First, our data indicate that T-cell mediated signaling plays an important role in selection and outgrowth of CLL, even in the aggressive U-CLL subset. Therefore, targeting T cell help in CLL could be an effective strategy.

Second, we demonstrate that phosphatases such as SHIP2 play an essential role in survival of CLL cells in both mouse and human. Thus, targeted inhibition of SHIP2 (-or perhaps other phosphates that are overexpressed in CLL cells) may provide a novel potential therapeutic target in treating CLL.

Third, we observed independent activation of ERK and BTK/PI3K/AKT pathways in CLL, suggesting redundancy in survival signaling in CLL. Such redundancy should be considered when using inhibitors that have specificity for certain kinases in cancer therapy. Moreover, our findings indicate that combination therapy with multiple kinase inhibitors would be an effective strategy to target CLL.

Finally, we show that ERK activation, beyond being a marker of anergy in CLL, was also associated with increased apoptosis susceptibility. Our finding of this dual role of ERK activation may provide a molecular explanation for the observation that CLL patients show progression despite kinase targeting therapy.

Further clinical evaluation upon targeting these pathways is warranted. Importantly, to completely block all survival signals and to fully eradicate the disease, combination therapy is needed. In this context, it is important to develop personalized medicine strategies, because patients with different molecular and biological characteristics are expected to benefit from different combination therapies.

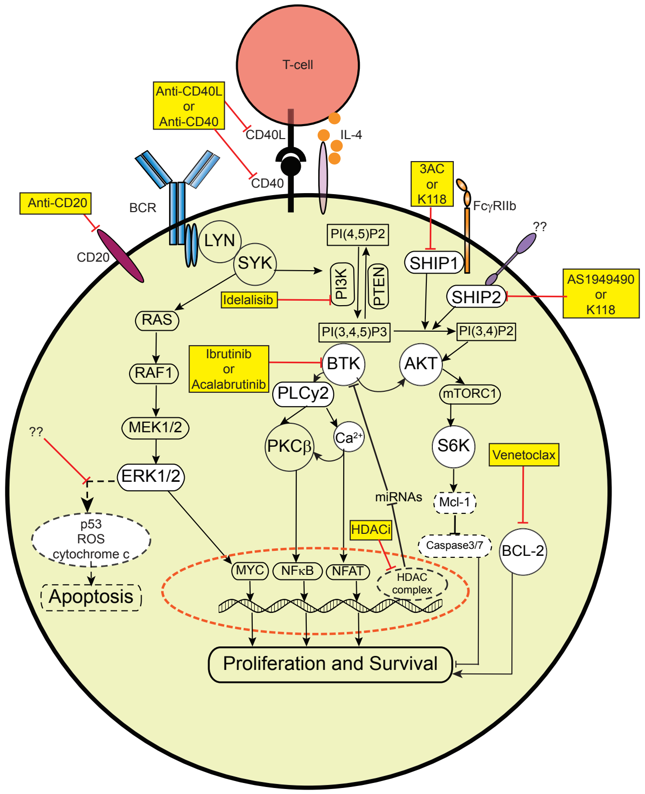
T-cell
Anti-CD40L
or
Anti-CD40
CD40L
IL-4
CD40
3AC
or
K118
FcγRIIb
??
Anti-CD20
BCR
CD20
LYN
SYK
PI(4,5)P2
PI3K
PTEN
SHIP1
SHIP2
AS1949490
or
K118
Idelalisib
RAS
PI(3,4,5)P3
PI(3,4)P2
Ibrutinib
or
Acalabrutinib
BTK
AKT
RAF1
PLCγ2
mTORC1
MEK1/2
PKCβ
Ca²⁺
S6K
Venetoclax
??
ERK1/2
miRNAs
Mcl-1
HDACi
p53
ROS
cytochrome c
Caspase3/7
BCL-2
MYC
NFκB
NFAT
HDAC
complex
Apoptosis
Proliferation and Survival

Figure 4. Therapeutic targets in CLL.
Signaling cascade showing important molecular pathways that are either targeted by clinically approved small molecule inhibitors or can be therapeutically targeted to abrogate survival and proliferation in CLL.

REFERENCES

1. Damle RN, Wasil T, Fais F, Ghiotto F, Valetto A, Allen SL, *et al.* Ig V gene mutation status and CD38 expression as novel prognostic indicators in chronic lymphocytic leukemia. *Blood* 1999 Sep 15; **94**(6)**:** 1840-1847.
2. Hamblin TJ, Davis Z, Gardiner A, Oscier DG, Stevenson FK. Unmutated Ig V(H) genes are associated with a more aggressive form of chronic lymphocytic leukemia. *Blood* 1999 Sep 15; **94**(6)**:** 1848-1854.
3. Agathangelidis A, Darzentas N, Hadzidimitriou A, Brochet X, Murray F, Yan XJ, *et al.* Stereotyped B-cell receptors in one-third of chronic lymphocytic leukemia: a molecular classification with implications for targeted therapies. *Blood* 2012 May 10; **119**(19)**:** 4467-4475.
4. Baliakas P, Agathangelidis A, Hadzidimitriou A, Sutton LA, Minga E, Tsanousa A, *et al.* Not all IGHV3-21 chronic lymphocytic leukemias are equal: prognostic considerations. *Blood* 2015 Jan 29; **125**(5)**:** 856-859.
5. Baliakas P, Hadzidimitriou A, Sutton LA, Minga E, Agathangelidis A, Nichelatti M, *et al.* Clinical effect of stereotyped B-cell receptor immunoglobulins in chronic lymphocytic leukaemia: a retrospective multicentre study. *Lancet Haematol* 2014 Nov; **1**(2)**:** e74-84.
6. Herve M, Xu K, Ng YS, Wardemann H, Albesiano E, Messmer BT, *et al.* Unmutated and mutated chronic lymphocytic leukemias derive from self-reactive B cell precursors despite expressing different antibody reactivity. *J Clin Invest* 2005 Jun; **115**(6)**:** 1636-1643.
7. Catera R, Silverman GJ, Hatzi K, Seiler T, Didier S, Zhang L, *et al.* Chronic lymphocytic leukemia cells recognize conserved epitopes associated with apoptosis and oxidation. *Mol Med* 2008 Nov-Dec; **14**(11-12)**:** 665-674.
8. Chu CC, Catera R, Zhang L, Didier S, Agagnina BM, Damle RN, *et al.* Many chronic lymphocytic leukemia antibodies recognize apoptotic cells with exposed nonmuscle myosin heavy chain IIA: implications for patient outcome and cell of origin. *Blood* 2010 May 13; **115**(19)**:** 3907-3915.
9. Myhrinder AL, Hellqvist E, Sidorova E, Soderberg A, Baxendale H, Dahle C, *et al.* A new perspective: molecular motifs on oxidized LDL, apoptotic cells, and bacteria are targets for chronic lymphocytic leukemia antibodies. *Blood* 2008 Apr 1; **111**(7)**:** 3838-3848.
10. Zwick C, Fadle N, Regitz E, Kemele M, Stilgenbauer S, Buhler A, *et al.* Autoantigenic targets of B-cell receptors derived from chronic lymphocytic leukemias bind to and induce proliferation of leukemic cells. *Blood* 2013 Jun 6; **121**(23)**:** 4708-4717.
11. Ghia EM, Widhopf GF, 2nd, Rassenti LZ, Kipps TJ. Analyses of recombinant stereotypic IGHV3-21-encoded antibodies expressed in chronic lymphocytic leukemia. *J Immunol* 2011 Jun 1; **186**(11)**:** 6338-6344.
12. Steininger C, Widhopf GF, 2nd, Ghia EM, Morello CS, Vanura K, Sanders R, *et al.* Recombinant antibodies encoded by IGHV1-69 react with pUL32, a phosphoprotein of cytomegalovirus and B-cell superantigen. *Blood* 2012 Mar 8; **119**(10)**:** 2293-2301.
13. Hoogeboom R, Wormhoudt TA, Schipperus MR, Langerak AW, Dunn-Walters DK, Guikema JE, *et al.* A novel chronic lymphocytic leukemia subset expressing mutated IGHV3-7-encoded rheumatoid factor B-cell receptors that are functionally proficient. *Leukemia* 2013 Mar; **27**(3)**:** 738-740.
14. Kostareli E, Gounari M, Janus A, Murray F, Brochet X, Giudicelli V, *et al.* Antigen receptor stereotypy across B-cell lymphoproliferations: the case of IGHV4-59/IGKV3-20 receptors with rheumatoid factor activity. *Leukemia* 2012 May; **26**(5)**:** 1127-1131.
15. Hoogeboom R, van Kessel KP, Hochstenbach F, Wormhoudt TA, Reinten RJ, Wagner K, *et al.* A mutated B cell chronic lymphocytic leukemia subset that recognizes and responds to fungi. *J Exp Med* 2013 Jan 14; **210**(1)**:** 59-70.
16. Duhren-von Minden M, Ubelhart R, Schneider D, Wossning T, Bach MP, Buchner M, *et al.* Chronic lymphocytic leukaemia is driven by antigen-independent cell-autonomous signalling. *Nature* 2012 Sep 13; **489**(7415)**:** 309-312.
17. Iacovelli S, Hug E, Bennardo S, Duehren-von Minden M, Gobessi S, Rinaldi A, *et al.* Two types of BCR interactions are positively selected during leukemia development in the Emu-TCL1 transgenic mouse model of CLL. *Blood* 2015 Mar 5; **125**(10)**:** 1578-1588.
18. Coscia M, Pantaleoni F, Riganti C, Vitale C, Rigoni M, Peola S, *et al.* IGHV unmutated CLL B cells are more prone to spontaneous apoptosis and subject to environmental prosurvival signals than mutated CLL B cells. *Leukemia* 2011 May; **25**(5)**:** 828-837.
19. Klein U, Tu Y, Stolovitzky GA, Mattioli M, Cattoretti G, Husson H, *et al.* Gene expression profiling of B cell chronic lymphocytic leukemia reveals a homogeneous phenotype related to memory B cells. *J Exp Med* 2001 Dec 3; **194**(11)**:** 1625-1638.
20. Seifert M, Kuppers R. Molecular footprints of a germinal center derivation of human IgM+(IgD+)CD27+ B cells and the dynamics of memory B cell generation. *J Exp Med* 2009 Nov 23; **206**(12)**:** 2659-2669.
21. Damle RN, Ghiotto F, Valetto A, Albesiano E, Fais F, Yan XJ, *et al.* B-cell chronic lymphocytic leukemia cells express a surface membrane phenotype of activated, antigen-experienced B lymphocytes. *Blood* 2002 Jun 1; **99**(11)**:** 4087-4093.
22. Chu CC, Catera R, Hatzi K, Yan XJ, Zhang L, Wang XB, *et al.* Chronic lymphocytic leukemia antibodies with a common stereotypic rearrangement recognize nonmuscle myosin heavy chain IIA. *Blood* 2008 Dec 15; **112**(13)**:** 5122-5129.
23. Lanemo Myhrinder A, Hellqvist E, Sidorova E, Soderberg A, Baxendale H, Dahle C, *et al.* A new perspective: molecular motifs on oxidized LDL, apoptotic cells, and bacteria are targets for chronic lymphocytic leukemia antibodies. *Blood* 2008 Apr 01; **111**(7)**:** 3838-3848.
24. Matejuk A, Beardall M, Xu Y, Tian Q, Phillips D, Alabyev B, *et al.* Exclusion of natural autoantibody-producing B cells from IgG memory B cell compartment during T cell-dependent immune responses. *J Immunol* 2009 Jun 15; **182**(12)**:** 7634-7643.
25. Muschen M. Autoimmunity checkpoints as therapeutic targets in B cell malignancies. *Nat Rev Cancer* 2018 Feb; **18**(2)**:** 103-116.

26. Pal Singh S, Dammeijer F, Hendriks RW. Role of Bruton's tyrosine kinase in B cells and malignancies. *Mol Cancer* 2018 Feb 19; **17**(1)**:** 57.
27. Muggen AF, Singh SP, Hendriks RW, Langerak AW. Targeting Signaling Pathways in Chronic Lymphocytic Leukemia. *Curr Cancer Drug Targets* 2016; **16**(8)**:** 669-688.
28. Contri A, Brunati AM, Trentin L, Cabrelle A, Miorin M, Cesaro L*, et al.* Chronic lymphocytic leukemia B cells contain anomalous Lyn tyrosine kinase, a putative contribution to defective apoptosis. *J Clin Invest* 2005 Feb; **115**(2)**:** 369-378.
29. Buchner M, Fuchs S, Prinz G, Pfeifer D, Bartholome K, Burger M*, et al.* Spleen tyrosine kinase is overexpressed and represents a potential therapeutic target in chronic lymphocytic leukemia. *Cancer Res* 2009 Jul 01; **69**(13)**:** 5424-5432.
30. Cesano A, Perbellini O, Evensen E, Chu CC, Cioffi F, Ptacek J*, et al.* Association between B-cell receptor responsiveness and disease progression in B-cell chronic lymphocytic leukemia: results from single cell network profiling studies. *Haematologica* 2013 Apr; **98**(4)**:** 626-634.
31. Herman SE, Gordon AL, Wagner AJ, Heerema NA, Zhao W, Flynn JM*, et al.* Phosphatidylinositol 3-kinase-delta inhibitor CAL-101 shows promising preclinical activity in chronic lymphocytic leukemia by antagonizing intrinsic and extrinsic cellular survival signals. *Blood* 2010 Sep 23; **116**(12)**:** 2078-2088.
32. Herman SE, Gordon AL, Hertlein E, Ramanunni A, Zhang X, Jaglowski S*, et al.* Bruton tyrosine kinase represents a promising therapeutic target for treatment of chronic lymphocytic leukemia and is effectively targeted by PCI-32765. *Blood* 2011 Jun 9; **117**(23)**:** 6287-6296.
33. Kil LP, de Bruijn MJ, van Hulst JA, Langerak AW, Yuvaraj S, Hendriks RW. Bruton's tyrosine kinase mediated signaling enhances leukemogenesis in a mouse model for chronic lymphocytic leukemia. *Am J Blood Res* 2013; **3**(1)**:** 71-83.
34. Woyach JA, Smucker K, Smith LL, Lozanski A, Zhong Y, Ruppert AS*, et al.* Prolonged lymphocytosis during ibrutinib therapy is associated with distinct molecular characteristics and does not indicate a suboptimal response to therapy. *Blood* 2014 Mar 20; **123**(12)**:** 1810-1817.
35. Kil LP, Yuvaraj S, Langerak AW, Hendriks RW. The role of B cell receptor stimulation in CLL pathogenesis. *Curr Pharm Des* 2012; **18**(23)**:** 3335-3355.
36. Rassenti LZ, Huynh L, Toy TL, Chen L, Keating MJ, Gribben JG*, et al.* ZAP-70 compared with immunoglobulin heavy-chain gene mutation status as a predictor of disease progression in chronic lymphocytic leukemia. *N Engl J Med* 2004 Aug 26; **351**(9)**:** 893-901.
37. Blix ES, Irish JM, Husebekk A, Delabie J, Forfang L, Tierens AM*, et al.* Phospho-specific flow cytometry identifies aberrant signaling in indolent B-cell lymphoma. *BMC Cancer* 2012; **12:** 478.
38. Petlickovski A, Laurenti L, Li X, Marietti S, Chiusolo P, Sica S*, et al.* Sustained signaling through the B-cell receptor induces Mcl-1 and promotes survival of chronic lymphocytic leukemia B cells. *Blood* 2005 Jun 15; **105**(12)**:** 4820-4827.
39. Gobessi S, Laurenti L, Longo PG, Sica S, Leone G, Efremov DG. ZAP-70 enhances B-cell-receptor signaling despite absent or inefficient tyrosine kinase activation in chronic lymphocytic leukemia and lymphoma B cells. *Blood* 2007 Mar 1; **109**(5)**:** 2032-2039.

40. Muggen AF, Pillai SY, Kil LP, van Zelm MC, van Dongen JJ, Hendriks RW*, et al.* Basal Ca signaling is particularly increased in mutated chronic lymphocytic leukemia. *Leukemia* 2014 Jun 11.
41. Gimenez N, Martinez-Trillos A, Montraveta A, Lopez-Guerra M, Rosich L, Nadeu F*, et al.* Mutations in RAS-BRAF-MAPK-ERK pathway define a specific subgroup of patients with adverse clinical features and provide new therapeutic options in chronic lymphocytic leukemia. *Haematologica* 2018 Sep 27.
42. Brown JR. Relapsed CLL: sequencing, combinations, and novel agents. *Hematology Am Soc Hematol Educ Program* 2018 Nov 30; **2018**(1)**:** 248-255.
43. Srivastava N, Iyer S, Sudan R, Youngs C, Engelman RW, Howard KT*, et al.* A small-molecule inhibitor of SHIP1 reverses age- and diet-associated obesity and metabolic syndrome. *JCI Insight* 2016 Jul 21; **1**(11).
44. Suwa A, Kurama T, Shimokawa T. SHIP2 and its involvement in various diseases. *Expert Opin Ther Targets* 2010 Jul; **14**(7)**:** 727-737.
45. Ecker V, Braun M, Neumayer T, Muschen M, Ruland J, Buchner M. SHIP1 Inhibition As Novel Therapeutic Approach in Chronic Lymphocytic Leukemia. Am Soc Hematology; 2018.
46. Brooks R, Fuhler GM, Iyer S, Smith MJ, Park MY, Paraiso KH*, et al.* SHIP1 inhibition increases immunoregulatory capacity and triggers apoptosis of hematopoietic cancer cells. *J Immunol* 2010 Apr 1; **184**(7)**:** 3582-3589.
47. Pan Z, Scheerens H, Li SJ, Schultz BE, Sprengeler PA, Burrill LC*, et al.* Discovery of selective irreversible inhibitors for Bruton's tyrosine kinase. *ChemMedChem* 2007 Jan; **2**(1)**:** 58-61.
48. Middendorp S, Dingjan GM, Maas A, Dahlenborg K, Hendriks RW. Function of Bruton's tyrosine kinase during B cell development is partially independent of its catalytic activity. *J Immunol* 2003 Dec 1; **171**(11)**:** 5988-5996.
49. Byrd JC, Harrington B, O'Brien S, Jones JA, Schuh A, Devereux S*, et al.* Acalabrutinib (ACP-196) in Relapsed Chronic Lymphocytic Leukemia. *N Engl J Med* 2016 Jan 28; **374**(4)**:** 323-332.
50. Corneth OB, Klein Wolterink RG, Hendriks RW. BTK Signaling in B Cell Differentiation and Autoimmunity. *Curr Top Microbiol Immunol* 2016; **393:** 67-105.
51. Bottoni A, Rizzotto L, Lai TH, Liu C, Smith LL, Mantel R*, et al.* Targeting BTK through microRNA in chronic lymphocytic leukemia. *Blood* 2016 Dec 29; **128**(26)**:** 3101-3112.
52. Bichi R, Shinton SA, Martin ES, Koval A, Calin GA, Cesari R*, et al.* Human chronic lymphocytic leukemia modeled in mouse by targeted TCL1 expression. *Proc Natl Acad Sci U S A* 2002 May 14; **99**(10)**:** 6955-6960.
53. Blum KA, Advani A, Fernandez L, Van Der Jagt R, Brandwein J, Kambhampati S*, et al.* Phase II study of the histone deacetylase inhibitor MGCD0103 in patients with previously treated chronic lymphocytic leukaemia. *British journal of haematology* 2009; **147**(4)**:** 507-514.
54. Hoellenriegel J, Meadows SA, Sivina M, Wierda WG, Kantarjian H, Keating MJ*, et al.* The phosphoinositide 3'-kinase delta inhibitor, CAL-101, inhibits B-cell receptor signaling and chemokine networks in chronic lymphocytic leukemia. *Blood* 2011 Sep 29; **118**(13)**:** 3603-3612.
55. Brown JR, Byrd JC, Coutre SE, Benson DM, Flinn IW, Wagner-Johnston ND*, et al.* Idelalisib, an inhibitor of phosphatidylinositol 3-kinase p110delta, for relapsed/refractory chronic lymphocytic leukemia. *Blood* 2014 May 29; **123**(22)**:** 3390-3397.

56. Furman RR, Sharman JP, Coutre SE, Cheson BD, Pagel JM, Hillmen P, *et al.* Idelalisib and rituximab in relapsed chronic lymphocytic leukemia. *N Engl J Med* 2014 Mar 13; **370**(11)**:** 997-1007.
57. Burger JA, Keating MJ, Wierda WG, Hartmann E, Hoellenriegel J, Rosin NY, *et al.* Safety and activity of ibrutinib plus rituximab for patients with high-risk chronic lymphocytic leukaemia: a single-arm, phase 2 study. *Lancet Oncol* 2014 Sep; **15**(10)**:** 1090-1099.
58. Jones JA, Robak T, Brown JR, Awan FT, Badoux X, Coutre S, *et al.* Efficacy and safety of idelalisib in combination with ofatumumab for previously treated chronic lymphocytic leukaemia: an open-label, randomised phase 3 trial. *Lancet Haematol* 2017 Mar; **4**(3)**:** e114-e126.
59. Danial NN, Korsmeyer SJ. Cell death: critical control points. *Cell* 2004 Jan 23; **116**(2)**:** 205-219.
60. Fulda S, Debatin KM. Extrinsic versus intrinsic apoptosis pathways in anticancer chemotherapy. *Oncogene* 2006 Aug 7; **25**(34)**:** 4798-4811.
61. Elmore S. Apoptosis: a review of programmed cell death. *Toxicol Pathol* 2007 Jun; **35**(4)**:** 495-516.
62. Youle RJ, Strasser A. The BCL-2 protein family: opposing activities that mediate cell death. *Nat Rev Mol Cell Biol* 2008 Jan; **9**(1)**:** 47-59.
63. Galonek HL, Hardwick JM. Upgrading the BCL-2 network. *Nat Cell Biol* 2006 Dec; **8**(12)**:** 1317-1319.
64. Green DR. At the gates of death. *Cancer Cell* 2006 May; **9**(5)**:** 328-330.
65. Cimmino A, Calin GA, Fabbri M, Iorio MV, Ferracin M, Shimizu M, *et al.* miR-15 and miR-16 induce apoptosis by targeting BCL2. *Proc Natl Acad Sci U S A* 2005 Sep 27; **102**(39)**:** 13944-13949.
66. Roberts AW, Seymour JF, Brown JR, Wierda WG, Kipps TJ, Khaw SL, *et al.* Substantial susceptibility of chronic lymphocytic leukemia to BCL2 inhibition: results of a phase I study of navitoclax in patients with relapsed or refractory disease. *J Clin Oncol* 2012 Feb 10; **30**(5)**:** 488-496.
67. Schoenwaelder SM, Jarman KE, Gardiner EE, Hua M, Qiao J, White MJ, *et al.* Bcl-xL-inhibitory BH3 mimetics can induce a transient thrombocytopathy that undermines the hemostatic function of platelets. *Blood* 2011 Aug 11; **118**(6)**:** 1663-1674.
68. Roberts AW, Davids MS, Pagel JM, Kahl BS, Puvvada SD, Gerecitano JF, *et al.* Targeting BCL2 with Venetoclax in Relapsed Chronic Lymphocytic Leukemia. *N Engl J Med* 2016 Jan 28; **374**(4)**:** 311-322.
69. Smit LA, Hallaert DY, Spijker R, de Goeij B, Jaspers A, Kater AP, *et al.* Differential Noxa/Mcl-1 balance in peripheral versus lymph node chronic lymphocytic leukemia cells correlates with survival capacity. *Blood* 2007 Feb 15; **109**(4)**:** 1660-1668.
70. Hallaert DY, Jaspers A, van Noesel CJ, van Oers MH, Kater AP, Eldering E. c-Abl kinase inhibitors overcome CD40-mediated drug resistance in CLL: implications for therapeutic targeting of chemoresistant niches. *Blood* 2008 Dec 15; **112**(13)**:** 5141-5149.
71. Seymour JF, Kipps TJ, Eichhorst B, Hillmen P, D'Rozario J, Assouline S, *et al.* Venetoclax-Rituximab in Relapsed or Refractory Chronic Lymphocytic Leukemia. *N Engl J Med* 2018 Mar 22; **378**(12)**:** 1107-1120.

Addendum

Abbreviations

Summary

Samenvatting

Acknowledgements

About the author

PhD Portfolio

Publications

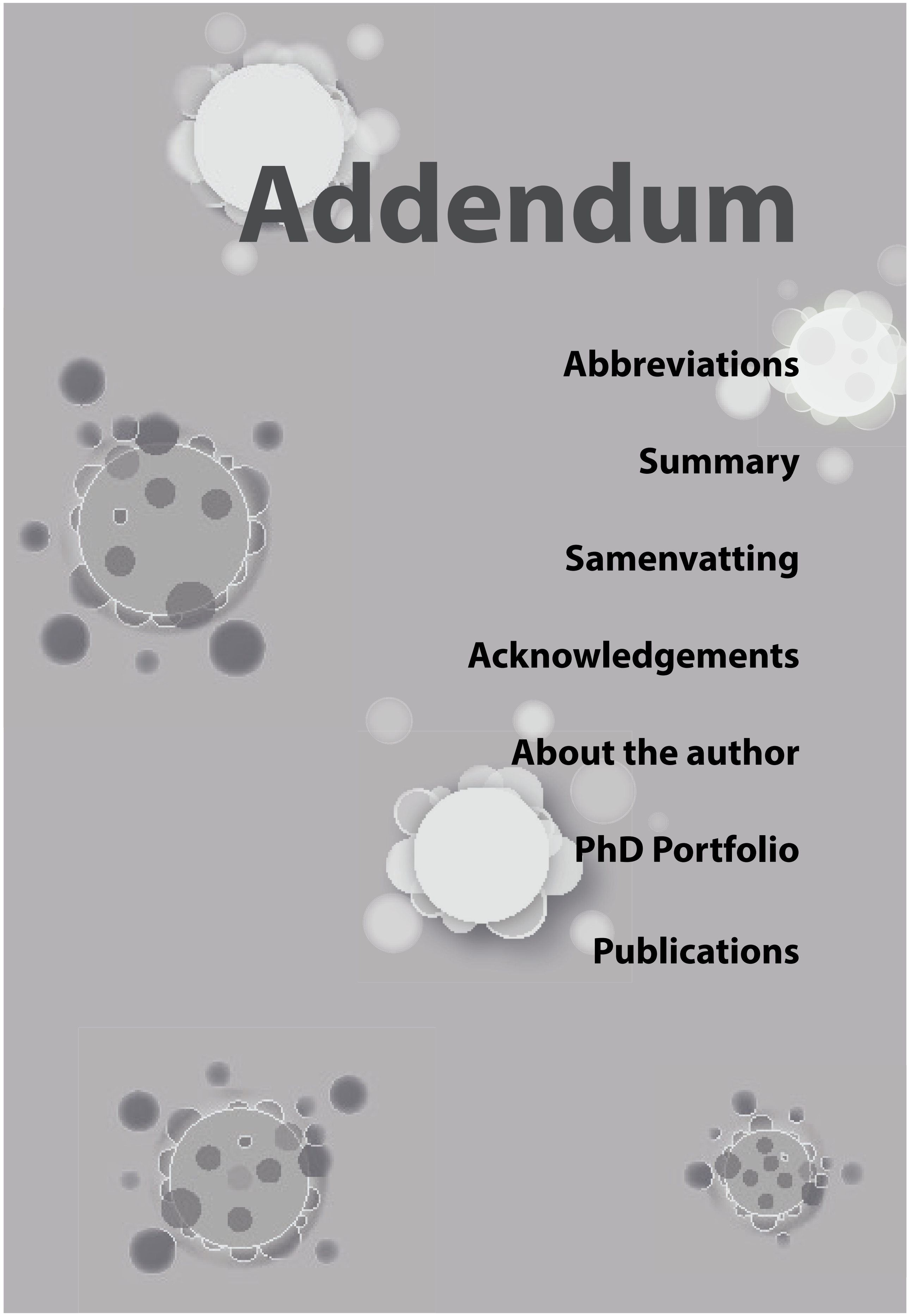

ABBREVIATIONS

7-AAD	7-aminoactinomycin
ABC-DLBCL	Activated B-cell-like diffuse large B-cell lymphoma
ADCC	Antibody mediated cytotoxicity
AID	Activation induced cytidine deaminase
AKT	serine/threonine kinase or protein kinase B
AS1949490	SHIP2-specific inhibitor 3-[(4-Chlorophenyl)methoxy]-N-[(1S)-1-phenylethyl]-2-thiophenecarboxamide
BCAP	B-cell PI3K adaptor
Bcl-2	B-cell lymphoma 2
BCR	B cell receptor
BMX	bone marrow expressed kinase
BTK	Bruton's Tyrosine Kinase
CD19-hBTK	B cell-specific overexpression of Btk
CDR3	Complementarity determining region 3
CLL	Chronic lymphocytic leukemia
CR	Complete response
DLBCL	Diffuse large B-cell lymphoma
E-Btk-2 mice	Mice expressing constitutive active E41K-BTK mutant selectively in the B-cell
ERK	Extracellular signal regulated kinase
FL	Follicular Lymphoma
Fo-B	Follicular B cells
GAPDH	Glyceraldehyde-3-phosphate dehydrogenase
GC	Germinal Center
GC-DLBCL	GC B-cell-like diffuse large B-cell lymphoma
HDAC	Histone deacetylase
IGH	Immunoglobulin heavy chain
IGHD	Immunoglobulin heavy constant delta gene
IGHJ	Immunoglobulin heavy chain joining gene
IGHV	Immunoglobulin heavy chain variable gene
IGL	Immunoglobulin light chain
INPP	Inositol polyphosphate phosphatases
IP4	Inositol (1,3,4,5) tetraphosphate

ITAMs	Immune tyrosine activation motifs
ITIMs	Immune tyrosine Inhibitory motifs
ITK	Interleukin-2-inducible T cell kinase
K118	pan-SHIP1/2 inhibitor, 3β-Amino-5α-androstanane hydrochloride
LYN	Lck/Yes-related novel protein tyrosine kinase
MACS	Magnetic-activated cell sorting
MALT	Mucosa-associated lymphoid tissue
MAPK	Mitogen-activated protein kinase
MCL	Mantle cell lymphoma
Mcl-1	Myeloid leukemia cell differentiation protein
M-CLL	Mutated chronic lymphocytic leukemia
MM	Multiple Myeloma
mTOR	Mammalian target of rapamycin
MYD88	Myeloid differentiation primary response 88
MZ	Marginal zone
MZL	Marginal zone lymphoma
NFAT	Nuclear factor of activated T cells
NF-κB	Nuclear factor kappa-light-chain-enhancer of activated B cells
NHLs	Non-Hodgkin lymphomas
ORR	Overall response rate
OS	Overall survival
PCNSL	Primary central nervous system lymphoma
PCR	Polymerase chain reaction
PH	Pleckstrin homology
PI(3,4)P2 or PIP2	Phosphatidylinositol (3,4)-bisphosphate
PI(3,4,5)P3 or PIP3	Phosphatidylinositol (3,4,5)-trisphosphate
PI3K	Phosphatidylinositol-3-Kinase
PLCy or PLCg	Phospholipase C gamma
PtC	Phosphatidylcholine
PTEN	Phosphatase and tensin homolog
PTPN	Protein tyrosine phosphatases of the non-receptor type
QVD	Quinoline-Val-Asp-Difluorophenoxymethyl Ketone
RLK	Resting lymphocyte kinase
RPKM	Reads per kilobase of a transcript per million
S6	Ribosomal protein S6 kinase

SH	SRC homology
SHIP	SH2-containing inositol phosphatase
SHM	Somatic hypermutation
SHP1	SH2 domain containing protein tyrosine phosphatase-1
sIgM	Surface IgM
SLL	Small lymphocytic leukemia
SLP65	SH2-domain-containing leukocyte protein of 65kDa
SYK	Spleen tyrosine kinase
TD	T cell-dependent
TEC	Tyrosine kinase expressed in hepatocellular carcinoma
TI	T cell-independent
TLR	Toll-like receptor
U-CLL	Unmutated chronic lymphocytic leukemia
VCAM-1	Vascular cell adhesion molecule-1
WM	Waldenström's Macroglobulinemia
XID	X-linked immunodeficiency
XLA	X-linked agammaglobulinemia

SUMMARY

Chronic lymphocytic leukemia (CLL) is the most frequently occurring type of leukemia in adults in the Western world. CLL is characterized by accumulation of a monoclonal population of small B cells with a typical immunophenotype (CD19^{+}CD20^{dim}CD5^{+}CD23^{+}CD27^{+}CD43^{+}surface Ig^{dim}) in the blood. Several lines of evidence indicate that important prognostic information resides in the B cell receptor (BCR) that is expressed by CLL cells and its downstream signaling pathways. First, based on somatic hypermutation (SHM) status of the immunoglobulin heavy chain variable (IGHV) genes of the BCR CLL patients can be grouped into unmutated CLL (U-CLL) and mutated CLL (M-CLL). This division is also clinically relevant, because U-CLL tend to have an unfavorable prognosis with a more aggressive course of the disease and shorter time to first treatment, while M-CLL is associated with a more indolent disease form with a relatively favorable prognosis. Second, approximately one-third of all CLL cases can be grouped on the basis of their restricted IGHV, IGHD, and IGHJ gene usage, and similarities in length and amino acid sequence of the complementarity determining region 3 (CDR3). These so-called stereotypic BCRs are found in multiple CLL patients and is indicative of a contribution of similar antigens, thus implicating antigenic stimulation and thereby BCR specificity in CLL pathogenesis. Third, it is now well known that aberrant kinase activation is critical for survival of leukemic cells in CLL. Bruton's tyrosine kinase (BTK) and phosphatidylinositol 3-kinase (PI3K), particularly the PI3Kδ isoform, are constitutively phosphorylated in CLL B cells and are crucial for their survival. A critical role for BTK in CLL leukemogenesis was confirmed in two preclinical mouse models for human disease, showing that either CLL-like disease did not develop in the absence of BTK, or that BTK inhibition significantly delayed CLL development. Importantly, small molecule inhibitors targeting BTK (ibrutinib and acalabrutinib) or PI3Kδ (idelalisib) have shown impressive clinical responses and are now part of routine standard of care in the clinic.

Although the overall response rates for treatment with kinase inhibitors are very good, the important limitation is that the percentage of patients with a complete response(CRs) is low and that patients with a minimal residual disease-negative CRs are rare. Hence, these targeted therapies are currently prescribed indefinitely and resistance can occur over time. There is a clinical need for more effective targeted and/or combination therapy that result in deep remission. Therefore, better understanding of the relevant signaling pathways in the pathogenesis of CLL is required.

In this thesis we describe studies that aim to unravel the role of B-cell intrinsic factors (such as BCR signaling) and extrinsic factors (such as signaling induced by anti-CD40, which is expressed on activated T cells) in the pathogenesis of the CLL. For these studies, we employed both CLL B cells from patients and the *IgH.TEμ* CLL mouse model. In this mouse model, the SV40 oncogene is sporadically expressed in B cells, on which mice develop a B cell leukemia from about 16 weeks of age, with large similarities with CLL in humans. In **Chapter 2**, we discuss the role of BTK in B cell development and B cell malignancies and highlight the importance of BTK inhibition in cancer therapy.

In **Chapter 3**, we used a total RNA deep sequencing approach to compare genome-wide gene expression profiles of unmutated *IgH.TEμ* CLL cells to those of wild type (Wt) and Btk-overexpressing splenic B cells, either unstimulated or *in vitro* stimulated with anti-IgM antibodies. In addition, we also compared gene expression profiles of unmutated *IgH.TEμ* CLL cells to available profiles of follicular B cells induced by in vitro stimulation with anti-CD40 antibodies and recombinant IL4 (α-CD40/IL-4). We found that 3,611 genes were differentially expressed between primary CLL cells from *IgH.TEμ* mice and naïve splenic B cells from wild-type mice. While approximately half of this CLL signature is related to BCR signaling, Btk overexpression and α-CD40/IL-4 stimulation additionally contribute to this signature, particularly concerning genes involved in cellular proliferation. These findings may help to define targets for therapeutic strategies in human CLL disease.

Despite proven usefulness of *IgH.TEμ* CLL mouse model as a pre-clinical tool to study human disease, it takes substantial time (>6 months) for these mice to develop CLL. Therefore, this model is not suitable for large-scale screens of novel compounds or combination therapies. In **Chapter 4** we aimed to obtain stable CLL cell lines from *IgH.TEμ* mice splenocytes (named EMC cell lines) by exploiting their constitutive active kinase signaling phenotype. The EMC cell lines exhibit a stable CD5$^+$CD43$^+$IgM$^+$CD19$^+$ CLL phenotype over prolonged culture and can be adoptively transferred into *Rag1*$^{-/-}$ mice. Treatment of the cell lines with ibrutinib or idelalisib resulted in reduced proliferation and fibronectin-dependent cell adhesion. Treatment of cell line-engrafted *Rag1*$^{-/-}$ mice with ibrutinib was associated with transient lymphocytosis, reduced splenomegaly and increased overall survival. These EMC cell lines thus provide a novel *in vitro* and *in vivo* preclinical platform to study CLL cell biology and to test efficacy of novel targeted therapy combinations.

In addition to kinases, optimal activity of phosphatases downstream of the BCR is essential for B cell function and selection at various cellular differentiation checkpoints. Although the role of aberrant kinase activation for survival of CLL cells is well established, it is currently unclear how the activity of phosphatases is dysregulated in CLL. In **Chapter 5** we identified ~100 phosphatase genes that were differentially expressed is a comparison of *IgH.TEμ* CLL cells wild-type splenic B cells. We explored the involvement of the SH2-containing inositol phosphatases SHIP1 and SHIP2 in CLL pathogenesis. Targeted B-cell specific deletion of *Ship2* (but not *Ship1*) significantly reduced CLL formation in the *IgH.TEμ* mouse model. Treatment of EMC cell lines and in human CLL samples with Ship1/2 inhibitors *in vitro* reduced cell survival and proliferation. Our data further indicate that SHIP1/2 promotes CLL survival by exerting dual effects on the BCR signaling cascade. On one hand SHIP1/2 increases PI(3,4)P2 levels and thereby enhances the AKT/S6 pathway, resulting in increased Mcl-1 protein expression, which mediates survival of CLL B-cells. On the other hand, SHIP1 seems to play a role in maintaining optimal Ca^{2+} levels in the presence of constitutive active kinase signaling, thereby engaging an anergic response to BCR stimulation in CLL B-cells. These findings thus provide a novel therapeutic pathway to target CLL.

In addition to B cell-intrinsic signaling pathways, CLL cells have been shown to exhibit a variable dependence on various components of the tumor micro-environment. Transcriptome analyses of human CLL revealed that U-CLL derives from unmutated mature CD5$^+$CD27$^-$ B cells and M-CLL derives from a distinct, previously unrecognized, CD5$^+$CD27$^+$ post-germinal center B cell subset. However, direct *in vivo* evidence for such origin of CLL subgroups is not established. In **Chapter 6** we investigated the role of antigenic pressure on clonal selection of CLL cells in the *IgH.TEμ* CLL mouse model. We found that U-CLL tumors that develop in these mice can be classified into two different groups based on their *IghV* usage. The stereotypic V$_H$11-2/Vκ14-126 CLL subset recognized the phosphatidylcholine self-antigen, developed independently of T cell help or GC formation and represented a somewhat more aggressive type of CLL. Conversely, *in vivo* T cell-dependent immunization decreased the proportions of V$_H$11/Vκ14-expressing CLL. Genome-wide gene expression analysis further supported the notion that V$_H$11 and non-V$_H$11 CLL resemble BCR-stimulated and anti-CD40-stimulated B cells, respectively. Moreover, we found evidence that this "non-V$_H$11" expression signature may be partly associated with non-stereotypic human U-CLL. These findings have implications for the origin of CLL and suggest that the development of human U-CLL can also be T cell dependent.

In **Chapter 7**, we used phospho-specific flow cytometry to study signaling properties of human CLL cells. We observed independent activation of ERK and BTK/PI3K/AKT pathways in CLL, suggesting redundancy in survival signaling in CLL. Such redundancy is important to consider when using kinase inhibitors in cancer therapy. Moreover, we found that high basal ERK phosphorylation correlated with enhanced spontaneous apoptosis of CLL *in vitro*. These findings point to apoptosis-inducing signaling downstream of ERK and support the idea that ERK activation has a role as an inducer of apoptosis, beyond its association with anergy in CLL. Such a mechanism may have implications in patients that show progression on current kinase targeting therapeutic regimens, because these therapies may also result in the abrogation of ERK-mediated apoptosis induction.

Taken together, the results described in this thesis provide further insight into the role of both kinases and phosphatases in signaling pathways that are important for the survival and proliferation of CLL cells. Our data indicate that combination therapy with multiple kinase inhibitors would be an effective strategy to target CLL. Moreover, combining agents with different modes of action can help achieve deeper remission and prevent

development of drug resistance. In **Chapter 8** our results are discussed in light of new treatment strategies for CLL.

SAMENVATTING

Chronische lymfatische leukemie (CLL) is het meest voorkomende type leukemie bij volwassenen in de westerse wereld. CLL wordt gekenmerkt door accumulatie van een monoklonale populatie van kleine B-cellen met een typisch immunofenotype ($CD19^{+}CD20^{laag}CD5^{+}CD23^{+}CD27^{+}CD43^{+}sIgD^{laag}$) in het bloed. Er zijn verschillende aanwijzingen dat belangrijke prognostische informatie aanwezig is zowel in de B-cel receptor (BCR) die tot expressie wordt gebracht door CLL-cellen, als in de onderliggende signaleringsroutes. Ten eerste kunnen - op basis van de somatische hypermutatie (SHM) status van de immunoglobuline zware keten variabele (IGHV) genen van de BCR - CLL-patiënten worden gegroepeerd in ongemuteerde CLL (U-CLL) en gemuteerde CLL (M-CLL). Deze verdeling is ook klinisch relevant, omdat U-CLL vaker een ongunstige prognose heeft met een agressiever beloop van de ziekte en kortere tijd tot de eerste behandeling. M-CLL is daarentegen geassocieerd met een mildere ziektevorm en een relatief gunstige prognose. Ten tweede, ongeveer een derde van alle CLL patiënten kan worden gegroepeerd op basis van hun beperkte IGHV-, IGHD- en IGHJ-gengebruik en hun overeenkomsten in lengte en aminozuursequentie van het CDR3 (‘*complementarity determing region 3*’) gebied van het variable deel van de zware keten. Deze zogenaamde stereotypische BCR’s worden in meerdere CLL-patiënten gevonden en suggereren binding van vergelijkbare antigenen. Dit zou een rol van antigeenstimulatie en BCR-specificiteit in de pathogenese van CLL ondersteunen. Ten derde, afwijkende kinase activiteit is essentieel voor de overleving van leukemische cellen in CLL: Bruton’s tyrosine kinase (BTK) en fosfatidylinositol 3-kinase (PI3K), met name de PI3Kδ isovorm, zijn constitutief gefosforyleerd. Een cruciale rol voor BTK bij CLL-leukemogenese werd bevestigd in twee preklinische muismodellen, die aantoonden dat er geen CLL-achtige ziekte ontstond in de afwezigheid van BTK, of dat BTK remming de ontwikkeling van CLL significant vertraagde. Bovendien hebben zgn. small-molecule remmers van BTK (ibrutinib en acalabrutinib) of PI3Kδ (idelalisib) indrukwekkende klinische effecten laten zien en maken ze op het ogenblik deel uit van de standaard zorg in de kliniek.

Hoewel de overall response rates voor de behandeling met kinaseremmers zeer goed zijn, is de belangrijkse beperking dat het percentage patiënten met een volledige respons laag is en dat patienten met een *minimal residual disease*-vrije volledige respons zeldzaam zijn. Vandaar dat deze gerichte therapieën momenteel ‘levenslang’ worden voorgeschreven, wat kan leiden tot therapieresistentie. Er is derhalve een klinische behoefte aan effectievere gerichte en/of combinatietherapieën, die tot diepe remissie leiden. Daarom is een beter inzicht in de relevante signaleringsroutes betrokken bij de pathogenese van CLL vereist.

In dit proefschrift beschrijven we onderzoek dat gericht is op het ontrafelen van de rol van B cel-intrinsieke factoren (zoals BCR signalering) en van extrinsieke factoren. Belangrijk hier bij is de signalering geïnduceerd door CD40 na interactie met CD40L dat tot expressie wordt gebracht op geactiveerde T-cellen). We hebben gebruik gemaakt van zowel CLL B cellen van patienten als van het *IgH.TEμ* CLL muismodel. In dit muismodel wordt sporadisch het SV40 oncogen tot expressie gebracht in B cellen, waarop vanaf een leeftijd van ongeveer 16 weken muizen een B cel leukemie ontwikkelen met grote overeenkomsten met CLL bij de mens. In **hoofdstuk 2** bespreken we de rol van BTK in de ontwikkeling van B cellen en B cel maligniteiten en wijzen we op het belang van BTK-remming in kankertherapie.

In **Hoofdstuk 3** hebben we genoomwijde totale RNA-sequencing technologie gebruikt om expressieprofielen te vergelijken tussen ongemuteerde CLL cellen uit *IgH.TE*μ muizen en B cellen (zowel ongestimuleerd en na stimulatie met anti-IgM antilichamen) afkomstig uit de milt van wild-type muizen en transgene muizen die BTK tot overexpressie brengen. Daarnaast vergeleken we ongemuteerde *IgH.TEμ* CLL cellen met beschikbare profielen van folliculaire B cellen na stimulatie met anti-CD40 antilichamen en IL-4. Wij konden hiermee een signatuur identificeren van 3.611 genen die differentieel tot expressie kwamen tussen CLL cellen en wild-type B cellen. Terwijl ongeveer de helft van deze CLL signatuur verband houdt met BCR signalering, vonden we een additionele rol van BTK en CD40/IL-4-signalering bij het moduleren van het *IgH.TEμ* CLL genoom. Deze bevindingen laten het belang zien van BCR-, BTK- en CD40-afgeleide stimulerende signalen in de pathogenese van ongemuteerd CLL in *IgH.TEμ*-muizen. Deze kennis kan een bijdrage leveren bij het definiëren van doelen voor therapiestrategieën voor CLL bij de mens.

Ondanks de bewezen bruikbaarheid van het *IgH.TEμ* CLL-muismodel als pre-klinisch hulpmiddel om CLL bij de mens te bestuderen, duurt het relatief lang (>6 maanden) voordat de muizen CLL ontwikkelen. Daarom is dit model minder geschikt voor grootschalige screening van nieuwe verbindingen of combinatietherapieën. Daarom hebben we in **Hoofdstuk 4** gestreefd naar het ontwikkelen van stabiele CLL-cellijnen vanuit de milt van *IgH.TEμ*-muizen die CLL hebben ontwikkeld (EMC-cellijnen genoemd), daarbij gebruik makend van hun signaleringprofiel met constitutief actieve kinases. De EMC-cellijnen vertonen een stabiel $CD5^+CD43^+IgM^+CD19^+$ CLL fenotype, zelfs na langdurige kweek *in vitro,* en kunnen adoptief worden overgebracht in *Rag1*$^{-/-}$ muizen, die geen rijpe B of T cellen hebben. Behandeling van de cellijnen met ibrutinib of idelalisib resulteerde in verminderde proliferatie en fibronectine-afhankelijke adhesie. Toen *Rag1*$^{-/-}$ muizen waarin EMC-cellijnen waren ingebracht werden behandeld met ibrutinib zagen we een kortstondige lymfocytose, een verminderde splenomegalie en verhoogde algehele overleving. Deze EMC cellijnen bieden dus een nieuw *in vitro* en *in vivo* preklinisch platform om CLL celbiologie te bestuderen en de werkzaamheid van nieuwe doelgerichte therapiecombinaties te testen.

Naast kinasefunctie is ook optimale activiteit van fosfatasen geassocieerd met de BCR signaleringsroute essentieel voor de werking en selectie van B cellen op verschillende cellulaire differentiatie checkpoints. Hoewel de rol van afwijkende activering van kinases voor overleving van CLL cellen goed is vastgesteld, is het momenteel onduidelijk hoe de activiteit van fosfatasen in CLL wordt ontregeld. In **Hoofdstuk 5** identificeerden we de betrokkenheid van de SH2-bevattende inositolfosfatasen SHIP1 en SHIP2 in CLL pathogenese. Gerichte B cel specifieke deletie van het *Ship2* gene in *IgH.TEμ* muizen en farmacologische remming van SHIP1/2 in EMC-cellijnen en humane CLL cellen verminderde hun overleving en proliferatiecapaciteit. Onze bevindingen geven verder aan dat SHIP1/2 de overleving van CLL cellen bevordert via twee afzonderlijke effecten op de BCR-signaleringsroute. Aan de ene kant verhoogt SHIP1/2 de PI-(3,4)-P2-niveaus en versterkt daardoor de AKT/S6-route, resulterend in verhoogde expressie van Mcl-1, een eiwit dat de overleving van CLL B cellen bevordert. Aan de andere kant speelt SHIP1 een rol in het handhaven van optimale Ca^{2+}-niveaus in de aanwezigheid van constitutieve actieve kinase signalering, leidend tot een anergische respons op BCR-stimulatie in CLL B cellen. Deze bevindingen geven derhalve een mogelijke nieuwe therapeutische route aan voor CLL.

Naast B cel-intrinsieke signaleringsroutes is aangetoond dat CLL-cellen een variabele afhankelijkheid van verschillende signalen vanuit de leukemie micro-omgeving vertonen. Gepubliceerde transcriptoomanalyses gaven sterke aanwijzingen dat U-CLL afkomstig is van ongemuteerde rijpe $CD5^+CD27^-$ B cellen en dat M-CLL afkomstig is van een bijzondere, voorheen onbekende $CD5^+CD27^+$ post-germinal center (GC, kiemscentrum) B cel subset. Direct *in vivo* bewijs voor een dergelijke oorsprong van CLL-subgroepen was echter niet aanwezig. In **Hoofdstuk 6** hebben we de rol van antigene druk op de klonale selectie van CLL cellen in het *IgH.TE*μ CLL-muismodel onderzocht. We vonden dat de U-CLL tumoren die zich ontwikkelen in deze muizen kunnen worden ingedeeld in twee verschillende groepen op basis van hun IghV-gebruik. De stereotypische V_H11-2/Vκ14-126 CLL-subset die het phosphatidylcholine auto-antigeen herkent, ontwikkelde zich onafhankelijk van de hulp van T cellen of GC vorming, en vertegenwoordigde een wat agressievere vorm van CLL. *In vivo* T cel-afhankelijke immunisatie verlaagde de verhouding van V_H11/Vκ14 tot niet-V_H11 CLL. Genoomwijde genexpressie analyse bevestigde verder dat V_H11 en niet-V_H11 CLL respectievelijk lijken op BCR-gestimuleerde en anti-CD40-gestimuleerde B-cellen. Bovendien vonden we bewijs dat deze "niet- V_H11" expressiesignatuur gedeeltelijk kan worden geassocieerd met niet-stereotypisch humaan U-CLL. Deze bevindingen hebben implicaties voor de oorsprong van CLL en suggereren dat de ontwikkeling van humaan U-CLL ook T cel-afhankelijk kan zijn.

In **Hoofdstuk 7** hebben we fosfo-specifieke flowcytometrie gebruikt om de signaleringseigenschappen van CLL cellen te bestuderen. We zagen onafhankelijke activatie van ERK- en BTK/PI3K/AKT-routes in CLL, hetgeen suggereert dat deze twee routes een parallele en deels overlappende functie kunnen hebben. Een dergelijke functionele overlap is belangrijk bij de overweging van het gebruik van kinase-remmers bij kankertherapie. Bovendien hebben we gevonden dat hoge basale fosforylering van ERK *in vitro* gecorreleerd was met spontane apoptose van CLL. Deze bevindingen wijzen erop dat ERK betrokken is bij apoptose-geassocieerde signalering en ondersteunen het idee dat ERK niet alleen een rol heeft in CLL anergie, maar ook in de inductie van apoptose. Een dergelijk mechanisme kan implicaties hebben voor patiënten die progressie vertonen ondanks hun behandeling met kinase remmers, aangezien dit therapeutische regime zou kunnen leiden tot vermindering van ERK-gemedieerde celdood.

Samenvattend geven de resultaten die in dit proefschrift worden beschreven verder inzicht in kinases en fosfatases in signaleringsroutes die belangrijk zijn voor de overleving en proliferatie van CLL cellen. Onze bevindingen wijzen erop dat combinatietherapie met meerdere kinase-remmers een effectieve strategie zou kunnen zijn voor CLL therapie. Bovendien kan het combineren van middelen met verschillende werkingsmethoden helpen om diepere remissie te bereiken en de ontwikkeling van resistentie tegen geneesmiddelen te voorkomen. In **Hoofdstuk 8** worden onze resultaten besproken in het kader van mogelijke nieuwe behandelingsstrategieën voor CLL.

ACKNOWLEDGEMENTS

This PhD thesis would not have been possible without the help, support and inspiration from people around me. I would like to take this opportunity to thank everyone who made this journey exciting, enjoyable and delightful.

First, I would like to express my sincere gratitude to my promotor **Prof. dr. Rudi W. Hendriks** for providing me the opportunity to work in his lab. Dear Rudi, I admire your extraordinary talent, immense knowledge and amazing way to find solutions to scientific problems. Your dedication to your students is superb. You have a friendly personality. Thanks for accompanying me to conferences, where I was sole participant from lab. Thanks for appreciating me at high times and motivating me at low times of my projects. You never minded discussing data even if we have to spend a few hundred hours late in the evening or between your hectic days. I always felt comfortable and confident with you by my side. Now working with you for over six years I feel that I have grown both scientifically as well as personally. I could not have imagined having a better mentor for my PhD study.

My sincere thanks also goes to my co-promotor **Dr. Anton W. Langerak** who provided me an opportunity to write and initiate this PhD project. Dear Ton, thanks for letting me join your team. Without your precious support it would not be possible to conduct this research. I am very thankful for your advices, tips, practical solutions and discussions. Thank you for the thorough criticism and insights to my projects. It was a pleasure working with you and was an honor to have you as a co-promotor.

I would also like to thank my reading committee. Dear **Prof. dr. Ruud Delwel** and **Dr. Jeroen Guikema**, thank you for joining the reading committee and for the efforts to judge my dissertation. Dear **Prof. dr. Arnon Kater**, thank you not only for being the member of the reading committee and evaluating the dissertation, but also being a valuable collaborator on parts of KWF project included in this dissertation. The meetings I had with you at AMC were very productive and your input on my manuscripts has certainly improved their quality.

I am really thankful to **Dr. Marc Seifert** for taking a seat in my promotion committee. I had the chance to meet you in person several times at B-cell meetings in Germany. Your talks and valuable discussions during those meetings enhanced my enthusiasm towards CLL research.

Dear **Prof. dr. Annemiek van Spriel** thank you very much for your willingness to join my promotion committee.

I extend my acknowledgement to our collaborators in Amsterdam university medical center. Dear **Prof. dr. Erik Eldering** many thanks for joining my promotion committee. Also thank you and your team (**Hanneke**, **Raquel**, **Marco** and **Ingrid**) for giving me access to your laboratory and research facilities and teaching me western blot technique. It is

because of your support that I am able to finish SHIP manuscript. Thank you **Dr. Marcel Spaargaren**, **Annemieke Kuil** and **Dr. Erik Slinger** for all assistance with experiments that helped finishing EMC cell lines manuscript.

Dear **Saravanan** you played a very critical part in realizing this PhD journey. First, thank you for bringing me to Rudi's lab and educating me about different projects during my internship. Soon after I joined your group you started trusting me and let me handle your experiments which ultimately made me an independent researcher. The work I did in my internship with you made a firm base for my PhD and I decided to continue building over it. Thanks for starting all those studies and mentoring me. Thanks for motivating and guiding me.

Special thanks to our B-cell study group in pulmonary medicine lab. Dear **Marjolein**, a large part of this thesis would not have been possible without your help. Thanks for helping me out in many ways (planning and performing experiments, arranging materials, guiding students along etc..). Thanks for motivating and supporting me in various difficult situations. Also, many thanks for accepting the request for being my paranymph and it is because of your contributions that I cannot imagine receiving this degree without you. Thanks **Odilia** and **Jasper** for all wonderful brainstorm sessions, doing experiment together and reviewing my manuscripts. I enjoyed the phase establishing phospho-flow technique in our lab. It is now specialty of our department, great job guys. It was also lot of fun going to several conferences with you guys. Also, Jasper thanks for organizing trip to Dresden, one of the best visit I had and continuing lab-longdrinks tradition. Special thanks to the two students I have been able to supervise. **Catarina**, it was wonderful to see how quickly you grew in your internship from an inquisitive student to a smart, independent and fun colleague. I wish you good luck with your PhD. **Mariana**, thanks for your great help in finishing up V_H11 manuscript which is now published with you as one of the author. You are a hard-working scientist and I wish you great success with your PhD.

Dear **Ralph**, you have been such a great addition to our lab and group. Sincere thanks for performing and teaching me RNA-seq analysis. I cannot imagine finishing bioinformatics part for three main chapters in this thesis without your help. Despite the fact that you work with so many groups, you returned my manuscripts well read, commented and criticized sometimes the very same day. I enjoyed and learned a lot working with you.

I also want to thank all other colleagues in the department of pulmonary medicine.

Thank you **Mirjam** (for thinking along, giving valuable advice during lab-meetings and clarifying my doubts), **Alex** (for all care, discussions, help with EDC and improving my Dutch speaking), **Hellen** (for all guidance and I wish you lot of happiness with the new born).

Thank you **Bobby** for being awesome mate, desk-neighbor, solving my computer problems, teaching me illustrator and giving all those valuable advices. I hope you enjoyed having Indian snacks/food with me and now you are much more tolerated to these spices that we know are not as chilly as everybody thinks. Also many thanks for accepting request to be my paranymph.

Thank you **Pauline** for helping me with R, illustrator, job applications, Dutch exams, career-counselling and starting lab-longdrinks with others. I learnt a lot form those late-evening discussions in lab. I wish you great success in managing final bits of your PhD. Thank you **Irma** for being nice roommate, guidance and all fun together. Thank you **Tridib** for guidance during Dutch exams, being weekend lab-buddy and all the out of lab fun. I wish you good luck with finishing your PhD. Thanks **Floris** for thinking along during experiments, valuable discussions and being a co-author. Good luck with rapping up your PhD thesis. Thank you **Sai Ping**, **Mandy**, **Esmee**, **Anne**, **Bob**, **Joanna** (all for being awesome room-mates), **Jelle** (for being nice neighbor and all fun get-together we had, and I will never forget that Oktoberfest), **Denise** (for organizing longdrinks games together with others), **Stefan** (welcome to our group), **Peter** and **Thomas**. I wish you all great success in finishing your PhD.

Thanks to all technical experts: **Melanie**, **Jennifer**, **Ingrid**, **Myrthe**, **Margaretha**, **Koen** and **Menno** for extending your help whenever I needed without hesitation, answering my questions, having fun together and coping up with my way of working in lab.

Very sincere thanks to **Orisia** for managing all paperwork, arranging my contract, visa and helping me during final phase of my PhD. Thank you **Wilma** for your kindness and care at start of my internship and PhD.

This thesis would not have been possible without the help of the Immunology department.

Special thanks to our EMCLL group. Dear **Alice** and **Ruud**, thanks for doing all the experiments, scientific discussions, reading, reviewing and writing together. I could not have completed the human CLL part in my publications without your help. Also, Alice thanks for introducing me to Immunology lab in the beginning of my PhD and helping me settle in new environment.

Thanks to all the group leaders, teachers and principal investigators at Immunology department:

Dear **Prof. dr. Jacques van Dongen**, **Dr. Menno van Zelm**, **Dr. Wim Dik**, **Dr. Vincent van der Velden**, **Dr. Mirjam van der Burg** thanks for all valuable discussions at every Tuesday morning meetings. Your tips and advices helped me advance in my projects.

Dear **Prof. dr. Peter Katsikis**, **Dr. Yvonne Mueller**, **Dr. Stefan Erkeland**, **Dr. Christopher Schliehe**, **Dr. Pieter Leenen**, **Dr. Marjan Versnel** and **Dr. Ruth Huzinga** thanks for all valuable discussions during journal clubs, histology teachings, department meetings and otherwise. Your tips, advices and motivational words meant a lot to me. Also special thanks to Peter Katsikis and Marjan Versnel for yearly PhD evaluation meetings that help me keep track of my PhD.

Special thanks to **Danielle** and **Bibi** for doing a fabulous job in making layout of this thesis and other members of Immunology secretariat for organizing meetings, conferences and Lab day outings.

Of course I cannot miss here thanking all the fellow PhD students from Immunology department: **Fabian**, **Jorn**, **Marjolein**, **Martine**, **Prisca**, **Wendy**, **Wida**, **Liza**, **Christina**, **Malou**, **Bri**, **Marieke**, **Rina**, **Prayer**, **Jenna**, **Christopher**, **Wouter**, **Willem Jan**, **Anne**, **Jamie**, **Manzhi**, **Xiafoei**, **Dew**, **Iris**, **Olivia**, **Steven**, **Christiaan**, **Jorn**, **Mahnaz**, **Olivia**, **Hannah** for all discussions, support and great fun during PhD retreat, PhD dinner and Journal clubs.

I would like to express my gratitude to different facilities within the Erasmus MC. Many thanks to the animal caretakers (**John**, **Patrick**, **Yvette**, **Henk**, **Eva**, **Vincent**, **Ingeborg**, **Helen**) and animal testing experts from the EDC for all alertness, good care for the mice and for enormous help during all experiments. Thanks to the Center for Biomics and in particular **Dr. Wilfred van IJcken** for performing mRNA sequencing. Thanks to **Henk Jan** from virology department for performing mRNA seq analysis.

Of course, I would also like to thank **Dr. Frank van Vliet** and **Dr. Jan Nouwen** who by setting up great Research Master Infection and Immunity (I&I) program made it possible for me to come to Netherlands and pursue such valuable education. Dear Frank and Jan, thanks for the wonderful time at I&I program and taking good care of all the students at educational and personal levels. I am also grateful to all core teachers of I&I for providing such valuable education that have formed firm base for my career. Also, many thanks to **Dr. Guus F. Rimmelzwaan**, **Dr. Mirjam van der Burg**, **Dr. Teun van Gelder** and post-graduate molecular medicine school (Frank & Jan) for selecting me for the NWO fellowship that helped me get into PhD program and taking care of all my bills during these four years.

I am also grateful to **Dr. Jaap Kwekkeboom** and **Dr. Alexander** from MDL department. Thanks for all the lab-training and education you provided during my master internship. You were essentially the first with whom I had real lab working experience.

I would also like to thank all people who I became friends with here in Netherlands and who made me feel like home. **Chinmoy**, you are my first buddy in Netherlands. Thanks for your help, support and all motivational words when I needed the most. I wish you great success with your PhD. Thank you **Gadissa** for being such a support. I haven't seen such a lively person in my life who never losses his cool even in most stressful situations. Good luck with everything in Ethiopia. Thank you **Rajendra bhai** and **Chaitali bhabhi** for always being there. You are like my second family here in Netherlands. Thank you **Smriti** for being wonderful friend and all the fun together.

I would like to thank some special people from DIPSAR. Thank you **Majumdar Sir**, **Pathak Sir**, **Meenakshi Mam** for recommending me for I&I Master's program. I thank my best friend **Mohd. Tariq Roomi** for motivating me to come abroad and pursue career in research. Tariq, you laid down the foundation stone of my research career with that pharmacovigilance study and I am glad that we presented our first ever conference paper and published first manuscript together. I owe you a lot. Thanks for sticking around with me and all the fun we had during our stay at DIPSAR. Thank you **Gaurav** for all the fun we had together. Your advice and guidance has been so valuable to me from the point I got admission to Masters until today. Thank you **Bharat**, **Vineet**, **Japneet**, **Harpreet**, **Bhupinder**, **Jassi Sir**, **Tushar pajji**, **Jasmine**, **Rahul**, **Mukul**, **Geet**, **Manesh**, **Harish**, **Farhan** and **Rahis** for all valuable advices and spending awesome time together.

At last, I would like to thank my family. Dear **Mom** and **Dad**, your contribution to this book is almost impossible to capture in words. This accomplishment is only feasible because you made me capable of doing this. Thanks for all your love, support, prayers and care. My dear brother **Charan**, thank you for believing in me and supporting my idea to come abroad. You have always been there to take all responsibilities and I would not have imagined living away from home if you was not there. Dear **Gulshan bhabhi** thanks for being part of our family and your love, support and care. Finally, special thanks to our little angel **Jasmayra**, my niece. Seeing you grow day by day refreshes me, make me forget all my pains and bring smile on my face. I wish you all the happiness in this world.

Simar Pal Singh

ABOUT THE AUTHOR

Simar Pal Singh was born on March 26th, 1988 in Delhi, India. At S.S. Mota Singh Senior Secondary School, Delhi he completed his schooling in 2005. In that year he started his study in pharmaceutical sciences at the University of Delhi in India and obtained his Diploma in Pharmacy in 2007. With this diploma he was registered as community pharmacist in Pharmacy council of India. After that he continued his pharmacy education and obtained his Bachelor's degree in Pharmacy in 2011 from University of Delhi, India. In 2012, he moved to the Netherlands to pursue the Research Master's Infection and Immunity at Post-graduate Molecular Medicine School, Erasmus MC, Erasmus University Rotterdam. As part of this study he completed two internships. The first master internship was performed at Department of Gastroenterology and Hepatology, Erasmus MC, under supervision of Dr. Jaap Kwekkeboom, where he studied the effect of a CTLA4 blocker and GITR ligation on regulatory T cells isolated from tissue samples from liver carcinoma patients in an *in-vitro* co-culture system. During his second internship at the Department of Pulmonary Medicine, Erasmus MC he worked on generating novel mouse cell lines that can be used as tools for pre-clinical research in the field of chronic lymphocytic leukemia (CLL) under supervision of Prof. dr. Rudi Hendriks. In August 2014 he received his Research Master's degree. At the end of Research Master training, he wrote a four-year research project and successfully received a NWO fellowship to pursue a PhD program. As a PhD student he started working on a collaborative project entitled "*Studying the role of B cell receptor (BCR) signaling and important associated other signal transduction cascades in the pathogenesis of CLL*" under supervision of Prof. dr. Rudi Hendriks (Department of Pulmonary Medicine) and Dr. Ton Langerak (Department of Immunology) at the Erasmus MC in Rotterdam.

PHD PORTFOLIO:

Name PhD student	S.P.(Simar Pal) Singh
Department	Pulmonary Medicine and Immunology, ErasmusMC
Research School	Postgraduate Molecular Medicine
PhD period	September 2014 – September 2019
Promotor	Prof. Dr. R.W. Hendriks
Co-promotor	Dr. A.W. Langerak

PhD Training

Courses:

2017	Galaxy Course
2017	Ensembl Course
2016	Basic & Advanced Flowcytometry course, BD Biosciences
2016	Basic Course on R
2016	Analysis of microarray and RNA Seq expression data using R/BioC and web tools
2015	Advanced Immunology course
2015	Introductory course in GraphPad Prism
2013	Laboratory animal science (art.9)
2013	Biomedical English Writing course

National Conferences:

2018	Oral	12th Dutch Hematology Congress, Papendal
2018	Oral	22nd Molecular Medicine Day, Rotterdam
2016	Oral	25th KWF Tumor Cell Biology meeting, Lunteren
2014	Oral	23rd KWF Tumor Cell Biology meeting, Lunteren
2017	Poster	26th KWF Cancer Biology meeting, Lunteren
2016	Poster	20th Molecular Medicine Day, Rotterdam
2015	Poster	19th Molecular Medicine Day, Rotterdam
2014	Poster	50th anniversary Dutch Society for Immunology (NVVI) Annual Meeting, Efteling

International Conferences:

2018	Oral	16th B cell forum meeting, Masserberg, Germany
2017	Oral	15th B cell forum meeting, Budenheim, Germany
2018	Poster	Keystone Symposia: B cells in Immunity & Autoimmunity, Dresden, Germany
2017	Poster	XVIIth International CLL workshop, New York, USA
2016	Poster	14th B cell forum meeting, Zeist
2016	Poster	Xth International CLL workshop, Cologne, Germany
2015	Poster	13th B cell forum meeting, Hitzacker, Germany
2015	Poster	ESF-EMBO B-cell symposium, Sant Feliu de Guixols, Spain
2015	Poster	1st International Bcell Symposia, Erlangen, Germany

Seminars and Journal Clubs:

2014-2018	Weekly Journal Club at department of Immunology and Pulmonary Medicine, Erasmus MC
2014-2018	Seminars and mini-symposia at department of Immunology, Erasmus MC

Teaching:

2016-2018	Assisted teaching during immune-histology lectures for medicine and clinical technology students at Erasmus MC
2017-2018	Supervised MSc thesis project of MSc Infection and Immunity student
2016-2017	Supervised MSc internship of MSc Molecular Medicine student

Awards & Honors:

2016	Registration and accommodation grant for Xth iWCLL, Cologne, Germany
2015	Represented Molecular Medicine school for the site visit accreditation
2015	Travel grant and 1st Poster prize at ESF-EMBO B-cell conference, Spain
2014-2018	PhD Grant from Molecular Medicine School, Erasmus MC
2007-Present	Registered pharmacist at Pharmacy council of India

PUBLICATIONS

1. Jasper Rip, Marjolein J. W. de Bruijn, Marjolein K. Appelman**, Simar P. Singh,** Rudi W. Hendriks and Odilia B. J. Corneth; Toll-Like Receptor Signaling Drives Btk-Mediated Autoimmune Disease, Frontiers in Immunology, Volume 10, Article 95, 2019.
2. **Simar P. Singh,** Marjolein J. W. de Bruijn, Mariana P. de Almeida, Ruud W. J. Meijers, Lars Nitschke, Anton W. Langerak, Saravanan Y. Pillai, Ralph Stadhouders and Rudi W. Hendriks; Identification of Distinct Unmutated Chronic Lymphocytic Leukemia Subsets in Mice Based on Their T Cell Dependency, Frontiers in Immunology, Volume 9, Article 1996, 2018.
3. **Simar P. Singh**, Floris Dammeijer, Rudi W. Hendriks; Role of Bruton's tyrosine kinase in B cells and malignancies, Molecular Cancer, Volume 17, Article 57, 2018.
4. **Simar P. Singh***, Jasper Rip*, Rudi W. Hendriks**,** Targeting Bruton's tyrosine kinase expression levels through microRNAs in chronic lymphocytic leukemia treatment, Translational Cancer Research, Volume 6, Supplementary 3, 2017. (**contributed equally*)
5. **Simar P. Singh**, Saravanan Y. Pillai, de Bruijn MJW, Stadhouders R, Corneth OBJ, van den Ham HJ, Muggen A, van IW, Slinger E, Kuil A, Marcel Spaargaren, Arnon P. Kater, Anton W. Langerak and Rudi W. Hendriks; Cell lines generated from a chronic lymphocytic leukemia mouse model exhibit constitutive Btk and Akt signaling, Oncotarget, Volume 8, Number 42, 2017.
6. Alice F. Muggen, **Simar P. Singh**, Rudi W. Hendriks, Anton W. Langerak; Targeting Signaling Pathways in Chronic Lymphocytic Leukemia, Current Cancer Drug Targets, Volume 16, Issue 8, 2016.
7. Alexander P. Gonzalez, Guoying Zhou, **Simar P. Singh**, Patrick P.C. Boor, Qiuwei Pan, Dirk Grunhagen, Jeroen de Jonge, T.K. Tran, Cornelis Verhoef, Jan N.M. IJzermans, Harry L.A. Janssen, Katharina Biermann, Jaap Kwekkeboom and Dave Sprengers; GITR engagement in combination with CTLA-4 blockade completely abrogates immunosuppression mediated by human liver tumor-derived regulatory T cells ex vivo, Oncoimmunology, Volume 4, Issue 12, 2015.
8. Amrita Parle, **Simar P. Singh** and Vineet Kumar; Status of Adverse Drug Reaction Reporting by Health Care Professionals of Delhi, Indian Journal of Pharmacy Practice, Volume 5, Issue 4, 2012.
9. Amrita Parle and **Simar P. Singh**; Status of spontaneous reporting of adverse drug reaction by physicians in Delhi, Indian Journal of Pharmacy Practice, Volume 4, Issue 2, 2011.